



National Library  
of Canada

Bibliothèque nationale  
du Canada

Canadian Theses Service    Service des thèses canadiennes

Ottawa, Canada  
K1A 0N4

## NOTICE

The quality of this microform is heavily dependent upon the quality of the original thesis submitted for microfilming. Every effort has been made to ensure the highest quality of reproduction possible.

If pages are missing, contact the university which granted the degree.

Some pages may have indistinct print especially if the original pages were typed with a poor typewriter ribbon or if the university sent us an inferior photocopy.

Reproduction in full or in part of this microform is governed by the Canadian Copyright Act, R.S.C. 1970, c. C-30, and subsequent amendments.

## AVIS

La qualité de cette microforme dépend grandement de la qualité de la thèse soumise au microfilmage. Nous avons tout fait pour assurer une qualité supérieure de reproduction.

S'il manque des pages, veuillez communiquer avec l'université qui a conféré le grade.

La qualité d'impression de certaines pages peut laisser à désirer, surtout si les pages originales ont été dactylographiées à l'aide d'un ruban usé ou si l'université nous a fait parvenir une photocopie de qualité inférieure.

La reproduction, même partielle, de cette microforme est soumise à la Loi canadienne sur le droit d'auteur, SRC 1970, c. C-30, et ses amendements subséquents.

**Synthesis, Characterization, and Reactivity  
of Iron(II) Sandwich Complexes.**

by

Kevin Craig Sturge

Submitted in partial fulfillment of the requirements  
for the degree of Doctor of Philosophy

at

Dalhousie University  
Halifax, Nova Scotia  
April, 1991

© Copyright by Kevin Craig Sturge, 1991.



National Library  
of Canada

Bibliothèque nationale  
du Canada

Canadian Theses Service    Service des thèses canadiennes

Ottawa, Canada  
K1A 0N4

The author has granted an irrevocable non-exclusive licence allowing the National Library of Canada to reproduce, loan, distribute or sell copies of his/her thesis by any means and in any form or format, making this thesis available to interested persons.

The author retains ownership of the copyright in his/her thesis. Neither the thesis nor substantial extracts from it may be printed or otherwise reproduced without his/her permission.

L'auteur a accordé une licence irrévocable et non exclusive permettant à la Bibliothèque nationale du Canada de reproduire, prêter, distribuer ou vendre des copies de sa thèse de quelque manière et sous quelque forme que ce soit pour mettre ces exemplaires de cette thèse à la disposition des personnes intéressées.

L'auteur conserve la propriété du droit d'auteur qui protège sa thèse. Ni la thèse ni des extraits substantiels de celle-ci ne doivent être imprimés ou autrement reproduits sans son autorisation.

ISBN 0-315-64453-2

Canada

## TABLE OF CONTENTS

	<u>Page</u>
Table of Contents	iv
List of Figures	ix
List of Schemes	xiii
List of Tables	xiv
Abstract	xx
Acknowledgements	xxi
Preface	1
Chapter 1. Introduction	2
Chapter 2. Reactions of $[(\text{arene})_2\text{Fe}]^{2+}$ and $[(\text{arene})(\text{cyclopentadienyl})\text{Fe}]^+$ Cations with Trialkylaluminum Compounds	14
2.1 Characterization of Starting Materials	15
2.2 Reaction of $[(\text{arene})_2\text{Fe}]^{2+}$ Dications with Triethylaluminum	19
2.3 Reaction of $[(\text{arene})_2\text{Fe}]^{2+}$ Dications with Trimethylaluminum	33
2.4 Reaction of $[(\text{arene})(\text{cyclopentadienyl})\text{Fe}]^+$ Cations with Trialkylaluminum Compounds	44

<b>Chapter 3. Reaction of <math>[(\text{arene})_2\text{Fe}]^{2+}</math> and <math>[(\text{arene})(\text{cyclohexadienyl})\text{Fe}]^+</math> Cations with Borohydride, Alkylolithium, and Grignard Reagents</b>	46
3.1 Reaction of $[(\text{arene})_2\text{Fe}]^{2+}$ Dications with $\text{NaBH}_4$	47
3.2 $^1\text{H}$ and $^{13}\text{C}$ NMR Spectroscopy of $[(\text{R}-1,4\text{-C}_6\text{H}_4\text{Me}_2)(1,4\text{-C}_6\text{H}_4\text{Me}_2)\text{Fe}]^+$ Monocations	55
3.3a Double Carbanion Addition to $[(\text{arene})_2\text{Fe}]^{2+}$ Dications	57
3.3b Single Carbanion Addition to $[(\text{arene})_2\text{Fe}]^{2+}$ Dications	68
3.4 Decomplexation of Cyclohexadienyl Complexes	70
3.5 Reaction of $[(\text{arene})(\text{cyclohexadienyl})\text{Fe}]^+$ Monocations with Methylolithium	72
<b>Chapter 4. Synthesis of <math>[(\text{arene})(\text{arene}')\text{Fe}]^{2+}</math> Dications and Reaction with Borohydride, Triethylborohydride, and Carbanions</b>	77
4.1 Synthesis of $[(\text{arene})(\text{arene}')\text{Fe}]^{2+}$ Dications	78
4.2 Ring Regioselectivity in the Addition of Anions to $[(1,4\text{-C}_6\text{H}_4\text{Me}_2)(\text{C}_6\text{Me}_6)\text{Fe}]^{2+}$ and $[(1,4\text{-C}_6\text{H}_4\text{Me}_2)(\text{C}_6\text{Et}_6)\text{Fe}]^{2+}$ Dications	88

4.3 Reaction of $[(1,4-C_6H_4Me_2)(C_6Me_6)Fe]^{2+}$ and $[(1,4-C_6H_4Me_2)(C_6Et_6)Fe]^{2+}$ Dications with $NaBEt_3H$	93
4.4 Regioselectivity in the Addition of Anions to the meta-xylene Ligand of the $[(1,3-C_6H_4Me_2)(C_6Me_6)Fe]^{2+}$ Dication	95
<b>Chapter 5. Net Addition of Carbanions and Electrophiles to <math>[(arene)(cyclopentadienyl)Fe]^+</math> Cations</b>	100
5.1 Net Phenide Addition to the $[(1,3,5-C_6H_3Me_3)(C_5H_5)Fe]^+$ Cation	101
5.2 Base Assisted Electrophilic Addition of $CH_2C_6H_5^+$ to the $[(C_6Me_6)(C_5H_5)Fe]^+$ Monocation and Decomplexation of $C_6(CH_2CH_2C_6H_5)_6$ . Solution and Solid State Behaviour of the Complex and Free Ligand	104
<b>Chapter 6. X-ray Crystallographic Comparison of the <math>\pi</math>-Bonding Abilities of Arene, Cyclopentadienyl, Cyclohexadienyl, and Pentadienyl Ligands in Iron(II) Sandwich Complexes</b>	115
<b>Chapter 7. General Conclusions and Suggestions for Future Research</b>	123
7.1 General Conclusions	124
7.2 Suggestions for Future Research	125

<b>Chapter 8. Experimental</b>	<b>128</b>
8.1 General	129
8.1a Chemicals and Apparatus	129
8.1b Spectroscopy	130
8.1c Analysis	131
8.2 Synthetic Procedures and Product Characterization	131
8.2a Synthesis of Starting Materials	131
8.2b Synthesis of Ethylation Products	133
8.2c Synthesis of Halomethylation Products	136
8.2d Synthesis of Hydride Addition Products	138
8.2e Synthesis of Pseudoferrocenes	141
8.2f Synthesis of Monoaddition Products	145
8.2g Decomplexation of Cyclohexadienyl Complexes	147
8.2h Synthesis of ( $\eta^4$ -5-Methylene- <del>exo</del> -6-ethyl- 1,2,3,4,6-pentamethyl-1,3-cyclohexadiene) ( $\eta^6$ - hexamethylbenzene) iron(0)	150
8.2i Synthesis of [(arene) (arene') Fe] <sup>2+</sup> Dications	151

8.2j Synthesis of Products Derived from Single Carbanion Addition to [(arene)(arene')Fe] <sup>2+</sup> Dications	153
8.2k Synthesis of [(Ph-1,3,5-C <sub>6</sub> H <sub>3</sub> Me <sub>3</sub> )(C <sub>5</sub> H <sub>5</sub> )Fe]	158
8.2l Synthesis of [(C <sub>6</sub> (CH <sub>2</sub> CH <sub>2</sub> Ph) <sub>6</sub> )(C <sub>5</sub> H <sub>5</sub> )Fe]PF <sub>6</sub> and Decomplexation of C <sub>6</sub> (CH <sub>2</sub> CH <sub>2</sub> Ph) <sub>3</sub>	159
<b>Chapter 9. Appendix. X-ray Crystallography</b>	<b>160</b>
<b>Chapter 10. References</b>	<b>261</b>

## LIST OF FIGURES

<u>FIGURE</u>	<u>TITLE</u>	<u>PAGE</u>
1.1	Arene Reactivity upon Complexation to a Transition Metal	6
1.2	Single Carbanion Addition to a Coordinated Arene to Yield a Transition Metal Cyclohexadienyl Complex	11
2.1	ORTEP Perspective View of the Dicationic Portion of [(1,3,5-C <sub>6</sub> H <sub>3</sub> Me <sub>3</sub> ) <sub>2</sub> Fe](PF <sub>6</sub> ) <sub>2</sub> , <b>1a</b>	18
2.2	<sup>1</sup> H NMR Spectrum of [(Et-1,3,5-C <sub>6</sub> H <sub>3</sub> Me <sub>3</sub> )(1,3,5-C <sub>6</sub> H <sub>3</sub> Me <sub>3</sub> )Fe] <sup>+</sup> , <b>2c</b>	21
2.3	ORTEP Perspective View of the Cationic Portion of [(Et-1,3,5-C <sub>6</sub> H <sub>3</sub> Me <sub>3</sub> )(1,3,5-C <sub>6</sub> H <sub>3</sub> Me <sub>3</sub> )Fe]PF <sub>6</sub> , <b>2c</b>	26
2.4	ORTEP Overhead View of the [(Et-C <sub>6</sub> Me <sub>6</sub> )(C <sub>6</sub> Me <sub>6</sub> )Fe] <sup>+</sup> Cation, <b>2e</b>	27
2.5	<sup>1</sup> H NMR Spectrum of [(CH <sub>2</sub> Cl-1,3,5-C <sub>6</sub> H <sub>3</sub> Me <sub>3</sub> )(1,3,5-C <sub>6</sub> H <sub>3</sub> Me <sub>3</sub> )Fe]PF <sub>6</sub> , <b>3c</b>	35
2.6	<sup>13</sup> C NMR Spectrum of [(CH <sub>2</sub> Cl-1,3,5-C <sub>6</sub> H <sub>3</sub> Me <sub>3</sub> )(1,3,5-C <sub>6</sub> H <sub>3</sub> Me <sub>3</sub> )Fe]PF <sub>6</sub> , <b>3c</b>	36
2.7	ORTEP Perspective View of the Cationic Portion of [(CH <sub>2</sub> Cl-1,3,5-C <sub>6</sub> H <sub>3</sub> Me <sub>3</sub> )(1,3,5-C <sub>6</sub> H <sub>3</sub> Me <sub>3</sub> )Fe]PF <sub>6</sub> , <b>3c</b>	40

2.8	ORTEP Perspective View of the [(CH <sub>2</sub> Cl-C <sub>6</sub> Me <sub>6</sub> )(C <sub>6</sub> Me <sub>6</sub> )Fe] <sup>+</sup> Cation, <b>3e</b>	42
3.1	Use of Hydride as a Protecting Group in the Conversion of C <sub>6</sub> Me <sub>6</sub> to a Difunctionalized Cyclohexadiene via Temporary Coordination to Iron	47
3.2	<sup>1</sup> H NMR Spectrum of [(H-C <sub>6</sub> H <sub>6</sub> )(C <sub>6</sub> H <sub>6</sub> )Fe]PF <sub>6</sub> , <b>5a</b>	51
3.3	Partial <sup>1</sup> H NMR Spectrum of [(H-1,4-C <sub>6</sub> H <sub>4</sub> Me <sub>2</sub> )(1,4- C <sub>6</sub> H <sub>4</sub> Me <sub>2</sub> )Fe]PF <sub>6</sub> , <b>5b</b>	56
3.4	<sup>1</sup> H NMR Spectrum of [( <sup>t</sup> Bu-C <sub>6</sub> H <sub>6</sub> ) <sub>2</sub> Fe], <b>8a</b>	62
3.5	ORTEP Perspective View of [( <sup>t</sup> Bu-C <sub>6</sub> H <sub>6</sub> ) <sub>2</sub> Fe], <b>8a</b>	63
3.6	Syn-eclipsed, Anti-eclipsed, and Gauche-eclipsed Conformations of Pseudoferrocenes	64
3.7	Calculated Rotational Barrier of Dipentadienyliron(II)	65
3.8	Perspective View of Bis(η <sup>5</sup> -exo-6-tert-butyl- 1,3,5-trimethylcyclohexadienyl)iron(II)	73
3.9	<sup>13</sup> C NMR Spectrum of [(Et-1,3,5-C <sub>6</sub> H <sub>3</sub> Me <sub>3</sub> )(Me-1,3,5- C <sub>6</sub> H <sub>3</sub> Me <sub>3</sub> )Fe], <b>12c</b>	75
4.1	Reaction of [(arene) <sub>2</sub> Fe] <sup>2+</sup> Dications with Excess Carbanion	78
4.2	<sup>1</sup> H NMR Spectrum of [(1,4-C <sub>6</sub> H <sub>4</sub> Me <sub>2</sub> )(C <sub>6</sub> Et <sub>6</sub> )Fe](PF <sub>6</sub> ) <sub>2</sub> , <b>16</b>	82

4.3	ORTEP Perspective View of the Dicationic Portion of [(1,3-C <sub>6</sub> H <sub>4</sub> Me <sub>2</sub> )(C <sub>6</sub> Me <sub>6</sub> )Fe](PF <sub>6</sub> ) <sub>2</sub> , 15	86
4.4	ORTEP Perspective View of the Dicationic Portion of [(1,4-C <sub>6</sub> H <sub>4</sub> Me <sub>2</sub> )(C <sub>6</sub> Me <sub>6</sub> )Fe](PF <sub>6</sub> ) <sub>2</sub> , 16	87
4.5	Major and Minor Products from the Reactions of NaBH <sub>4</sub> , MeLi, AlEt <sub>3</sub> , and <sup>t</sup> BuLi with [(1,4-C <sub>6</sub> H <sub>4</sub> Me <sub>2</sub> )(C <sub>6</sub> Me <sub>6</sub> )Fe](PF <sub>6</sub> ) <sub>2</sub>	89
4.6	Partial <sup>1</sup> H NMR Spectrum of the Products Obtained from Reaction of [(1,4-C <sub>6</sub> H <sub>4</sub> Me <sub>2</sub> )(C <sub>6</sub> Me <sub>6</sub> )Fe](PF <sub>6</sub> ) <sub>2</sub> with NaBH <sub>4</sub> (aq)	90
4.7	Possible Products in the Reaction of [(1,4-C <sub>6</sub> H <sub>4</sub> Me <sub>2</sub> )(C <sub>6</sub> Me <sub>6</sub> )Fe](PF <sub>6</sub> ) <sub>2</sub> with Excess BEt <sub>3</sub> H <sup>-</sup>	94
4.8	Unsubstituted Ring Positions in m-xylene	96
4.9	Expected Electron Density Distribution in m-xylene	96
4.10	Possible Quinone-like Structure of the m-xylene Ring in the 19e <sup>-</sup> [(1,3-C <sub>6</sub> H <sub>4</sub> Me <sub>2</sub> )(C <sub>6</sub> Me <sub>6</sub> )Fe] <sup>+</sup> Radical	97
4.11	Proposed Electron Density Distribution in the 18e <sup>-</sup> [(1,3-C <sub>6</sub> H <sub>4</sub> Me <sub>2</sub> )(C <sub>6</sub> Me <sub>6</sub> )Fe] <sup>2+</sup> and 19e <sup>-</sup> [(1,3-C <sub>6</sub> H <sub>4</sub> Me <sub>2</sub> )(C <sub>6</sub> Me <sub>6</sub> )Fe] <sup>+</sup> Cations	99
5.1	ORTEP Perspective View of [(Ph-1,3,5-C <sub>6</sub> H <sub>3</sub> Me <sub>3</sub> )(C <sub>5</sub> H <sub>5</sub> )Fe], 21c.	103
5.2	Observed Solid State Conformations of C <sub>6</sub> Et <sub>6</sub> when Complexed to a Transition Metal Moiety	105

5.3	Functionalization of the Methyl Group of [(arene)(cyclopentadienyl)Fe] <sup>+</sup> Cations	106
5.4	ORTEP Perspective View of C <sub>6</sub> (CH <sub>2</sub> CH <sub>2</sub> C <sub>6</sub> H <sub>5</sub> ) <sub>6</sub> , 23	108
5.5	ORTEP Perspective View of the Cationic Portion of [(C <sub>6</sub> (CH <sub>2</sub> CH <sub>2</sub> C <sub>6</sub> H <sub>5</sub> ) <sub>6</sub> )(C <sub>5</sub> H <sub>5</sub> )Fe]PF <sub>6</sub> , 22	109
5.6	<sup>1</sup> H NMR Spectrum of [(C <sub>6</sub> (CH <sub>2</sub> CH <sub>2</sub> C <sub>6</sub> H <sub>5</sub> ) <sub>6</sub> )(C <sub>5</sub> H <sub>5</sub> )Fe]PF <sub>6</sub> , 21, at 25°C	110
5.7	<sup>1</sup> H NMR Spectrum of C <sub>6</sub> (CH <sub>2</sub> CH <sub>2</sub> C <sub>6</sub> H <sub>5</sub> ) <sub>6</sub> , 22, at -92°C	111

## LIST OF SCHEMES

<u>SCHEME</u>	<u>TITLE</u>	<u>PAGE</u>
1.1	One-pot Successive Functionalization of the Methyl Substituents of $[(C_6Me_6)(C_5H_5)Fe]^+$ via Reaction with $tBuOK$ and $RX$	9
2.1	Suggested Mechanism for the Reaction of $AlEt_3$ with $[(arene)_2Fe]^{2+}$ Dications	30
2.2	Suggested Mechanism for the Reaction of $AlMe_3$ with $[(arene)_2Fe]^{2+}$ Dications in $CH_2X_2$	43

LIST OF TABLES

<u>TABLE</u>	<u>TITLE</u>	<u>PAGE</u>
2.1	Comparison of $^1\text{H}$ and $^{13}\text{C}$ NMR Chemical Shifts (ppm) of $[(\text{arene})_2\text{Fe}]^{2+}$ Dications and the Corresponding Free Aromatics	17
2.2	$^1\text{H}$ NMR Chemical Shifts (ppm) of the Ring Hydrogen Atoms of $[(\text{Et-cyclohexadienyl})(\text{arene})\text{Fe}]^+$ Monocations	22
2.3	$^{13}\text{C}$ NMR Chemical Shifts (ppm) of the Ring Carbon Atoms of $[(\text{Et-cyclohexadienyl})(\text{arene})\text{Fe}]^+$ Monocations	23
2.4	$^1\text{H}$ NMR Chemical Shifts (ppm) of the Ring and Halomethyl Fragment Hydrogen Atoms of $[(\text{CH}_2\text{X-1,3,5-C}_6\text{H}_3\text{Me}_3)(1,3,5\text{-C}_6\text{H}_3\text{Me}_3)\text{Fe}]\text{PF}_6$ (X = Cl, Br)	37
2.5	$^{13}\text{C}$ NMR Chemical Shifts (ppm) of the Ring and Halomethyl Fragment Carbon Atoms of $[(\text{CH}_2\text{X-C}_6\text{H}_n\text{Me}_{6-n})(\text{C}_6\text{H}_n\text{Me}_{6-n})\text{Fe}]\text{PF}_6$ (X = Cl, Br; n = 0, 3)	38
3.1	$^1\text{H}$ NMR Chemical Shifts (ppm) of the Ring Hydrogen Atoms of $[(\text{H-cyclohexadienyl})(\text{arene})\text{Fe}]^+$ Monocations	49
3.2	$^{13}\text{C}$ NMR Chemical Shifts (ppm) of the Ring Carbon Atoms of $[(\text{H-cyclohexadienyl})(\text{arene})\text{Fe}]^+$ Monocations	50
3.3	$^1\text{H}$ NMR Chemical Shifts (ppm) of the Ring Hydrogen Atoms of $[(\text{cyclohexadienyl})_2\text{Fe}]$ Complexes	60

3.4	$^{13}\text{C}$ NMR Chemical Shifts (ppm) of the Ring Carbon Atoms of [(cyclohexadienyl) $_2\text{Fe}$ ] Complexes	61
4.1	$^1\text{H}$ NMR Chemical Shifts (ppm) of [(arene)(arene') $\text{Fe}$ ] $^{2+}$ Dications	83
4.2	$^{13}\text{C}$ NMR Chemical Shifts (ppm) of the Ring Carbon Atoms of [(arene)(arene') $\text{Fe}$ ] $^{2+}$ Dications	84
4.3	Percentage of Product Derived from net $\text{R}^-$ Addition to the p-xylene Ligand of [(1,4- $\text{C}_6\text{H}_4\text{Me}_2$ )( $\text{C}_6\text{R}_6$ ) $\text{Fe}$ ]( $\text{PF}_6$ ) $_2$ ( $\text{R} = \text{Me}, \text{Et}$ )	92
6.1	Crystallographic Comparison of the Metal-Ligand Interactions in Iron(II) Sandwich Complexes	118
A1	Crystal Data and Refinement Parameters for [(1,3,5- $\text{C}_6\text{H}_3\text{Me}_3$ ) $_2\text{Fe}$ ]( $\text{PF}_6$ ) $_2$	162
A2	Final Fractional Coordinates for [(1,3,5- $\text{C}_6\text{H}_3\text{Me}_3$ ) $_2\text{Fe}$ ]( $\text{PF}_6$ ) $_2$	163
A3	Bond Distances ( $\text{\AA}$ ) and Angles ( $^\circ$ ) for [(1,3,5- $\text{C}_6\text{H}_3\text{Me}_3$ ) $_2\text{Fe}$ ]( $\text{PF}_6$ ) $_2$	164
A4	Crystal Data and Refinement Parameters for [(Et-1,3,5- $\text{C}_6\text{H}_3\text{Me}_3$ )(1,3,5- $\text{C}_6\text{H}_3\text{Me}_3$ ) $\text{Fe}$ ] $\text{PF}_6$	165
A5	Final Fractional Coordinates for [(Et-1,3,5- $\text{C}_6\text{H}_3\text{Me}_3$ )(1,3,5- $\text{C}_6\text{H}_3\text{Me}_3$ ) $\text{Fe}$ ] $\text{PF}_6$	166
A6	Bond Distances ( $\text{\AA}$ ) and Angles ( $^\circ$ ) for [(Et-1,3,5- $\text{C}_6\text{H}_3\text{Me}_3$ )(1,3,5- $\text{C}_6\text{H}_3\text{Me}_3$ ) $\text{Fe}$ ] $\text{PF}_6$	168

A7	Least Squares Best Planes Calculations for [(Et-1,3,5-C <sub>6</sub> H <sub>3</sub> Me <sub>3</sub> )(1,3,5-C <sub>6</sub> H <sub>3</sub> Me <sub>3</sub> )Fe]PF <sub>6</sub>	170
A8	Crystal Data and Refinement Parameters for [(Et-C <sub>6</sub> Me <sub>6</sub> )(C <sub>6</sub> Me <sub>6</sub> )Fe]PF <sub>6</sub>	172
A9	Final Fractional Coordinates for [(Et-C <sub>6</sub> Me <sub>6</sub> )(C <sub>6</sub> Me <sub>6</sub> )Fe]PF <sub>6</sub>	173
A10	Bond Distances (Å) and Angles (°) for [(Et-C <sub>6</sub> Me <sub>6</sub> )(C <sub>6</sub> Me <sub>6</sub> )Fe]PF <sub>6</sub>	175
A11	Least Squares Best Plane Calculations for [(Et-C <sub>6</sub> Me <sub>6</sub> )(C <sub>6</sub> Me <sub>6</sub> )Fe]PF <sub>6</sub>	178
A12	Crystal Data and Refinement Parameters for [(CH <sub>2</sub> Cl-1,3,5-C <sub>6</sub> H <sub>3</sub> Me <sub>3</sub> )(1,3,5-C <sub>6</sub> H <sub>3</sub> Me <sub>3</sub> )Fe]PF <sub>6</sub>	180
A13	Final Fractional Coordinates for [(CH <sub>2</sub> Cl-1,3,5-C <sub>6</sub> H <sub>3</sub> Me <sub>3</sub> )(1,3,5-C <sub>6</sub> H <sub>3</sub> Me <sub>3</sub> )Fe]PF <sub>6</sub>	181
A14	Bond Distances (Å) and Angles (°) for [(CH <sub>2</sub> Cl-1,3,5-C <sub>6</sub> H <sub>3</sub> Me <sub>3</sub> )(1,3,5-C <sub>6</sub> H <sub>3</sub> Me <sub>3</sub> )Fe]PF <sub>6</sub>	183
A15	Least Squares Best Planes Calculations for [(CH <sub>2</sub> Cl-1,3,5-C <sub>6</sub> H <sub>3</sub> Me <sub>3</sub> )(1,3,5-C <sub>6</sub> H <sub>3</sub> Me <sub>3</sub> )Fe]PF <sub>6</sub>	185
A16	Crystal Data and Refinement Parameters for [(CH <sub>2</sub> Cl-C <sub>6</sub> Me <sub>6</sub> )(C <sub>6</sub> Me <sub>6</sub> )Fe]PF <sub>6</sub>	187
A17	Final Fractional Coordinates for [(CH <sub>2</sub> Cl-C <sub>6</sub> Me <sub>6</sub> )(C <sub>6</sub> Me <sub>6</sub> )Fe]PF <sub>6</sub>	188
A18	Bond Distances (Å) and Angles (°) for [(CH <sub>2</sub> Cl-C <sub>6</sub> Me <sub>6</sub> )(C <sub>6</sub> Me <sub>6</sub> )Fe]PF <sub>6</sub>	192

A19	Least Squares Best Planes Calculations for [(CH <sub>2</sub> Cl-C <sub>6</sub> Me <sub>6</sub> )(C <sub>6</sub> Me <sub>6</sub> )Fe]PF <sub>6</sub>	195
A20	Crystal Data and Refinement Parameters for [( <sup>t</sup> Bu-C <sub>6</sub> H <sub>6</sub> ) <sub>2</sub> Fe]	197
A21	Final Fractional Coordinates for [( <sup>t</sup> Bu-C <sub>6</sub> H <sub>6</sub> ) <sub>2</sub> Fe]	198
A22	Bond Distances (Å) and Angles (°) for [( <sup>t</sup> Bu-C <sub>6</sub> H <sub>6</sub> ) <sub>2</sub> Fe]	203
A23	Least Squares Best Planes Calculations for [( <sup>t</sup> Bu-C <sub>6</sub> H <sub>6</sub> ) <sub>2</sub> Fe]	206
A24	Crystal Data and Refinement Parameters for [(1,3-C <sub>6</sub> H <sub>4</sub> Me <sub>2</sub> )(C <sub>6</sub> Me <sub>6</sub> )Fe](PF <sub>6</sub> ) <sub>2</sub>	209
A25	Final Fractional Coordinates for [(1,3- C <sub>6</sub> H <sub>4</sub> Me <sub>2</sub> )(C <sub>6</sub> Me <sub>6</sub> )Fe](PF <sub>6</sub> ) <sub>2</sub>	210
A26	Bond Distances (Å) and Angles (°) for [(1,3-C <sub>6</sub> H <sub>4</sub> Me <sub>2</sub> )(C <sub>6</sub> Me <sub>6</sub> )Fe](PF <sub>6</sub> ) <sub>2</sub>	212
A27	Least Squares Best Planes Calculations for [(1,3-C <sub>6</sub> H <sub>4</sub> Me <sub>2</sub> )(C <sub>6</sub> Me <sub>6</sub> )Fe](PF <sub>6</sub> ) <sub>2</sub>	215
A28	Crystal Data and Refinement Parameters for [(1,4-C <sub>6</sub> H <sub>4</sub> Me <sub>2</sub> )(C <sub>6</sub> Me <sub>6</sub> )Fe](PF <sub>6</sub> ) <sub>2</sub>	217
A29	Final Fractional Coordinates for [(1,4- C <sub>6</sub> H <sub>4</sub> Me <sub>2</sub> )(C <sub>6</sub> Me <sub>6</sub> )Fe](PF <sub>6</sub> ) <sub>2</sub>	218
A30	Bond Distances (Å) and Angles (°) for [(1,4-C <sub>6</sub> H <sub>4</sub> Me <sub>2</sub> )(C <sub>6</sub> Me <sub>6</sub> )Fe](PF <sub>6</sub> ) <sub>2</sub>	220

A31	Least Squares Best Planes Calculations for [(1,4-C <sub>6</sub> H <sub>4</sub> Me <sub>2</sub> )(C <sub>6</sub> Me <sub>6</sub> )Fe](PF <sub>6</sub> ) <sub>2</sub>	222
A32	Crystal Data and Refinement Parameters for [(C <sub>5</sub> H <sub>5</sub> )(C <sub>6</sub> H <sub>5</sub> -1,3,5-C <sub>6</sub> H <sub>3</sub> Me <sub>3</sub> )Fe]	224
A33	Final Fractional Coordinates for [(C <sub>5</sub> H <sub>5</sub> )(C <sub>6</sub> H <sub>5</sub> - 1,3,5-C <sub>6</sub> H <sub>3</sub> Me <sub>3</sub> )Fe]	225
A34	Bond Distances (Å) and Angles (°) for [(C <sub>5</sub> H <sub>5</sub> )(C <sub>6</sub> H <sub>5</sub> -1,3,5-C <sub>6</sub> H <sub>3</sub> Me <sub>3</sub> )Fe]	227
A35	Least Squares Best Planes Calculations for [(C <sub>5</sub> H <sub>5</sub> )(C <sub>6</sub> H <sub>5</sub> -1,3,5-C <sub>6</sub> H <sub>3</sub> Me <sub>3</sub> )Fe]	229
A36	Crystal Data and Refinement Parameters for [(C <sub>5</sub> H <sub>5</sub> )(C <sub>6</sub> (CH <sub>2</sub> CH <sub>2</sub> C <sub>6</sub> H <sub>5</sub> ) <sub>6</sub> )Fe]PF <sub>6</sub>	231
A37	Final Fractional Coordinates for [(C <sub>5</sub> H <sub>5</sub> )(C <sub>6</sub> (CH <sub>2</sub> CH <sub>2</sub> C <sub>6</sub> H <sub>5</sub> ) <sub>6</sub> )Fe]PF <sub>6</sub>	232
A38	Bond Distances (Å) and Angles (°) for [(C <sub>5</sub> H <sub>5</sub> )(C <sub>6</sub> (CH <sub>2</sub> CH <sub>2</sub> C <sub>6</sub> H <sub>5</sub> ) <sub>6</sub> )Fe]PF <sub>6</sub>	236
A39	Least Squares Best Planes Calculations for [(C <sub>5</sub> H <sub>5</sub> )(C <sub>6</sub> (CH <sub>2</sub> CH <sub>2</sub> C <sub>6</sub> H <sub>5</sub> ) <sub>6</sub> )Fe]PF <sub>6</sub>	241
A40	Crystal Data and Refinement Parameters for C <sub>6</sub> (CH <sub>2</sub> CH <sub>2</sub> Ph) <sub>6</sub>	247
A41	Final Fractional Coordinates for C <sub>6</sub> (CH <sub>2</sub> CH <sub>2</sub> C <sub>6</sub> H <sub>5</sub> ) <sub>6</sub>	248
A42	Bond Distances (Å) and Angles (°) for C <sub>6</sub> (CH <sub>2</sub> CH <sub>2</sub> C <sub>6</sub> H <sub>5</sub> ) <sub>6</sub>	251

A43 Least Squares Best Planes Calculations for  
 $C_6(CH_2CH_2C_6H_5)_6$

255

## ABSTRACT

Reactions of  $[(\text{arene})_2\text{Fe}]^{2+}$  dications with carbanion sources  $\text{AlR}_3$ ,  $\text{RLi}$ , and  $\text{RMgX}$  have been investigated. In reactions with  $\text{AlR}_3$  ( $\text{R} = \text{Me}, \text{Et}$ ) in  $\text{CH}_2\text{X}_2$  ( $\text{X} = \text{Cl}, \text{Br}$ ), monocationic  $[(\text{arene})(\text{cyclohexadienyl})\text{Fe}]^+$  complexes are produced where the cyclohexadienyl ligand is derived from single net  $\text{Et}^-$  ( $\text{AlEt}_3$ ) or  $\text{CH}_2\text{X}^-$  ( $\text{AlMe}_3$ ) addition to an arene ring. Reactions with alkyllithium or Grignard reagents yield  $[(\text{cyclohexadienyl})_2\text{Fe}]$  complexes for arene = benzene, p-xylene, or mesitylene; and  $[(\text{arene})(\text{cyclohexadienyl})\text{Fe}]^+$  complexes for arene = pentamethylbenzene or hexamethylbenzene.

Mixed-arene iron dications of the general formula  $[(\text{arene})(\text{arene}')\text{Fe}]^{2+}$  have been synthesized and their reactivity towards carbanions and borohydride has been investigated. This investigation has revealed that there is a preference for addition at the less substituted arene ligand. These results are rationalized as occurring via a single electron transfer process rather than a nucleophilic mechanism.

Finally, X-ray crystallographic characterization of a number of the aforementioned compounds with previously reported structures has allowed an analysis of Fe(II) sandwich complexes containing cyclopentadienyl, cyclohexadienyl, pentadienyl, and arene ligands. This analysis ranks the four ligands with respect to their ability to  $\pi$ -bond to iron as: arene > cyclohexadienyl  $\approx$  pentadienyl > cyclopentadienyl.

## ACKNOWLEDGEMENTS

The author wishes to express his sincere appreciation, first and foremost, to Drs. Stanley Cameron and Michael Zaworotko for their guidance, suggestions, and the opportunities they have presented throughout the course of this endeavour. In addition, he would like to thank Drs. Anthony Linden, Robin Rogers, Peter White, and Ms. Kathy Beveridge for X-ray structural determinations; Dr. Donald Hooper, Mr. Bruce Macdonald, and Ms. Maureen Yates for NMR spectroscopy; and Mr. Michael Clerk for assistance in the laboratory. He would also like to acknowledge the financial support of the Walter C. Sumner Foundation, Dalhousie University, and Saint Mary's University.

"One should not be deterred from doing an experiment because somebody says it won't work."

Professor Sir Geoffrey Wilkinson

**Chapter 1**

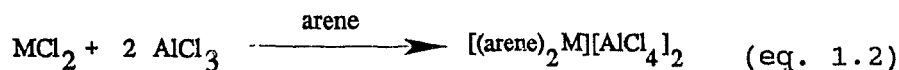
**Introduction**

It is believed that as early as 1919 Hein synthesized a compound in which an aromatic hydrocarbon was bonded to a transition metal centre<sup>1</sup>. It was not until 1954, however, that the true nature of this, the first example of a transition metal arene complex, was fully realized. In 1955 E.O. Fischer prepared<sup>2</sup> the prototypical arene sandwich complex  $\text{Cr}(\text{C}_6\text{H}_6)_2$  and in 1973 he shared the Nobel Prize in Chemistry with G. Wilkinson for his pioneering work in this field. The chemistry of complexed aromatic hydrocarbons has subsequently received considerable attention from organometallic chemists<sup>3-10</sup> and, as a result, there are arene complexes known and structurally characterized for almost all of the transition metals<sup>3,11,12</sup> as well as some lanthanide<sup>13,14</sup>, actinide<sup>15-18</sup>, and main group<sup>19-24</sup> elements.

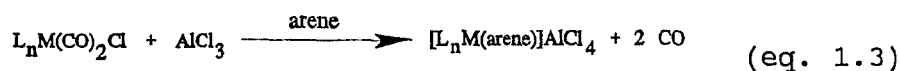
Several experimental techniques have proven successful in the preparation of transition metal arene complexes, including the "Fischer-Hafner" synthesis, carbonyl replacement, metal vapour synthesis, and cyclic condensation. The most widely used synthetic method is the "Fischer-Hafner" synthesis which involves activation of a transition metal halide substrate, normally by  $\text{AlCl}_3$ <sup>2</sup>. In the presence of the arene and aluminum metal the following reaction occurs (equation 1.1).



If reduction of the transition metal salt is not required, aluminum metal is not used (equation 1.2):



This technique is most effective in the preparation of bis(arene) and (arene)(cyclopentadienyl) sandwich complexes although mono(arene) dimers such as  $[(C_6Me_6)NbCl_2]_2$ <sup>25</sup> and  $[(C_6H_6)Pd(AlCl_4)]_2$ <sup>26</sup> have also been synthesized by this route. A similar method, carbonyl replacement, involves halide abstraction by  $AlCl_3$  and/or substitution of CO by the arene in a metal carbonyl halide (equation 1.3) or metal carbonyl.



This technique has been most successful in the preparation of "piano-stool" arene complexes such as  $[(arene)M(CO)_3]^{n+}$  where  $M = Mn$ ,  $n = 1$ <sup>27-29</sup> and  $M = Cr$ <sup>30-33</sup>,  $Mo$ <sup>34</sup>,  $W$ <sup>35</sup>;  $n = 0$ . The other two methods, metal vapour synthesis<sup>36-38</sup> and cyclic condensation<sup>39-41</sup>, have been used successfully where the other methods have failed.

In these and related compounds, arene ligands act as  $\pi$ -electron donor ligands when bonded to the transition metal. The most common mode of coordination is symmetric hexahapto ( $\eta^6$ ) and the ligand is treated as a formal 6-electron

neutral donor for effective atomic number (EAN) counting purposes. In recent years aromatics have also been observed to bond in  $\eta^2$ ,<sup>42-46</sup>  $\eta^4$ ,<sup>41,47-51</sup>  $\mu^2-\eta^2\eta^2$ ,<sup>52-54</sup>  $\mu^3-\eta^2\eta^2\eta^2$ ,<sup>55</sup> and  $\mu^2-\eta^6\eta^6$ <sup>56-58</sup> fashions; the delocalized nature of the ring is greatly reduced in such complexes and they are less common than  $\eta^6$  bonded arene moieties.

A molecular orbital treatment of the bonding in transition metal arene complexes yields a meaningful description of the electronic framework of these molecules<sup>6</sup>. In the prototypical bis(arene) complex,  $[(C_6H_6)_2Cr]$ , there are components of  $\sigma$ ,  $\pi$ , and  $\delta$  symmetry in the bonding of the ligand to the metal. The most important bonding interactions are:  $\sigma$  bonds between the  $\pi$ -orbitals of the ligand and metal s and  $p_z$  orbitals, and  $\pi$ -bonds between the  $\pi$ -orbitals of the ligand and  $d_{xz}$ ,  $d_{yz}$  metal orbitals. There is a smaller component of  $\delta$  symmetry between ligand  $\pi^*$ -orbitals and metal  $d_{x^2-y^2}$ ,  $d_{xy}$  orbitals. These interactions constitute the six bonding molecular orbitals of the complex and are fully occupied. In addition, six electrons are housed in three non-bonding orbitals that are primarily metal d in character, completing the 18-electron configuration. It is a combination of electron donation to the metal and  $\pi$ -backbonding from the metal which act to reinforce each other synergically, lend stability to the complexes, and, most importantly, profoundly affect the reactivity of the ligand.

In terms of reactivity, the transition metal effectively acts as an electron-sink, withdrawing electron density from the delocalized  $\pi$ -system of the arene. The electron deficiency of the ring renders it susceptible to reduction and nucleophilic attack as well as making ring and  $\alpha$ -substituent protons relatively acidic (Figure 1.1), i.e. the arene ring reactivity is reversed when compared with uncomplexed aromatics<sup>5</sup>.

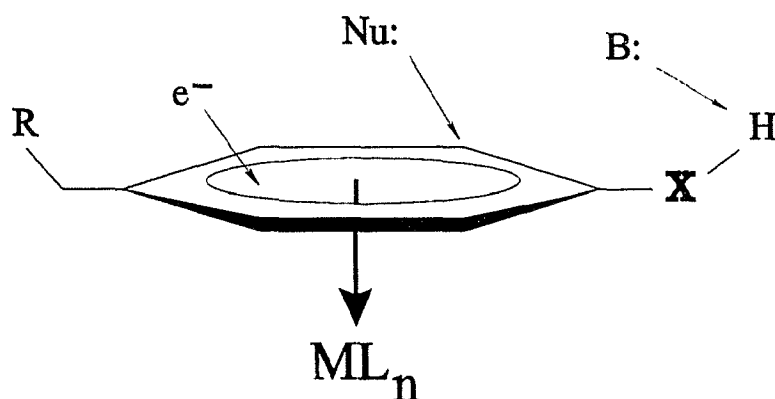
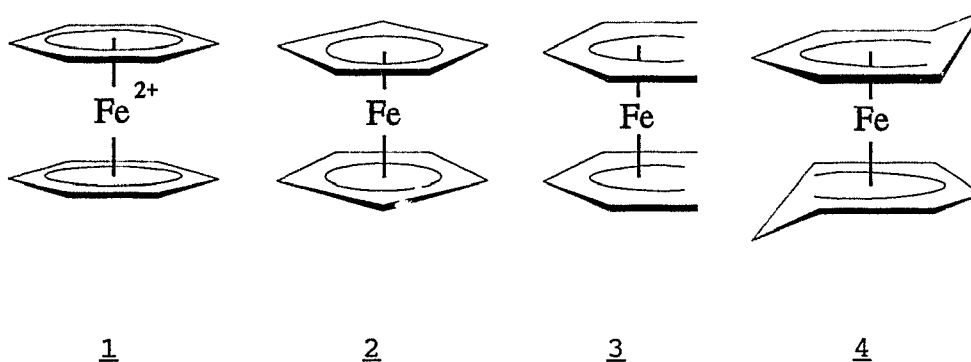


Figure 1.1 Arene Reactivity upon Complexation to a Transition Metal.

One class of compounds that fits into this category of altered arene reactivity is  $[(\text{arene})_2\text{Fe}]^{2+}$  dications, 1. The  $[(\text{arene})_2\text{Fe}]^{2+}$  dications also fall into the larger grouping of organoiron sandwich complexes, which contain the prototypical sandwich complex ferrocene,  $[(\text{cyclopentadienyl})_2\text{Fe}]^{59}$ , 2. Other analogues include the

recently characterized [(pentadienyl)<sub>2</sub>Fe] systems (sometimes referred to as "open ferrocenes")<sup>60-64</sup>, 3; the relatively unexplored [(cyclohexadienyl)<sub>2</sub>Fe] complexes (sometimes referred to as "pseudoferrocenes")<sup>65-68</sup>, 4; and mixed-sandwich complexes derived from combinations of the four ligands (eg. [(arene)(cyclopentadienyl)Fe]<sup>+</sup> cations).



The similarities that these complexes share are mainly in terms of structure and bonding in that they are isoelectronic  $\pi$ -ligand sandwich complexes. Whereas an arene is formally a  $6\pi$ -electron neutral donor ligand, the cyclopentadienyl, pentadienyl, and cyclohexadienyl ligands are formally monoanionic. [(arene)<sub>2</sub>Fe]<sup>2+</sup> complexes are therefore dicationic, [(arene)(cyclopentadienyl)Fe]<sup>+</sup> and [(arene)(cyclohexadienyl)Fe]<sup>+</sup> complexes are monocationic, and [(cyclopentadienyl)<sub>2</sub>Fe], [(pentadienyl)<sub>2</sub>Fe], and [(cyclohexadienyl)<sub>2</sub>Fe], compounds are neutral.

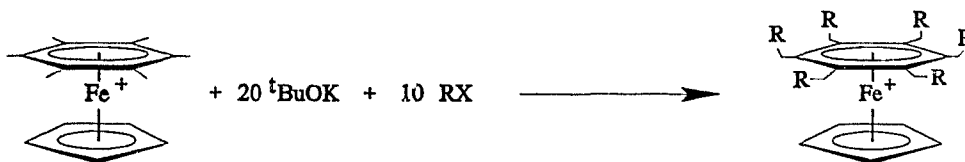
Iron-arene complexes exhibit four general aspects of

organotransition metal arene chemistry: susceptibility to reduction, acidity of ring and  $\alpha$ -substituent hydrogen atoms, conformational effects upon flexible substituents, and reactivity towards nucleophiles.

The first of these effects, susceptibility of the arene moiety towards reduction, has been extensively studied by Astruc et al. Chemical or electrochemical reduction of highly substituted  $[(\text{arene})_2\text{Fe}]^{2+}$  dications and  $[(\text{arene})(\text{cyclopentadienyl})\text{Fe}]^+$  cations has yielded relatively stable 19- and 20-electron complexes<sup>69-72</sup>. The stability of these so called "electron reservoirs" has been attributed to a combination of the  $\pi$ -ligand's ability to delocalize electron density and a high degree of steric crowding kinetically preventing decomposition pathways. Indeed,  $19e^-$   $[(\text{arene})(\text{cyclopentadienyl})\text{Fe}]$  complexes are the most electron-rich molecules known to date<sup>70</sup>. The 19<sup>th</sup> electron in the  $[(\text{C}_6\text{Me}_6)_2\text{Fe}]^+$  radical cation is predominantly metal-based (80%)<sup>71</sup>.

A number of workers have also taken advantage of the acidity of substituent protons on the arene rings of  $[(\text{arene})(\text{cyclopentadienyl})\text{Fe}]^+$  cations. Helling first used<sup>73</sup> the enhanced acidity of  $-\text{XH}$  ( $X = \text{N}, \text{O}, \text{S}$ ) substituted aromatics to prepare the methylated analogues ( $-\text{XMe}$ ) via reaction with base and methyl iodide. Sutherland has shown<sup>74-79</sup> that substituent C-H protons also undergo deprotonation with a suitable base and has used this

methodology in the preparation of novel heterocyclic complexes. Astruc has recently found<sup>80</sup> that reaction of [(arene)(cyclopentadienyl)Fe]<sup>+</sup> cations with excess base (such as <sup>t</sup>BuO<sup>-</sup>K<sup>+</sup>) and primary organic halides (RX, where R = -CH<sub>3</sub>, -CH<sub>2</sub>C<sub>6</sub>H<sub>5</sub>, for example) is a useful and facile means of converting methylated aromatics to higher substituted aromatics, according to scheme 1.1. Alternately, under milder conditions (KOH, DME), functionalities such as -CH<sub>2</sub>CH=CH<sub>2</sub>, and -(CH<sub>2</sub>)<sub>6</sub>OMe have been introduced cleanly and in high yield<sup>81</sup>.



Scheme 1.1 One-pot Successive Functionalization of the Methyl Substituents of [(C<sub>6</sub>Me<sub>6</sub>)(C<sub>5</sub>H<sub>5</sub>)Fe]<sup>+</sup> via Reaction with <sup>t</sup>BuOK and RX.

The effect on conformation of coordinated arene ligands with flexible substituents (eg. hexaethylbenzene) in transition metal sandwich and half-sandwich complexes has been investigated by a number of workers<sup>80,82-96</sup>. The steric strain caused by the proximity of ancillary ligands tends,

in general, to force flexible substituents into a distal (away from the metal) arrangement. As a result, crystallographic characterizations of such complexes reveal conformations of the coordinated arene that would normally be unexpected in the uncomplexed arene. It has even been shown that the solid state conformation of  $C_6Et_6$  in the  $[(C_6Et_6)(C_5H_5)Fe]^+$  cation is affected by choice of counterion, exhibiting 4 distal ethyl groups (2 proximal) when hexafluorophosphate is the counterion<sup>80</sup>, and 5 distal ethyl groups (1 proximal) when tetraphenylborate is the counterion<sup>95</sup>. In the absence of any unusual interionic contacts, this example illustrates the low energy differences between such conformations, which has been borne out by calculations on uncomplexed hexaethylbenzene<sup>82</sup>.

Perhaps the most widely studied aspect of transition metal arene chemistry is the reactivity of the arene towards net nucleophilic addition. Numerous examples of single net addition of nucleophiles to transition metal arene complexes, from neutral phosphines (eg.  $PBu_3$ ) to carbanions (eg.  $tBu^-$ ), have been reported<sup>4,5,8,68,97-109</sup> for a wide range of substrates. The net addition of carbanions occurs invariably at the *exo* face of the arene, yielding a metal-cyclohexadienyl species, as depicted in Figure 1.2.

Unlike free cyclohexadienyl anions, metal-cyclohexadienyl complexes are often stable, isolable species. Reactions of organometallic arene compounds with

nucleophiles do not always yield these derivatives, however. Depending on the choice of reagent, solvent, and temperature, competing reactions such as single electron

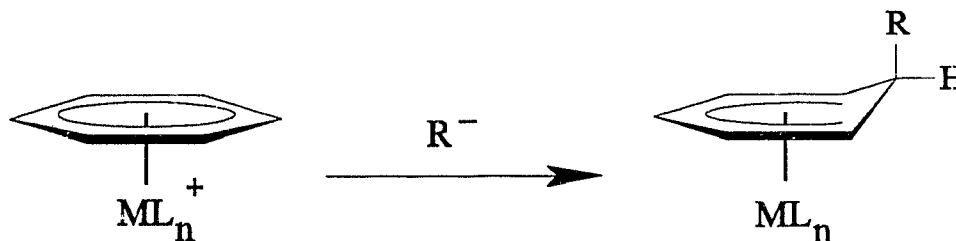


Figure 1.2 Single Carbanion Addition to a Coordinated Arene to Yield a Transition Metal Cyclohexadienyl Complex.

transfer (SET) to generate 19-electron complexes<sup>110,111</sup>, reaction at ancillary ligands<sup>112-114</sup>, and deprotonation<sup>115</sup> have been observed.

Facilitated by the ease of synthesis and isolation, workers have focused attention on cyclohexadienyl moieties as key intermediates in the conversion of aromatics to substituted aromatics or stereospecifically difunctionalized cyclohexadienes. Decomplexation of the cyclohexadienyl ligand using oxidizing reagents has resulted in functionalized arene molecules<sup>65,100,103,114,116-120</sup>. It is thus apparent that complexation of an arene to a transition metal followed by the addition of nucleophiles and subsequent

decomplexation offers a viable alternative to electrophilic substitution of uncomplexed aromatics.

A second addition of a nucleophile to a coordinated cyclohexadienyl ring may result in cyclohexadiene formation. Several elegant multi-step routes to complexed cyclohexadienes have been reported<sup>104-108,110,111,121,122</sup> but attempts at developing a widely applicable, facile process have been thwarted by the unavailability of a convenient route to the required cyclohexadienyl intermediate or deactivation of the complex towards further carbanion addition. This is, in part, due to the observation that traditional alkylating reagents, such as alkyllithium and Grignard reagents, often fail to react in the desired fashion<sup>111,120</sup>. Additionally, substituted ring carbon atoms are typically inert to attack by nucleophiles other than hydride, so, for example, alkylated cyclohexadienyl complexes derived from hexamethylbenzene have only been prepared indirectly via multi-step processes<sup>107,111</sup>.

One such case in which traditional alkylating reagents have hitherto failed to produce desired products is with  $[(\text{arene})_2\text{Fe}]^{2+}$  dications. This is unfortunate since the combination of a high degree of arene activation<sup>8</sup>, 2+ charge, and ease of synthesis make the  $[(\text{arene})_2\text{Fe}]^{2+}$  dications appear to be ideal substrates for conversion of aromatics to cyclohexadienes. It has been reported that these dications (other than arene = mesitylene) fail to

react with  $R^-$  sources under standard conditions ( $RMgX$  or  $RLi$ ,  $-78^\circ C$ , THF) to give carbon-carbon bond formation<sup>111</sup>.

A class of alkylating reagent that has been overlooked by organotransition metal chemists for the purpose of carbanion addition to complexed arenes are the trialkylaluminums,  $AlR_3$ , although they have been used effectively for alkyl metathesis of metal halides<sup>123-129</sup>, and as alkylating reagents by organic chemists<sup>130</sup>. Recently Zaworotko et al. have demonstrated that anionic trialkylaluminum reagents are effective for the alkylation of  $[(arene)Mn(CO)_3]^+$  cations<sup>99</sup>. The parent trialkylaluminum compounds  $AlR_3$  ( $R = Me, Et$ ) are extremely air and moisture sensitive liquids that react violently or even explosively with water or oxygen. However, they are very soluble in hydrocarbon solvents, are comparatively mild alkylating reagents because the Al-C bond polarity is relatively low, and are air stable in their anionic form (eg.  $(AlR_3)_n X^-$ ).

In light of this previous work, the primary goal of this thesis is to extend the reaction chemistry of the  $[(arene)_2Fe]^{2+}$  and  $[(arene)(cyclopentadienyl)Fe]^+$  systems in terms of functionalization of the arene ring, with the aim of converting arene complexes to functionalized or sterically crowded aromatics or cyclohexadienes.

## Chapter 2

Reactions of  $[(\text{arene})_2\text{Fe}]^{2+}$  and  
 $[(\text{arene})(\text{cyclopentadienyl})\text{Fe}]^+$  Cations with  
Trialkylaluminum Compounds

## 2.1 Characterization of Starting Materials

The dications  $[(\text{arene})_2\text{Fe}]^{2+}$  (arene = benzene, **1a**, para-xylene, **1b**, mesitylene, **1c**, pentamethylbenzene, **1d**, and hexamethylbenzene, **1e**) were prepared according to the method of Helling et al.<sup>131</sup> and subsequently isolated as the hexafluorophosphate salts. **1a-e** were characterized by  $^1\text{H}$  and  $^{13}\text{C}$  NMR spectroscopy and infrared spectrophotometry, details of which are presented in full in the experimental section.

A well known feature of the  $^1\text{H}$  NMR spectroscopy of aromatic hydrocarbons is that the chemical shifts of the ring hydrogen atoms resonate downfield (at higher  $\delta$  values) of those in comparable olefins<sup>132</sup>. This trait is due to the anisotropy of the local magnetic field of the molecule as electrons circle the  $\pi$ -cloud of the aromatic ring. This ring current is manifested as a conical region of shielding (associated with upfield shifts) above and below the ring plane, and deshielding (associated with downfield shifts) on the exterior of the ring plane. Upon complexation of the arene to a metal moiety, electron density is withdrawn from this  $\pi$ -cloud. The net result is to reduce both shielding and deshielding effects in transition metal arene complexes, causing  $^1\text{H}$  (as well as  $^{13}\text{C}$ ) NMR resonances to come, in general, upfield of the free aromatics. This characteristic is exemplified by the NMR data of **1a-e** and the corresponding

free arene molecules presented in Table 2.1. For all of the [(arene)<sub>2</sub>Fe]<sup>2+</sup> dications listed, the <sup>1</sup>H and <sup>13</sup>C NMR chemical shifts of the aromatic hydrogen and carbon atoms come at lower δ values than in the corresponding uncomplexed aromatics.

In addition to spectroscopic characterization, **1c** was also characterized by single crystal X-ray diffraction\*. Crystallographic data collection and refinement parameters are given in Table A1 and final fractional coordinates and bond distances and angles are presented in Tables A2 and A3. A perspective view of the dicationic portion of the salt is presented in Figure 2.1 (hydrogen atoms and iron-carbon bonds are omitted, in this and other crystallographic figures, for clarity).

**1c** was observed to adopt a solid state conformation in which the two mesitylene rings are eclipsed with the substituent methyl carbon atoms staggered. The eclipsed/staggered disposition of the arene rings and methyl substituents is expected<sup>6</sup> from electronic and steric considerations, respectively. Average Fe-C and ring C-C bond distance are 2.12(2) and 1.35(6) Å, and the perpendicular distance from the metal to the ring planes is 1.594(1) Å.

---

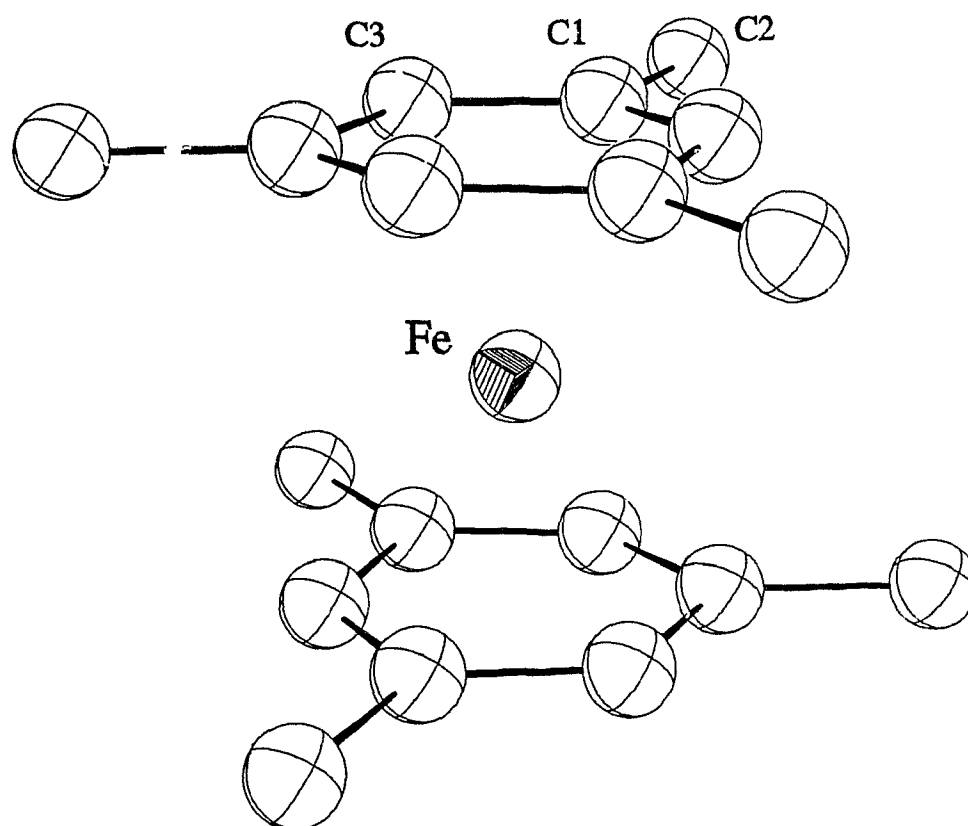
\* The X-ray crystal structure of **1a** was solved by Drs. Stanley Cameron and Anthony Linden at Dalhousie University using data collected on an Enraf-Nonius CAD-4 diffractometer.

Table 2.1 Comparison of  $^1\text{H}$  and  $^{13}\text{C}$  NMR Chemical Shifts (ppm) of  $[(\text{arene})_2\text{Fe}]^{2+}$  Dications and the Corresponding Free Aromatics $^\ddagger$ .

Compound	Arene Chemical Shift(s)	
	$^1\text{H}$	$^{13}\text{C}$
benzene*	7.54	129.3
$[(\text{C}_6\text{H}_6)_2\text{Fe}](\text{PF}_6)_2^*$	6.93	95.2
para-xylene	7.04	135.3, 129.7
$[(1,4-\text{C}_6\text{H}_4\text{Me}_2)_2\text{Fe}](\text{PF}_6)_2$	7.01	112.0, 94.0
mesitylene	6.76	138.3, 127.8
$[(1,3,5-\text{C}_6\text{H}_3\text{Me}_3)_2\text{Fe}](\text{PF}_6)_2$	6.50	113.3, 92.0
pentamethylbenzene	6.75	133.5, 132.6, 129.7
$[(\text{C}_6\text{HMe}_5)_2\text{Fe}](\text{PF}_6)_2$	6.36	107.7, 106.8, 105.3, 92.5
hexamethylbenzene	-	138.1
$[(\text{C}_6\text{Me}_6)_2\text{Fe}](\text{PF}_6)_2$	-	104.6

$^\ddagger$  Acetone- $\text{d}_6$ .

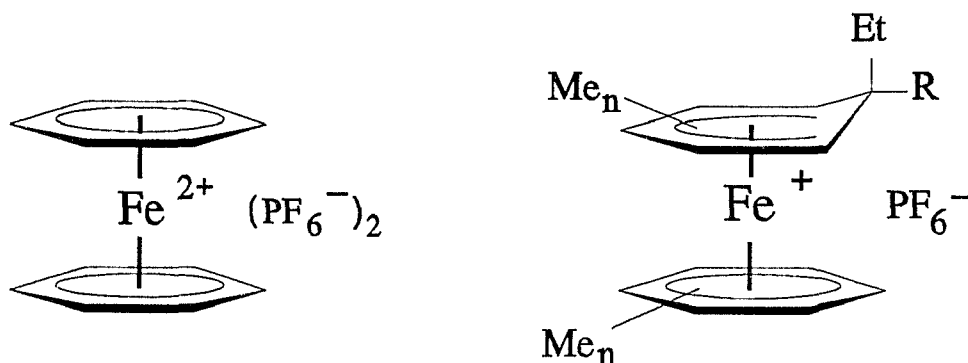
\* Acetonitrile- $\text{d}_3$ .



**Figure 2.1** ORTEP<sup>133</sup> Perspective View of the Dicationic Portion of  $[(1,3,5\text{-C}_6\text{H}_3\text{Me}_3)_2\text{Fe}](\text{PF}_6)_2$ , **1a**.

## 2.2 Reaction of $[(\text{arene})_2\text{Fe}]^{2+}$ Dications with Triethylaluminum

**1a-e** were reacted with a 4-fold excess of  $\text{AlEt}_3$  in dichloromethane producing the monocationic mixed arene-cyclohexadienyl complexes,  $[(\text{arene})(\text{cyclohexadienyl})\text{Fe}]\text{PF}_6$ , **2a-e**, derived from net  $\text{Et}^-$  addition



- |   |   |
|---|---|
| 1. (a) arene = $\text{C}_6\text{H}_6$               | 2. (a) $n = 0$ , $\text{R} = \text{H}$              |
| (b) arene = $1,4\text{-C}_6\text{H}_4\text{Me}_2$   | (b) $n = 1,4\text{-Me}_2$ , $\text{R} = \text{H}$   |
| (c) arene = $1,3,5\text{-C}_6\text{H}_3\text{Me}_3$ | (c) $n = 1,3,5\text{-Me}_3$ , $\text{R} = \text{H}$ |
| (d) arene = $\text{C}_6\text{HMe}_5$                | (d) $n = 5$ , $\text{R} = \text{H}$                 |
| (e) arene = $\text{C}_6\text{Me}_6$                 | (e) $n = 6$ , $\text{R} = \text{Me}$                |

to a single arene ring.  $\text{Et}^-$  addition was shown via X-ray crystallography to occur in the expected<sup>4</sup> exo fashion for **2c** and **2e**. In complexes possessing both substituted and unsubstituted ring carbon atoms (**1b-d**), ethylation occurred exclusively at the sterically favoured unsubstituted position. The isolated yields of **2a-e** unexpectedly (based

on steric considerations) increased with the degree of substitution of the arene ring, giving **2e** in greater than 90% yield. The high yield of **2e** is particularly unexpected as addition necessarily occurs at a substituted ring carbon atom, a reaction hitherto disfavoured in nucleophilic addition reactions to transition metal complexes<sup>4</sup>.

**2a-e** were characterized by <sup>1</sup>H and <sup>13</sup>C NMR spectroscopy and IR spectrophotometry. The <sup>1</sup>H NMR spectrum of **2c** is presented in Figure 2.2. There are several features of this spectrum that are typical of [(arene)(cyclohexadienyl)Fe]<sup>+</sup> cations: the peak labelled H<sub>A</sub> corresponds to the diene ring protons which are shifted to lower field with respect to the mesitylene aromatic C-H; H<sub>B</sub> and H<sub>E</sub> correspond to the hydrogen atoms of the one and two equivalent methyl groups of the cyclohexadienyl ligand, respectively, and have chemical shifts which reflect the decreased deshielding of the cyclohexadienyl ligand towards the sp<sup>3</sup> hybridized carbon atom of the ring; H<sub>C</sub> corresponds to the *endo* hydrogen atom of the cyclohexadienyl ligand and appears as a triplet due to coupling with the two methylene hydrogen atoms of the ethyl group; the H<sub>F</sub> and H<sub>G</sub> resonances of ~0.6 and ~0.4 ppm are assigned to the methylene and methyl fragments of the ethyl moiety, respectively, and are typical of *exo* R groups; and the aromatic ring hydrogen atoms of the complexed mesitylene ligand (H<sub>Ar</sub>) resonate, as expected, at lower field than in the free molecule.

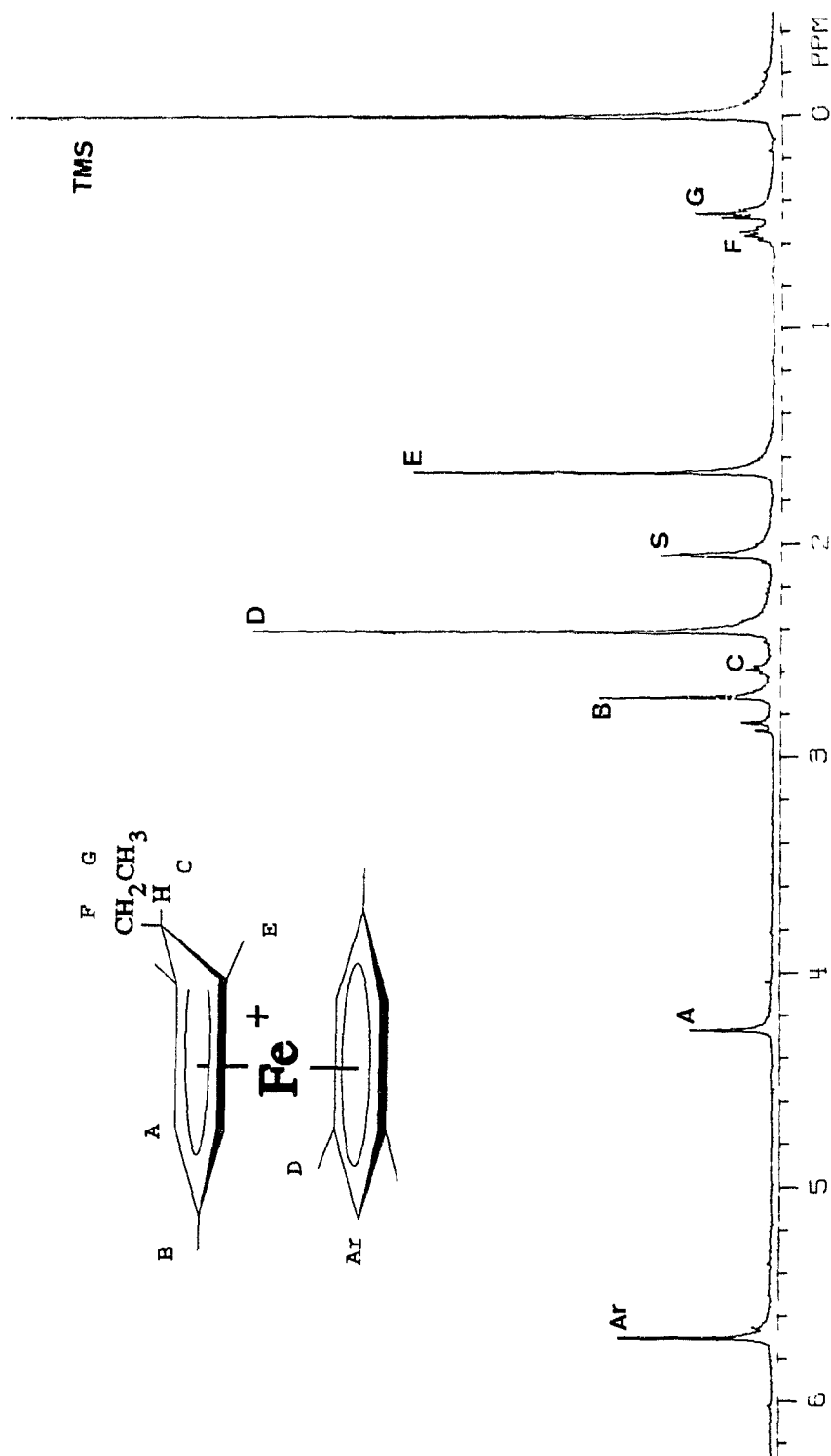
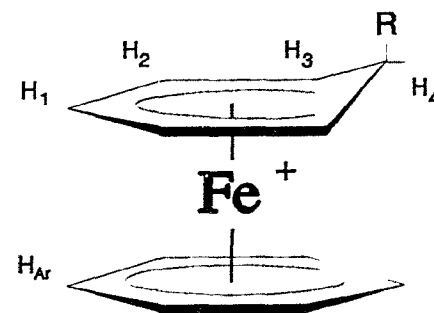


**Figure 2.2**  $^1\text{H}$  NMR Spectrum of  $[(\text{Et-}1,3,5\text{-C}_6\text{H}_3\text{Me}_3)\text{Fe}]^+$ , **2c**.

**Table 2.2**  $^1\text{H}$  NMR Chemical Shifts (ppm) of the Ring Hydrogen Atoms of  
 $[(\text{Et-cyclohexadienyl})(\text{arene})\text{Fe}]^+$  Monocations.<sup>‡</sup>

<u>Complex</u>	<u>Complex #</u>	<u>H<sub>Ar</sub></u>	<u>H<sub>1</sub></u>	<u>H<sub>2</sub></u>	<u>H<sub>3</sub></u>	<u>H<sub>4</sub></u>
$[(\text{Et-C}_6\text{H}_6)(\text{C}_6\text{H}_6)\text{Fe}]\text{PF}_6$	<b>2a</b>	6.46s	6.98t	4.94t	3.94t	2.60t
$[(\text{Et-C}_6\text{H}_4\text{Me}_2)(\text{C}_6\text{H}_4\text{Me}_2)\text{Fe}]\text{PF}_6$	<b>2b</b>	6.32d	6.59d	4.56d	3.38d	?
		5.39d	-	-	-	-
$[(\text{Et-C}_6\text{H}_3\text{Me}_3)(\text{C}_6\text{H}_3\text{Me}_3)\text{Fe}]\text{PF}_6$	<b>2c</b>	5.86s	-	4.37s	-	2.61t
$[(\text{Et-C}_6\text{HMe}_5)(\text{C}_6\text{HMe}_5)\text{Fe}]\text{PF}_6$	<b>2d</b>	5.22s	-	-	-	?

<sup>‡</sup> Acetone-d<sub>6</sub>.



The  $^1\text{H}$  NMR chemical shifts of the ring hydrogen atoms of **2a-d** and  $^{13}\text{C}$  NMR chemical shifts of the ring carbon atoms of **2a-e** are given in Tables 2.2 and 2.3, respectively. The trends in chemical shifts and multiplicity patterns exemplified by the spectrum of **2c** are observed for the other monocations in Table 2.2 and are consistent with the proposed structures. The spectrum of **2b** is somewhat unusual and will be discussed in section 3.2. The  $^{13}\text{C}$  NMR chemical shifts of **2a-e** emphasize the reduction in magnetic anisotropy experienced by the carbon atoms of the cyclohexadienyl ligand towards the  $\text{sp}^3$  carbon atom of the ring and are characteristic of the coordinated cyclohexadienyl ligand<sup>99,100,102,103,134-138</sup>.

The infrared spectra of **2a-e** exhibit strong absorptions centered at approximately  $840\text{ cm}^{-1}$  which have been assigned to a P-F stretching frequency, confirming the presence of hexafluorophosphate as the counterion. Additionally, the absence of any absorption bands centered near  $2800\text{ cm}^{-1}$ , indicative of metal-cyclohexadienyl complexes containing an exo C-H fragment<sup>139</sup>, suggest that net  $\text{Et}^-$  addition occurs in the proposed exo fashion.

In order to confirm the stereochemistry, **2c** and **2e** were also characterized by single crystal X-ray diffraction\*.

---

\* The X-ray crystal structures of **2c** and **2e** were solved by Drs. Stanley Cameron and Anthony Linden at Dalhousie University using data collected on an Enraf-Nonius CAD-4 diffractometer.

The structure of **2c** represents, to our knowledge, the first example of an X-ray crystallographically characterized [(arene)(cyclohexadienylFe)]<sup>+</sup> sandwich complex. A view of the cation is presented in Figure 2.3, and data collection and refinement parameters, final fractional coordinates, bond distances and angles, and least squares best planes calculations are given in Tables A4, A5, A6, and A7 respectively. The cation again displays the expected eclipsed/staggered conformation of the  $\eta^5$ - and  $\eta^6$ - rings and methyl carbon atoms. The arene ring and the dienyl portion of the cyclohexadienyl ring are essentially planar, with maximum deviations from planarity of 0.01(1) Å and 0.02(1) Å, respectively. The average Fe-C bond distances to the  $\eta^6$ - and  $\eta^5$ -rings are 2.11(2) Å and 2.10(5) Å, respectively. Average C-C bond distances in the arene ring and dienyl portion of the cyclohexadienyl ring are 1.41(1) Å and 1.42(2) Å, respectively. The perpendicular distances from the ring plane to the iron atom are 1.570(4) Å for the arene ligand and 1.586(4) Å for the cyclohexadienyl ligand. The sp<sup>3</sup> carbon atom of the cyclohexadienyl ring resides 0.66(1) Å above the dienyl plane.

An overhead view of the cation of **2e** is shown in Figure 2.4 and data collection and refinement parameters are given in Table A8. Final fractional coordinates, bond distances and angles, and least squares best planes calculations are presented in Tables A9, A10, and A11. The average Fe-C bond

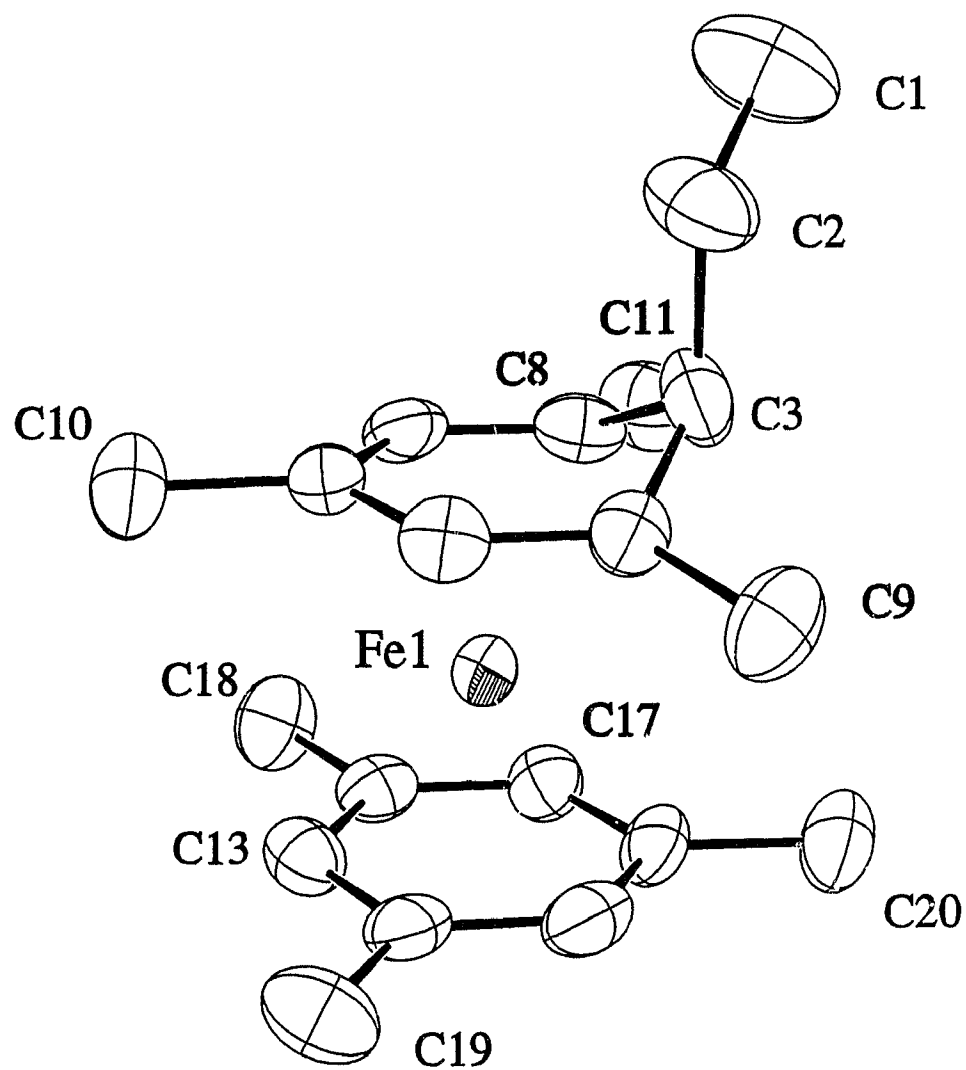


**Figure 2.3** ORTEP<sup>133</sup> Perspective View of the Cationic Portion of [(Et-1,3,5-C<sub>6</sub>H<sub>3</sub>Me<sub>3</sub>)(1,3,5-C<sub>6</sub>H<sub>3</sub>Me<sub>3</sub>)Fe]PF<sub>6</sub>, **2c**.

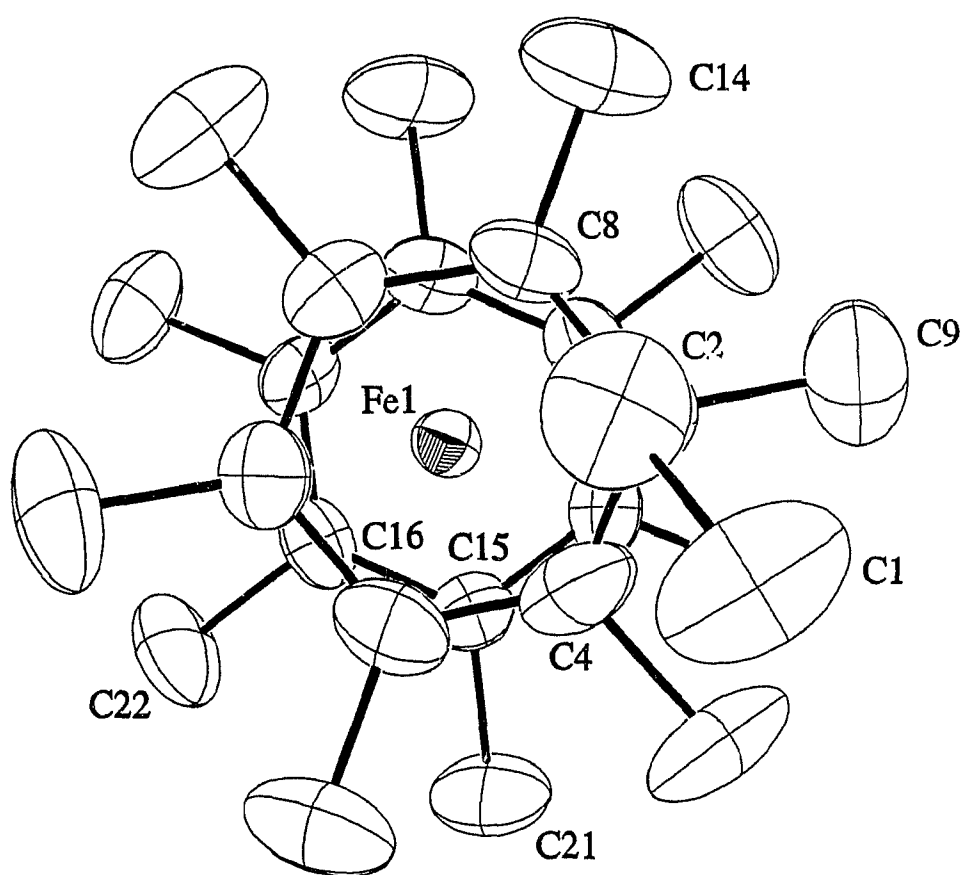
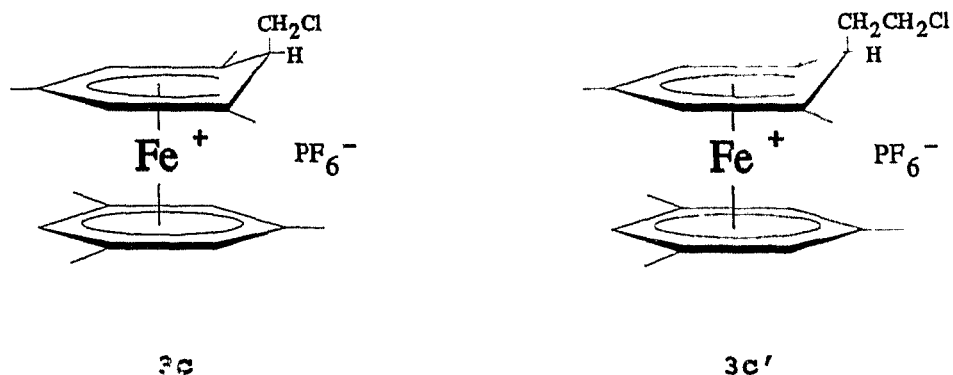


**Figure 2.4** ORTEP<sup>133</sup> Overhead View of the  
 $[(Et-C_6Me_6)(C_6Me_6)Fe]^+$  Cation, 2e.

length is 2.16(1) Å and the perpendicular distance from the iron atom to the arene ring plane is 1.631(3) Å. The carbon atoms of C<sub>6</sub>Me<sub>6</sub> ring deviate from planarity by a maximum of only 0.01(1) Å, with an average C-C bond length of 1.41(2) Å. The dienyl portion of the cyclohexadienyl ring has a maximum deviation from planarity of 0.03(1) Å, Fe-ring plane distance of 1.616(4) Å, and has average Fe-C and C-C bond lengths of 2.12(4) and 1.41(2) Å, respectively. The sp<sup>3</sup> carbon atom of the cyclohexadienyl ring is 0.60(1) Å above the dienyl plane. The cation exhibits two manifestations of steric strain: the methyl carbon atoms of the hexamethylbenzene ligand all point away from the metal at an average distance of 0.13(2) Å from the C<sub>6</sub> plane; and the ring carbons atoms of the arene and cyclohexadienyl rings are staggered.

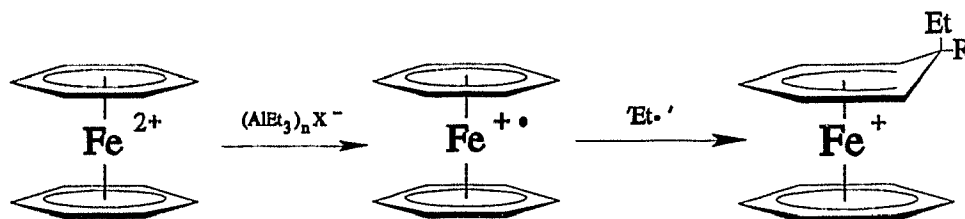
The reaction of **1c** with AlEt<sub>3</sub>, in addition to producing **2c**, afforded a chloromethylated major product (60%) **3c**, and when conducted in 1,2-dichloroethane gave a minor product (20%) identified by <sup>1</sup>H NMR as the chloroethylated analogue **3c'**. The reaction of **1d** with AlEt<sub>3</sub> also gave an additional chloromethylated product (20%), **3d**, but gave only **2d** in 1,2-dichloroethane.

It is conventionally accepted that addition of R<sup>-</sup> to transition metal arene complexes results from nucleophilic attack upon the coordinated arene, facilitated by the reduced electron density in the arene upon complexation<sup>4,5,8</sup>.



The experimental results presented in this thesis, however, suggest that a single electron transfer (SET) mechanism is more likely to be occurring in the reaction of **1a-e** with AlEt<sub>3</sub>. A process can be envisioned whereby AlEt<sub>3</sub>, or more likely an (AlEt<sub>3</sub>)<sub>n</sub>PF<sub>6</sub><sup>-</sup> complex anion (which have been reported<sup>99</sup> to result from the interaction of [(arene)Mn(CO)<sub>3</sub>]PF<sub>6</sub> salts with trialkylaluminum compounds), reduces the organometallic dication. Subsequent coupling of the 19-electron [(arene)<sub>2</sub>Fe]<sup>+</sup> cation and either an ethyl radical or ethyl-containing species would therefore yield the observed reaction products (see Scheme 2.1). It is important to note that cyclohexadienyl formation is consistent with either a SET or nucleophilic mechanism and that reactions previously assumed to be a result of nucleophilic addition could therefore also result from SET processes.

The following observations support such a SET mechanism: (i) the purple solutions that form upon the



**Scheme 2.1** Suggested Mechanism for the Reaction of  $\text{AlEt}_3$  with  $[(\text{arene})_2\text{Fe}]^{2+}$  Dications.

addition of  $\text{AlEt}_3$  to the reaction mixtures are indicative of the 19-electron  $[(\text{arene})_2\text{Fe}]^+$  cations reported<sup>69-71</sup> by Astruc et al.

(ii) The observation that no double addition occurs can be attributed to an increase in reduction potential between  $[(\text{arene})_2\text{Fe}]^{2+}$  and  $[(\text{arene})(\text{cyclohexadienyl})\text{Fe}]^+$  species. The reduction potential for **1e** has been measured<sup>140</sup> as -0.48v vs. SCE (in DMF) and the other complexes **1a-d** should be approximately equal. However, the reduction potential of  $[(\text{H-C}_6\text{Me}_6)(\text{C}_6\text{Me}_6)\text{Fe}]^+$  has been measured<sup>110</sup> as -1.45v vs. SCE (in DMF) and since simple alkyl substituted  $[(\text{arene})(\text{cyclopentadienyl})\text{Fe}]^+$  cations are typically in the same range (-1.30 to -1.55v vs. SCE in acetone,  $[\text{n-Bu}_4\text{N}]\text{BF}_4$ <sup>141</sup>), it is reasonable to assume that **2a-e** also have values of approximately -1.5v. Since none of the reduction potentials of these complexes have been measured in dichloromethane we cannot make a direct comparison, although

it is important to note the relatively large difference in reduction potentials (approximately 1v) between the dicationic and monocationic complexes. To our knowledge, the oxidation potentials of  $\text{AlEt}_3$  complexes have not been reported, but if they fall in the 1v range between the reduction potentials of the dications and monocations they would be capable of transferring an electron to **1a-e** (making  $\text{Et}^\cdot$  addition favourable) but not to  $[(\text{arene})(\text{cyclohexadienyl})\text{Fe}]^+$  cations, precluding further reaction.

(iii) The observation that product yields increase with the degree of substitution of the complexed arene is consistent with a SET process since increased stability of the organometallic radical cation comes with higher arene substitution<sup>69,70,80</sup>. Therefore the lifetime of the  $[(\text{C}_6\text{Me}_6)_2\text{Fe}]^+$  radical would be expected to be longer than that of  $[(\text{C}_6\text{H}_6)_2\text{Fe}]^+$  and would likely react more completely with  $\text{Et}^\cdot$ . This observation is contrary to what one would expect for a nucleophilic attack of  $\text{Et}^\cdot$ , based on steric considerations.

(iv) Formation of the chloroalkyl products **3c**, **3c'**, and **3d** can be attributed to reaction of the  $19\text{e}^-$  cation with solvent molecules (discussed in the following section).

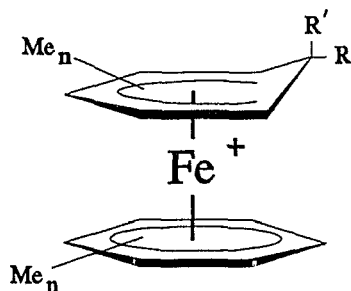
In addition to these experimental observations there is precedent in the scientific literature for trialkylaluminum compounds undergoing SET reactions, not only in transition

metal systems, but reactions of organic substrates as well. Zaworotko et al. have shown<sup>99</sup> that the interaction of  $\text{AlR}_3$  ( $\text{R} = \text{Me}, \text{Et}$ ) with  $[(\text{arene})\text{Mn}(\text{CO})_3]^+$  cations affords reduction products and have confirmed the existence of radical species in solution via ESR spectroscopy. Ashby has also confirmed<sup>142</sup>, via ESR, the existence of paramagnetic species in reactions of trialkylaluminums with diaryl ketones, and more importantly has correlated the rate of product formation with the decay of the radical intermediates.

To our knowledge the ethylation of **1e** represents the first example of direct high-yield carbanionic alkylation at an alkylated arene ring position, and the ethylation of **1a**, **1b**, **1d**, and **1e** are the first reported<sup>98</sup> examples of direct  $\text{R}^-$  addition to these species. Astruc has shown that it is possible to add a variety of carbanions to both **1a**<sup>106,108,111</sup> and **1e**<sup>107,111</sup>, however the synthesis requires three steps: (1) hydride addition to form  $[(\text{arene})(\text{cyclohexadienyl})\text{Fe}]^+$ , (2)  $\text{R}^-$  addition to either the complexed cyclohexadienyl (**1a**) or arene (**1e**), (3) removal of  $\text{H}^-$  by  $\text{Ph}_3\text{C}^+$ . Reaction of **1a-e** with  $\text{AlEt}_3$  therefore offers a convenient, facile route to alkylated  $[(\text{arene})(\text{cyclohexadienyl})\text{Fe}]^+$  complexes.

### 2.3 Reaction of [(arene)<sub>2</sub>Fe]<sup>2+</sup> Dications with Trimethylaluminum

To investigate further the interaction of trialkylaluminum compounds with [(arene)<sub>2</sub>Fe]<sup>2+</sup> dications, **1a-e** were reacted with AlMe<sub>3</sub> using benzene, dichloromethane, and dibromomethane as solvents. Monocationic [(arene)(cyclopentadienyl)Fe]<sup>+</sup> complexes were again isolated, with R' addition being dependent upon the solvent used. Only **1c** gave an isolable product from reaction with AlMe<sub>3</sub> in benzene. The expected methylation product [(Me-1,3,5-C<sub>6</sub>H<sub>3</sub>Me<sub>3</sub>)(1,3,5-C<sub>6</sub>H<sub>3</sub>Me<sub>3</sub>)Fe]PF<sub>6</sub> (**9c**) was isolated but the yield was small (20%). Reaction of **1c** and **1e** in CH<sub>2</sub>Cl<sub>2</sub> and CH<sub>2</sub>Br<sub>2</sub> gave [(arene)(cyclohexadienyl)Fe]PF<sub>6</sub> complexes in which cyclohexadienyl formation occurred as the result of net addition of CH<sub>2</sub>Cl<sup>-</sup> (**3c** and **3e**), and CH<sub>2</sub>Br<sup>-</sup> (**4c** and **4e**).



**3c.** n=1,3,5-Me<sub>3</sub>, R'=CH<sub>2</sub>Cl, R=H

**3e.** n=6, R'=CH<sub>2</sub>Cl, R=Me

**4c.** n=1,3,5-Me<sub>3</sub>, R'=CH<sub>2</sub>Br, R=H

**4e.** n=6, R'=CH<sub>2</sub>Br, R=Me

**9c.** n=1,3,5-Me<sub>3</sub>, R'=Me, R=H

The resulting compounds have been characterized by <sup>1</sup>H and <sup>13</sup>C NMR spectroscopy which reveal that **3c** and **4c** contain minor impurities of **9c**. The NMR chemical shifts of the ring

hydrogen atoms and ring carbon atoms, summarized in Tables 2.4 and 2.5 reveal chemical shift and multiplicity patterns similar to **2a-e**. The  $^1\text{H}$  NMR spectrum of **3c** is shown in Figure 2.5 in which the resonances associated with **3c** are denoted by  $^\circ$ . The spectrum is, as expected, similar to that given by **2c** with the exception that there is a doublet at 2.60 ppm that is assigned to the two equivalent hydrogen atoms of the chloromethyl group (which couple with the *endo* hydrogen atom). The spectrum also reveals the minor product (**9c**), denoted by  $*$ . Missing from the figure (although present in the spectrum) is a doublet at 0.3 ppm which is assigned to the *exo* methyl group of **9c**.

The  $^1\text{H}$  decoupled  $^{13}\text{C}$  NMR spectrum of **3c** is shown in Figure 2.6. Similar to that observed in the  $^1\text{H}$  NMR spectrum, there is a pattern of decreasing chemical shifts of the cyclohexadienyl ring carbon atoms (B, D, E, F) towards the  $\text{sp}^3$  hybridized carbon atom of the ring. In addition, resonances due to the impurity **9c** (denoted by  $*$ ) can be seen.

Infrared spectra of the halomethyl complexes reveal the P-F stretching frequency at  $\sim 840\text{ cm}^{-1}$  associated with the hexafluorophosphate anion and, in the case of **3c** and **4c**, show no absorptions near  $2800\text{ cm}^{-1}$ , suggesting that the  $-\text{CH}_2\text{X}$  fragment adds in an *exo* fashion.

In addition to spectroscopic characterization, **3c** and

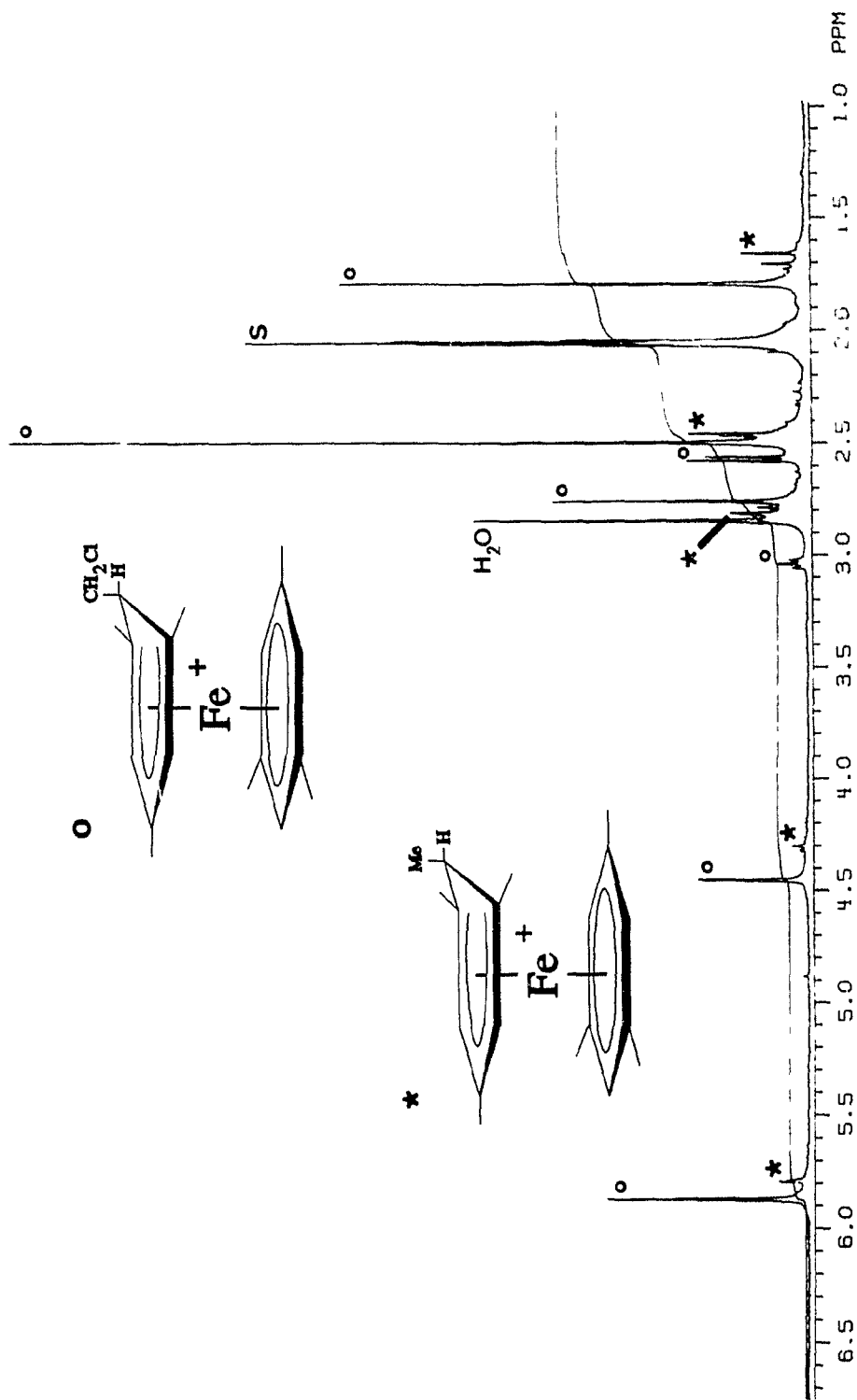


Figure 2.5  $^1\text{H}$  NMR Spectrum of  $[(\text{CH}_2\text{Cl-1,3,5-C}_6\text{H}_3\text{Me}_3)\text{Fe}]\text{PF}_6$ , 3c.

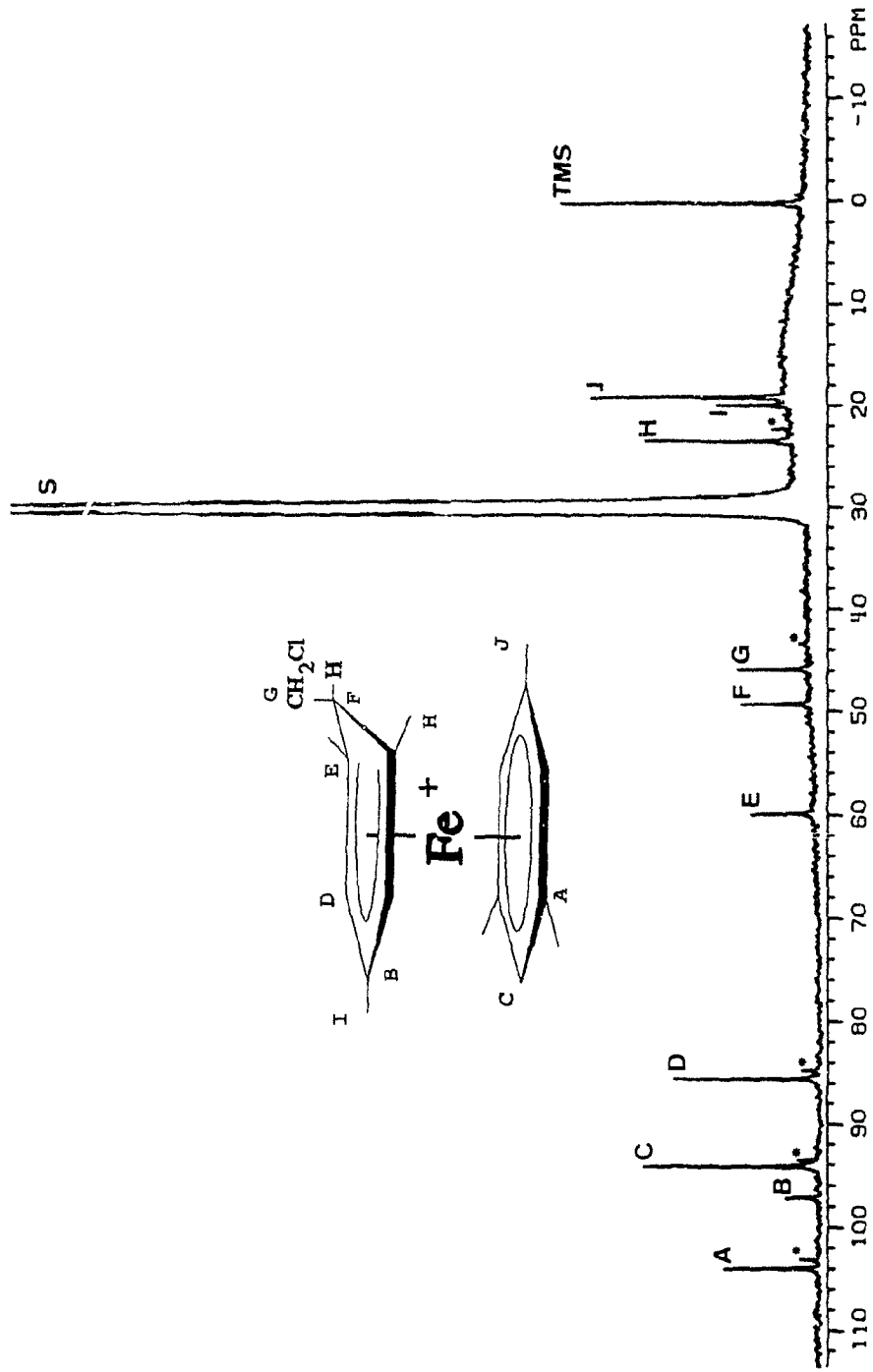
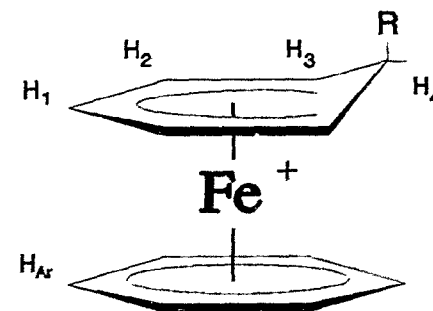


Figure 2.6  $^{13}\text{C}$  NMR Spectrum of  $[(\text{CH}_2\text{Cl}-1,3,5\text{-C}_6\text{H}_3\text{Me}_3)\text{Fe}]\text{PF}_6$ , **3c**.

**Table 2.4**  $^1\text{H}$  NMR Chemical Shifts (ppm) of the Ring and Halomethyl Fragment Hydrogen Atoms of  $[(\text{CH}_2\text{X}-1,3,5-\text{C}_6\text{H}_3\text{Me}_3)(1,3,5-\text{C}_6\text{H}_3\text{Me}_3)\text{Fe}]\text{PF}_6$  ( $\text{X} = \text{Cl}, \text{Br}$ ).<sup>‡</sup>

<u>Complex</u>	<u>Complex #</u>	<u>H<sub>Ar</sub></u>	<u>H<sub>1</sub></u>	<u>H<sub>2</sub></u>	<u>H<sub>3</sub></u>	<u>H<sub>4</sub></u>	<u>R</u>
$[(\text{CH}_2\text{Cl}-\text{C}_6\text{H}_3\text{Me}_3)(\text{C}_6\text{H}_3\text{Me}_3)\text{Fe}]\text{PF}_6$	<b>3c</b>	5.87s	-	4.45s	-	3.03t	2.60d
$[(\text{CH}_2\text{Br}-\text{C}_6\text{H}_3\text{Me}_3)(\text{C}_6\text{H}_3\text{Me}_3)\text{Fe}]\text{PF}_6$	<b>4c</b>	5.88s	-	4.46s	-	3.05t	2.09d

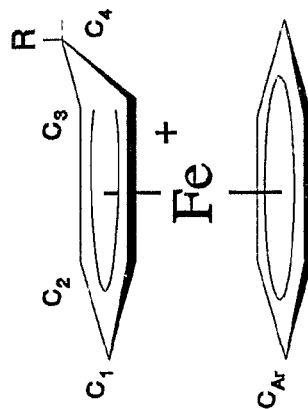
<sup>‡</sup> Acetone- $\text{d}_6$ .



**Table 2.5**  $^{13}\text{C}$  NMR Chemical Shifts (ppm) of the Ring and Halomethyl Fragment Carbon Atoms of  $[(\text{CH}_2\text{X}-\text{C}_6\text{H}_n\text{Me}_{6-n})(\text{C}_6\text{H}_3\text{Me}_3)\text{Fe}] \text{PF}_6$  ( $\text{X} = \text{Cl}, \text{Br}; n = 0, 3$ ).<sup>†</sup>

Complex	Complex #	$\text{C}_{\text{Ar}}$	$\text{C}_1$	$\text{C}_2$	$\text{C}_3$	$\text{C}_4$	R
$[(\text{CH}_2\text{Cl}-\text{C}_6\text{H}_3\text{Me}_3)(\text{C}_6\text{H}_3\text{Me}_3)\text{Fe}] \text{PF}_6$	<b>3c</b>	103.8s 94.0d	97.0s	85.4d	59.7s	49.1d	45.7t
$[(\text{CH}_2\text{Br}-\text{C}_6\text{H}_3\text{Me}_3)(\text{C}_6\text{H}_3\text{Me}_3)\text{Fe}] \text{PF}_6$	<b>4c</b>	103.8s 93.9d	97.5s	85.1d	60.2s	48.7d	33.2t
$[(\text{CH}_2\text{Cl}-\text{C}_6\text{Me}_6)(\text{C}_6\text{Me}_6)\text{Fe}] \text{PF}_6$	<b>3e</b>	101.5s	92.3s	93.4s	53.5s	45.5s	52.6t
$[(\text{CH}_2\text{Br}-\text{C}_6\text{Me}_6)(\text{C}_6\text{Me}_6)\text{Fe}] \text{PF}_6$	<b>4e</b>	101.6s	92.4s	93.3s	52.8s	44.7s	42.4t

<sup>†</sup> Acetone- $\text{d}_6$ .



**3e** have been characterized by X-ray crystallography\*. Data collection and refinement parameters, final fractional coordinates, bond distances and angles, and least squares best planes calculations for **3c** and **3e** are given in Tables A12, A13, A14 and A15; and A16, A17, A18, and A19; respectively.

The structure of **3c**, shown in Figure 2.7, is similar to **2c**. The two  $\pi$ -bonded ligands again show the eclipsed/staggered disposition of the ring and substituent carbon atoms. The mesitylene C<sub>6</sub> ring deviates a maximum of 0.06(1) Å from planarity with an average C-C bond length of 1.40(3) Å. The average Fe-C and Fe-C<sub>6</sub> plane distances are 2.11(2) and 1.555(4) Å, respectively. The dienyl portion of the cyclohexadienyl ring has a maximum deviation from planarity of 0.04(1) Å and an average C-C bond distance of 1.42(1) Å. The average Fe-C bond length is 2.09(5) Å and the dienyl plane is 1.570(4) Å from the metal center. The sp<sup>3</sup> carbon atom of the cyclohexadienyl ring is 0.66(1) Å from the dienyl plane and *exo* CH<sub>2</sub>Cl<sup>-</sup> addition is confirmed from the crystallographic characterization.

**3e** is isostructural with **2e** and displays the same manifestations of steric strain. A perspective view of the

---

\* The crystal structure of **3c** was solved by Drs. Stanley Cameron and Anthony Linden at Dalhousie University using data collected on an Enraf-Nonius CAD-4 diffractometer, and the crystal structure of **3e** was solved by Dr. Peter White at the University of New Brunswick using data collected on an Enraf-Nonius CAD-4 diffractometer.

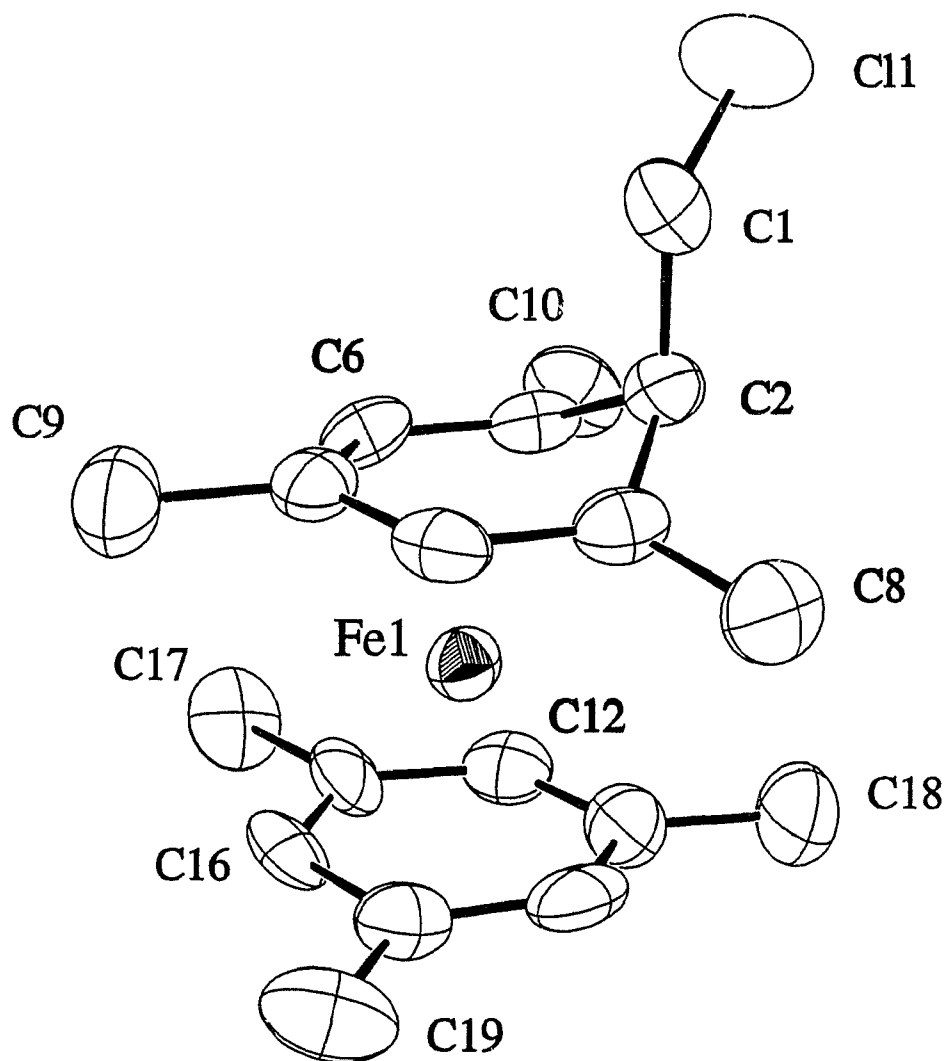


**Figure 2.7** ORTEP<sup>133</sup> Perspective View of the Cationic Portion of  $[(\text{CH}_2\text{Cl}-1,3,5-\text{C}_6\text{H}_3\text{Me}_3)(1,3,5-\text{C}_6\text{H}_3\text{Me}_3)\text{Fe}]\text{PF}_6$ , **3c**.

cation is given in Figure 2.8. The average C-C bond length of the hexamethylbenzene ring is 1.41(1) Å, which deviates by only 0.01(1) Å from planarity. Average Fe-C and Fe-C<sub>6</sub> plane distances are 2.155(9) and 1.627(4) Å, respectively. The dienyl portion of the η<sup>5</sup>-ring has a maximum deviation from planarity of 0.02(1) Å and an average C-C bond length of 1.41(1) Å. The cyclohexadienyl plane is 1.608(4) Å away from the iron atom with an average Fe-C bond length of 2.12(3) Å. The sp<sup>3</sup> carbon atom of the cyclohexadienyl ring resides 0.60(1) Å above the dienyl plane, and the structure confirms exo addition of CH<sub>2</sub>Cl<sup>-</sup>.

Reactions of **1b** with AlMe<sub>3</sub> gave products with complicated NMR spectra that indicated the presence of two or more products in approximately equal proportions. <sup>1</sup>H NMR revealed that one of the p-xylene rings had reacted and IR analysis showed intense bands centered near 840 cm<sup>-1</sup> indicative of the PF<sub>6</sub><sup>-</sup> anion. It is therefore likely that the products are the methylated and chloromethylated [(arene)(cyclohexadienyl)Fe]<sup>+</sup> complexes. Attempts to grow crystals suitable for X-ray crystallography were unsuccessful. The reactions of **1a** and **1d** with AlMe<sub>3</sub> gave NMR spectra revealing complex mixtures of products that were not investigated further.

The isolation of **9c** and the halomethylated complexes is consistent with a SET mechanism. Formation of **9c** could occur in a manner essentially the same as for formation of

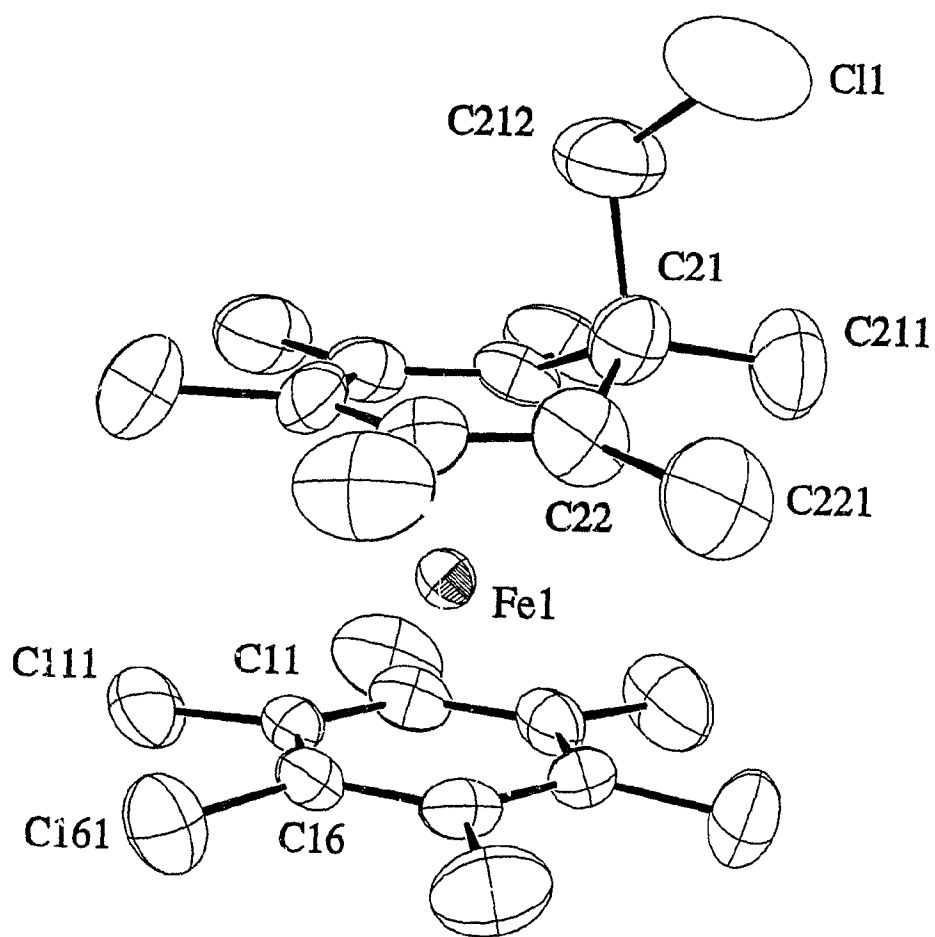
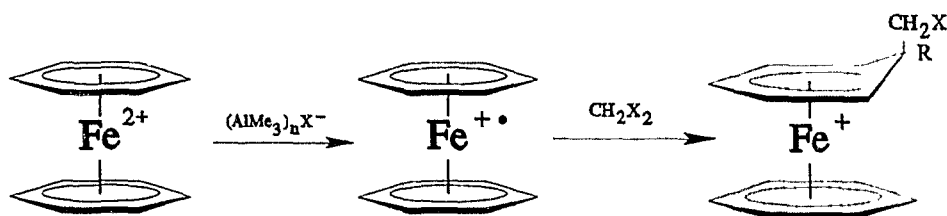


**Figure 2.8** ORTEP<sup>133</sup> Perspective View of the  
 $[(\text{CH}_2\text{Cl}-\text{C}_6\text{Me}_6)(\text{C}_6\text{Me}_6)\text{Fe}]^+$  Cation, **3e**.

2c, the only difference being that radical coupling involves a methyl-containing (rather than ethyl-containing) radical. Generation of the halomethylated moieties involves a more active role on the part of the solvent. A plausible mechanism for their formation is that  $(\text{AlMe}_3)_n\text{PF}_6^-$  reduces the  $[(\text{arene})_2\text{Fe}]^{2+}$  dication to the 19-electron radical cation  $[(\text{arene})_2\text{Fe}]^+$  which subsequently reacts with solvent molecules as indicated by scheme 2.2.



Scheme 2.2 Suggested Mechanism for the Reaction of  $\text{AlMe}_3$  with  $[(\text{arene})_2\text{Fe}]^{2+}$  Dications in  $\text{CH}_2\text{X}_2$ .

Addition of  $-\text{CH}_2\text{Cl}$  to reduced organometallic species via reaction with  $\text{CH}_2\text{Cl}_2$  and  $\text{RX}$  has already been documented<sup>69,143</sup>, and most notably, Vol'kenau has reported<sup>144</sup> that the  $19e^- (\text{C}_6\text{H}_6)(\text{C}_5\text{H}_5)\text{Fe}$  radical reacts with  $\text{CCl}_4$  to give the  $[(\text{cyclohexadienyl})(\text{cyclopentadienyl})\text{Fe}]$  complex  $[(\text{CCl}_3-\text{C}_6\text{H}_6)(\text{C}_5\text{H}_5)\text{Fe}]$ , further supporting the proposed SET mechanism.

In summary, it is apparent from the present study that

$R^-$  addition to  $[(\text{arene})_2\text{Fe}]^{2+}$  dications to yield  $[(\text{arene})(\text{cyclohexadienyl})\text{Fe}]^+$  complexes is not limited to  $[(1,3,5\text{-C}_6\text{H}_3\text{Me}_3)_2\text{Fe}]^{2+}$  and can be achieved in a facile, one-step, high yield process. The synthesis of **3c**, **3e**, **4c**, and **4e** is also significant as further functionalization of  $[(\text{arene})(\text{cyclohexadienyl})\text{Fe}]^+$  cations is feasible via the  $-\text{CH}_2\text{X}$  moiety. For example, metathesis of  $X^-$  in these complexes could provide a route to functionalized cyclohexadienyl complexes that would not otherwise be possible due to the unavailability of suitable carbanionic reagents. Another potential mode of reactivity of the halomethylated complexes is via formation of the corresponding Grignard reagents from these cations. This would allow reaction with electrophiles.

#### 2.4 Reaction of $[(\text{arene})(\text{cyclopentadienyl})\text{Fe}]^+$ Cations with Trialkylaluminum Compounds

$[(1,3,5\text{-C}_6\text{H}_3\text{Me}_3)(\text{C}_5\text{H}_5)\text{Fe}]\text{PF}_6$  was prepared according to the procedure described by Nesmeyanov<sup>145</sup> and reacted with  $\text{AlEt}_3$  in benzene, and  $\text{AlMe}_3$  in dichloromethane. In both cases the reactions failed to produce net addition products. This observation is in keeping with the idea of SET mechanisms occurring for the reactions involving trialkylaluminum reagents. The  $(\text{AlR}_3)_n\text{PF}_6^-$  anions are presumably not capable of transferring an electron to

[(arene)(cyclopentadienyl)Fe]<sup>+</sup> complexes due to the relatively unfavourable reduction potentials<sup>141</sup> (eg. -1.30 to -1.55v vs SCE) of [(arene)(cyclopentadienyl)Fe]<sup>+</sup> cations.

When [(1,3,5-C<sub>6</sub>H<sub>3</sub>Me<sub>3</sub>)(C<sub>5</sub>H<sub>5</sub>)Fe]PF<sub>6</sub> was suspended in benzene and 4 equivalents of AlEt<sub>3</sub> added, a two-phase system was produced consisting of a dark brown salt-rich lower phase, and a pale yellow upper phase containing mostly aromatic solvent. This phenomenon, dubbed a "liquid clathrate" by Atwood, is well documented<sup>146-156</sup> for the interaction of trialkylaluminums with salts, including transitic metal arene salts<sup>99</sup>.

### Chapter 3

Reaction of  $[(\text{arene})_2\text{Fe}]^{2+}$  and  $[(\text{arene})(\text{cyclohexadienyl})\text{Fe}]^+$   
Cations with Borohydride, Alkyl lithium, and Grignard  
Reagents

### 3.1 Reaction of $[(\text{arene})_2\text{Fe}]^{2+}$ Dications with $\text{NaBH}_4$

The net addition of hydride to  $[(\text{arene})_2\text{Fe}]^{2+}$  dications is not a novel idea. Astruc has used hydride addition to  $[(\text{C}_6\text{H}_6)_2\text{Fe}]^{2+}$  and  $[(\text{C}_6\text{Me}_6)_2\text{Fe}]^{2+}$  successfully as the key first step in conversion of these arene complexes to cyclohexadienes<sup>106,107,111</sup> (Figure 3.1). The systematic

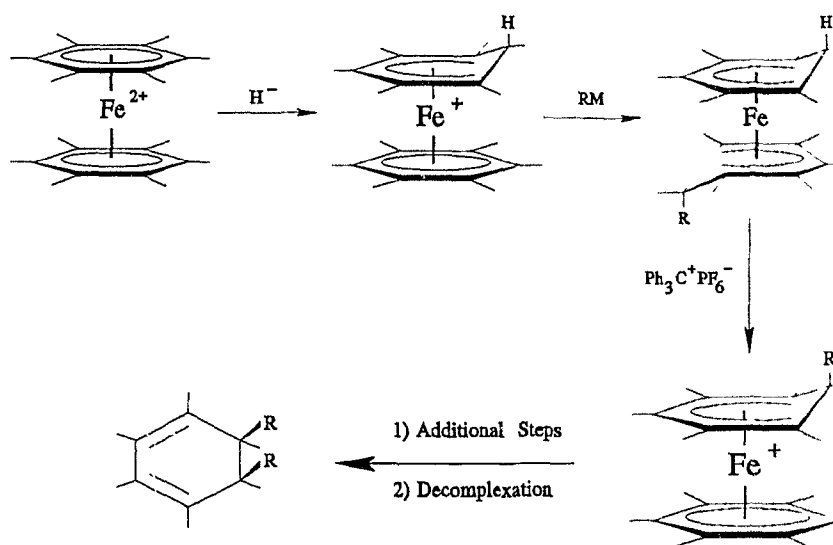
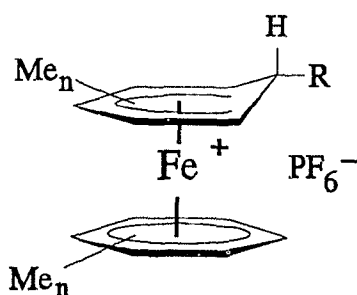


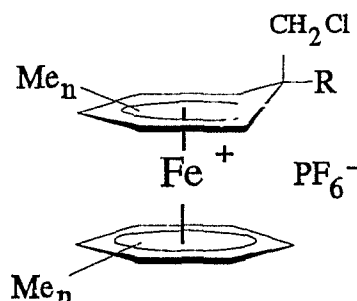
**Figure 3.1** Use of Hydride as a Protecting Group in the Conversion of  $\text{C}_6\text{Me}_6$  to a Difunctionalized Cyclohexadiene via Temporary Coordination to Iron.

synthesis and characterization of hydride addition products for a range of  $[(\text{arene})_2\text{Fe}]^{2+}$  dications, however, has not been investigated. It is in this context that the following work was completed.

The  $[(\text{arene})_2\text{Fe}]^{2+}$  dications **1a-e** were reacted with a 10-fold excess of aqueous  $\text{NaBH}_4$  in dichloromethane (since  $\text{CH}_2\text{Cl}_2$  proved to be a better solvent than tetrahydrofuran for reactions of  $[(\text{arene})_2\text{Fe}]^{2+}$  dications with trialkylaluminum compounds). In contrast to Astruc's work employing THF as solvent in which he isolated  $[(\text{arene})(\text{cyclohexadiene})\text{Fe}]$  complexes<sup>108</sup>, only monocationic  $[(\text{arene})(\text{cyclohexadienyl})\text{Fe}]^+$  complexes were formed. Furthermore, in addition to the expected monohydride adducts **5a-e** expected,  $^1\text{H}$  NMR spectroscopy revealed that the  $-\text{CH}_2\text{Cl}$  adducts **3a-e** were obtained as minor products (up to 30%) in these reactions.



- 5. (a)**  $n = 0, R = H$   
**(b)**  $n = 1, 4\text{-Me}_2, R = H$   
**(c)**  $n = 1, 3, 5\text{-Me}_3, R = H$   
**(d)**  $n = 5, R = H$   
**(e)**  $n = 6, R = \text{Me}$



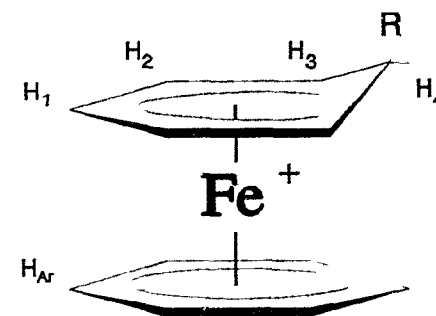
- 3. (a)**  $n = 0, R = H$   
**(b)**  $n = 1, 4\text{-Me}_2, R = H$   
**(c)**  $n = 1, 3, 5\text{-Me}_3, R = H$   
**(d)**  $n = 5, R = H$   
**(e)**  $n = 6, R = \text{Me}$

The  $^1\text{H}$  NMR chemical shifts of the ring hydrogen atoms and  $^{13}\text{C}$  NMR chemical shifts of the ring carbon atoms of **5a-e**

**Table 3.1**  $^1\text{H}$  NMR Chemical Shifts (ppm) of the Ring Hydrogen Atoms of  
 $[(\text{H-cyclohexadienyl})(\text{arene})\text{Fe}]^+$  Monocations.<sup>‡</sup>

<u>Complex</u>	<u>Complex #</u>	<u>H<sub>Ar</sub></u>	<u>H<sub>1</sub></u>	<u>H<sub>2</sub></u>	<u>H<sub>3</sub></u>	<u>H<sub>4</sub></u>	<u>R</u>
$[(\text{H-C}_6\text{H}_6)(\text{C}_6\text{H}_6)\text{Fe}]\text{PF}_6$	<b>5a</b>	6.44s	7.14t	4.98t	3.58t	2.85dt	1.10d
$[(\text{H-C}_6\text{H}_4\text{Me}_2)(\text{C}_6\text{H}_4\text{Me}_2)\text{Fe}]\text{PF}_6$	<b>5b</b>	6.38dd, 5.34dd	6.76d	4.59d	3.13d	?	1.39d
$[(\text{H-C}_6\text{H}_3\text{Me}_3)(\text{C}_6\text{H}_3\text{Me}_3)\text{Fe}]\text{PF}_6$	<b>5c</b>	5.78s	-	4.39s	-	2.59d	?
$[(\text{H-C}_6\text{HMe}_5)(\text{C}_6\text{HMe}_5)\text{Fe}]\text{PF}_6$	<b>5d</b>	5.21s	-	-	-	?	1.23d
$[(\text{H-C}_6\text{Me}_6)(\text{C}_6\text{Me}_6)\text{Fe}]\text{PF}_6$	<b>5e</b>	-	-	-	-	-	0.95q

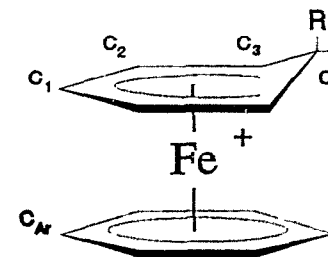
<sup>‡</sup> Acetone- $\text{d}_6$ .



**Table 3.2**  $^{13}\text{C}$  NMR Chemical Shifts (ppm) of the Ring Carbon Atoms of  
 $[(\text{H-cyclohexadienyl})(\text{arene})\text{Fe}]^+$  Monocations.<sup>‡</sup>

<u>Complex</u>	<u>Complex #</u>	<u>C<sub>Ar</sub></u>	<u>C<sub>1</sub></u>	<u>C<sub>2</sub></u>	<u>C<sub>3</sub></u>	<u>C<sub>4</sub></u>
$[(\text{H-C}_6\text{H}_6)(\text{C}_6\text{H}_6)\text{Fe}]\text{PF}_6$	<b>5a</b>	91.7u	86.5d	85.0d	40.5d	24.8t
$[(\text{H-C}_6\text{H}_4\text{Me}_2)(\text{C}_6\text{H}_4\text{Me}_2)\text{Fe}]\text{PF}_6$	<b>5b</b>	105.9s, 93.5d 89.6d	85.3d -	82.9d 102.7s	43.2d 60.8s	32.0t -
$[(\text{H-C}_6\text{H}_3\text{Me}_3)(\text{C}_6\text{H}_3\text{Me}_3)\text{Fe}]\text{PF}_6$	<b>5c</b>	103.1s, 93.4d	96.0s	86.5d	58.9s	37.8t
$[(\text{H-C}_6\text{HMe}_5)(\text{C}_6\text{HMe}_5)\text{Fe}]\text{PF}_6$	<b>5d</b>	102.9s, 101.5s, 100.2s, 91.5d	86.5s	94.4s	52.2s	41.5t
$[(\text{H-C}_6\text{Me}_6)(\text{C}_6\text{Me}_6)\text{Fe}]\text{PF}_6$	<b>5e</b>	100.8s	91.6s	95.0s	50.3s	39.1d

<sup>‡</sup> Acetone-d<sub>6</sub>.



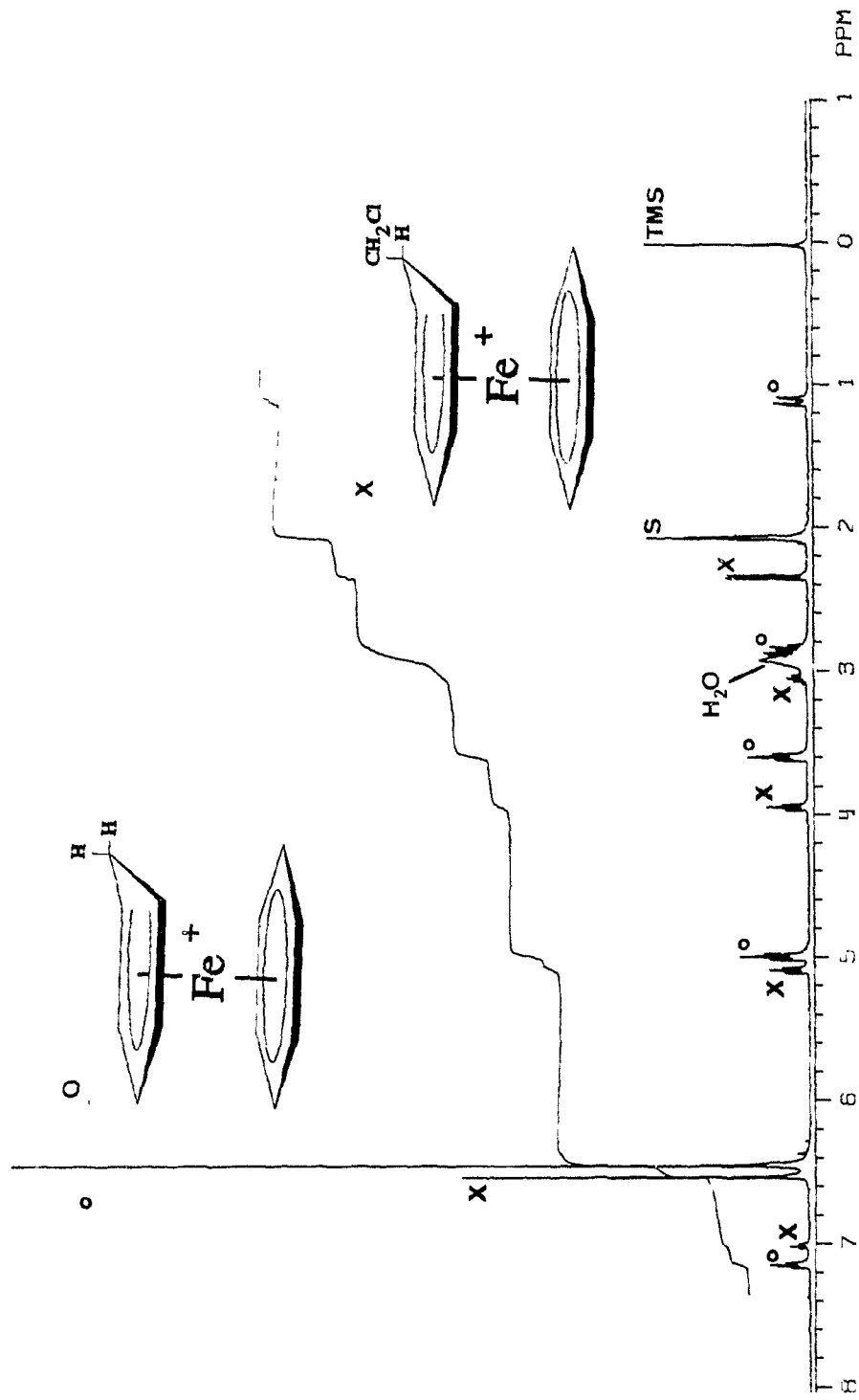


Figure 3.2  $^1\text{H}$  NMR Spectrum of  $[(\text{H-C}_6\text{H}_6)\text{Fe}]^+\text{PF}_6^-$ , 5a.

are given in Tables 3.1 and 3.2, respectively. The  $^1\text{H}$  NMR spectrum of **5a** is shown in Figure 3.2 (denoted by  $^\circ$ ). The characteristic pattern of decreasing chemical shifts associated with the cyclohexadienyl ligand are exemplified by the triplets centered at 7.14, 4.98, and 3.58 ppm and correspond to  $\text{H}_1$ ,  $\text{H}_2$ , and  $\text{H}_3$ , respectively. The observation that  $\text{H}_2$  and  $\text{H}_3$  are triplets instead of doublets of doublets reveals that the coupling constants of adjacent ring hydrogen atoms ( $\text{H}_1$  and  $\text{H}_3$  for  $\text{H}_2$ ,  $\text{H}_2$  and  $\text{H}_4$  for  $\text{H}_3$ ) are approximately equal. The singlet at 6.44 ppm is assigned to the benzene ring hydrogen atoms. The doublet of triplets pattern (distorted by  $\text{H}_2\text{O}$  resonance) is assigned to the *endo* hydrogen atom of the cyclohexadienyl ring ( $\text{H}_4$ ) and is a result of couplings with  $\text{H}_3$  and the *exo* hydrogen atom. The most shielded resonance, at 1.10 ppm, corresponds to the *exo* hydrogen atom and appears as a doublet due to coupling with  $\text{H}_4$ .

Also present in the spectrum of **5a** are peaks associated with  $[(\text{CH}_2\text{Cl}-\text{C}_6\text{H}_6)(\text{C}_6\text{H}_6)\text{Fe}]^+$ , a minor product, denoted by  $^*$ . The resonances between 7.1 and 3.8 ppm correspond to the arene and dienyl portion of the cyclohexadienyl ring ( $\text{H}_1$ ,  $\text{H}_2$ , and  $\text{H}_3$ ) and are, as expected, similar to **5a** in both chemical shift and multiplicity. The other resonances, a quintet at  $\sim 3.1$  ppm and a doublet at  $\sim 2.4$  ppm, are assigned to the *endo* cyclohexadienyl and chloromethyl hydrogen atoms, respectively.

One possible explanation for the formation of the  $-\text{CH}_2\text{Cl}$  adducts is activation of solvent molecules by borohydride to produce the  $\text{CH}_2\text{Cl}^-$  anion with subsequent nucleophilic addition to an arene ring of  $[(\text{arene})_2\text{Fe}]^{2+}$ . We have, however, not found any experimental evidence to suggest that such a mechanism is occurring. A more plausible mechanism is a SET mechanism similar to that suggested in Scheme 2.2, with the exception that borohydride reduces the transition metal moiety.

There is both experimental evidence as well as precedent in the literature to support such a claim. Intense purple or black solutions are formed upon addition of  $\text{NaBH}_4(\text{aq})$  to the reaction mixture, suggestive of the  $19e^-$  organometallic complexes. Additionally, yields of **5a-e** increased with degree of substitution of the arene ring. These observations are more consistent with SET than with a nucleophilic attack, for reasons discussed in Section 2.1. In the case of **5a**, a shiny metallic coating is deposited upon the walls of the reaction vessel suggesting that  $\text{Fe(II)}$  is reduced to  $\text{Fe(0)}$  in the reaction. Furthermore, Astruc has shown<sup>110</sup> that the reaction of  $[(\text{arene})(\text{cyclopentadienyl})\text{Fe}]^+$  with  $\text{NaBH}_4$  and  $\text{LiAlH}_4$  at  $-60^\circ\text{C}$  in THF yield  $19e^-$  intermediates which were characterized by ESR and Mossbauer spectroscopy. When these solutions are allowed to warm to room temperature the net hydride addition products result.

There are, however, important inconsistencies in this evaluation. First, Astruc has claimed that reactions of  $\text{NaBH}_4$  and  $\text{LiAlH}_4$  with  $[(\text{C}_6\text{Me}_6)_2\text{Fe}]^{2+}$  in THF (which yield the arene-diene complex  $[(\text{C}_6\text{H}_2\text{Me}_6)(\text{C}_6\text{Me}_6)\text{Fe}]$ ) do not proceed by a SET mechanism but rather via hydride transfer, although he has stated that the reactions are highly solvent dependent. It is possible that by changing the solvent to  $\text{CH}_2\text{Cl}_2$  a SET mechanism is favoured. Second, double net addition of hydride to give neutral products was not observed. While the formation of only monocationic products from the reaction of  $[(\text{arene})_2\text{Fe}]^{2+}$  with trialkylaluminum reagents (Chapter 2) is consistent with a SET mechanism, double addition products might be expected from the reaction of  $[(\text{arene})_2\text{Fe}]^{2+}$  with  $\text{NaBH}_4$  (and indeed have been shown to occur under different conditions<sup>110</sup>) since  $\text{NaBH}_4$  is known<sup>110</sup> to reduce a variety of monocationic organoiron complexes with reduction potentials in the range -1.4 to -1.8 V vs. SCE. That the  $[(\text{arene})(\text{cyclohexadienyl})\text{Fe}]^+$  cations that are formed do get reduced to the  $19e^-$  complexes cannot be ruled out, however. The instability of these radicals or the conditions under which the experiment is conducted (room temperature,  $\text{CH}_2\text{Cl}_2$ , aqueous  $\text{NaBH}_4$ ) presumably precludes further net addition of either hydride or  $\text{CH}_2\text{Cl}^-$ .

### 3.2 $^1\text{H}$ and $^{13}\text{C}$ NMR Spectroscopy of $[(\text{R}-1,4-\text{C}_6\text{H}_4\text{Me}_2)(1,4-\text{C}_6\text{H}_4\text{Me}_2)\text{Fe}]^+$ Monocations

The  $^1\text{H}$  and  $^{13}\text{C}$  NMR spectra of the  $[(\text{R}-1,4-\text{C}_6\text{H}_4\text{Me}_2)(1,4-\text{C}_6\text{H}_4\text{Me}_2)\text{Fe}]^+$  ( $\text{R} = \text{H}, \text{Et}$ ) deserve additional attention due the unusual number of non-equivalent peaks and multiplicity patterns. Figure 3.3 shows the  $^1\text{H}$  NMR spectrum of  $[(\text{H}-1,4-\text{C}_6\text{H}_4\text{Me}_2)(1,4-\text{C}_6\text{H}_4\text{Me}_2)\text{Fe}]\text{PF}_6$  in the region 3.6 - 7.2 ppm. In this region we might expect to see two doublets corresponding to the ring hydrogen atoms of the cyclohexadienyl ligand (with integrations of 1 proton each) and a singlet corresponding to the four "equivalent" hydrogen atoms of the p-xylene ring. However, the p-xylene ring hydrogen atoms appear as two doublets integrated to two protons each.

The source of this unexpected multiplicity lies with the asymmetry in the cyclohexadienyl ring, which renders the complex asymmetric. The NMR spectrum of the monocation arises as a result of its intrinsic symmetry. A close analogy would be diastereotopism. In this example, the iron atom acts as a chiral center and the p-xylene ring hydrogen atoms are diastereotopic, as is shown below. It should be emphasized that this does not imply a restricted rotation about the iron-ring centroid bond, but merely reflects the different chemical environments experienced by  $\text{H}_1$  and  $\text{H}_2$  as the p-xylene ligand rotates freely about this bond. The  $^{13}\text{C}$

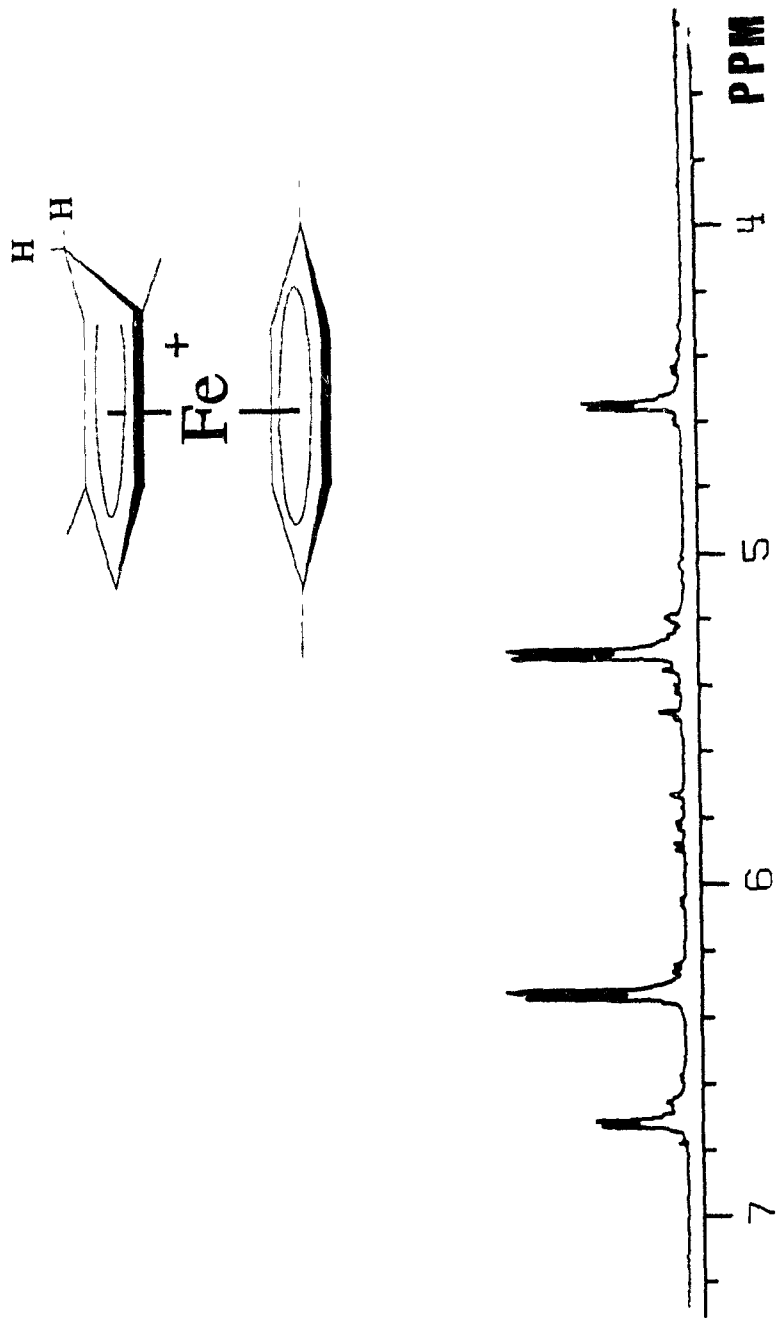
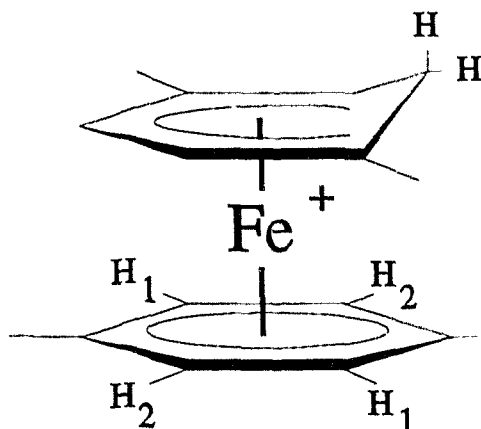


**Figure 3.3** Partial  $^1H$  NMR Spectrum of  $[(H-1,4-C_6H_4Me_2) Fe]PF_6$ , **5b**.

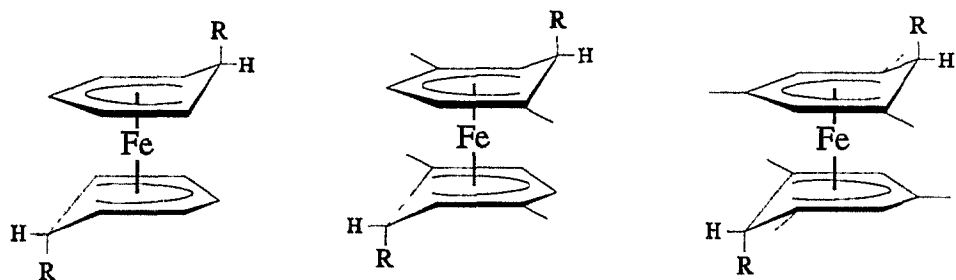


NMR spectra of these complexes are in agreement with this interpretation.

### 3.3a Double Carbanion Addition to [(arene)<sub>2</sub>Fe]<sup>2+</sup> Dications

The reaction of carbanions (organolithium and Grignard reagents) with [(arene)<sub>2</sub>Fe]<sup>2+</sup> has been investigated by Helling<sup>65,120</sup>, Astruc<sup>104,111</sup>, and Zaworotko<sup>67,68</sup>. Helling et al. showed that reaction of [(1,3,5-C<sub>6</sub>H<sub>3</sub>Me<sub>3</sub>)<sub>2</sub>Fe](PF<sub>6</sub>)<sub>2</sub> with one or two molar equivalents of RLi (R = phenyl, tert-butyl, vinyl) gives the corresponding [(arene)(cyclohexadienyl)Fe]<sup>+</sup> cations and [(cyclohexadienyl)<sub>2</sub>Fe] complexes, respectively. However, Astruc has stated<sup>111</sup> that reactions of carbanions with [(arene)<sub>2</sub>Fe]<sup>2+</sup> dications (arene ≠ mesitylene) fail to yield addition products, but rather give intractable

reduction products. Upon reinvestigation of these reactions employing dichloromethane as solvent, we find carbanions will add cleanly to  $[(\text{arene})_2\text{Fe}]^{2+}$  to give either  $[(\text{arene})(\text{cyclohexadienyl})\text{Fe}]^+$  or  $[(\text{cyclohexadienyl})_2\text{Fe}]$  complexes depending upon the degree of substitution of the arene ring. For reaction of phenyllithium (PhLi), benzylmagnesium bromide (BzMgBr), and tert-butyllithium ( $^t\text{BuLi}$ ) with  $[(\text{arene})_2\text{Fe}]^{2+}$ , where arene = benzene, para-xylene, or mesitylene, the corresponding  $[(\text{cyclohexadienyl})_2\text{Fe}]$  complexes  $[(\text{Ph}-\text{C}_6\text{H}_6)_2\text{Fe}]$ , **6a**;  $[(\text{Bz}-\text{C}_6\text{H}_6)_2\text{Fe}]$ , **7a**;  $[(^t\text{Bu}-\text{C}_6\text{H}_6)_2\text{Fe}]$ , **8a**;  $[(\text{Bz}-1,4-\text{C}_6\text{H}_4\text{Me}_2)_2\text{Fe}]$ , **7b**;  $[(^t\text{Bu}-1,4-\text{C}_6\text{H}_4\text{Me}_2)_2\text{Fe}]$ , **8b**; and  $[(\text{R}-1,3,5-\text{C}_6\text{H}_3\text{Me}_3)_2\text{Fe}]$ <sup>65-67</sup> are



**6a:** R = Ph

**7a:** R = Bz

**8a:** R =  $^t\text{Bu}$

**7b:** R = Bz

**8b:** R =  $^t\text{Bu}$

R = Ph,  $^t\text{Bu}$ , Bz

formed. For more completely alkylated  $[(\text{arene})_2\text{Fe}]^{2+}$  dications (arene = pentamethylbenzene and hexamethylbenzene) the corresponding  $[(\text{arene})(\text{cyclohexadienyl})\text{Fe}]^+$  cations are

isolated and will be discussed further in the following section.

The [(cyclohexadienyl)<sub>2</sub>Fe] complexes have been characterized by <sup>1</sup>H and <sup>13</sup>C NMR spectroscopy and resonances are tabulated in Tables 3.3 and 3.4. The chemical shifts and multiplicity patterns are typical of transition metal cyclohexadienyl complexes. The <sup>1</sup>H NMR spectrum of **8a** is shown in Figure 3.4. The spectrum reveals the 1:2:2:1 sequence of triplets (A, B, C, D), characteristic of cyclohexadienyl complexes derived from benzene. In addition the singlet (E) at ~0.6 ppm is assigned to the <sup>t</sup>Bu moiety. **7b** and **8b** are diastereomeric and exhibit temperature dependent NMR spectra that have been assigned to restricted rotation models of the complexes in solution<sup>157</sup>. Restricted rotation of pseudoferrocenes will be discussed in more detail in Section 3.5.

To confirm the structure and conformation of the [(cyclohexadienyl)<sub>2</sub>Fe] complexes, **8a** was characterized via single crystal X-ray diffraction\*. A perspective view of the crystal structure of **8a** is presented in Figure 3.5, and data collection and refinement parameters, final fractional coordinates, bond distances and angles, and least squares best planes calculations are presented in Tables A20, A21, A22, and A23, respectively.

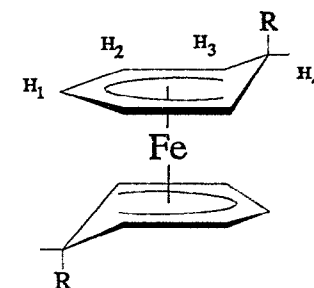
---

\* The X-ray crystal structure of **8a** was solved by Dr. Michael Zaworotko at Saint Mary's University using data collected on an Enraf-Nonius CAD-4 diffractometer at the University of Victoria by Ms. Kathy Beveridge.

**Table 3.3**  $^1\text{H}$  NMR Chemical Shifts (ppm) of the Ring Hydrogen Atoms of  
 [(cyclohexadienyl) $_2\text{Fe}$ ] Complexes.<sup>‡</sup>

Complex	Complex #	H <sub>1</sub>	H <sub>2</sub>	H <sub>3</sub>	H <sub>4</sub>	R
(Ph-C <sub>6</sub> H <sub>6</sub> ) <sub>2</sub> Fe	<b>6a</b>	4.59t	4.10t	3.12t	3.81t	7.20m
(Bz-C <sub>6</sub> H <sub>6</sub> ) <sub>2</sub> Fe	<b>7a</b>	4.67t	3.95t	2.71t	2.51qnt	7.20t, 7.10t, 7.02d, 1.76d
( <sup>t</sup> Bu-C <sub>6</sub> H <sub>6</sub> ) <sub>2</sub> Fe	<b>8a</b>	4.53t	4.14t	2.85t	2.50t	0.63s
(Et-C <sub>6</sub> H <sub>6</sub> ) (Me-C <sub>6</sub> H <sub>6</sub> ) Fe	<b>13a</b>	4.60m	3.92t	2.83t	1.27m	0.51m, 0.24d
( <sup>t</sup> Bu-C <sub>6</sub> H <sub>4</sub> Me <sub>2</sub> ) <sub>2</sub> Fe	<b>8b</b>	4.17t	3.82d	2.31d	1.27d	0.66s
(Et-C <sub>6</sub> H <sub>3</sub> Me <sub>3</sub> ) (Me-C <sub>6</sub> H <sub>3</sub> Me <sub>3</sub> ) Fe	<b>13c</b>	-	3.25s	-	2.15m	0.66m, 0.30d

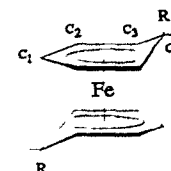
<sup>‡</sup> Benzene-d<sub>6</sub>.



**Table 3.4**  $^{13}\text{C}$  NMR Chemical Shifts (ppm) of the Ring Carbon Atoms of [(cyclohexadienyl) $_2\text{Fe}$ ] Complexes.<sup>‡</sup>

<u>Complex</u>	<u>Complex #</u>	<u>C<sub>1</sub></u>	<u>C<sub>2</sub></u>	<u>C<sub>3</sub></u>	<u>C<sub>4</sub></u>
(Ph-C <sub>6</sub> H <sub>6</sub> ) <sub>2</sub> Fe	<b>6a</b>	84.8d	77.9d	43.2d	41.2d
(Bz-C <sub>6</sub> H <sub>6</sub> ) <sub>2</sub> Fe	<b>7a</b>	83.7d	77.9d	42.3d	38.8d
( <sup>t</sup> Bu-C <sub>6</sub> H <sub>6</sub> ) <sub>2</sub> Fe	<b>8a</b>	85.6d	75.9d	48.0d	42.8d
( <sup>t</sup> Bu-C <sub>6</sub> H <sub>4</sub> Me <sub>2</sub> ) <sub>2</sub> Fe	<b>8b</b>	87.6d	80.1d	54.1s	38.7d
		-	75.5s	53.5s	36.9d
		-	-	52.3d	-
		-	-	43.7d	-
(Et-C <sub>6</sub> H <sub>3</sub> Me <sub>3</sub> )(Me-C <sub>6</sub> H <sub>3</sub> Me <sub>3</sub> )Fe	<b>13c</b>	84.5s	87.9d,br	52.0s,br	49.7d
		-	-	50.8s,br	42.8d

<sup>‡</sup> Benzene-d<sub>6</sub>.



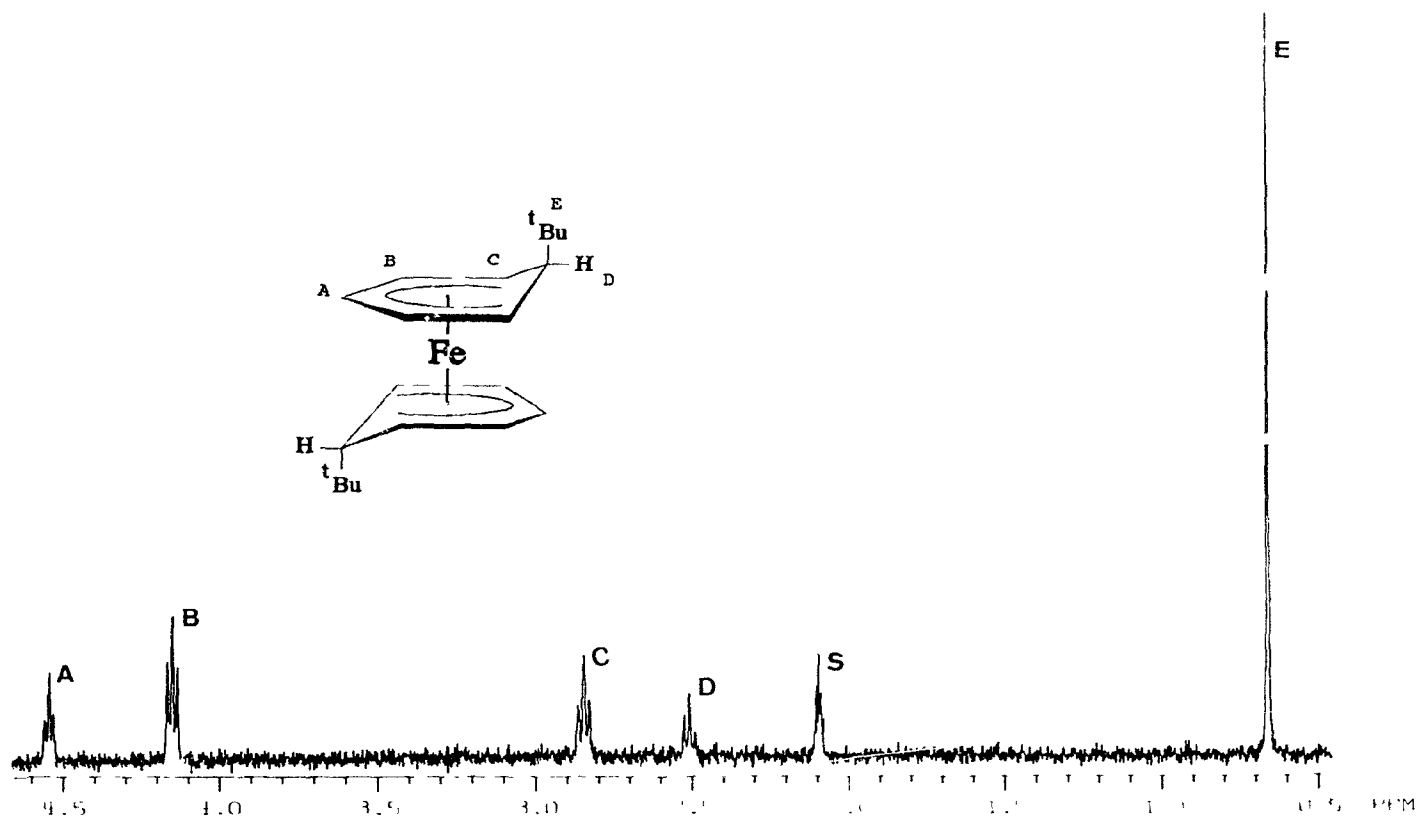


Figure 3.4  $^1\text{H}$  NMR Spectrum of  $[(^t\text{Bu-C}_6\text{H}_6)_2\text{Fe}]$ , **8a**.

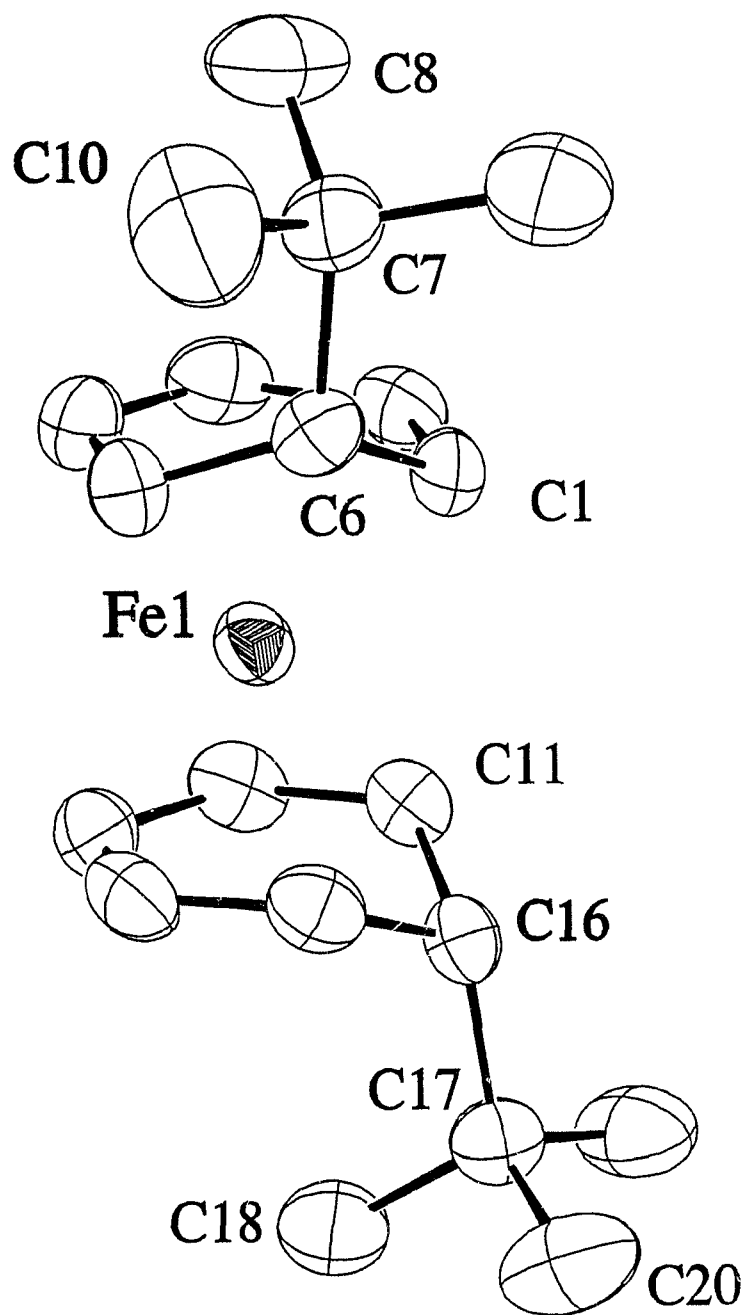


Figure 3.5 ORTEP<sup>133</sup> Perspective View of [<sup>t</sup>Bu-C<sub>6</sub>H<sub>6</sub>]<sub>2</sub>Fe, 8a.

**8a** crystallizes in the triclinic space group P1 with two independent molecules in the asymmetric unit. The average Fe-C and Fe-dienyl plane distances are 2.06(3) Å and 1.556(3) Å, respectively. An interesting feature of this molecule is the gauche-eclipsed conformation adopted by the two cyclohexadienyl ligands. The twist angle between the rings is 59.5° and 57.5° for the two molecules, based on a syn-eclipsed conformation = 0° and an anti-eclipsed conformation = 180° (Figure 3.6). Since steric effects are

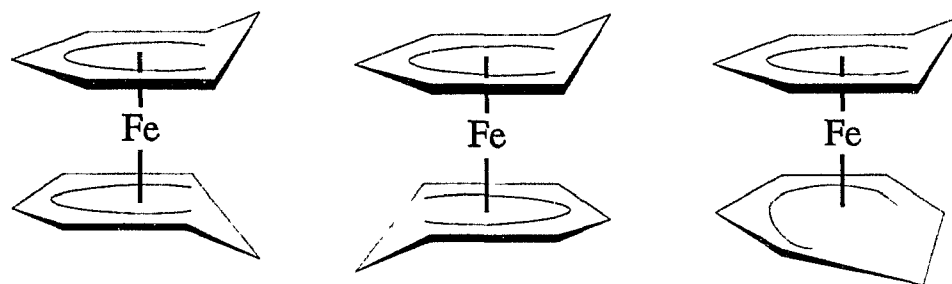


Figure 3.6 Syn-eclipsed, Anti-eclipsed, and Gauche-eclipsed Conformations of Pseudoferrocenes.

minimized with the absence of dienyl methyl groups, the energetically preferred conformation of the pseudoferrocene appears to be gauche-eclipsed rather than anti-eclipsed in which the two <sup>t</sup>Bu groups would be as far apart as possible. This result is in agreement with X-ray structural observations and EHMO calculations which predict energy minima at ~60° (Figure 3.7) on the related

[(pentadienyl)<sub>2</sub>Fe] complexes investigated by Ernst<sup>158</sup>.

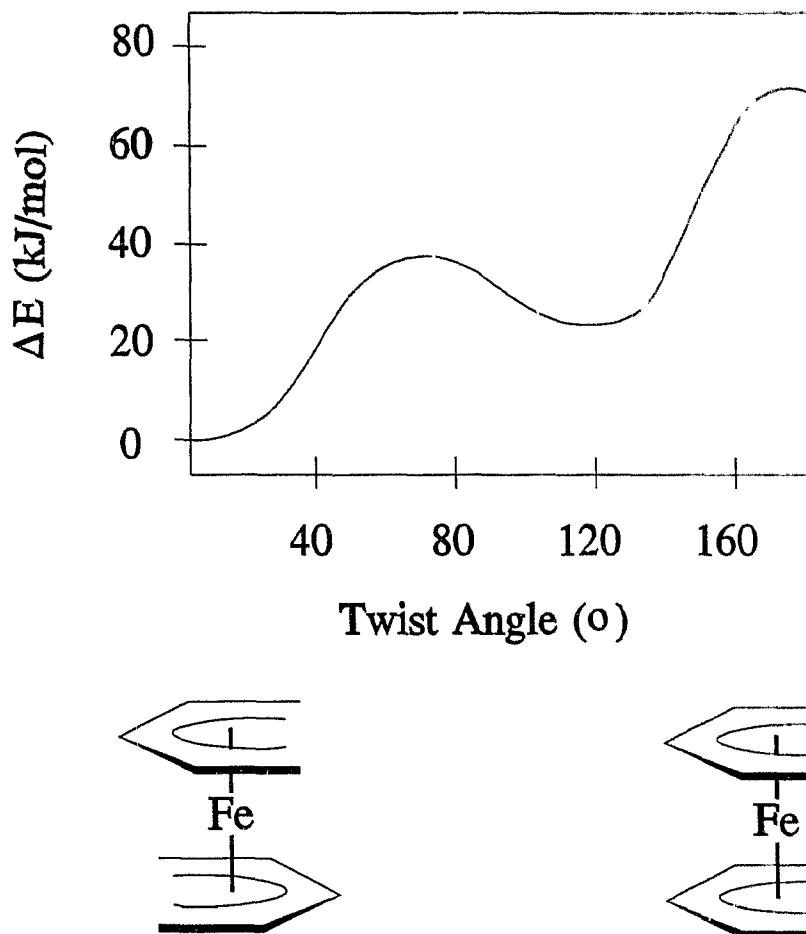


Figure 3.7 Calculated Rotational Barrier of Dipentadienyliron(II).

Astruc has shown that carbanions add to the cyclohexadienyl ring of [(arene)(cyclohexadienyl)Fe]<sup>+</sup> cations to yield [(arene)(cyclohexadiene)Fe] complexes<sup>106</sup> (Figure 3.7). In doing so, the rules for nucleophilic

addition to coordinated polyenes set down by Davies, Green, and Mingos<sup>4</sup> are violated. Astruc has attributed the formation of the pseudoferrocene complexes synthesized by Helling to the 1,3,5- disposition of the methyl groups in the starting arene complex. In addition, he has explained<sup>108</sup> the reaction of hydride with  $[(C_6H_6)_2Fe]^{2+}$  to give  $[(C_6H_8)(C_6H_6)Fe]$  and not  $[(C_6H_7)_2Fe]$  as being a result of frontier orbital control rather than charge control (necessary to invoke the Davies, Green, and Mingos rules). We find, however, that under different conditions in one-step reactions, only  $[(cyclohexadienyl)_2Fe]$  products are isolated.

Astruc has recently claimed<sup>104</sup> that the reaction between  $[(1,4-C_6H_4Me_2)_2Fe]^{2+}$  and PhLi in THF yields the arene-diene complex, based on a 60 MHz <sup>1</sup>H NMR spectrum of a decomposing solution. Our own investigation of this reaction in CH<sub>2</sub>Cl<sub>2</sub> suggests from NMR data that at least two products are formed and at least one of the products is unstable, decomposing in solution. We have been unable to identify the products, however, it is possible that both the  $[(cyclohexadienyl)_2Fe]$  and  $[(arene)(cyclohexadiene)Fe]$  complexes are produced.

In terms of conversion of a coordinated arene to a stereospecifically difunctionalized cyclohexadiene, the formation of  $[(cyclohexadienyl)_2Fe]$  complexes from the reactions of carbanions with  $[(arene)_2Fe]^{2+}$  dications is

discouraging. However, this should not lessen the significance of the pseudoferrocene molecules.

Pseudoferrocenes are a relatively new and unexplored area of organometallic chemistry and, as the name implies, analogues of one of the most widely recognized and studied organometallic compounds, ferrocene. It is possible that the diverse chemistry of ferrocene can be applied to pseudoferrocenes.

In addition, [(cyclohexadienyl)<sub>2</sub>Fe] complexes have the potential to be the key intermediates in functionalization of aromatic hydrocarbons. For example, decomplexation of the cyclohexadienyl ligand with *endo* hydride removal could yield the substituted aromatic (a procedure that has been accomplished for other metal-cyclohexadienyl complexes<sup>65,100,103,114,116-120</sup>). Decomplexation of cyclohexadienyl moieties will be discussed in Section 3.4.

Alternatively, *endo* hydride removal without decomplexation could yield [(arene)<sub>2</sub>Fe]<sup>2+</sup> dications that are not accessible by conventional routes. We can envision a procedure whereby with successive net carbanion addition and *endo* hydride removal steps we could synthesize a target molecule by choosing desired carbanions. When we also consider the conformational effect of complexation to a metal there is the potential to control, not only the choice of functionalities, but also the three dimensional shape of the molecule; an approach that is becoming more and more

important in chemistry with respect to molecular recognition and "unnatural" product syntheses.

### 3.3b Single Carbanion Addition to [(arene)<sub>2</sub>Fe]<sup>2+</sup> Dications

Reaction of excess MeLi, BzMgBr, and <sup>t</sup>BuLi with [(C<sub>6</sub>HMe<sub>5</sub>)<sub>2</sub>Fe](PF<sub>6</sub>)<sub>2</sub> and [(C<sub>6</sub>Me<sub>6</sub>)<sub>2</sub>Fe](PF<sub>6</sub>)<sub>2</sub> were conducted employing the same conditions utilized for reaction of the [(C<sub>6</sub>H<sub>6-n</sub>Me<sub>n</sub>)<sub>2</sub>Fe]<sup>2+</sup> (n = 0, 2, 3) dications discussed in the previous section. Single net addition of R<sup>-</sup> occurred yielding [(R-C<sub>6</sub>HMe<sub>5</sub>)(C<sub>6</sub>HMe<sub>5</sub>)Fe]PF<sub>6</sub> (R = Me, **9d**; Bz, **10d**; <sup>t</sup>Bu, **11d**) and [(R-C<sub>6</sub>Me<sub>6</sub>)(C<sub>6</sub>Me<sub>6</sub>)Fe]PF<sub>6</sub> (R = Me, **9e**; Bz, **10e**). The products were characterized by <sup>1</sup>H and <sup>13</sup>C NMR spectroscopy and infrared spectrophotometry and spectra are in agreement with the proposed structures. No double addition products were isolated. Minor products were observed via NMR spectroscopy and are believed to be complexes derived from net CH<sub>2</sub>Cl<sup>-</sup> addition. In the reaction of <sup>t</sup>BuLi with [(C<sub>6</sub>Me<sub>6</sub>)<sub>2</sub>Fe](PF<sub>6</sub>)<sub>2</sub>, <sup>1</sup>H NMR revealed a complex mixture of products in which at least two major products were formed in approximately equal ratios. One set of resonances was identified as **3e**, and the other is consistent with what one would expect for [(<sup>t</sup>Bu-C<sub>6</sub>Me<sub>6</sub>)(C<sub>6</sub>Me<sub>6</sub>)Fe]<sup>+</sup>. The spectrum, however, could not be fully assigned and the reaction was not investigated further.

The observation that only monocationic products are

produced from the reaction of lithium and Grignard reagents with higher substituted  $[(\text{arene})_2\text{Fe}]^{2+}$  dications (arene =  $\text{C}_6\text{HMe}_5$ ,  $\text{C}_6\text{Me}_6$ ) reas neutral  $[(\text{cyclohexadienyl})_2\text{Fe}]$  complexes are formed with less substituted  $[(\text{arene})_2\text{Fe}]^{2+}$  dications (arene =  $\text{C}_6\text{H}_6$ ,  $1,4\text{-C}_6\text{H}_4\text{Me}_2$ ,  $1,3,5\text{-C}_6\text{H}_3\text{Me}_3$ ) is attributed to steric effects. The three pseudoferrocene complexes that have been crystallographically characterized, **8a**,  $[(^t\text{Bu-}1,3,5\text{-C}_6\text{H}_3\text{Me}_3)_2\text{Fe}]^{159}$ , and  $[(\text{Ph-}1,3,5\text{-C}_6\text{H}_3\text{Me}_3)_2\text{Fe}]^{67}$ , adopt a gauche-eclipsed conformation in which the twist angle of the cyclohexadienyl rings is  $\sim 60^\circ$ . In this conformation the steric pressure between the staggered methyl groups on opposing rings (except **8a**) is minimized. This is particularly relevant since methyl substituents in the 1- and 5-position of a cyclohexadienyl ring point out of the dienyl plane toward the iron atom in direct proportion to the upward angle of the  $\text{sp}^3$  carbon atom of the ring, thereby increasing steric repulsion between methyl groups<sup>67</sup>. Pseudoferrocenes derived from **1d** or **1e** would have their 1- or 5-Me groups pointing toward methyl groups on the opposing ring (instead of hydrogen atoms) in a gauche-eclipsed conformation. Presumably this unfavourable steric interaction precludes their formation.

Finally, the formation of minor products derived from net  $\text{CH}_2\text{Cl}^-$  addition to a single arene ring of **1d** and **1e** in reactions with Grignard and lithium reagents suggests that a SET transfer mechanism plays a role in product formation or

is a competing reaction. As was discussed in Chapter 2, these products would likely be formed if the  $19e^-$  organometallic radical is present in solution.

### 3.4 Decomplexation of Cyclohexadienyl Complexes

As was discussed in Chapter 1 an important synthetic application of net carbanion addition to transition metal arene complexes is decomplexation and conversion of the cyclohexadienyl moieties to functionalized aromatics. A number of workers have successfully converted metal-cyclohexadienyl complexes to substituted aromatics using oxidizing reagents such as:  $I_2$ <sup>114</sup>, Jones' reagent ( $CrO_3$ ,  $H_2SO_4$ ,  $H_2O$ )<sup>103,119</sup>,  $Ce^{IV}$ <sup>65,100,114,120</sup>,  $KMnO_4$ <sup>65</sup>, and 2,3-dichloro-5,6-dicyanoquinone (DDQ)<sup>79,136,138</sup>, as well as subjecting the cyclohexadienyl complexes to pyrolysis.

Particularly relevant in this context are  $[(cyclohexadienyl)_2Fe]$  compounds for a number of reasons: they are inexpensive to prepare; they can be synthesized in high yield; and they possess two cyclohexadienyl ligands. We have therefore investigated the reactions of two of the pseudoferrocenes discussed in Section 3.3a with various oxidizing reagents and pyrolysis.

**7a** and **7b** were reacted with the following oxidizing reagents:  $Br_2$ ,  $Ce^{IV}$ , DDQ,  $I_2$ ,  $KMnO_4$ , Jones' reagent, and  $HCl(g)$ ; as well as being subjected to pyrolysis. In

reactions with  $\text{Ce}^{\text{IV}}$  and  $\text{KMnO}_4$ , the starting materials were recovered unchanged and were not investigated further. This result is surprising since Helling has reported<sup>65</sup> that reactions of  $[(\text{R}-1,3,5\text{-C}_6\text{H}_3\text{Me}_3)_2\text{Fe}]$  ( $\text{R} = \text{Ph}$ ,  $^t\text{Bu}$ , and vinyl) with  $\text{Ce}^{\text{IV}}$  and  $\text{KMnO}_4$  result in phenylmesitylene,  $^t$ butylmesitylene, and vinylmesitylene. They give few details of the reaction procedure and workup, however. In reactions of **7b** with  $\text{Br}_2$  and  $\text{I}_2$  decomposition of the pseudoferrocene gave mixtures of p-xylene and  $\text{C}_6\text{H}_5\text{CH}_2\text{X}$  ( $\text{X} = \text{Br}$ ,  $\text{I}$ ) and were not investigated further.

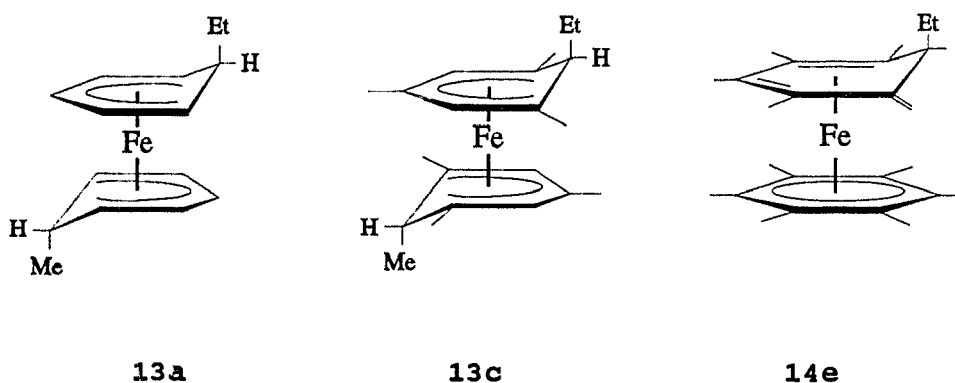
Reaction with  $\text{HCl}$ ,  $\text{DDQ}$ , and pyrolysis, however, after workup yielded oils or liquids identified as diphenylmethane,  $\text{C}_6\text{H}_5\text{-CH}_2\text{-C}_6\text{H}_5$ , **12a** (from **7a**); and 1-benzyl-2,5-dimethylbenzene,  $\text{C}_6\text{H}_3\text{Me}_2\text{-CH}_2\text{-C}_6\text{H}_5$ , **12b** (from **7b**); based upon their  $^1\text{H}$  NMR spectra. Reaction of **7a** and **7b** with  $\text{HCl}$  gave the highest crude yields of **12a** (83%) and **12b** (60%). Yields from reaction with  $\text{DDQ}$  were reduced (55% of **12a** and 43% of **12b**) but gave the highest purity of decomplexation products. Results from pyrolysis gave intermediate yields and purity.

Unfortunately, NMR revealed that **12a** and **12b** contained significant amounts of impurities that were not identified and attempts at purifying the compounds were only moderately successful. This may be in part due to the fact that reaction conditions were not optimized. Nevertheless, the high yields of products that were obtained are encouraging

and serve to emphasize the synthetic potential of pseudoferrocenes.

### 3.5 Reaction of [(arene)(cyclohexadienyl)Fe]<sup>+</sup> Monocations with Methylithium

Reactions of the [(Et-cyclohexadienyl)(arene)Fe]<sup>+</sup> complexes **2a**, **2c**, and **2e** with methylithium were investigated. Two classes of reaction were observed: (1) net addition of Me<sup>-</sup> to the complexed arene ring of **2a** and **2c** to give the [(cyclohexadienyl)<sub>2</sub>Fe] complexes **13a** and **13c**, respectively; (2) proton abstraction from a methyl group at carbon 1- or 5- of the cyclohexadienyl ring of **2e** to yield a triene complex **14e**, which contains an exocyclic double bond.



The exocyclic double bond is reactive and **14e** slowly reverts to **2d** in air, presumably via reaction with water vapour.

**13a** and **13c** were characterized by <sup>1</sup>H and <sup>13</sup>C NMR spectroscopy and the ring carbon and hydrogen atom

resonances are presented in Tables 3.4 and 3.5. The room temperature  $^{13}\text{C}$  NMR spectrum of **12c** warrants additional discussion due to the fluxional behaviour of the complex. Helling and Braitsch first demonstrated<sup>66</sup> that the  $^1\text{H}$  NMR spectra of  $[(\text{R}-1,3,5\text{-C}_6\text{H}_3\text{Me}_3)_2\text{Fe}]$  ( $\text{R} = \text{Ph}, \text{tBu}$ ) exhibit temperature dependence. They suggested that their results in no way implied a restricted rotation about the iron-cyclohexadienyl ring axis, because the molecule could not adopt an orientation that would account for the low temperature spectra. However, the validity of this conclusion must be questioned in light of the crystal structure of  $[(\text{tBu}-1,3,5\text{-C}_6\text{H}_3\text{Me}_3)_2\text{Fe}]$  published<sup>159</sup> two years later. The molecule adopts a solid state conformation (Figure 3.8) in which the two rings are gauche-eclipsed. If

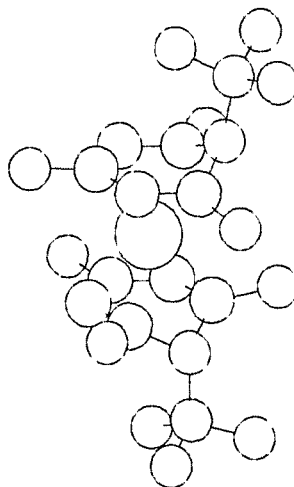


**Figure 3.8** Perspective View of Bis( $\eta^5$ -exo-6-tert-butyl-1,3,5-trimethylcyclohexadienyl) iron(II).

there was indeed restricted rotation, the substituent protons of carbon atoms 2, 4, 7, and 9 would be expected to be influenced by fluxionality. This is exactly what is observed in the low temperature spectrum of the molecule.

In light of this assessment we can presume that the unexpected room temperature  $^{13}\text{C}$  NMR of **13c** (Figure 3.9) is a result of fluxionality. The peaks labelled A, B, and C have been assigned to the correspondingly labelled atoms in the figure. The  $^{13}\text{C}$  NMR chemical shifts of these carbon atoms would be expected to be affected by a "freezing out" of the molecule since the atoms would be chemically non-equivalent in a gauche-eclipsed conformation. Therefore, the broadness of these peaks can likely be attributed to the beginning of coalescence of the peaks predicted by a restricted rotation model. This assessment is borne out by the variable temperature spectra of analogous pseudoferrocenes<sup>67,157</sup> and solid state conformation of **8a**.

The formation of **13c** is not unexpected since it has been shown<sup>65,67</sup> that reaction of **1c** with 2 equivalents of alkyllithium reagents yield  $[(\text{cyclohexadienyl})_2\text{Fe}]$  complexes. The net addition of  $\text{Me}^-$  to the arene ring of **2a** is also expected as it obeys the Davies, Green and Mingos rules.

**14e** was characterized by  $^1\text{H}$  and  $^{13}\text{C}$  NMR spectroscopy which showed resonances and multiplet patterns in agreement with the proposed structure. Additionally, crystals of the

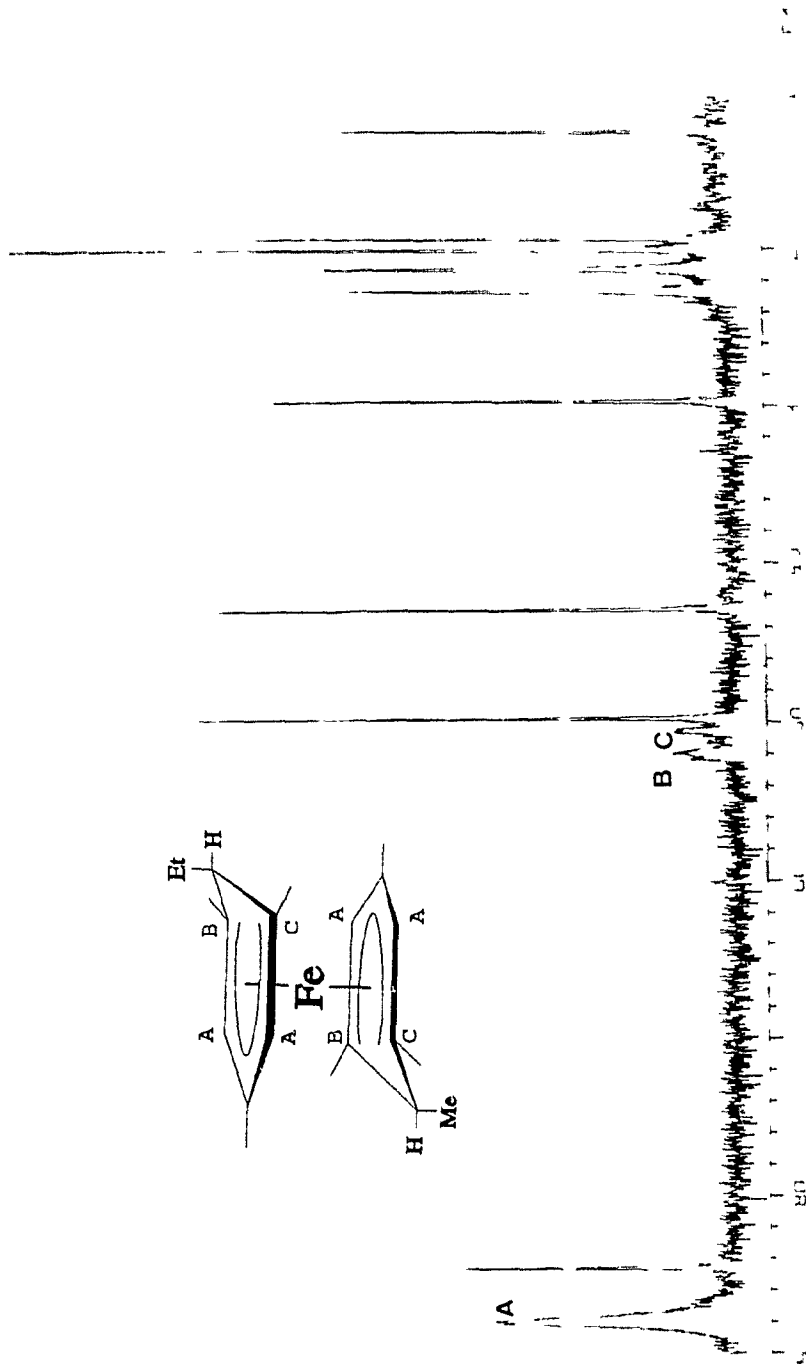


**Figure 3.9**  $^{13}\text{C}$  NMR Spectrum of  $[(\text{Et-1,3,5-C}_6\text{H}_3\text{Me}_3)\text{Fe}]$ , **12c**.

complex were obtained and submitted for X-ray crystallographic analysis but the structure could not be determined accurately due to crystal disorder. This disorder is attributed to two enantiomers being present in the crystal, however, the gross structure and conformation of **14e** was confirmed.

Although nucleophiles have been documented<sup>107,111</sup> to react with  $[(H-C_6Me_6)(C_6Me_6)Fe]^+$  producing  $[(R-C_6Me_6)(H-C_6Me_6)Fe]$ , the formation of molecules such as **14e** is not entirely without precedent. In fact, in the same report it was demonstrated that  $tBuO^-$  may be used to abstract  $H^+$  from the methyl group attached to carbon atoms 1- or 5- of the R-cyclohexadienyl moiety. In generation of **14e**,  $Me^-$  acts as base. The exocyclic double bonds of similar compounds are reactive towards electrophiles forming C-C, C-Si, C-P, C-Mn, C-Fe, C-Cr, C-Mo, and C-halogen bonds<sup>160</sup>, thus it should prove possible to add electrophiles to the double bond of the triene complex. Successive proton abstraction and electrophilic addition steps could therefore provide a means of selectively functionalizing the  $C_6$  ring.

## Chapter 4

Synthesis of [(arene)(arene')Fe]<sup>2+</sup> Dications and Reaction  
with Borohydride, Triethylborohydride, and Carbanions

#### 4.1 Synthesis of [(arene)(arene')Fe]<sup>2+</sup> Dications

As was demonstrated in Chapter 3, net addition of R<sup>-</sup> to [(arene)<sub>2</sub>Fe]<sup>2+</sup> dications (arene = benzene, p-xylene, mesitylene) produces [(cyclohexadienyl)<sub>2</sub>Fe] complexes according to the rules of Davies, Green, and Mingos rather than [(arene)(cyclohexadiene)Fe] complexes (Figure 4.1).

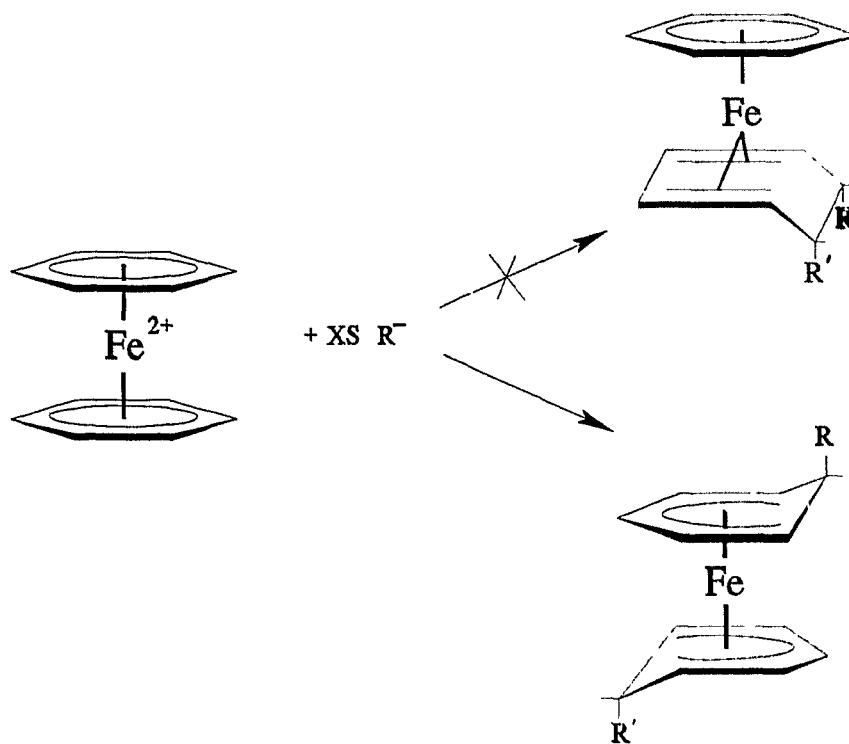
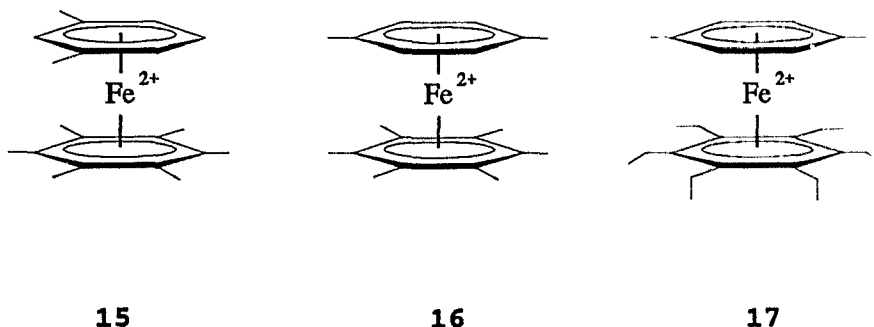


**Figure 4.1** Reaction of [(arene)<sub>2</sub>Fe]<sup>2+</sup> Dications with Excess Carbanion.

In an attempt to control the regioselectivity of the second net R<sup>-</sup> addition, mixed-arene salts with the general formula



$\text{C}_6\text{H}_4\text{Me}_2(\text{C}_6\text{Me}_6)\text{Fe}]^{2+}$ , **15**, and  $[(1,4\text{-C}_6\text{H}_4\text{Me}_2)(\text{C}_6\text{Me}_6)\text{Fe}]^{2+}$ , **16**, were synthesized and precipitated from aqueous solution as their hexafluorophosphate salts. A slightly different procedure was used to synthesize  $[(1,4\text{-C}_6\text{H}_4\text{Me}_2)(\text{C}_6\text{Et}_6)\text{Fe}]^{2+}$ , **17**, in that an approximately 2:1 ratio of  $\text{C}_6\text{Et}_6$  to  $\text{FeCl}_3$  was employed. The reactions afforded mixtures of the  $[(\text{arene})(\text{arene}')\text{Fe}](\text{PF}_6)_2$  and  $[(\text{arene})_2\text{Fe}](\text{PF}_6)_2$  complexes. Fortunately, the mixed-arene salts are the less soluble of the products and could be isolated by fractional recrystallization from acetone/water in yields of 26-51%. It should be pointed out that this synthesis is not general since it only works for certain combinations of arene molecules. For example, attempts to synthesize  $[(\text{arene})(\text{arene}')\text{Fe}]^{2+}$  in which benzene was one of the ligands failed. Reasons for this discrimination are unclear and a thorough investigation of different combinations of aromatic ligands was not undertaken.



The mixed-arene salts were characterized by  $^1\text{H}$  and  $^{13}\text{C}$  NMR spectroscopy and infrared spectrophotometry. The

infrared spectra showed strong absorption bands centered near  $840\text{ cm}^{-1}$  indicative of the  $\text{PF}_6^-$  anion. The  $^1\text{H}$  NMR spectrum of **17** is presented in Figure 4.2. The singlets labelled A and C (with integrations of 4 and 6 hydrogen atoms, respectively) are assigned to the ring and methyl hydrogen atoms of the p-xylene ring, respectively. The quartet labelled B and the triplet labelled D (with integrations of 12 and 18 hydrogen atoms) are assigned to the hydrogen atoms of the six equivalent ethyl substituents of the  $\text{C}_6\text{Et}_6$  ligand. Resonances due to a minor impurity (designated by  $\circ$ ) are attributed to the presence of either  $[(1,4\text{-C}_6\text{H}_4\text{Me}_2)_2\text{Fe}]^{2+}$  or uncomplexed p-xylene.

$^1\text{H}$  and  $^{13}\text{C}$  NMR data for the  $[(\text{arene})(\text{arene}')\text{Fe}]^{2+}$  complexes are presented in Tables 4.1 and 4.2. An interesting example of the way in which the electron density of the arene rings is delocalized over the whole  $[(\text{arene})_2\text{Fe}]^{2+}$  dication can be seen when the chemical shifts of **1b** and **1e** are compared with **16**. **1b** has  $^{13}\text{C}$  NMR chemical shifts of 112.0 and 94.0 ppm for the ring carbon atoms, whereas the shifts corresponding to the same carbon atoms in **16** are 111.2 and 93.6 ppm. Both resonances are shifted upfield in **16** corresponding to the increased electron density in the p-xylene ring imparted to it by the electron-rich hexamethylbenzene ligand. In comparing the  $^{13}\text{C}$  NMR shifts of the  $\text{C}_6\text{Me}_6$  ring in **1e** (104.6 ppm) with that of **16** (107.1 ppm), a downfield shift is observed corresponding to

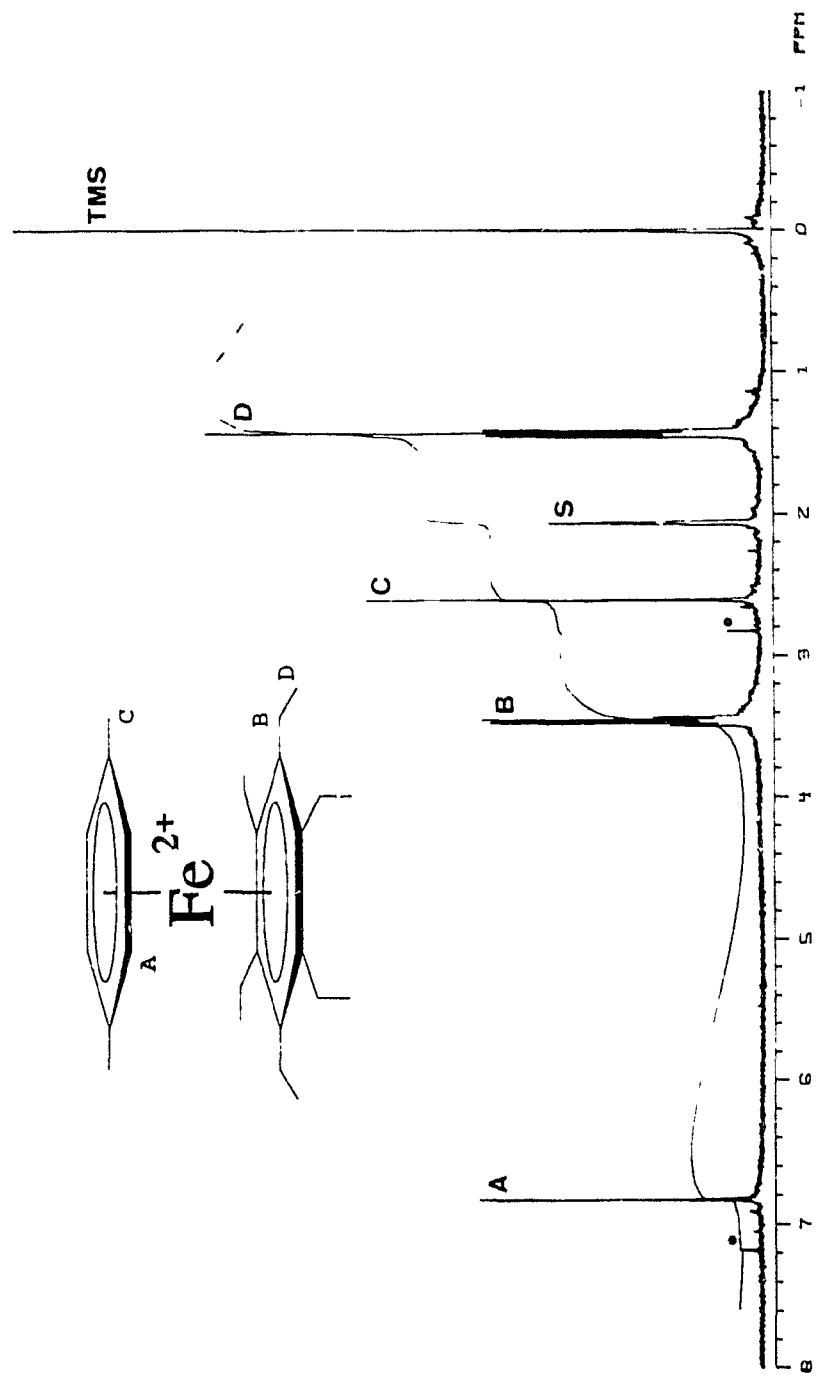


Figure 4.2 <sup>1</sup>H NMR Spectrum of [(1,4-C<sub>6</sub>H<sub>4</sub>Me<sub>2</sub>)(C<sub>6</sub>Et<sub>6</sub>)Fe](PF<sub>6</sub>)<sub>2</sub>, 16.

Table 4.1 <sup>1</sup>H NMR Chemical Shifts (ppm) of [(arene)(arene')Fe]<sup>2+</sup> Dications.†

<u>Complex</u>	<u>Complex #</u>	<u>C<sub>6</sub>H<sub>4</sub>Me<sub>2</sub> ligand</u>		<u>C<sub>6</sub>R<sub>6</sub> ligand</u>	
		<u>H<sub>Ar</sub></u>	<u>CH<sub>3</sub></u>	<u>CH<sub>3</sub></u>	<u>CH<sub>2</sub></u>
[(1,3-C <sub>6</sub> H <sub>4</sub> Me <sub>2</sub> )(C <sub>6</sub> Me <sub>6</sub> )Fe](PF <sub>6</sub> ) <sub>2</sub>	15	7.10t, 6.98d, 6.79s	2.65s	2.79s	-
[(1,4-C <sub>6</sub> H <sub>4</sub> Me <sub>2</sub> )(C <sub>6</sub> Me <sub>6</sub> )Fe](PF <sub>6</sub> ) <sub>2</sub>	16	6.89s	2.60s	2.75s	-
[(1,4-C <sub>6</sub> H <sub>4</sub> Me <sub>2</sub> )(C <sub>6</sub> Et <sub>6</sub> )Fe](PF <sub>6</sub> ) <sub>2</sub>	17	6.83s	2.60s	1.43t	3.46q

† Acetone-d<sub>6</sub>.

**Table 4.2**  $^{13}\text{C}$  NMR Chemical Shifts (ppm) of the Ring Carbon Atoms of  $[(\text{arene})(\text{arene}')\text{Fe}]^{2+}$  Dications.<sup>‡</sup>

<u>Complex</u>	<u>Complex #</u>	$\text{C}_6\text{H}_4\text{Me}_2$ ligand <u>C<sub>Ar</sub></u>	$\text{C}_6\text{R}_6$ ligand <u>C<sub>Ar</sub></u>
$[(1,3\text{-C}_6\text{H}_4\text{Me}_2)(\text{C}_6\text{Me}_6)\text{Fe}](\text{PF}_6)_2$	15	112.7s, 96.2d, 92.4d, 92.1d	107.2s
$[(1,4\text{-C}_6\text{H}_4\text{Me}_2)(\text{C}_6\text{Me}_6)\text{Fe}](\text{PF}_6)_2$	16	111.2s, 93.6d	107.1s
$[(1,4\text{-C}_6\text{H}_4\text{Me}_2)(\text{C}_6\text{Et}_6)\text{Fe}](\text{PF}_6)_2$	17	112.5s, 93.4d	111.7s

<sup>‡</sup> Acetone- $\text{d}_6$ .

the decreased electron density in the hexamethylbenzene ring of the [(arene)(arene')Fe]<sup>2+</sup> dication. A similar trend is observed with the <sup>1</sup>H NMR chemical shifts of the methyl substituents of **1b** (2.70 ppm), **1e** (2.52 ppm), and **16** (2.60, 2.75 ppm).

**15** and **16** are the second and third reported [(arene)(arene')Fe]<sup>2+</sup> dications and the first to be characterized crystallographically\*. Perspective views of the dicationic portions of these salts are shown in Figures 4.3 and 4.4. Data collection and refinement parameters, final fractional coordinates, bond distances and angles and least squares best planes calculations for **15** and **16** are given in Tables A24, A25, A26 and A27; and A28, A29, A30, and A31; respectively.

**15** adopts a solid state conformation in which the ring carbon atoms are staggered with Fe-C and Fe-ring plane distances to the hexamethylbenzene and m-xylene rings of 2.131(8) Å and 1.594(4) Å, and 2.12(3) Å and 1.587(5) Å, respectively. The arene ligands are essentially planar (maximum deviation of 0.03 Å from planarity) and parallel (torsion angle = 1.9°). With one exception, the methyl carbon atoms of the hexamethylbenzene ring point away from

---

\* The X-ray crystal structure of **15** was solved by Dr. Michael Zaworotko at Saint Mary's University using data collected at the University of Victoria by Ms. Kathy Beveridge on an Enraf-Nonius CAD-4 diffractometer, and the X-ray crystal structure of **16** was solved by Dr. Robin Rogers at Northern Illinois University using data collected on an Enraf-Nonius CAD-4 diffractometer.

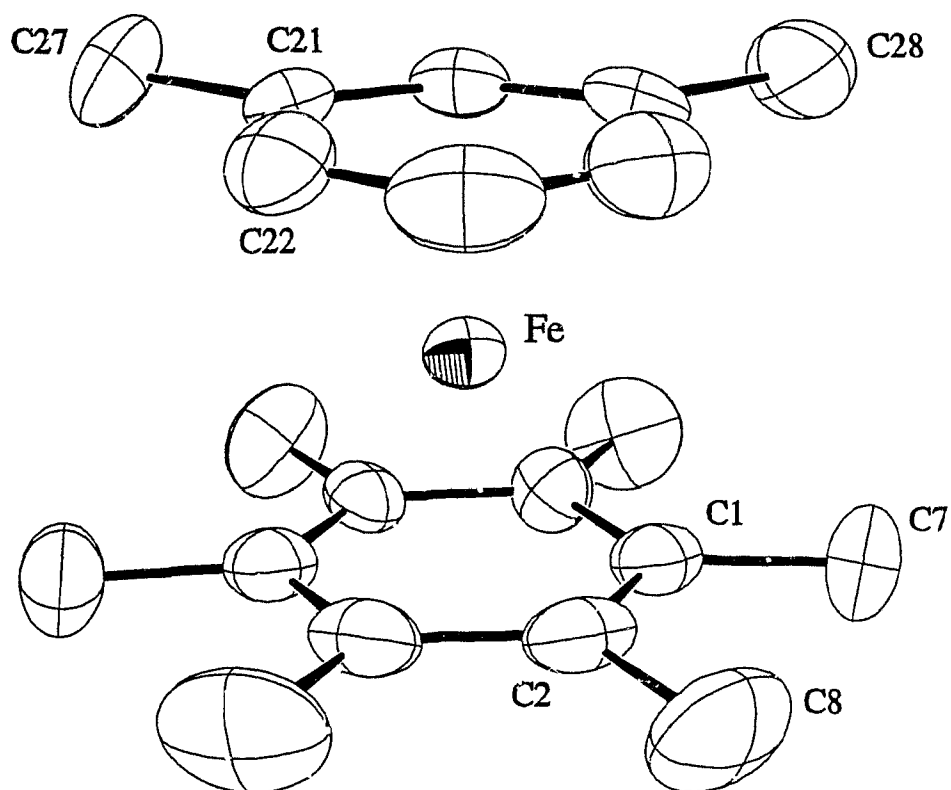


**Figure 4.3** ORTEP<sup>133</sup> Perspective View of the Dicationic Portion of  $[(1,3\text{-C}_6\text{H}_4\text{Me}_2)(\text{C}_6\text{Me}_6)\text{Fe}](\text{PF}_6)_2$ , 15.

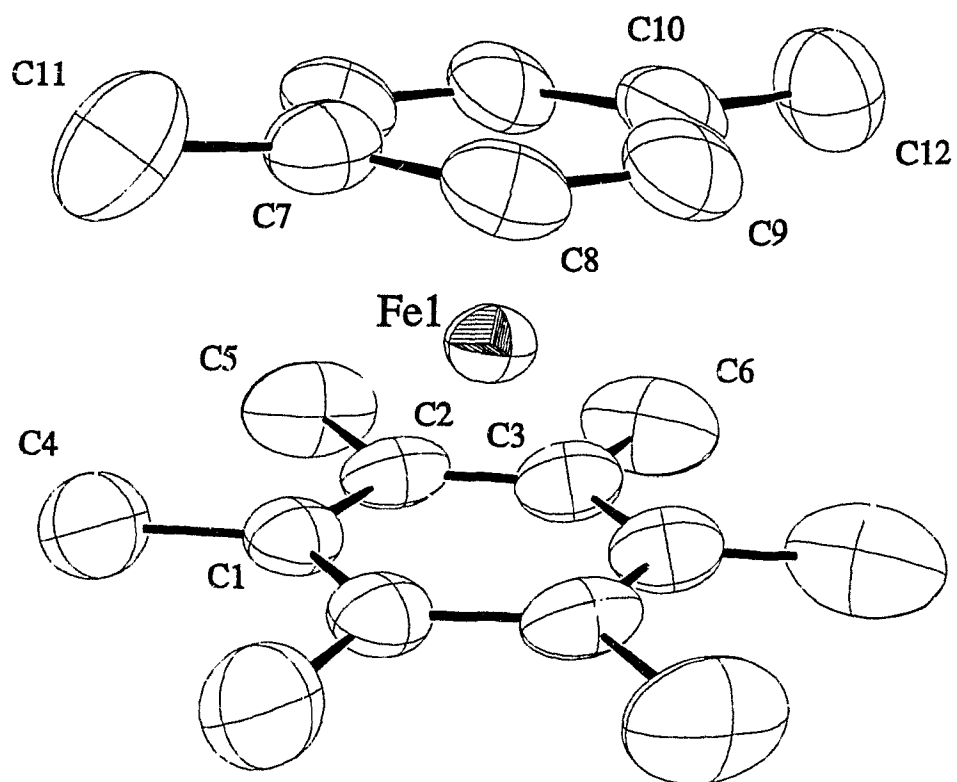
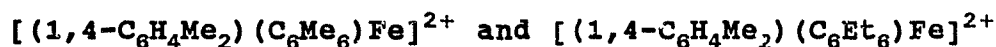


**Figure 4.4** ORTEP<sup>133</sup> Perspective View of the Dicationic  
Portion of  $[(1,4\text{-C}_6\text{H}_4\text{Me}_2)(\text{C}_6\text{Me}_6)\text{Fe}](\text{PF}_6)_2$ , **16**.

the metal at an average distance of 0.05 Å from the C<sub>6</sub> plane.

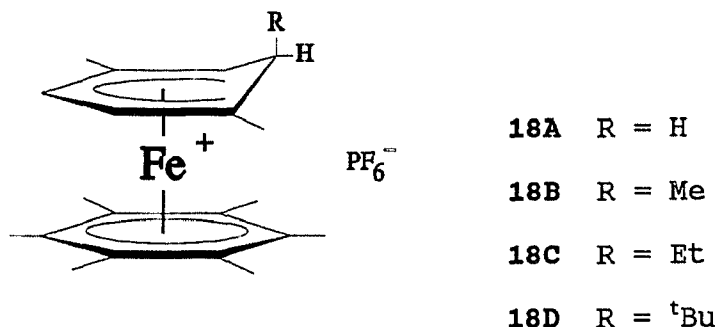
The two arene rings of **16** are essentially planar (maximum deviation = 0.03 Å) and parallel (torsion angle = 0.5°) in the solid state and adopt a conformation in which the ring carbon atoms of the arene ligands are staggered. Average Fe-C and Fe-ring plane distances to the hexamethylbenzene and p-xylene rings are 2.13(1) Å and 1.60 Å, and 2.13(4) Å and 1.59 Å, respectively.

#### 4.2 Ring Regioselectivity in the Addition of Anions to



#### Dications

Reactions of excess NaBH<sub>4</sub>, MeLi, AlEt<sub>3</sub>, and <sup>t</sup>BuLi with **16** were conducted in dichloromethane at -95°C in the hope that double addition to the p-xylene ligand would result to yield the corresponding [(arene)(cyclohexadiene)Fe] complexes. Unfortunately, no double addition occurred; only single net addition of H<sup>-</sup>, Me<sup>-</sup>, Et<sup>-</sup>, and <sup>t</sup>Bu<sup>-</sup> yielding [(arene)(cyclohexadienyl)Fe]PF<sub>6</sub> salts was observed. The anions added, as expected, to the unsubstituted position of the p-xylene ring to give [(R-1,4-C<sub>6</sub>H<sub>4</sub>Me<sub>2</sub>)(C<sub>6</sub>Me<sub>6</sub>)Fe]<sup>+</sup> cations as the major products (**18A** - **18D** for R = H, Me, Et, <sup>t</sup>Bu, respectively). No addition to the substituted position of p-xylene was observed, but <sup>1</sup>H NMR revealed that minor



products resulted from addition to the hexamethylbenzene ring yielding  $[(R-C_6Me_6)(1,4-C_6H_4Me_2)Fe]^+$  monocations (Figure 4.5).

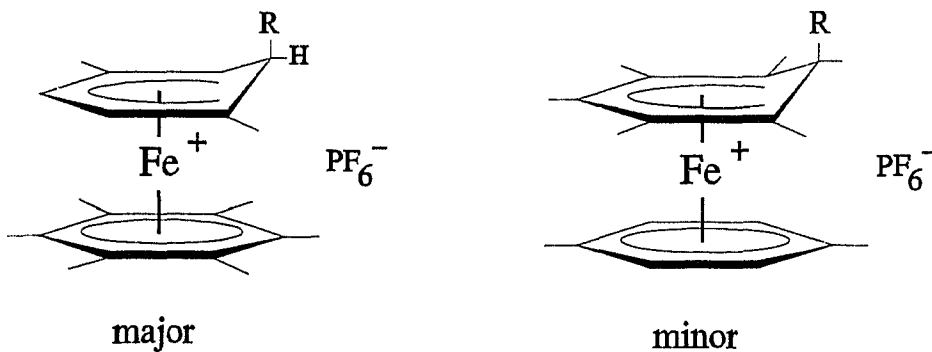


**Figure 4.5** Major and Minor Products from the Reactions of  $NaBH_4$ ,  $FeLi$ ,  $AlEt_3$ , and  $^tBuLi$  with  $[(1,4-C_6H_4Me_2)(C_6Me_6)Fe](PF_6)_2$ .

The  $^1H$  NMR spectrum of the aromatic region of a typical reaction mixture is shown in Figure 4.6. The two doublets labelled A correspond to the 2- and 3- hydrogen atoms of the

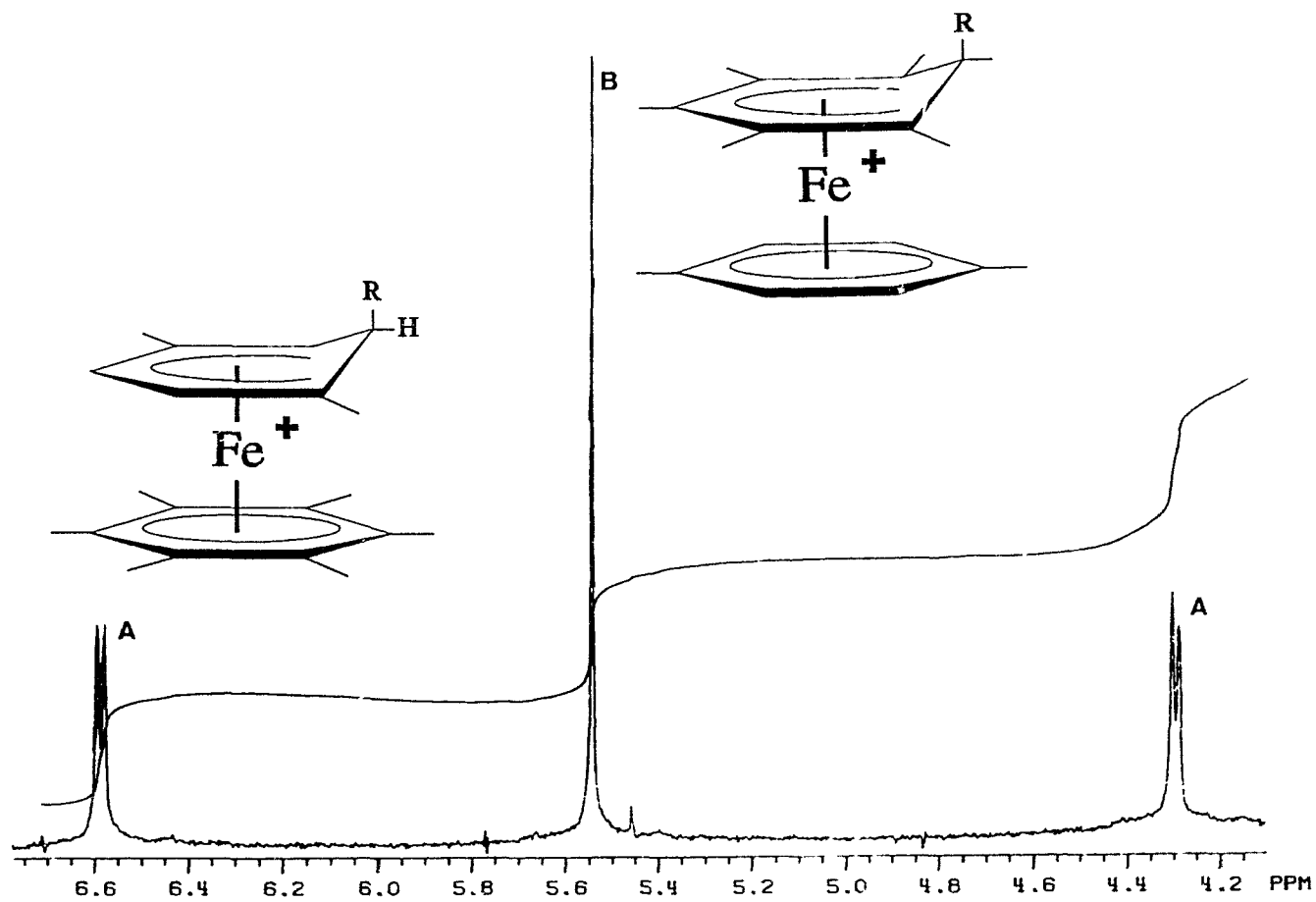


Figure 4.6 Partial  $^1\text{H}$  NMR Spectrum of the Products Obtained from Reaction of  $[(1,4\text{-C}_6\text{H}_4\text{Me}_2)(\text{C}_6\text{Me}_6)\text{Fe}](\text{PF}_6)_2$  with  $\text{NaBH}_4(\text{aq})$ .

cyclohexadienyl ligand in the  $[(R-1,4-C_6H_4Me_2)(C_6Me_6)Fe]^+$  cation and the singlet labelled B corresponds to the 4 equivalent p-xylene ring hydrogen atoms in the  $[(R-C_6Me_6)(1,4-C_6H_4Me_2)Fe]^+$  cation. Integration of these signals reveal that net anion addition to the hexamethylbenzene ring occurred as 7-17% of the product mixture.

To see if the regioselectivity of the addition could be controlled by increasing the steric bulk of the ancillary ligand, the reactivity towards the same anions was investigated with 17. Again, only  $[(arene)(cyclohexadienyl)Fe]^+$  cations were isolated.  $^1H$  NMR showed, however, that addition to the  $C_6Et_6$  ligand, with one exception, did not occur. Table 4.3 shows the percentage of products derived from  $R^-$  addition to the p-xylene ring of the  $[(arene)(arene')Fe]^{2+}$  dications. Net carbanion addition to the  $C_6Et_6$  ring is now effectively deterred. This is presumably a result of the increased steric bulk of the ethyl substituents (expected to be predominantly distally arranged due to the proximity of the ancillary ligand). The significance of these results is that they show that it is possible to control the regioselectivity of net anion addition to  $[(arene)_2Fe]^{2+}$  dications via introduction of a sterically crowded ligand.

$[(^tBu-1,4-C_6H_4Me_2)(C_6Et_6)Fe]PF_6$  was characterized crystallographically but unfortunately the structure contained disorder that led to a high conventional R factor.

**Table 4.3** Percentage of Product Derived from Net R<sup>-</sup> Addition to the p-xylene Ligand of  
 $[(1,4\text{-C}_6\text{H}_4\text{Me}_2)(\text{C}_6\text{R}_6)\text{Fe}](\text{PF}_6)_2$  (R = Me, Et).

<u>Substrate</u>	<u>Complex #</u>	<u>H<sup>-</sup></u> <sup>a</sup>	<u>Me<sup>-</sup></u> <sup>b</sup>	<u>Et<sup>-</sup></u> <sup>c</sup>	<u><sup>t</sup>Bu<sup>-</sup></u> <sup>b</sup>
$[(\text{C}_6\text{H}_4\text{Me}_2)(\text{C}_6\text{Me}_6)\text{Fe}]^{2+}$	16	92	87	83	93
$[(\text{C}_6\text{H}_4\text{Me}_2)(\text{C}_6\text{Et}_6)\text{Fe}]^{2+}$	17	99	>99.9	>99.9	>99.9

<sup>a</sup> 10 eqv. NaBH<sub>4</sub>(aq), CH<sub>2</sub>Cl<sub>2</sub>, 25°C, 90 min.

<sup>b</sup> 4 eqv. RLi, CH<sub>2</sub>Cl<sub>2</sub>, -95°C, 60 min.

<sup>c</sup> 4 eqv. AlEt<sub>3</sub>, ClCH<sub>2</sub>CH<sub>2</sub>Cl, 25°C, 24 hr.

Nonetheless, the gross solid state structure and conformation was discernable and revealed that <sup>t</sup>Bu<sup>-</sup> had added to the unsubstituted position of the p-xylene ring. The nature of the disorder was with the ethyl substituent lying directly below the sp<sup>3</sup> hybridized carbon atom of the cyclohexadienyl ring and the PF<sub>6</sub><sup>-</sup> anion. The crystal contained two cations; one in which this ethyl substituent was distally arranged and one in which it was proximally arranged. It is reasonable to assume that the apparent low energy difference between the distal and proximal conformations is a result of the degree to which the sp<sup>3</sup> hybridized carbon atom of the cyclohexadienyl ring is forced (by steric pressure) away from the iron atom<sup>67</sup>.

#### 4.3 Reaction of [(1,4-C<sub>6</sub>H<sub>4</sub>Me<sub>2</sub>)(C<sub>6</sub>Me<sub>6</sub>)Fe]<sup>2+</sup> and [(1,4-C<sub>6</sub>H<sub>4</sub>Me<sub>2</sub>)(C<sub>6</sub>Et<sub>6</sub>)Fe]<sup>2+</sup> Dications with NaBEt<sub>3</sub>H

As was addressed in the previous section, reactions of the [(arene)(arene')Fe]<sup>2+</sup> dications 16 and 17 with aqueous NaBH<sub>4</sub> and alkyllithium reagents fail to give double net anion addition. It is therefore unclear whether a second net anion addition to 18A-D or 19A-D would result in the formation of diene-arene or pseudoferrocene products. In an attempt to force a second addition, reactions of 16 and 17 were conducted using BEt<sub>3</sub>H<sup>-</sup> as a hydride source under the conditions utilized for reactions with carbanions.

After workup of the reaction mixtures deep orange hexanes solutions were obtained suggesting the presence of neutral organoiron species. Unfortunately, the products proved to be too air- and solution-sensitive to obtain interpretable NMR spectra, and thus their identity remains unknown. Possible products include the corresponding pseudoferrocenes, [(arene)(cyclohexadiene)Fe], or proton-abstraction products as shown in Figure 4.7.

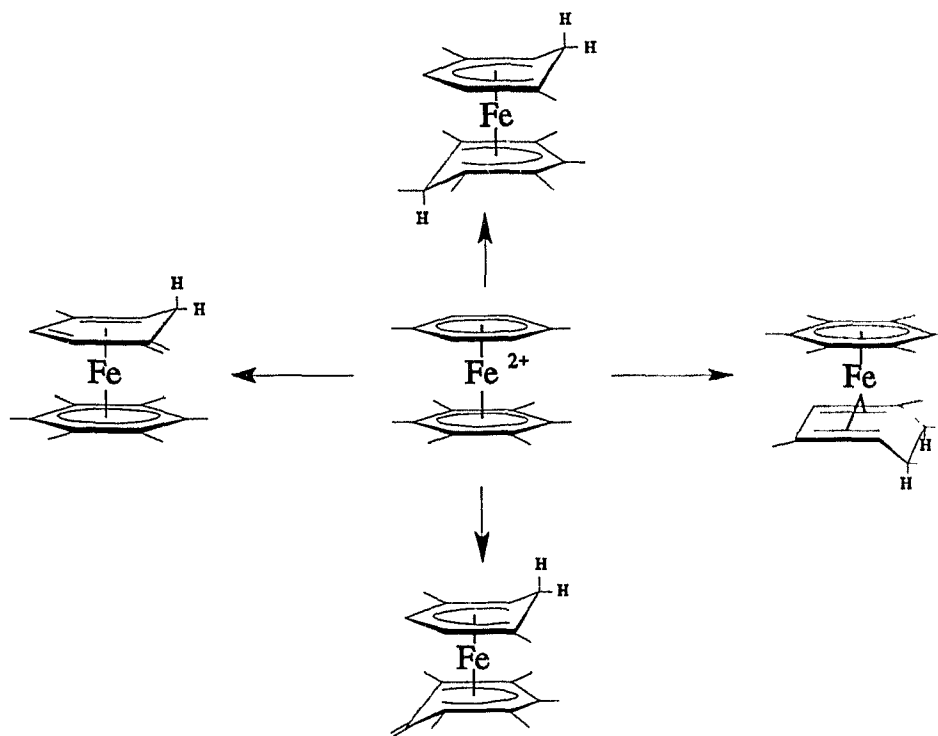


**Figure 4.7** Possible Products in the Reaction of [(1,4-C<sub>6</sub>H<sub>4</sub>Me<sub>2</sub>)(C<sub>6</sub>Me<sub>6</sub>)Fe](PF<sub>6</sub>)<sub>2</sub> with Excess BEt<sub>3</sub>H<sup>-</sup>.

Interestingly, Sweigart has recently shown<sup>97</sup> that reactions

of carbanions with  $[(C_6H_6)(arene)Ru]^{2+}$  dications (arene = 1,3,5- $C_6H_3Me_3$ , 1,3,5- $C_6H_3^iPr_3$ ,  $C_6Me_6$ ) yield  $[(cyclohexadienyl)_2Ru]$  complexes rather than the arene-diene complexes.

#### 4.4 Regioselectivity in the Addition of Anions to the meta-xylene Ligand of the $[(1,3-C_6H_4Me_2)(C_6Me_6)Fe]^{2+}$ Dication

$MeLi$ ,  $AlEt_3$ ,  $PhLi$ , and  $tBuLi$  were reacted with **15** in  $CH_2Cl_2$ . In all cases monocationic salts were formed from single net carbanion addition to either the 1,3- $C_6H_4Me_2$  (major product) or  $C_6Me_6$  (minor product) rings. If we ignore addition to the  $C_6Me_6$  ring, this series of reactions also provides an opportunity to evaluate the regioselectivity of carbanion addition to the m-xylene ring; an opportunity not available in the case of p-xylene.

There are 3 possible ring positions (2, 4, and 5) as unsubstituted sites for carbanion addition to the coordinated m-xylene, shown in Figure 4.8. Reactions with  $Me^-$ ,  $Et^-$ , and  $Ph^-$  were shown by  $^1H$  and  $^{13}C$  NMR spectroscopy to yield mixtures of addition products. Due to the complexity of overlapping multiplets in the NMR spectra, the positions of addition could not be determined. However, when  $tBuLi$  was employed as the carbanion source only one isomer was observed; addition at the 4-carbon atom, **20D**.

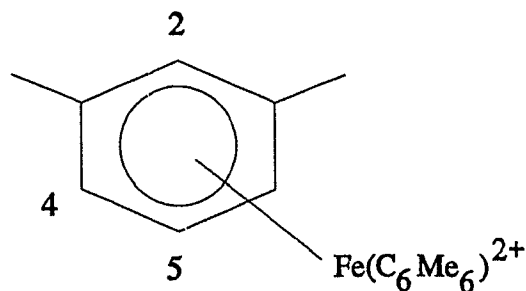


**Figure 4.8** Unsubstituted Ring Positions in m-xylene.

The regioselectivity observed for net  ${}^t\text{Bu}^-$  addition to **15** has important mechanistic implications with respect to nucleophilic attack of the carbanion versus SET/radical coupling. First let us consider the reaction of **15** with  ${}^t\text{BuLi}$  proceeding via nucleophilic attack of  ${}^t\text{Bu}^-$  to the complexed m-xylene. Since methyl substituents are *ortho-para* directing in electrophilic aromatic substitution, the distribution of electron density around the m-xylene ring would be expected to be as shown in Figure 4.9. The ring

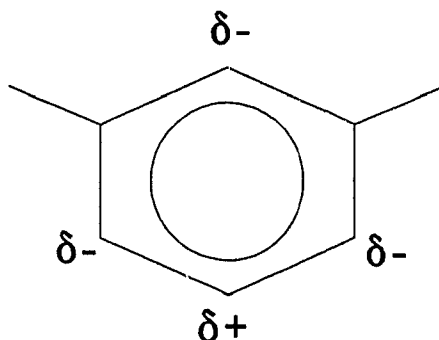


**Figure 4.9** Expected Electron Density Distribution in m-xylene.

carbon atom with the least amount of electron density is 5-, meta to the methyl groups. Therefore, if  $t\text{Bu}^-$  adds as a nucleophile, one would predict that the cyclohexadienyl formed would be the position 5- addition isomer. Indeed nucleophilic attack of carbanions meta to methyl substituents has been shown<sup>5</sup> to occur for the more electron-rich  $[(\text{arene})\text{Cr}(\text{CO})_3]$  systems, however this is not what is observed for  $[(\text{arene})(\text{arene}')\text{Fe}]^{2+}$  dications.

Should the reaction take place via SET transfer we must consider the distribution of electron density in the m-xylene ring of the  $19e^-$  complex. As a first approximation, we might view the m-xylene ring in the organometallic radical adopting the quinone-like structure (expected<sup>166</sup> for the m-xylene radical anion) shown in Figure 4.10, with the

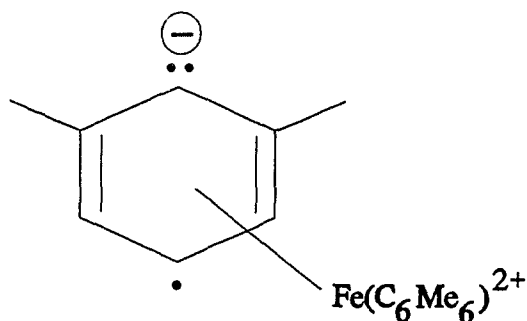


**Figure 4.10** Possible Quinone-like Structure of the m-xylene Ring in the  $19e^- [(1,3-\text{C}_6\text{H}_4\text{Me}_2)(\text{C}_6\text{Me}_6)\text{Fe}]^+$  Radical.

radical centered on the carbon atom *meta* to the two methyl substituents. If this were the case then the expected coupling product would again be <sup>t</sup>Bu addition to the 5-position.

This interpretation, however, probably does not accurately represent the true distribution of electron density in the 19e<sup>-</sup> radical cation. When we consider that in the one electron reduction of the [(arene)<sub>2</sub>Fe]<sup>2+</sup> dication to the 19e<sup>-</sup> [(arene)<sub>2</sub>Fe]<sup>+</sup> complex the 19<sup>th</sup> electron resides, for the most part, on the metal<sup>71</sup>; and that the arene ligands are symmetrically bound to the metal; the net effect of the electron transfer is likely to be an increase in the magnitude of the electron density on the *m*-xylene ring and not a redistribution of this electron density. The distribution of the electron density in the *m*-xylene ring of the 18e<sup>-</sup> and 19e<sup>-</sup> complexes, therefore, would probably be better represented as in Figure 4.11.

Coupling of R<sup>•</sup> with the organometallic radical would be expected to result in a new carbon-carbon bond formed where the electron density in the arene is greatest; namely *ortho* or *para* to the methyl groups (positions 2- and 4-). When we then consider the steric constraints that would be expected to be in effect for the reaction of the <sup>t</sup>Bu moiety, addition at the 4-position should predominate. This is exactly what is observed, thereby lending support to the argument that carbanions add to [(arene)<sub>2</sub>Fe]<sup>2+</sup> dications via a SET process.

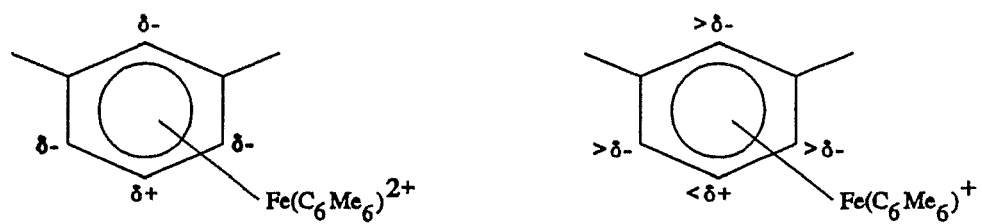


Figure 4.11 Proposed Electron Density Distribution in the  $18e^- [(1,3\text{-C}_6\text{H}_4\text{Me}_2)(\text{C}_6\text{Me}_6)\text{Fe}]^{2+}$  and  $19e^- [(1,3\text{-C}_6\text{H}_4\text{Me}_2)(\text{C}_6\text{Me}_6)\text{Fe}]^+$  Cations.

## Chapter 5

Net Addition of Carbanions and Electrophiles to  
[(arene)(cyclopentadienyl)Fe]<sup>+</sup> Cations

### 5.1 Net Phenide Addition to the $[(1,3,5\text{-C}_6\text{H}_3\text{Me}_3)(\text{C}_5\text{H}_5)\text{Fe}]^+$ Cation

The net addition of nucleophiles to the arene ring of  $[(\text{arene})(\text{cyclopentadienyl})\text{Fe}]^+$  cations is a well established facet of organometallic chemistry covering a wide range of both arene complexes and nucleophiles. However, the number of the resulting  $[(\text{cyclohexadienyl})(\text{cyclopentadienyl})\text{Fe}]$  complexes that have been X-ray crystallographically characterized is at best modest. To our knowledge, the only crystallographically characterized  $[(\text{cyclohexadienyl})(\text{cyclopentadienyl})\text{Fe}]$  moiety is  $(\eta^5\text{-exo-1-Acetyl-2,4,6-tris(trifluoromethyl)cyclohexadienyl})(\text{cyclopentadienyl})\text{iron(II)}$ <sup>167</sup>. This, however, is not a representative example of a  $[(\text{cyclohexadienyl})(\text{cyclopentadienyl})\text{Fe}]$  complex since the complex contains three strongly electron-withdrawing  $\text{CF}_3$  groups.

In order to investigate the relative  $\pi$ -bonding abilities of the arene, cyclopentadienyl, cyclohexadienyl, and pentadienyl ligands the synthesis and structural characterization\* of a  $[(\text{cyclohexadienyl})(\text{cyclopentadienyl})\text{Fe}]$  complex containing

---

\* The X-ray crystal structure of **21c** was solved by Dr. Peter White at the University of New Brunswick using data collected on an Enraf-Nonius CAD-4 diffractometer.

only hydrocarbon ligands, namely; ( $\eta^5$ -1,3,5-trimethyl-6-exo-phenylcyclohexadienyl)( $\eta^5$ -cyclopentadienyl)iron(II), **21c**, was undertaken. The results of this investigation are discussed in Chapter 6.

**21c** has a melting point that agrees with a previous report<sup>112</sup>. No NMR results were originally reported for this complex, however, our data are consistent with what one would expect for metal-cyclohexadienyl complexes and similar to that reported<sup>167</sup> for  $[(\text{CH}_3\text{CO}-\text{C}_6\text{H}_3(\text{CF}_3)_3)(\text{C}_5\text{H}_5)\text{Fe}]$ .

Crystallographic refinement and data collection parameters, final fractional coordinates, bond distances and angles, and least squares best planes calculations for **21c** are presented in Tables A32, A33, A34, and A35, respectively. A perspective view of the complex, depicted in Figure 5.1, shows that the two  $\eta^5$ -rings are essentially parallel making a dihedral angle of only  $2.4(2)^\circ$ , and addition of the phenyl moiety has occurred in the expected<sup>4</sup> exo fashion. The cyclopentadienyl and Ph rings are close to planarity with deviations of less than  $0.01 \text{ \AA}$ , while the dienyl portion of cyclohexadienyl ring deviates from planarity by a maximum of  $0.016 \text{ \AA}$ . The three methyl carbon atoms point significantly towards the iron atom;  $0.195$ ,  $0.193$ , and  $0.069 \text{ \AA}$  from the  $\text{C}_5$  plane for carbon atoms C27, C29, and C28, respectively. The phenyl moiety is twisted with respect to the mirror plane of cyclohexadienyl ring by  $40^\circ$  (based on the torsional angle between C36:C31 and

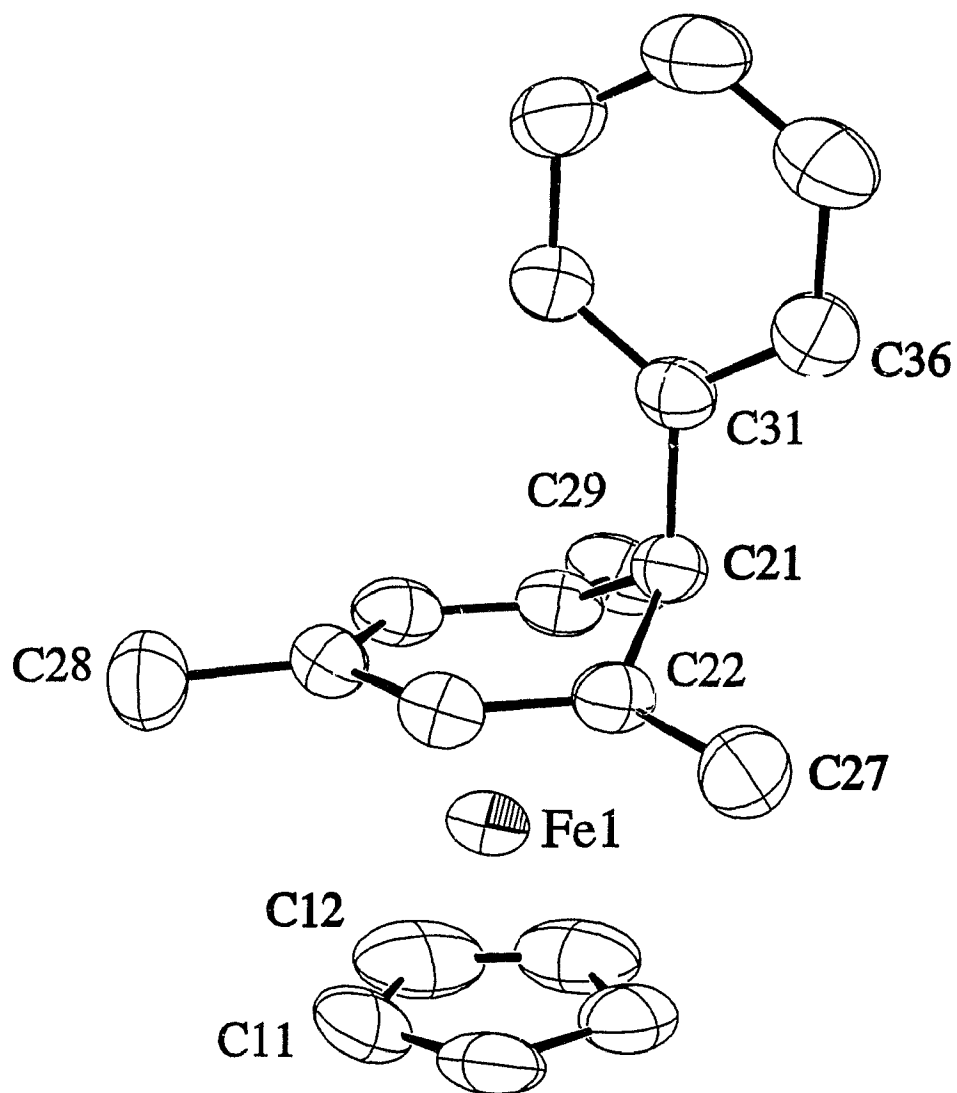


**Figure 5.1** ORTEP<sup>133</sup> Perspective View of [(Ph-1,3,5- $C_6H_3Me_3$ )( $C_5H_5$ )Fe], **21c**.

C21:C23).

Comparison of the results of this study with those obtained for the acetyl-tris(trifluoromethyl) analogue reveal surprisingly little structural differences between the two. Indeed, the net effect of replacing 1,3,5-methyl groups with 1,3,5-trifluoromethyl substituents is statistically non-existent as the solid state structural parameters of  $[(\text{CH}_3\text{CO}-\text{C}_6\text{H}_3(\text{CF}_3)_3)(\text{C}_5\text{H}_5)\text{Fe}]$  (see Table 6.1) and **21c** are almost identical.

**5.2 Base Assisted Electrophilic Addition of  $\text{CH}_2\text{C}_6\text{H}_5^+$  to the  $[(\text{C}_6\text{Me}_6)(\text{C}_5\text{H}_5)\text{Fe}]^+$  Monocation and Decomplexation of  $\text{C}_6(\text{CH}_2\text{CH}_2\text{C}_6\text{H}_5)_6$ . Solution and Solid State Behaviour of the Complex and Free Ligand**

In Chapter 1 the four main aspects of altered arene reactivity and conformation upon complexation to a transition metal were discussed. For the most part this thesis has dealt with the susceptibility of the coordinated arene to reduction and attack by nucleophiles. However, acidity of ring and substituent protons, as well as conformation of flexible arene substituents are important and well documented. The following section considers the latter two effects of metal complexation upon aromatic hydrocarbons.

The effect that ancillary ligands have upon the

conformation of coordinated aromatics was demonstrated<sup>82-84,87</sup> by Mislow using the "piano-stool" complexes  $[(C_6Et_6)M(CO)_2L]$  ( $M = Cr, Mo$ ). In his investigations,  $C_6Et_6$  was observed to adopt four of the eight possible conformations in the solid state (Figure 5.2) depending upon the size of L. In addition, these complexes exhibited dynamic behaviour in solution. This dynamic behaviour is a topic of ongoing controversy as the low temperature spectra may be interpreted either via invoking restricted rotation about the arene-metal tripod bond or arene-Et bonds.

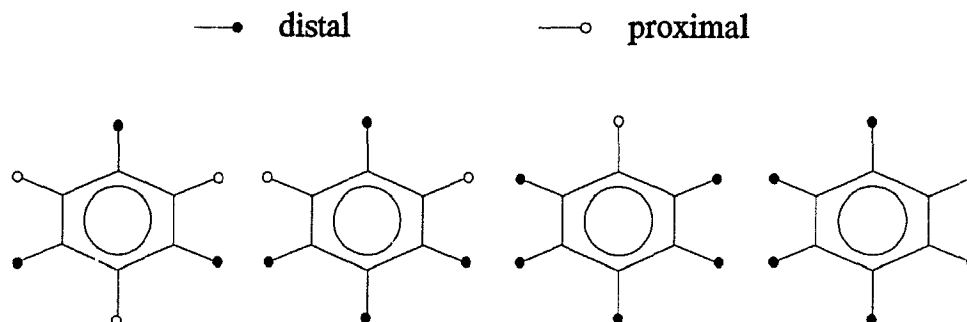
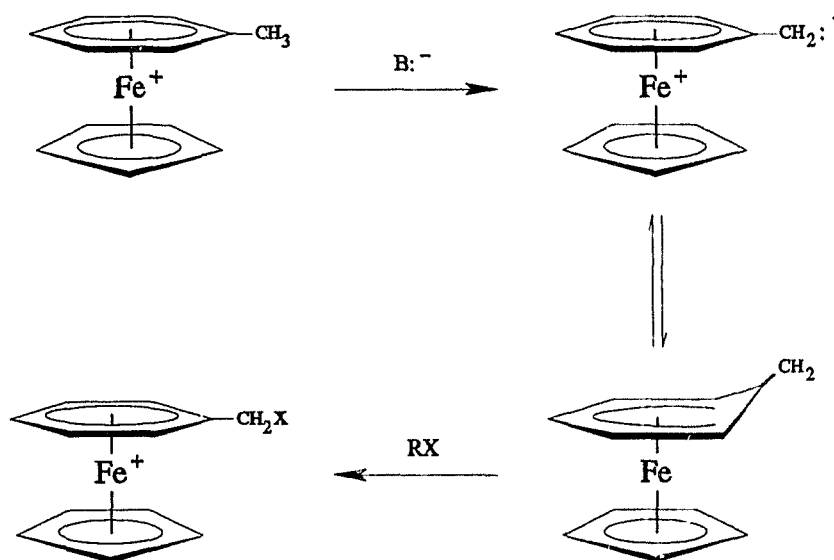


Figure 5.2 Observed Solid State Conformations of  $C_6Et_6$  when Complexed to a Transition Metal Moiety.

A number of workers have shown<sup>73-81</sup> that it is possible to functionalize the methyl groups on the arene ring of  $[(arene)(cyclopentadienyl)Fe]^+$  cations by abstraction of a proton by a suitable base followed by reaction of the

intermediate with electrophiles (Figure 5.3). In particular, addition of a large excess of both base and electrophile can produce, in a one-pot reaction, the fully substituted aromatic (see Scheme 1.1). It is then possible to chemically, photochemically, or thermally decomplex the aromatic molecule in good yields.

An example of this reaction is the conversion of  $[(C_6Me_6)(C_5H_5)Fe]PF_6$  to  $[(C_6(CH_2CH_2Ph)_6)(C_5H_5)Fe]PF_6^{80}$ . In order to determine the relative importance of intraligand versus ligand-metal steric repulsions, discussed above, we have



**Figure 5.3** Functionalization of the Methyl Group of  $[(\text{arene})(\text{cyclopentadienyl})Fe]^+$  Cations.

repeated this reaction and structurally characterized\* the reaction product,  $[(C_6(CH_2CH_2C_6H_5)_6)(C_5H_5)Fe]PF_6$ , **22**, and decomplexation product  $C_6(CH_2CH_2C_6H_5)_6$ , **23**. Crystallographic refinement and data collection parameters for **22** and **23** are given in Tables A36 and A40, respectively. Final fractional coordinates, bond distances and angles, and least squares best planes calculations for **22** and **23** are presented in Tables A37, A38, and A39, and A41, A42, and A43, respectively. Perspective views of **23**, and the cation of **22**, are shown in Figures 5.4 and 5.5.

**23** adopts the alternating up-down arrangement of phenylethyl groups which would be expected to predominate on the basis of steric repulsions between the phenylethyl substituents. Such a conformation was also adopted by  $C_6Et_6$  in the solid state, for which it was predicted to be approximately  $3.5 \text{ kcal mol}^{-1}$  more stable than any of the other seven up-down isomers<sup>82</sup>. The 360 MHz  $^1H$  NMR spectrum of **22** (Figure 5.6) exhibits two complex but symmetrical patterns in the ethylene region and is similar to that observed for the free ligand. The similarity between the two spectra might be anticipated since, assuming fast rotation around the  $CH_2-Ph$ ,  $CH_2-CH_2$  and Fe-arene bonds, the six phenylethylene moieties are equivalent if the

---

\* The X-ray crystal structures of **22** and **23** were solved by Dr. Robin Rogers at Northern Illinois University using data collected on an Enraf-Nonius CAD-4 diffractometer.

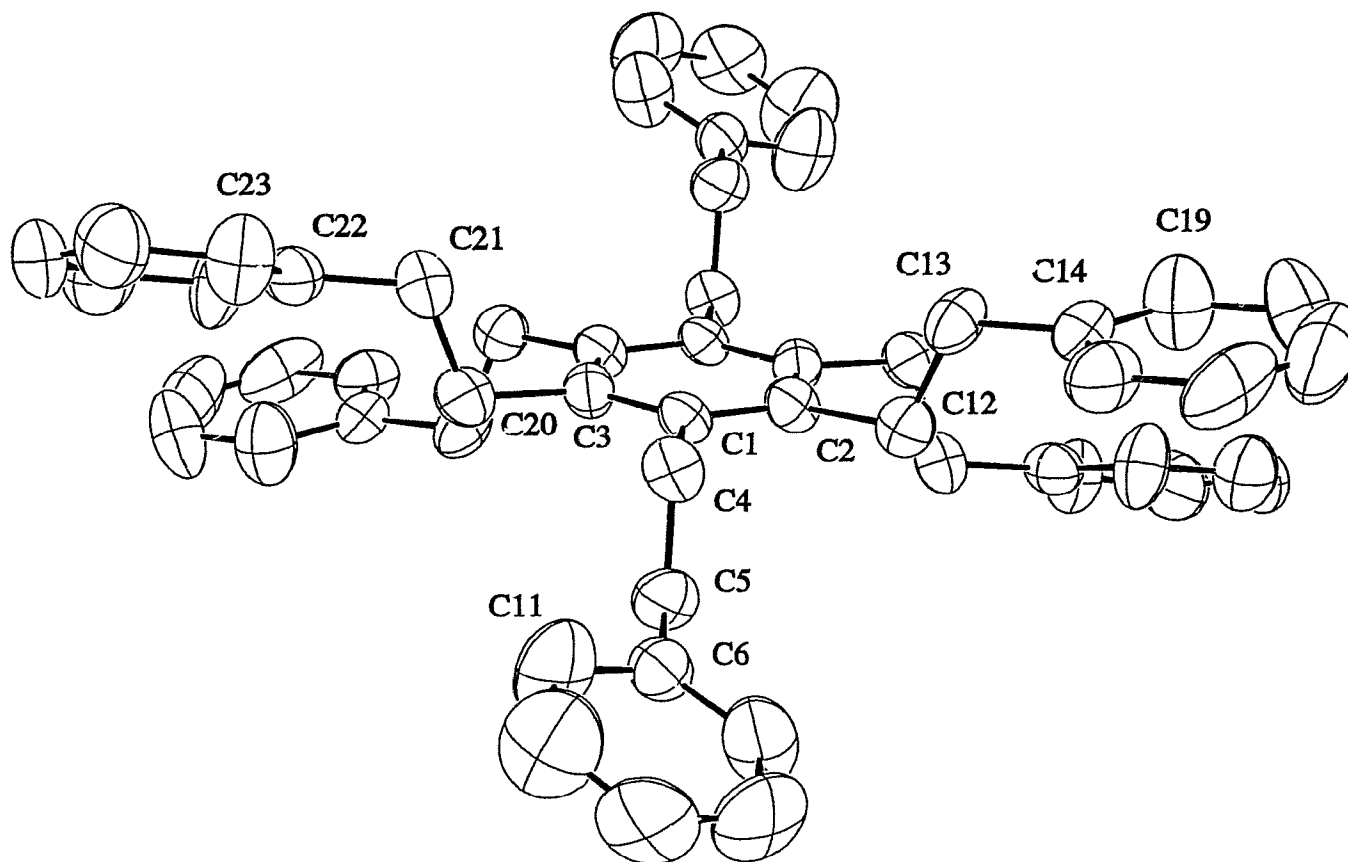


Figure 5.4 ORTEP<sup>133</sup> Perspective View of  $C_6(CH_2CH_2C_6H_5)_6$ , 23.

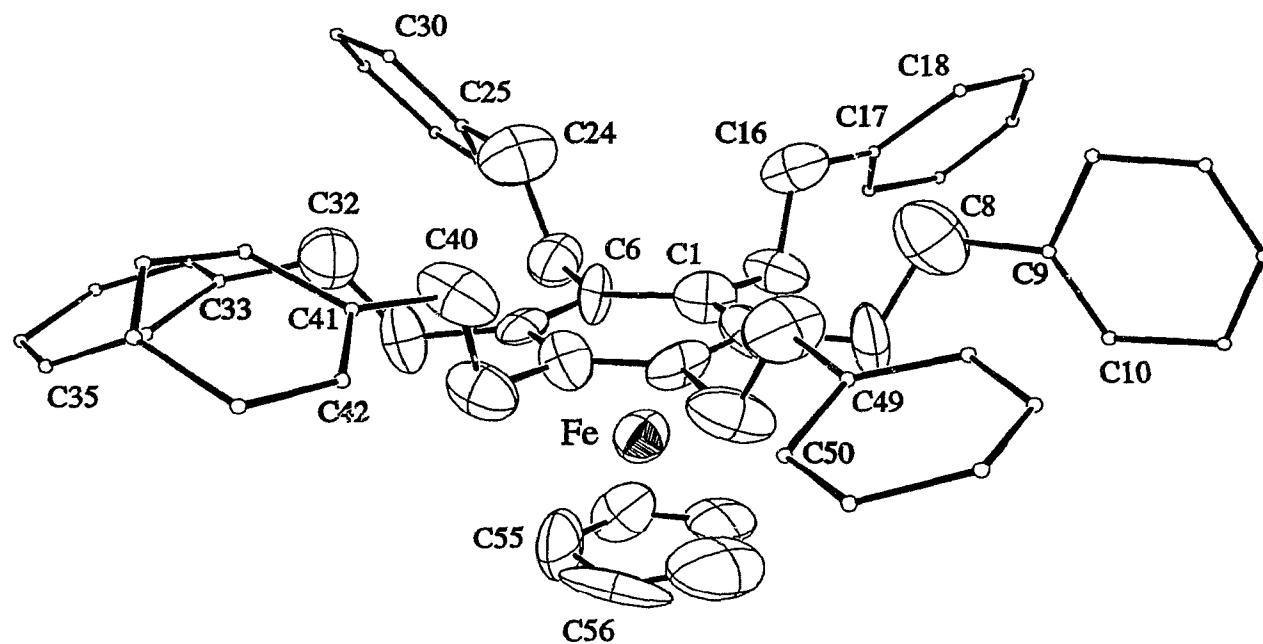


Figure 5.5 ORTEP<sup>133</sup> Perspective View of the Cationic Portion of  
 $[(C_6(CH_2CH_2C_6H_5)_6)(C_5H_5)Fe]PF_6$ , 22.

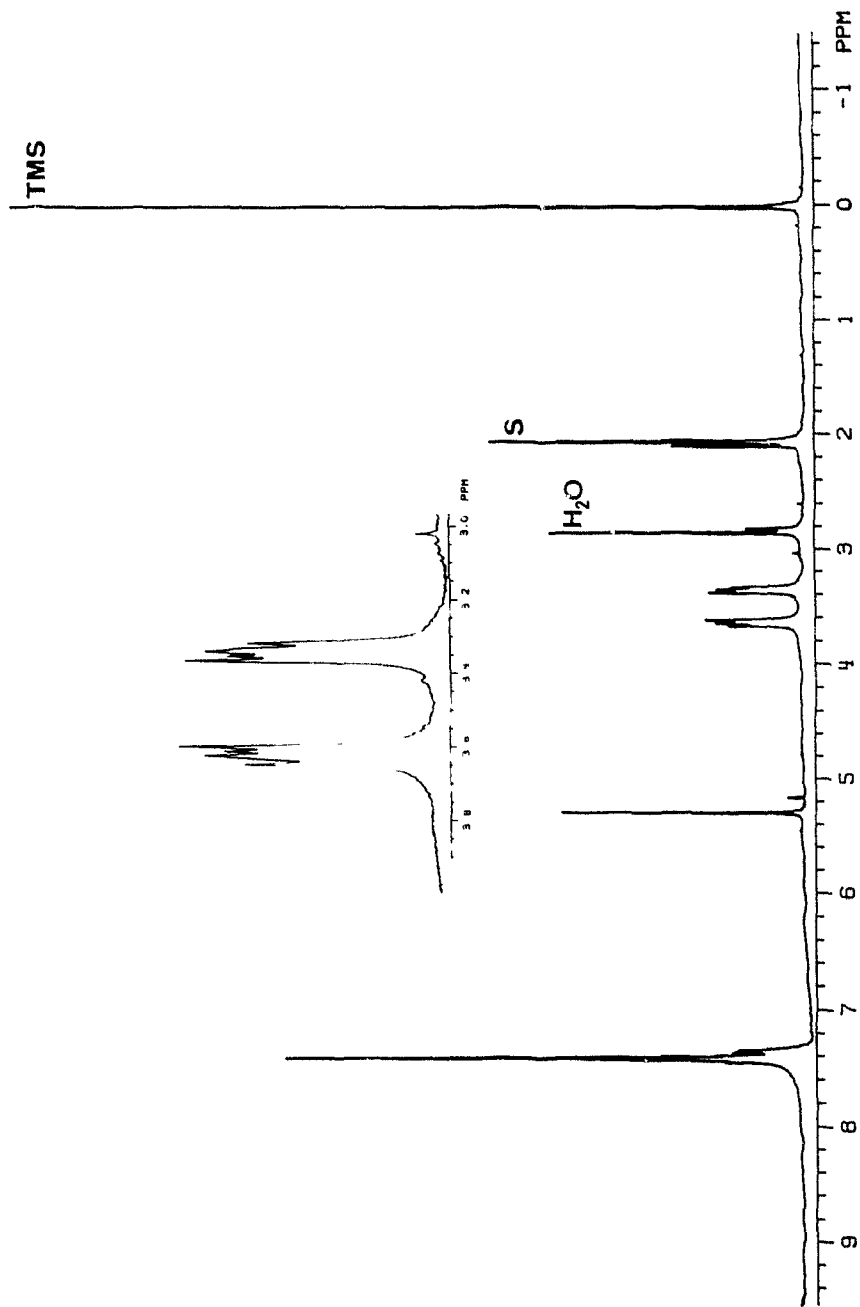


Figure 5.6 <sup>1</sup>H NMR Spectrum of  $[(C_6(CH_2CH_2C_6H_5)_6)(C_5H_5)Fe]PF_6$ , **21**, at 25°C.

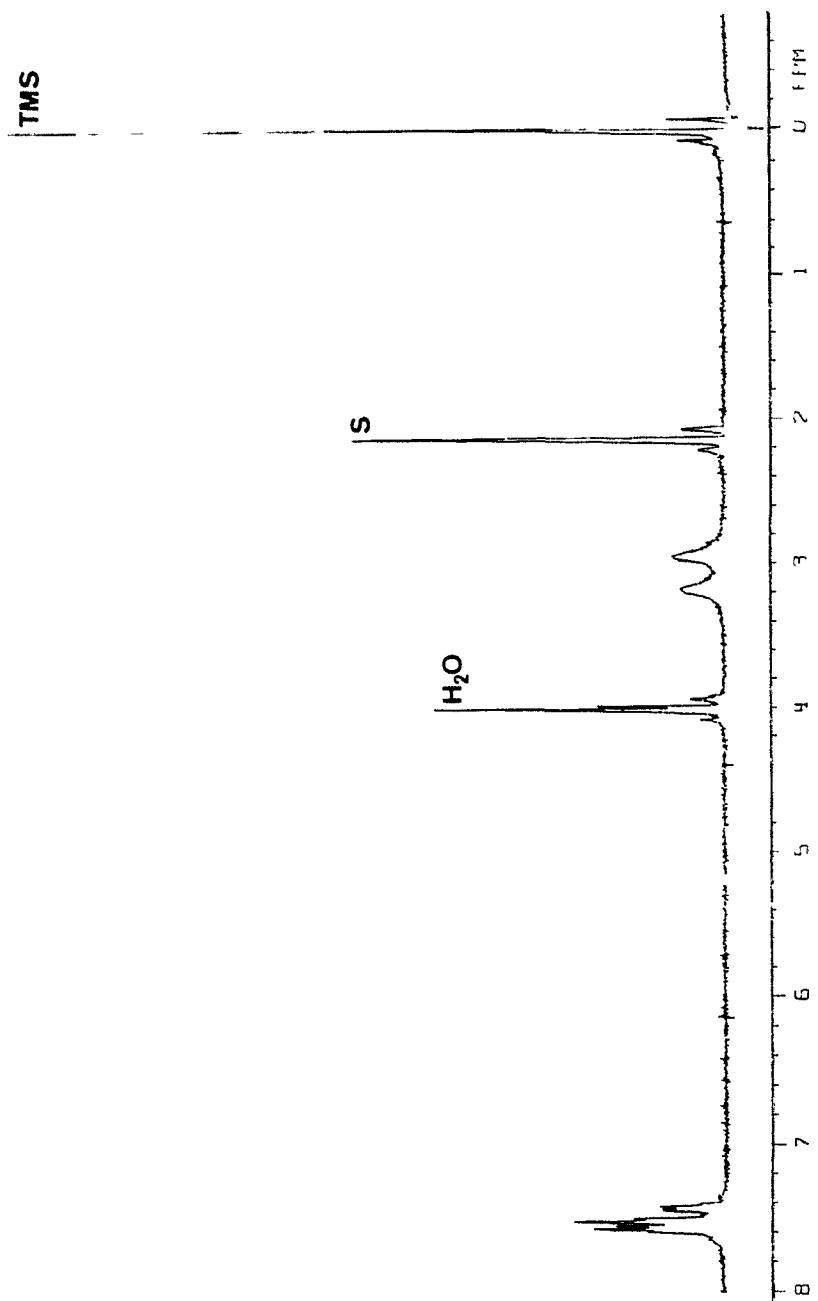


Figure 5.7  $^1\text{H}$  NMR spectrum of  $\text{C}_6(\text{CH}_2\text{CH}_2\text{C}_6\text{H}_5)_6$ , 22, at  $-92^\circ\text{C}$ .

conformations adopted in the solid state predominate in solution (effective  $D_{3d}$  or  $S_6$  symmetry for **23**,  $C_{6v}$  for **22**).

Neither **22** nor **23** exhibit temperature dependence in their NMR spectra between room temperature and  $-92^\circ\text{C}$ . However, **23** appears to be approaching decoalescence at  $-92^\circ\text{C}$  as the ethylene multiplets broaden considerably relative to the rest of the spectrum (Figure 5.7). The spectrum of **22** also broadens at lower temperatures but this is presumably a solubility effect as all peaks in the spectrum are affected. It is therefore not possible to unambiguously determine whether **22** and **23** are undergoing rapid interconversion of conformers on the NMR time scale (the observed solid state conformations predominating) or whether they are rigid, however the data are consistent with the former for **23** and the latter for **22**.

The conformation adopted by hexa(phenylethyl)benzene when complexed to  $[\text{Fe}(\text{C}_5\text{H}_5)]^+$  is quite different from that seen in the free molecule. Figure 5.5 illustrates how all six ethylene moieties are distal to the iron atom, making **22** the first compound to exclusively adopt conformation D (Figure 5.2) for a  $\text{C}_6\text{R}_6$  ligand in the solid state. A six distal conformation was also observed for  $[(\text{C}_6\text{Et}_6)\text{Cr}(\text{CO})_2(\text{PPh}_3)]^{82}$ . One of the ethyl groups, however, was seen to be disordered and occupying a proximal site in approximately one third of the molecules. The closest X-ray crystallographically characterized analogues to **22** are

perhaps  $[(C_6Et_6)Fe(C_5H_5)]PF_6^{80}$  and  $[(C_6Et_6)Fe(C_5H_5)]BPh_4^{95}$ , which were observed to adopt conformations B and C, respectively, in the solid state. The effect of increasing the size of the R group is therefore, at least in this instance, adoption of the conformation which is least energetically favoured in the free ligand.

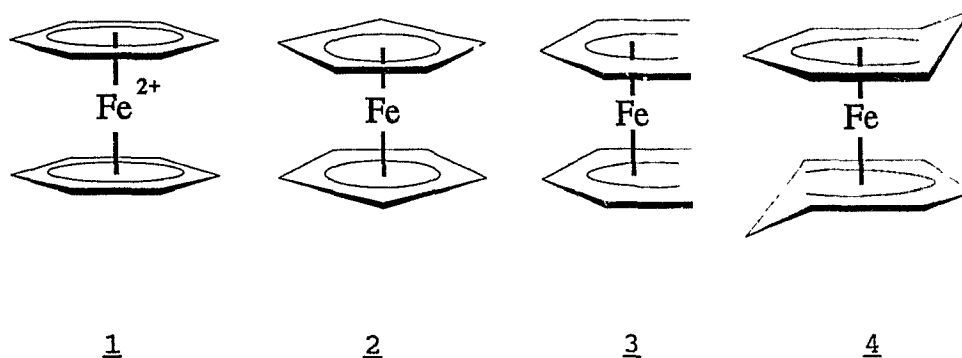
Steric strain might be expected to manifest itself, particularly in the Fe-C bond distances, the Fe-plane distances and the angles around the ethylene groups<sup>109</sup>. Unfortunately, the quality and amount of data and high thermal motion in the Ph moieties precludes close examination of individual bond lengths and angles. However, there are two apparent manifestations of steric strain: the average angle subtended at the ethylene carbon atoms bonded to the coordinated  $C_6$  ring ( $115(3)^\circ$ ); the Fe- $C_5$  and Fe- $C_6$  plane distances, which, at 1.54 Å and 1.64 Å, are relatively short and long, respectively, of a range of Fe(II)-plane distances<sup>109</sup>. The coordinated rings are planar to 0.02 Å and, surprisingly, four of the ethylene carbon atoms bonded to the coordinated  $C_6$  ring point towards the Fe atom (by 0.05 to 0.24 Å). Bending of ring substituents towards the metal has been predicted in  $[(arene)M(CO)_n]$  complexes<sup>168</sup>. The conformations adopted by the Ph groups are markedly different from those adopted in 23. As might be expected, the Ph groups are now unable to orient themselves parallel to the coordinated  $C_6$  ring, and the result is random

disposition of the Ph groups. The observed orientations are presumably strongly influenced by a combination of intraligand and packing effects.

## Chapter 6

X-ray Crystallographic Comparison of the  $\pi$ -Bonding Abilities  
of Arene, Cyclopentadienyl, Cyclohexadienyl, and Pentadienyl  
Ligands in Iron(II) Sandwich Complexes

Ferrocene,  $[(\text{cyclopentadienyl})_2\text{Fe}]$ , 2, is the prototypical<sup>59,169</sup> and perhaps the most generally recognized example of a full-sandwich iron(II) complex. Subsequent work spanning three decades has resulted in synthesis and characterization of several isoelectronic analogues, including the following:  $[(\text{arene})_2\text{Fe}]^{2+}$  <sup>170</sup>, 1;  $[(\text{pentadienyl})_2\text{Fe}]$ <sup>60</sup>, 3; and  $[(\text{cyclohexadienyl})_2\text{Fe}]$ <sup>65-68</sup>, 4.



A number of mixed ligand sandwiches have also been prepared and, as for the symmetric sandwiches, several have been characterized via X-ray crystallography. These include  $[(\text{pentadienyl})(\text{cyclopentadienyl})\text{Fe}]$ <sup>60</sup>, 5,  $[(\text{arene})(\text{cyclopentadienyl})\text{Fe}]^+$ ,<sup>80,95</sup> 6,  $[(\text{arene})(\text{cyclohexadienyl})\text{Fe}]^+$ ,<sup>98,171</sup> 7, and  $[(\text{cyclohexadienyl})(\text{cyclopentadienyl})\text{Fe}]$ <sup>109,167</sup>, 8.

An important question that can be asked with respect to these complexes is: which of four ligands is best able to  $\pi$ -bond to the metal, and why? Comparing the structures

described in this thesis with relevant literature compounds allows us to extend the comparisons already drawn between cyclopentadienyl and pentadienyl<sup>60</sup> to arene and cyclohexadienyl ligands.

Structural parameters for a range of symmetrical and mixed iron(II) full-sandwich complexes obtained via single crystal X-ray crystallography are presented in Table 6.1 and form the basis for the following discussion. Table 6.1 permits estimates of the relative interaction of the arene, cyclopentadienyl, pentadienyl, and cyclohexadienyl ligands with the iron atom by facilitating comparison of the structural parameters for the mixed complexes with those for the bis(ligand) complexes. Three parameters may be considered as measures of the iron-ligand interaction: (i) average Fe-C distance, (ii) Fe-ligand plane distance, (iii) average C-C ring distance.

One might initially expect Fe-C bond distance to be the most effective measure of Fe-ligand interaction. However this does not necessarily appear to be the case for this study. Comparison of the iron-carbon distances in [(pentadienyl)<sub>2</sub>Fe], [(cyclopentadienyl)<sub>2</sub>Fe], and [(pentadienyl)(cyclopentadienyl)Fe] complexes indicates that in the mixed ligand complex the pentadienyl ligand is 0.027 to 0.029 Å closer to the iron atom than it is in [(pentadienyl)<sub>2</sub>Fe] whereas the cyclopentadienyl ligand is the same distance as in ferrocene. Therefore, there is a

**Table 6.1** Crystallographic Comparison of the Metal-Ligand Interactions in Iron(II) Sandwich Complexes.

Complex	Type <sup>a</sup>	Average M-C distance (Å)	Average C-C distance (Å)	M-C plane distance (Å)	Reference
$[(C_5H_5)_2Fe]$	A	2.05(2)	1.40(4)	1.66	172
$[(C_6H_3Me_3)_2Fe](PF_6)_2$	B	2.12(1)	1.400(1)	1.594(1)	173
$[(^tBu-C_6H_6)_2Fe]$	C	2.06(3)	1.39(1)	1.556(3)	68
$[(^tBu-C_6H_3Me_3)_2Fe]$	C	2.09(4)	1.409(6)	1.571(3)	159
$[(Ph-C_6H_3Me_3)_2Fe]$	C	2.07(4)	1.41(1)	1.55	67
$[(2,3,4-C_8H_{13})_2Fe]$	D	2.087(1)	1.412(2)	1.46(1)	174
$[(2,4-C_7H_{11})_2Fe]$	D	2.089(1)	1.411(8)	1.458(8)	175

<sup>a</sup> A = [(cyclopentadienyl)<sub>2</sub>Fe], B = [(arene)<sub>2</sub>Fe]<sup>2+</sup>, C = [(cyclohexadienyl)<sub>2</sub>Fe], D = [(pentadienyl)<sub>2</sub>Fe], E = [(arene)(cyclopentadienyl)Fe]<sup>+</sup>, F = 19e<sup>-</sup> [(arene)(cyclopentadienyl)Fe], G = [(cyclohexadienyl)(cyclopentadienyl)Fe], H = [(pentadienyl)(cyclopentadienyl)Fe], I = [(arene)(cyclohexadienyl)Fe]<sup>+</sup>. <sup>b</sup> Not available.

Table 6.1 (con't) Crystallographic Comparison of the Metal-Ligand Interactions in Iron(II) Sandwich Complexes.

$\eta^5$ -ligand

Complex	Type <sup>a</sup>	Avg. M-C Dist. (Å)	Avg. C-C Dist. (Å)	M-C <sub>5</sub> Plane Dist. (Å)	Ref.
$[(C_5H_5)(C_6Et_6)Fe]PF_6$	E	2.05(1)	1.38(1)	1.683(1)	80
$[(C_5H_5)(C_6Et_6)Fe]BPh_4$	E	2.05(1)	1.40(1)	1.68	95
$[(C_5H_5)(C_6Me_6)Fe]$	F	2.144(2)	b	1.79(1)	176
$[(C_5H_5)[C_6H_3(CF_3)_3C(O)CH_3]Fe]$	G	2.06(1) 2.05(2)	1.40(1) 1.415(5)	1.68 1.52	167
$[(C_5H_5)(Ph-C_6H_3Me_3)Fe]$	G	2.059(3) 2.06(3)	1.405(9) 1.418(6)	1.677(2) 1.526(1)	109
$[(C_5H_5)(2,4-C_7H_{11})Fe]$	H	2.05(1) 2.06(2)	1.37(6) 1.43(1)	1.69 1.42	177
$[(Et-C_6H_3Me_3)(C_6H_3Me_3)Fe]PF_6$	I	2.09(5)	1.41(2)	1.586(4)	98
$[(CH_2Cl-C_6H_3Me_3)(C_6H_3Me_3)Fe]PF_6$	I	2.09(5)	1.42(1)	1.570(4)	171

Table 6.1 (con't) Crystallographic Comparison of the Metal-Ligand Interactions in Iron(II) Sandwich Complexes.

$\eta^6$ -ligand

Complex	Type <sup>a</sup>	Avg. M-C Dist. (Å)	Avg. C-C Dist. (Å)	M-C <sub>6</sub> Plane Dist. (Å)	Ref.
$[(C_5H_5)(C_6Et_6)Fe]PF_6$	E	2.11(2)	1.43(1)	1.55(1)	80
$[(C_5H_5)(C_6Et_6)Fe]BPh_4$	E	2.10(1)	1.423(9)	1.54	95
$[(C_5H_5)(C_6Me_6)Fe]$	F	2.100(7)	b	1.58(1)	176
$[(Et-C_6H_3Me_3)(C_6H_3Me_3)Fe]PF_6$	I	2.11(2)	1.41(1)	1.570(4)	98
$[(CH_2Cl-C_6H_3Me_3)(C_6H_3Me_3)Fe]PF_6$	I	2.11(2)	1.40(1)	1.555(4)	171

suggestion that pentadienyl interacts more favourably with iron(II) than cyclopentadienyl; the conclusion reached earlier by Ernst et. al. from their investigation of [(pentadienyl)(cyclopentadienyl)Fe].

An observation that must be considered, however, is that as the ligand plane approaches the Fe atom the C-C bond distances in the  $C_6$  ring increase (as one would expect if increased  $\pi$ -back bonding from the metal to a ligand antibonding orbital occurs) thereby partially offsetting the decrease in the M-C bond distance.

It might therefore be anticipated that the metal-ligand plane distance would be a more effective measure of metal-ligand interaction as it should be less influenced by changes in C-C bond distance. The Fe-cyclopentadienyl plane distance for [(Ph-1,3,5- $C_6H_3Me_3$ )( $C_5H_5$ )Fe] is 0.02 Å greater than that observed for ferrocene whereas the Fe-cyclohexadienyl plane distance is 0.02 - 0.04 Å less than that seen for the [(cyclohexadienyl) $_2$ Fe] complexes. The Fe-C bond distances exhibit a similar trend but it is not as extreme. Similarly, in mixed complexes containing the cyclopentadienyl and arene ligands the cyclopentadienyl ligand plane moves away from the metal vs. ferrocene (by as much as 0.13 Å in the 19-electron complex [( $C_5H_5$ )( $C_6Me_6$ )Fe]) while the M-arene plane distance contracts by as much as 0.05 Å vs. [(arene) $_2$ Fe] $^{2+}$ . Finally, in [(arene)(cyclohexadienyl)Fe] $^+$  complexes the Fe-

cyclohexadienyl plane distance increases by an average of 0.02 Å vs. [(cyclohexadienyl)<sub>2</sub>Fe], while the Fe-arene plane distance decreases on average 0.031 Å from that of the [(arene)<sub>2</sub>Fe]<sup>2+</sup> complexes. Similar trends are observed for [(pentadienyl)(cyclopentadienyl)Fe] vs. ferrocene and [(pentadienyl)<sub>2</sub>Fe], with the Fe-plane distances showing a greater change than the Fe-C bond distances. The metal plane distance therefore does indeed appear to be the most sensitive measure of Fe-ligand interaction.

Evaluation of these solid-state X-ray structural results therefore leads us to rank the ligands in following order of metal-ligand interaction: arene > cyclohexadienyl ~ pentadienyl > cyclopentadienyl. Although the steric differences between the four ligands are not considered, particularly the effects of 1,5 substituents in the cyclohexadienyl complexes, it should be noted that the order suggested above corresponds to the relative susceptibility of the [(ligand)<sub>2</sub>Fe] complexes to undergo reduction and/or nucleophilic addition. In this context [(arene)<sub>2</sub>Fe]<sup>2+</sup> complexes are known to be quite reactive ( $E^{\circ} = \sim -0.48\text{v}$ ), [(arene)(cyclohexadienyl)Fe]<sup>+</sup> and [(arene)(cyclopentadienyl)Fe]<sup>+</sup> complexes undergo attack at the arene ring ( $E^{\circ} = \sim -1.55\text{v}$ ), and [(cyclopentadienyl)<sub>2</sub>Fe] is relatively unreactive<sup>4</sup>. However, Table 6.1 is incomplete since there are no reported [(arene)(pentadienyl)Fe]<sup>+</sup> and [(pentadienyl)(cyclohexadienyl)Fe] complexes.

Chapter 7

**General Conclusions and Suggestions for Future Research**

## 7.1 General Conclusions

From the work presented in this thesis it has been shown that net addition of carbanions to  $[(\text{arene})_2\text{Fe}]^{2+}$  dications is facile, not only with alkylaluminum reagents, but with traditional  $\text{R}^-$  sources such as Grignard and lithium reagents, when dichloromethane is employed as solvent. The  $[(\text{arene})(\text{cyclohexadienyl})\text{Fe}]^+$  cations reported herein represent the first crystallographically characterized mixed arene-cyclohexadienyl complexes of iron and syntheses of  $[(\text{R}-\text{C}_6\text{Me}_6)(\text{C}_6\text{Me}_6)\text{Fe}]^+$  cations are the first examples of direct high-yield net carbanion addition at an alkylated arene ring position. Furthermore, when double net carbanion addition to  $[(\text{arene})_2\text{Fe}]^{2+}$  dications occurs under these conditions,  $[(\text{cyclohexadienyl})_2\text{Fe}]$  complexes are formed in preference to  $[(\text{cyclohexadiene})(\text{arene})\text{Fe}]$  molecules. It has also been established that the use of  $\text{AlMe}_3$  and dihalomethane solvents provide a novel means for introducing the  $-\text{CH}_2\text{X}$  functionality (cleanly in one case) onto coordinated aromatics. The bulk of experimental evidence suggests that the above reactions proceed via single electron transfer mechanisms rather than nucleophilic addition.

We have demonstrated that decomplexation of the cyclohexadienyl ligands of pseudoferrocenes via reaction with  $\text{HCl}$ ,  $\text{DDQ}$ , or pyrolysis yield functionalized aromatic molecules.

This work has also provided a synthetic route to several new mixed-arene iron(II) sandwich complexes and has contributed the first crystallographic characterizations of these compounds. Reactions of the  $[(\text{arene})(\text{arene}')\text{Fe}]^{2+}$  dications with borohydride and carbanion sources has shown that there is a preference for carbon-carbon bond formation at the least sterically hindered arene ring, and that by employing  $\text{C}_6\text{Et}_6$  as one of the ligands the regioselectivity of the reaction could be effectively controlled.

It has also been demonstrated that the previously synthesized  $[(\text{C}_6(\text{CH}_2\text{CH}_2\text{C}_6\text{H}_5)_6)(\text{C}_5\text{H}_5)\text{Fe}]^+$  cation adopts a six distal conformation of the arene ligands in the solid state. To our knowledge, this is the first example of an arene exclusively adopting such a conformation. Variable temperature  $^1\text{H}$  NMR spectra of this complex suggest that the six distal conformation is preserved in solution.

A crystallographic analysis of mixed iron(II) sandwich complexes containing the arene, cyclopentadienyl, cyclohexadienyl, and pentadienyl ligands has led us to conclude that the ability of the these ligands to  $\pi$ -bond to iron has the order arene > cyclohexadienyl ~ pentadienyl > cyclopentadienyl.

## 7.2 Suggestions for Future Research

While we have shown that the reaction of  $[(\text{arene})_2\text{Fe}]^{2+}$

dications with trialkylaluminum reagents is more consistent with a SET mechanism than a nucleophilic attack of  $R^-$ , we have not undertaken a mechanistic study of these reactions. As a result, the nature of the species involved in the electron transfer and coupling steps is unclear. A more detailed mechanistic study would therefore be a worthwhile undertaking and could shed some light on the reaction pathway.

The  $[(\text{cyclohexadienyl})_2\text{Fe}]$  and  $[(\text{arene})(\text{cyclohexadienyl})\text{Fe}]^+$  complexes that have been synthesized as part of this work have considerable potential for decomplexation of the cyclohexadienyl moiety to yield functionalized aromatics. However, problems still exist in the decomplexation reactions and isolation of pure aromatics and, as a result, more work needs to be done in this area. It is also possible that the range of R groups could be extended to include carbanions containing other functionalities (eg.  $\text{CH}_2\text{COCH}_3^-$ ,  $\text{CCl}_3^-$ ) as well as other non-metal and transition metal moieties.

While it is disappointing that  $[(\text{arene})(\text{arene}')\text{Fe}]^{2+}$  dications did not react with anions to produce  $[(\text{cyclohexadiene})(\text{arene})\text{Fe}]$  complexes, it is possible that further investigations will prove fruitful, for example, in the reaction of  $[(1,4-\text{C}_6\text{H}_4\text{Me}_2)(\text{C}_6\text{Et}_6)\text{Fe}]^{2+}$  with  $\text{NaBET}_3\text{H}$ .

Another prospect for future research lies with the synthesis and X-ray crystallographic characterization of, as

yet unreported, [(arene)(pentadienyl)Fe]<sup>+</sup> and [(cyclohexadienyl)(pentadienyl)Fe] complexes. Such complexes would provide a further opportunity to examine the relative  $\pi$ -bonding abilities of the arene, cyclohexadienyl, and pentadienyl ligands.

In more general terms, we believe [(arene)<sub>2</sub>Fe]<sup>2+</sup>, [(arene)(cyclohexadienyl)Fe]<sup>+</sup>, and [(cyclohexadienyl)<sub>2</sub>Fe] complexes have the potential to be used as templates for the design and assembly of unnatural molecules. When we consider such factors as ease and cost of synthesis, the range of charges of the complexes (0, 1+, 2+), altered reactivity of ligands, the steric influence upon ligands as a result of complexation, and susceptibility to reduction the potential uses of such complexes should be apparent. It is hoped that by extending the chemistry of these compounds we have laid the groundwork for others to make advances in this area of chemistry.

**Chapter 8**

**Experimental**

## 8.1 General

### 8.1a Chemicals and Apparatus

The following chemicals were purchased from the Aldrich Chemical Company, Inc. and were used as supplied: chloroform-d, acetone-d<sub>6</sub>, acetonitrile-d<sub>3</sub>, benzene-d<sub>6</sub>, hexamethylbenzene, ammonium hexafluorophosphate, methyllithium phenyllithium, tert-butyllithium, benzylmagnesium bromide, tert-butylmagnesium bromide, sodium borohydride, sodium triethylborohydride, ferrocene, benzyl bromide, anhydrous magnesium sulphate, decahydronaphthalene potassium metal, phosphorus pentoxide, pentamethylbenzene, and 2,3-dichloro-5,6-dicyanoquinone. Dibromomethane, which was distilled over phosphorus pentoxide under a nitrogen atmosphere prior to use, para-xylene, mesitylene, and 1,2-dichloroethane which were distilled over CaH<sub>2</sub> under a nitrogen atmosphere prior to use were also purchased from the Aldrich Chemical Company. Dichloromethane, hexanes, and tetrahydrofuran, purchased from BDH Chemicals, were distilled over calcium hydride under a nitrogen atmosphere prior to use. Anhydrous calcium chloride, diethyl ether, and acetone were also purchased from BDH and used as supplied. Benzene, which was distilled over CaH<sub>2</sub> under nitrogen, and acetonitrile, used as supplied, were purchased from Anachemia Chemicals Ltd. Anhydrous iron(III) chloride,

aluminum metal, and aluminum chloride, purchased from Johnson-Matthey Inc.; calcium hydride and hexaethylbenzene purchased from the Eastman Kodak Company; and trimethylaluminum and triethylaluminum, purchased from Texas Alkyls, were used as supplied. Meta-xylene, also purchased from the Eastman Kodak Company, was distilled over  $\text{CaH}_2$  under  $\text{N}_2$  prior to use. Nitrogen and argon gases were purchased from Atlantic Oxygen and hydrogen chloride gas was purchased from Matheson Gas Products Canada.

Glassware was thoroughly cleaned by soaking in alcoholic KOH, chromic acid, aqua regia, or a hydrogen peroxide solution of KOH, and oven-dried at  $100^\circ\text{C}$ . All manipulations involving neat trialkylaluminum reagents were conducted in a Vacuum Atmospheres' glove box under an atmosphere of argon. All other handling of air sensitive materials was conducted either in the glove box or with Schlenk glassware using standard vacuum line techniques. Nitrogen gas was passed through a tube containing anhydrous calcium chloride to ensure removal of water vapour.

### 8.1b Spectroscopy

Routine 60 MHz  $^1\text{H}$  NMR spectra were obtained on a Varian EM-360 spectrometer, while 360 MHz  $^1\text{H}$  and  $^{13}\text{C}$  NMR spectra were recorded by the staff of the Atlantic Regional Magnetic Resonance Centre using a Nicolet 360NB spectrometer.

Infrared spectra were obtained on a Perkin Elmer 1600 Fourier Transform Infrared Spectrophotometer. Samples for NMR spectroscopy were dissolved in an appropriate deuterated solvent and IR samples were prepared as 5% mixtures of the compounds in KBr and recorded using a diffuse reflectance accessory.

### 8.1c Analysis

Elemental analyses were performed by the Canadian Microanalytical Service Ltd., Vancouver.

## 8.2 Synthetic Procedures and Product Characterization

### 8.2a Synthesis of Starting Materials

The following procedures are based on those reported by Helling et al.<sup>131</sup> The complexes listed below were synthesized as follows: 5.00g (30.8 mmol) of anhydrous  $\text{FeCl}_3$  and 12.33g (92.5 mmol) of  $\text{AlCl}_3$  were refluxed in 100 ml of benzene (**1a**), or stirred at room temperature in para-xylene (**1b**) or mesitylene (**1c**) for 24 hours. The reaction flask was then cooled to  $0^\circ\text{C}$  and the contents extracted with 150 ml of  $\text{H}_2\text{O}$ . After filtration the aqueous phase was washed with hexanes, separated, and the complex precipitated as an orange solid with aqueous  $\text{NH}_4^+\text{PF}_6^-$ . The solids were washed

with hexanes or ether and dried under vacuum or, in the case of **1b**, recrystallized from acetone/H<sub>2</sub>O, washed with hexanes or ether, and dried under vacuum.

(**1a**) Bis( $\eta^6$ -benzene)iron(II) hexafluorophosphate -

Yield: 7.43g (14.8 mmol, 48%). <sup>1</sup>H NMR (CD<sub>3</sub>CN):  $\delta$  6.93(s); <sup>13</sup>C NMR (CD<sub>3</sub>CN):  $\delta$  95.2d. IR (cm<sup>-1</sup>): 3099s, 1455s, 1029m, 843s.

(**1b**) Bis( $\eta^6$ -para-xylene)iron(II) hexafluorophosphate -

Yield: 10.10g (18.1 mmol, 59%). <sup>1</sup>H NMR ((CD<sub>3</sub>)<sub>2</sub>CO):  $\delta$  7.01(s,4H), 2.70(s,6H); <sup>13</sup>C NMR ((CD<sub>3</sub>)<sub>2</sub>CO):  $\delta$  112.0s, 94.0d, 19.4q. IR (cm<sup>-1</sup>): 3089m, 3026w, 2998w, 2939m, 1558m, 1490m, 1450m, 1122m, 1031m, 843s.

(**1c**) Bis( $\eta^6$ -mesitylene)iron(II) hexafluorophosphate -

Yield: 9.58g (16.3 mmol, 53%). <sup>1</sup>H NMR ((CD<sub>3</sub>)<sub>2</sub>CO):  $\delta$  2.64(s,9H), 6.50(s,3H); <sup>13</sup>C NMR ((CD<sub>3</sub>)<sub>2</sub>CO):  $\delta$  113.3s, 92.0d, 19.7q. IR (cm<sup>-1</sup>): 3117m, 3076m, 2930w, 1548m, 1459s, 1388m, 1036m, 1016m, 842s.

The following complexes were synthesized by stirring 5.00g (30.8 mmol) of anhydrous FeCl<sub>3</sub>, 12.33g (92.5 mmol) of AlCl<sub>3</sub>, and 61.6 mmol of pentamethylbenzene (**1d**) or hexamethylbenzene (**1e**) in 100 ml of decalin at 90°C for 24 hours. The reaction flask was then cooled to 0°C and the

contents extracted with 200 ml of H<sub>2</sub>O. After filtration the aqueous phase was washed with hexanes, separated, and precipitated as orange solids with aqueous NH<sub>4</sub><sup>+</sup>PF<sub>6</sub><sup>-</sup>. The solids were subsequently recrystallized from acetonitrile/water or acetone/water, washed with hexanes, and dried under vacuum.

(1d) Bis( $\eta^6$ -pentamethylbenzene)iron(II)

hexafluorophosphate - Yield: 14.25g (22.2 mmol, 72%). <sup>1</sup>H NMR ((CD<sub>3</sub>)<sub>2</sub>CO):  $\delta$  6.36(s,1H), 2.36(s,9H), 2.26(s,6H); <sup>13</sup>C NMR ((CD<sub>3</sub>)<sub>2</sub>CO):  $\delta$  107.7s, 106.8s, 105.3s, 92.5d, 18.0q, 15.4q, 14.9q. IR (cm<sup>-1</sup>): 3107m, 3061m, 3006m, 2942m, 1466s, 1441s, 1393s, 1294m, 1081m, 1026m, 842s.

(1e) Bis( $\eta^6$ -hexamethylbenzene)iron(II)

hexafluorophosphate - Yield: 16.04g (23.9 mmol, 81%). <sup>1</sup>H NMR ((CD<sub>3</sub>)<sub>2</sub>CO):  $\delta$  2.52(s); <sup>13</sup>C NMR ((CD<sub>3</sub>)<sub>2</sub>CO):  $\delta$  104.6s, 15.9q. IR (cm<sup>-1</sup>): 3020w, 2923w, 1448m, 1394m, 1073m, 1019m, 1002m, 844s.

## 8.2b Synthesis of Ethylation Products

**2a-e** were prepared as follows: 2.00g of **1a** (3.98 mmol), **1b** (3.58 mmol), **1c** (3.41 mmol), **1d** (3.11 mmol), or **1e** (2.98 mmol) were stirred in 100 ml of CH<sub>2</sub>Cl<sub>2</sub> (or 1,2-dichloroethane in the case of **1c**) to which was added a four-

fold excess of  $\text{AlEt}_3$ . A black (**2a-b**) or purple (**2c-e**) suspension formed within one minute and the mixture was stirred for 24 hours. The reaction vessel was then cooled to  $0^\circ\text{C}$  and the solution was quenched with ice water. After filtration the halocarbon phase was concentrated under reduced pressure to afford orange (**2a-b**) or red (**2c-e**) solids which were recrystallized from acetone/ $\text{H}_2\text{O}$ .

(**2a**)  $(\eta^5\text{-exo-Ethylcyclohexadienyl})(\eta^6\text{-benzene})\text{iron(II)}$  hexafluorophosphate - Yield: 0.43g (1.1 mmol, 28%). The recrystallized product was shown via NMR spectroscopy to contain an impurity which could not be separated from the organometallic complex.  $^1\text{H}$  NMR ( $(\text{CD}_3)_2\text{CO}$ ):  $\delta$  6.98(t,1H), 6.46(s,6H), 4.94(t,2H), 3.94(t,2H), 2.60(t,1H), 0.46(t,3H), 0.37(q,2H);  $^{13}\text{C}$  NMR ( $(\text{CD}_3)_2\text{CO}$ ):  $\delta$  91.8d, 91.5d, 85.7d, 84.6d, 48.9d, 11.8dt, 6.2q. IR ( $\text{cm}^{-1}$ ): 3097m, 2958m, 2931m, 2874m, 1455m, 1379w, 920m, 842s, 668m.

(**2b**)  $(\eta^5\text{-exo-5-Ethyl-1,4-dimethylcyclohexadienyl})(\eta^6\text{-para-xylene})\text{iron(II)}$  hexafluorophosphate - Yield: 0.40g (0.92 mmol, 23%). The recrystallized product was shown via NMR spectroscopy to contain minor impurities which could not be separated from the organometallic species.  $^1\text{H}$  NMR ( $(\text{CD}_3)_2\text{CO}$ ):  $\delta$  6.59(d,1H), 6.32(d,2H), 5.39(d,2H), 4.56(d,1H), 3.38(d,1H), 2.65(s,6H), 2.00(s,3H), 1.72(s,3H), 0.47(m,5H), (the *endo*-H could not be located due to

overlapping resonances);  $^{13}\text{C}$  NMR ( $\text{CDCl}_3$ ):  $\delta$  104.4s, 99.4s, 92.1d, 89.6d, 83.2d, 81.9d, 68.2s, 47.9d, 43.9d, 31.6t, 23.5q, 20.4q, 19.6q, 9.1q. IR ( $\text{cm}^{-1}$ ): 3004m, 2890w, 1480m, 1458m, 1390m, 1184m, 1032m, 840s, 789m.

(2c) ( $\eta^5$ -exo-6-Ethyl-1,3,5-trimethylcyclohexadienyl)( $\eta^6$ -mesitylene)iron(II) hexafluorophosphate - 1.26g (78%) of a mixture of products were revealed through NMR spectroscopy: [(Et-1,3,5- $\text{C}_6\text{H}_3\text{Me}_3$ )(1,3,5- $\text{C}_6\text{H}_3\text{Me}_3$ )Fe]PF<sub>6</sub> (2.16 mmol, 80%) and [(CH<sub>2</sub>CH<sub>2</sub>Cl-1,3,5- $\text{C}_6\text{H}_3\text{Me}_3$ )(1,3,5- $\text{C}_6\text{H}_3\text{Me}_3$ )Fe]PF<sub>6</sub> (0.50 mmol, 20%). [(Et-1,3,5- $\text{C}_6\text{H}_3\text{Me}_3$ )(1,3,5- $\text{C}_6\text{H}_3\text{Me}_3$ )Fe]PF<sub>6</sub> -  $^1\text{H}$  NMR ( $(\text{CD}_3)_2\text{CO}$ ):  $\delta$  5.86(s,3H), 4.37(s,2H), 2.76(s,3H), 2.61(t,1H), 2.47(s,9H), 1.70(s,6H), 0.56(q,2H), 0.46(t,3H);  $^{13}\text{C}$  NMR ( $(\text{CD}_3)_2\text{CO}$ ):  $\delta$  102.0s, 94.8s, 92.5d, 84.0d, 63.0s, 49.0d, 29.8t, 23.3q, 18.7q, 11.3q, 5.3q. IR ( $\text{cm}^{-1}$ ): 3056w, 2975m, 2929m, 1540m, 1452m, 1383m, 1037m, 1012m, 875m, 840s.

(2d) ( $\eta^5$ -exo-6-Ethyl-1,2,3,4,5-pentamethylcyclohexadienyl)( $\eta^6$ -pentamethylbenzene)iron(II) hexafluorophosphate - Yield: 1.33g (2.53 mmol, 81%).  $^1\text{H}$  NMR ( $(\text{CD}_3)_2\text{CO}$ ):  $\delta$  5.22(s,1H), 2.53(s,3H), 2.46(s,6H), 2.35(s,6H), 1.95(s,3H), 1.85(s,6H), 1.53(s,6H), 0.46(dq,2H), 0.33(t,3H), (the *endo*-H could not be located due to overlapping resonances);  $^{13}\text{C}$  NMR ( $(\text{CD}_3)_2\text{CO}$ ):  $\delta$  102.8s, 101.7s, 100.3s, 98.5s, 92.6s, 91.4d, 57.0s, 53.5d, 29.9t,

20.7q, 19.7q, 18.2q, 15.6q, 14.4q, 13.9q, 11.2q. IR (cm<sup>-1</sup>):  
2964m, 2914m, 1468m, 1442m, 1388m, 1294m, 1074m, 1022m,  
839s.

(2e) ( $\eta^6$ -exo-Ethylhexamethylcyclohexadienyl) ( $\eta^6$ -  
hexamethylbenzene)iron(II) hexafluorophosphate - Yield:  
1.52g (2.74 mmol, 92%). <sup>1</sup>H NMR ((CD<sub>3</sub>)<sub>2</sub>CO):  $\delta$  2.51(s,3H),  
2.30(s,18H), 1.88(s,6H), 1.37(s,3H), 1.32(s,6H), 0.26(m,5H);  
<sup>13</sup>C NMR ((CD<sub>3</sub>)<sub>2</sub>CO):  $\delta$  100.8s, 92.7s, 91.8s, 56.8s, 45.3s,  
37.9t, 21.9q, 16.0q, 15.6q, 14.5q, 14.2q, 9.0q. IR (cm<sup>-1</sup>):  
2988m, 2957m, 2914m, 1458m, 1438m, 1390m, 1065m, 1024m,  
1004m, 876m, 842s.

### 8.2c Synthesis of Halomethylation Products

Halomethyl addition products were synthesized by stirring 2.00g of **1c** (3.41 mmol) or **1e** (2.98 mmol) in 100 ml of CH<sub>2</sub>Cl<sub>2</sub> (**3c**, **3e**) or CH<sub>2</sub>Br<sub>2</sub> (**4c**, **4e**) to which was added 4 molar equivalents of AlMe<sub>3</sub>. Within one minute purple solutions had formed with unreacted starting material still present. The mixtures were then stirred for 24 hours at which point the reaction vessels were cooled to 0°C and quenched with ice water. After filtration, the halocarbon phases were concentrated under reduced pressure to yield red solids which were recrystallized from acetone/H<sub>2</sub>O.

(3c) ( $\eta^5$ -exo-6-Chloromethyl-1,3,5-trimethylcyclohexadienyl)( $\eta^6$ -mesitylene)iron(II) hexafluorophosphate - 0.42g (25%) of a mixture of products were revealed through NMR spectroscopy that consisted of [(CH<sub>2</sub>Cl-1,3,5-C<sub>6</sub>H<sub>3</sub>Me<sub>3</sub>)(1,3,5-C<sub>6</sub>H<sub>3</sub>Me<sub>3</sub>)Fe]PF<sub>6</sub> (0.77 mmol, 90%) and [(Me-1,3,5-C<sub>6</sub>H<sub>3</sub>Me<sub>3</sub>)(1,3,5-C<sub>6</sub>H<sub>3</sub>Me<sub>3</sub>)Fe]PF<sub>6</sub> (0.09 mmol, 10%). [(CH<sub>2</sub>Cl-1,3,5-C<sub>6</sub>H<sub>3</sub>Me<sub>3</sub>)(1,3,5-C<sub>6</sub>H<sub>3</sub>Me<sub>3</sub>)Fe]PF<sub>6</sub> - <sup>1</sup>H NMR ((CD<sub>3</sub>)<sub>2</sub>CO):  $\delta$  5.87(s,3H), 4.45(s,2H), 3.03(t,1H), 2.76(s,3H), 2.60(d,2H), 2.50(s,9H), 1.80(s,6H); <sup>13</sup>C NMR ((CD<sub>3</sub>)<sub>2</sub>CO):  $\delta$  103.8s, 97.0s, 94.0d, 85.4d, 59.7s, 49.1d, 45.7t, 23.3q, 19.8q, 19.0q. IR (cm<sup>-1</sup>): 3056w, 2970m, 2917m, 1540m, 1455m, 1381m, 1038m, 841s, 737m.

(3e) ( $\eta^5$ -exo-Chloromethylhexamethylcyclohexadienyl)( $\eta^6$ -hexamethylbenzene)iron(II) hexafluorophosphate - Yield: 0.86g (1.5 mmol, 50%). <sup>1</sup>H NMR ((CD<sub>3</sub>)<sub>2</sub>CO):  $\delta$  2.53(s,3H), 2.32(s,18H), 2.20(s,2H), 1.92(s,6H), 1.51(s,3H), 1.41(s,6H); <sup>13</sup>C NMR ((CD<sub>3</sub>)<sub>2</sub>CO):  $\delta$  101.5s, 93.4s, 92.3s, 53.3s, 52.6t, 45.5s, 20.8q, 16.0q, 15.5q, 14.5q, 14.2q. IR (cm<sup>-1</sup>): 2992s, 2922s, 1440s, 1390s, 1063s, 1009m, 876m, 841s, 708m. Anal. Calcd for C<sub>25</sub>H<sub>38</sub>ClF<sub>6</sub>FeP: C, 52.24; H, 6.66%. Found: C, 52.01; H, 6.74.

(4c) ( $\eta^5$ -exo-6-Bromomethyl-1,3,5-trimethylcyclohexadienyl)( $\eta^6$ -mesitylene)iron(II) hexafluorophosphate - 0.62g (34%) of a mixture of products

was obtained containing  $[(\text{CH}_2\text{Br}-1,3,5\text{-C}_6\text{H}_3\text{Me}_3)(1,3,5\text{-C}_6\text{H}_3\text{Me}_3)\text{Fe}]\text{PF}_6$  (0.93 mmol, 80%) and  $[(\text{Me}-1,3,5\text{-C}_6\text{H}_3\text{Me}_3)(1,3,5\text{-C}_6\text{H}_3\text{Me}_3)\text{Fe}]\text{PF}_6$  (0.27 mmol, 20%).  $[(\text{CH}_2\text{Br}-1,3,5\text{-C}_6\text{H}_3\text{Me}_3)(1,3,5\text{-C}_6\text{H}_3\text{Me}_3)\text{Fe}]\text{PF}_6$  -  $^1\text{H NMR}$  ( $(\text{CD}_3)_2\text{CO}$ ):  $\delta$  5.88 (s, 3H), 4.46 (s, 2H), 3.05 (t, 1H), 2.75 (s, 3H), 2.50 (s, 9H), 2.09 (d, 2H), 1.83 (s, 6H);  $^{13}\text{C NMR}$  ( $(\text{CD}_3)_2\text{CO}$ ):  $\delta$  103.8s, 97.5s, 93.9d, 85.1d, 60.2s, 48.7d, 33.2t, 23.3q, 19.8q, 19.0q. IR ( $\text{cm}^{-1}$ ): 3001w, 2983m, 1538m, 1454m, 1384m, 1037m, 842s.

**(4e)**  $(\eta^6\text{-exo-Bromomethylhexamethylcyclohexadienyl})(\eta^6\text{-hexamethylbenzene})\text{iron(II) hexafluorophosphate}$  - Yield: 1.29g (2.08 mmol, 70%).  $^1\text{H NMR}$  ( $(\text{CD}_3)_2\text{CO}$ ):  $\delta$  2.52 (s, 3H), 2.33 (s, 18H), 2.14 (s, 2H), 1.93 (s, 6H), 1.51 (s, 3H), 1.46 (s, 6H);  $^{13}\text{C NMR}$  ( $(\text{CD}_3)_2\text{CO}$ ):  $\delta$  101.6s, 93.3s, 92.4s, 52.8s, 44.7s, 42.4t, 21.8q, 16.0q, 15.4q, 14.5q, 14.3q. Anal. Calcd for  $\text{C}_{20}\text{H}_{29}\text{FFeP}_6$ : C, 48.49%; H, 6.18%. Found: C, 48.94%; H, 6.22%. IR ( $\text{cm}^{-1}$ ): 3008m, 2914m, 1438m, 1390m, 1066m, 1009m, 876m, 843s.

## 8.2d Synthesis of Hydride Addition Products

The net hydride addition products

$[(\text{H}-\text{C}_6\text{H}_n\text{Me}_{6-n})(\text{C}_6\text{H}_n\text{Me}_{6-n})\text{Fe}]\text{PF}_6$  ( $n = 0, 1$ ), **5a-e**, were prepared by stirring 1.00g of **1a** (1.99 mmol), **1b** (1.79 mmol), **1c** (1.71 mmol), **1d** (1.56 mmol), or **1e** (1.49 mmol) in 50 ml of dichloromethane to which were added 10 molar equivalents of

NaBH<sub>4</sub> as a 20 ml aqueous solution. After stirring for 90 minutes the reaction mixtures were filtered and the filtrate concentrated under reduced pressure. The resulting solids were washed with H<sub>2</sub>O and ether and recrystallized from acetone/H<sub>2</sub>O.

(5a) ( $\eta^5$ -exo-Hydridocyclohexadienyl)( $\eta^6$ -benzene)iron(II) hexafluorophosphate - 0.04g (0.1 mmol, 6%) of a mixture of [(H-C<sub>6</sub>H<sub>6</sub>)(C<sub>6</sub>H<sub>6</sub>)Fe]PF<sub>6</sub> and [(CH<sub>2</sub>Cl-C<sub>6</sub>H<sub>6</sub>)(C<sub>6</sub>H<sub>6</sub>)Fe]PF<sub>6</sub> was obtained in the ratio 70/30, respectively. [(H-C<sub>6</sub>H<sub>6</sub>)(C<sub>6</sub>H<sub>6</sub>)Fe]PF<sub>6</sub> - <sup>1</sup>H NMR ((CD<sub>3</sub>)<sub>2</sub>CO):  $\delta$  7.14(t,1H), 6.44(s,6H), 4.98(t,2H), 3.58(t,2H), 2.85(dt,1H), 1.10(d,1H); <sup>13</sup>C NMR ((CD<sub>3</sub>)<sub>2</sub>CO): 91.7d, 86.5d, 85.0d, 40.5d, 24.8t. IR (cm<sup>-1</sup>): 3096m, 2833m, 1450m, 1299m, 839s.

(5b) ( $\eta^5$ -exo-5-Hydrido-1,4-dimethylcyclohexadienyl)( $\eta^6$ -para-xylene)iron(II) hexafluorophosphate - Yield: 0.27g (0.65 mmol, 36%) with a minor impurity (< 5%) of [(CH<sub>2</sub>Cl-1,4-C<sub>6</sub>H<sub>4</sub>Me<sub>2</sub>)(1,4-C<sub>6</sub>H<sub>4</sub>Me<sub>2</sub>)Fe]PF<sub>6</sub>. [(H-1,4-C<sub>6</sub>H<sub>4</sub>Me<sub>2</sub>)(1,4-C<sub>6</sub>H<sub>4</sub>Me<sub>2</sub>)Fe]PF<sub>6</sub> - <sup>1</sup>H NMR ((CD<sub>3</sub>)<sub>2</sub>CO):  $\delta$  6.76(d,1H), 6.38(dd,2H), 5.34(dd,2H), 4.59(d,1H), 3.13(d,1H), 2.66(s,6H), 1.99(s,3H), 1.61(s,3H), 1.39(br d,1H), (the endo-H could not be located due to overlapping resonances); <sup>13</sup>C NMR ((CD<sub>3</sub>)<sub>2</sub>CO):  $\delta$  105.9s, 102.7s, 93.5d, 89.6d, 85.3d, 82.9d, 60.8s, 43.2d, 32.0t, 24.4q, 20.4q, 19.8q. IR(cm<sup>-1</sup>): 3074m, 2922m, 2744w, 1489m, 1449m, 1385m, 1031s, 838s.

(5c) ( $\eta^5$ -exo-6-Hydrido-1,3,5-trimethylcyclohexadienyl)( $\eta^6$ -mesitylene)iron(II) hexafluorophosphate - Yield: 0.40g (0.90 mmol, 53%) with a minor impurity (< 5%) of 3c. [(H-1,3,5-C<sub>6</sub>H<sub>3</sub>Me<sub>3</sub>)(1,3,5-C<sub>6</sub>H<sub>3</sub>Me<sub>3</sub>)Fe]PF<sub>6</sub> - <sup>1</sup>H NMR ((CD<sub>3</sub>)<sub>2</sub>CO):  $\delta$  5.78(s,3H), 4.39(s,2H), 2.80(s,3H), 2.59(d,1H), 2.45(s,9H), 1.56(s,6H), (the endo-H could not be located due to overlapping resonances); <sup>13</sup>C NMR ((CD<sub>3</sub>)<sub>2</sub>CO):  $\delta$  103.1s, 96.0s, 93.4d, 86.5d, 58.9s, 37.8t, 24.0q, 20.1q, 18.9q. IR (cm<sup>-1</sup>): 3058m, 2977m, 2815m, 2449w, 1536m, 1449m, 1381m, 1039m, 920w, 838s.

(5d) ( $\eta^5$ -exo-6-Hydrido-1,2,3,4,5-pentamethylcyclohexadienyl)( $\eta^6$ -pentamethylbenzene)iron(II) hexafluorophosphate - Yield: 0.55g (1.1 mmol, 71%) with a minor impurity (< 5%) of [(CH<sub>2</sub>Cl-C<sub>6</sub>HMe<sub>5</sub>)(C<sub>6</sub>HMe<sub>5</sub>)Fe]PF<sub>6</sub>. [(H-C<sub>6</sub>HMe<sub>5</sub>)(C<sub>6</sub>HMe<sub>5</sub>)Fe]PF<sub>6</sub> - <sup>1</sup>H NMR ((CD<sub>3</sub>)<sub>2</sub>CO):  $\delta$  5.21(s,1H), 2.59(s,3H), 2.46(s,6H), 2.30(s,6H), 1.96(s,3H), 1.86(s,6H), 1.40(s,6H), 1.23(d,1H), (the endo-H could not be located due to overlapping resonances); <sup>13</sup>C NMR ((CD<sub>3</sub>)<sub>2</sub>CO):  $\delta$  102.9s, 101.5s, 100.2s, 94.4s, 91.5d, 86.5s, 52.2s, 41.5t, 21.1q, 18.4q, 15.8q, 14.7q, 14.6q, 13.9q. IR (cm<sup>-1</sup>): 3000m, 2916m, 2873m, 2790m, 1468m, 1441m, 1390m, 1324m, 1073m, 1025m, 838s.

(5e) ( $\eta^5$ -exo-Hydridohexamethylcyclohexadienyl)( $\eta^6$ -hexamethylbenzene)iron(II) hexafluorophosphate - Yield: 0.31g (0.59 mmol, 39%) with a minor impurity (< 5%) of 3e.  $[(H-C_6Me_6)(C_6Me_6)Fe]PF_6$  -  $^1H$  NMR ( $(CD_3)_2CO$ ):  $\delta$  2.55(s, 3H), 2.31(s, 18H), 1.86(s, 6H), 1.27(d, 3H), 1.20(s, 6H), 0.95(q, 1H);  $^{13}C$  NMR ( $(CD_3)_2CO$ ):  $\delta$  100.8s, 95.0s, 91.6s, 50.3s, 39.1d, 20.7q, 16.5q, 16.0q, 15.0q, 13.9q. IR( $cm^{-1}$ ): 2986m, 2918m, 2790w, 1459m, 1389m, 1067m, 1011m, 841s.

### 8.2e Synthesis of Pseudoferrocenes

The [(cyclohexadienyl) $_2$ Fe] complexes **6a-8b** were synthesized by the following procedure. 2.00g of **1a** (3.98 mmol) or **1b** (3.58 mmol) were suspended in 30 ml of  $CH_2Cl_2$  and the reaction flask was degassed with nitrogen and cooled to  $-95^\circ C$ . Under a positive pressure of  $N_2$ , 4 molar equivalents of the appropriate lithium (**6a**, **8a-b**) or Grignard (**7a-b**) reagent were added via syringe. The reaction mixture was allowed to slowly warm to room temperature with stirring at which point 5 ml of  $H_2O$  were added to the flask. The contents were filtered and the filtrate was concentrated to a red oil which was extracted with hexanes, stirred over anhydrous  $MgSO_4$  and decolourizing carbon, and filtered. The orange filtrate was then concentrated to a red-orange oily solid under reduced pressure and dried under vacuum. The pseudoferrocene

complexes formed from double net carbanion addition to **1b** yield four isomers (two of which are enantiomers) giving a total of three diastereomers. NMR spectra were recorded on the first diastereomers of **7b** and **8b** to crystallize upon cooling a hexanes solution to  $-20^{\circ}\text{C}$ . Crystals of **8a** were obtained by cooling a hexanes solution to  $-20^{\circ}\text{C}$ .

(**6a**) Bis( $\eta^5$ -exo-phenylcyclohexadienyl)iron(II) - Yield: 0.91g (1.7 mmol, 63%).  $^1\text{H}$  NMR ( $\text{C}_6\text{D}_6$ ):  $\delta$  7.20(m,5H), 4.59(t,1H), 4.10(t,2H), 3.81(t,1H), 3.12(t,2H);  $^{13}\text{C}$  NMR ( $\text{C}_6\text{D}_6$ ):  $\delta$  129.0d, 127.4d, 126.2s, 84.8d, 77.9d, 43.2d, 41.2d. m.p. 140-150  $^{\circ}\text{C}$ .

(**7a**) Bis( $\eta^5$ -exo-benzylcyclohexadienyl)iron(II) - Yield: 1.18g (2.99 mmol, 75%).  $^1\text{H}$  NMR ( $\text{C}_6\text{D}_6$ ):  $\delta$  7.20(t,2H), 7.10(t,1H), 7.02(d,2H), 4.67(t,1H), 3.95(t,2H), 2.71(t,2H), 2.51(quint,1H), 1.76(d,2H);  $^{13}\text{C}$  NMR ( $\text{C}_6\text{D}_6$ ):  $\delta$  139.5s, 129.5d, 128.6d, 125.7d, 83.7d, 77.9d, 47.7t, 42.3d, 38.8d. Anal. Calcd for  $\text{C}_{26}\text{H}_{26}\text{Fe}$ : C, 50.92%; H, 4.27%. Found: C, 51.37%; H, 4.33%. m.p. 100-103 $^{\circ}\text{C}$ .

(**7b**) Bis( $\eta^5$ -exo-5-Benzyl-1,4-dimethylcyclohexadienyl)iron(II)\* - Yield: 1.30g (2.89 mmol, 80%).  $^1\text{H}$  NMR ( $\text{C}_6\text{D}_5\text{CD}_3$ ): ( $40^{\circ}\text{C}$ )  $\delta$  7.12(t,2H), 7.02(t,1H), 6.91(d,2H), 4.33(dd,1H), 3.70(d,1H), 2.49(dt,1H), 2.12(m,1H), 1.98(dd,1H), 1.57(s,3H), 1.53(dd,1H), 1.45(br

s, 3H);  $^{13}\text{C}$  NMR ( $\text{C}_6\text{H}_6$ ):  $\delta$  140.1s, 129.4d, 128.3d, 125.6d, 95.0s, 85.3d, 76.4d, 52.2s, 45.3d, 44.5t, 43.9d, 22.8q, 22.0q. m.p. 111-113°C. \* least soluble diastereomer.

(8a) Bis( $\eta^5$ -exo-tert-butylcyclohexadienyl)iron(II) -

Yield: 1.22g (3.73 mmol, 94%).  $^1\text{H}$  NMR ( $\text{C}_6\text{D}_6$ ):  $\delta$  4.53(t, 1H), 4.14(t, 2H), 2.85(t, 2H), 2.50(t, 1H), 0.63(s, 9H);  $^{13}\text{C}$  NMR ( $\text{C}_6\text{D}_6$ ):  $\delta$  85.6d, 75.9d, 48.0d, 42.8d, 37.2s, 25.9q. m.p. 90-91°C.

(8b) Bis( $\eta^5$ -exo-5-tert-butyl-1,4-

dimethylcyclohexadienyl)iron(II)\* - Yield: 1.14g (2.98 mmol, 82%).  $^1\text{H}$  NMR ( $\text{C}_6\text{D}_6$ ):  $\delta$  4.17(d, 1H), 3.82(d, 1H), 2.31(d, 1H), 2.20(s, 3H), 1.66(s, 3H), 1.27(d, 1H), 0.66(s, 9H);  $^{13}\text{C}$  NMR ( $\text{C}_6\text{D}_6$ ):  $\delta$  87.6d, 80.1d, 75.5s, 54.1s, 53.5s, 52.3d, 43.7d, 38.7s, 36.9d, 29.4q, 27.6q, 26.4q, 22.1q. \* least soluble diastereomer.

(13a) ( $\eta^5$ -exo-Ethylcyclohexadienyl)( $\eta^5$ -exo-

methylcyclohexadienyl)iron(II) - 0.30g (0.78 mmol) of [(Et- $\text{C}_6\text{H}_6$ )( $\text{C}_6\text{H}_6$ )Fe]PF<sub>6</sub> were partially dissolved in 20 ml of THF and the reaction flask was cooled to 0°C. 2.23 ml (3.12 mmol) of a 1.4 M MeLi solution in diethyl ether were then added under a stream of N<sub>2</sub>(g) and the solution turned black. After stirring for 5 minutes the solution was allowed to warm to room temperature and the solvent was removed under

vacuum. The solid residue was extracted with hexanes and filtered. The filtrate was concentrated yielding 0.08g (0.3 mmol, 40%) of a yellow-orange solid.  $^1\text{H NMR}$  ( $\text{C}_6\text{H}_6$ ):  $\delta$  4.60(m, 2H), 3.92(t, 4H), 2.83(t, 4H), 1.27(br m, 2H), 0.51(m, 5H), 0.24(d, 3H).

(13c) ( $\eta^5$ -exo-6-Ethyl-1,3,5-trimethylcyclohexadienyl)( $\eta^5$ -exo-6-Methyl-1,3,5-trimethylcyclohexadienyl)iron(II) - 0.50g (1.06 mmol) of [(Et-1,3,5- $\text{C}_6\text{H}_3\text{Me}_3$ )(1,3,5- $\text{C}_6\text{H}_3\text{Me}_3$ )Fe]PF<sub>6</sub> were partially dissolved in 50 ml of THF and the reaction flask was cooled to 0°C. Under a stream of N<sub>2</sub>(g), 3.04 ml (4.25 mmol) of a 1.4 M MeLi solution in diethyl ether were added and a dark red solution formed immediately. After stirring for 40 minutes 10 ml of H<sub>2</sub>O were added to remove excess MeLi. The reaction mixture was then filtered and the filtrate concentrated to an orange aqueous suspension under reduced pressure. Extraction with hexanes gave an orange solution which was passed through a column of activated alumina yielding a single orange fraction. This solution was concentrated under reduced pressure to give an orange oil which crystallized upon cooling yielding 0.20g (0.59 mmol, 55%) of the pseudoferrocene.  $^1\text{H NMR}$  ( $\text{C}_6\text{D}_6$ ):  $\delta$  3.25(s, 4H), 2.15(m, 2H), 1.92(s, 3H), 1.89(s, 3H), 1.51(s, 6H), 1.44(s, 6H), 0.66(m, 5H), 0.30(d, 3H);  $^{13}\text{C NMR}$  ( $\text{C}_6\text{D}_6$ ):  $\delta$  87.9d, br, 84.5s, 52.0br s, 50.8br s, 49.7d, 42.8d, 29.6t, 22.6q, 21.2q,

19.9q, 19.3q, 12.4q. IR (cm<sup>-1</sup>): 2963s, 2926s, 2875m, 1544m, 1451m, 1377m, 1260w, 1022m, 848m. m.p. 69-70 °C.

### 8.2f Synthesis of Monoaddition Products

[(R-C<sub>6</sub>H<sub>n</sub>Me<sub>6-n</sub>)(C<sub>6</sub>H<sub>n</sub>Me<sub>6-n</sub>)Fe]PF<sub>6</sub> (n = 0, 1) complexes were synthesized via the following procedure. 2.00g of **1d** (3.11 mmol) or **1e** (2.98 mmol) were suspended in 30 ml of dichloromethane and the reaction vessel was degassed with N<sub>2</sub>. Under a positive pressure of N<sub>2</sub>, 4 molar equivalents of the appropriate lithium (**9d-e**, **11d-e**) or Grignard (**10d-e**) reagent were added via syringe. The reaction mixture was allowed to slowly warm to room temperature with stirring at which point 5 ml of H<sub>2</sub>O were added and the mixture was stirred for a further 5 minutes. The resulting slurry was filtered and the filtrate was concentrated to a red aqueous suspension. The solid was filtered, washed with H<sub>2</sub>O and ether, and recrystallized from acetone/H<sub>2</sub>O.

**(9d)** (η<sup>5</sup>-exo-6-Methyl-1,2,3,4,5-pentamethylcyclohexadienyl)(η<sup>6</sup>-pentamethylbenzene)iron(II) hexafluorophosphate - Yield: 0.78g (1.5 mmol, 49%). <sup>1</sup>H NMR ((CD<sub>3</sub>)<sub>2</sub>CO): δ 5.23(s,1H), 2.57(s,3H), 2.45(s,6H), 2.30(s,6H), 1.97(s,3H), 1.85(s,6H), 1.49(s,6H), 0.03(d,3H) (the exo-H could not be located due to overlapping resonances); <sup>13</sup>C NMR ((CD<sub>3</sub>)<sub>2</sub>CO): δ 102.8s, 101.6s, 100.2s,

92.3s, 91.7s, 91.4d, 58.4s, 47.2d, 20.8q, 19.4q, 18.5q,  
18.3q, 15.8q, 14.5q, 14.2q. IR (cm<sup>-1</sup>): 2967m, 2909m, 1469m,  
1441m, 1389m, 1047w, 1017m, 840s.

(9e) ( $\eta^5$ -exo-6-Methylhexamethylcyclohexadienyl)( $\eta^6$ -  
hexamethylbenzene)iron(II) hexafluorophosphate - Yield:  
0.84g (1.56 mmol, 52%). <sup>1</sup>H NMR ((CD<sub>3</sub>)<sub>2</sub>CO):  $\delta$  2.53(s,3H),  
2.33(s,18H), 2.31(s,3H), 1.92(s,6H), 1.41(s,6H), 1.28(s,3H);  
<sup>13</sup>C NMR ((CD<sub>3</sub>)<sub>2</sub>CO):  $\delta$  101.6s, 93.3s, 92.3s, 53.4s, 45.7s,  
20.9q, 16.9q, 16.4q, 16.1q, 15.6q, 14.3q. IR (cm<sup>-1</sup>): 3003m,  
1450m, 1393m, 1064w, 1015m, 840s.

(10d) ( $\eta^5$ -exo-6-Benzyl-1,2,3,4,5-  
pentamethylcyclohexadienyl)( $\eta^6$ -pentamethylbenzene)iron(II)  
hexafluorophosphate - Yield: 1.28g (2.18 mmol, 70%). <sup>1</sup>H NMR  
((CD<sub>3</sub>)<sub>2</sub>CO):  $\delta$  7.20(m,5H), 5.13(s,1H), 3.10(d,2H),  
2.38(s,6H), 2.28(s,6H), 2.02(s,3H), 1.89(s,3H), 1.69(s,6H),  
1.46(s,6H) (the endo-H could not be located due to  
overlapping resonances); <sup>13</sup>C NMR ((CD<sub>3</sub>)<sub>2</sub>CO):  $\delta$  138.8s,  
130.3d, 128.4d, 126.7d, 102.8s, 101.6s, 100.0s, 93.0s,  
91.3s, 91.1d, 56.4s, 54.0t, 39.9d, 20.1q, 19.4q, 18.3q,  
15.7q, 14.5q, 13.9q. IR (cm<sup>-1</sup>): 3023m, 2916m, 1452m, 1392m,  
1017m, 840s.

(10e) ( $\eta^5$ -exo-6-Benzylhexamethylcyclohexadienyl)( $\eta^6$ -hexamethylbenzene)iron(II) hexafluorophosphate - Yield: 1.58g (2.56 mmol, 86%).  $^1\text{H}$  NMR ( $(\text{CD}_3)_2\text{CO}$ ):  $\delta$  7.19(m,5H), 2.38(s,2H), 2.25(s,18H), 2.16(s,3H), 1.80(s,6H), 1.58(s,3H), 1.20(s,6H);  $^{13}\text{C}$  NMR ( $(\text{CD}_3)_2\text{CO}$ ):  $\delta$  131.5s, 130.8d, 128.5d, 126.8d, 100.5s, 93.8s, 92.0s, 56.5s, 48.0t, 47.8s, 25.2q, 15.9q, 15.4q, 14.7q, 14.5q. IR ( $\text{cm}^{-1}$ ): 2990m, 1452m, 1391m, 1070w, 1016m, 840s.

(11d) ( $\eta^5$ -exo-6-tert-Butyl-1,2,3,4,5-pentamethylcyclohexadienyl)( $\eta^6$ -pentamethylbenzene)iron(II) hexafluorophosphate - Yield: 1.28g (2.30 mmol, 74%).  $^1\text{H}$  NMR ( $(\text{CD}_3)_2\text{CO}$ ):  $\delta$  5.21(s,1H), 2.48(s,6H), 2.43(s,3H), 2.36(s,6H), 1.95(s,3H), 1.88(s,6H), 1.63(s,6H), 0.36(s,9H) (the *endo*-H could not be located due to overlapping resonances);  $^{13}\text{C}$  NMR ( $(\text{CD}_3)_2\text{CO}$ ):  $\delta$  103.8s, 102.6s, 101.1s, 92.9d, 92.5s, 91.9s, 61.3d, 55.2s, 39.8s, 24.9q, 18.6q, 18.5q, 18.4q, 15.9q, 14.7q, 13.7q. IR ( $\text{cm}^{-1}$ ): 2965m, 2907m, 1471m, 1442m, 1389m, 1071m, 1017m, 843s.

## 8.2g Decomplexation of Cyclohexadienyl Complexes

### (12a) Diphenylmethane -

**Reaction of  $[(\text{Bz}-\text{C}_6\text{H}_6)_2\text{Fe}]$  with HCl** - 3.36g (8.52 mmol) of  $[(\text{Bz}-\text{C}_6\text{H}_6)_2\text{Fe}]$  was dissolved in 60 ml of dichloromethane and cooled to  $-95^\circ\text{C}$ . A stream of HCl(g) was passed through the

solution for 5 minutes and the mixture was stirred as it was allowed to warm to room temperature. The resulting wine red solution was filtered through Celite and filtrate was concentrated under reduced pressure to a red oil. This oil was passed through a short column of alumina with  $\text{CH}_2\text{Cl}_2$  and the red colour remained on the column. The eluent was concentrated and dried under vacuum yielding 2.39g (14.2 mmol, 83%) of a colourless liquid.

**Reaction of  $[(\text{Bz}-\text{C}_6\text{H}_6)_2\text{Fe}]$  with DDQ** - 1.08g (2.74 mmol) of  $[(\text{Bz}-\text{C}_6\text{H}_6)_2\text{Fe}]$  was partially dissolved in 50 ml of acetonitrile followed by addition of 1.24g (5.48 mmol) of 2,3-dichloro-5,6-dicyanoquinone (DDQ). The resulting black solution was stirred for 30 minutes, filtered through Celite, and the filtrate was concentrated under reduced pressure to yield a brown oil which was chromatographed and dried as above (with the brown colour remaining on the column) to yield 0.51g (3.03 mmol, 55%) of a light yellow liquid.

**Pyrolysis of  $[(\text{Bz}-\text{C}_6\text{H}_6)_2\text{Fe}]$**  - 1.39g (3.52 mmol) of  $[(\text{Bz}-\text{C}_6\text{H}_6)_2\text{Fe}]$  was heated to  $145^\circ\text{C}$  in a sealed tube for 52 hours. After cooling to room temperature the contents of the reaction flask were extracted with 40 ml of diethyl ether, filtered through Celite, and concentrated to a yellow oil under reduced pressure. Chromatography of the oil, as

above, and drying under vacuum yielded 0.74g (4.40 mmol, 62%) of a colourless liquid.

$^1\text{H NMR}$  ( $\text{CDCl}_3$ ):  $\delta$  7.3(s,5H), 4.0(s,1H).

(12b) 1-Benzyl-2,5-dimethylbenzene

**Reaction of  $[(\text{Bz-1,4-C}_6\text{H}_4\text{Me}_2)_2\text{Fe}]$  with HCl** - 0.19g (0.42 mmol) of  $[(\text{Bz-1,4-C}_6\text{H}_4\text{Me}_2)_2\text{Fe}]$  was dissolved in 50 ml of dichloromethane and cooled to  $-95^\circ\text{C}$ . A stream of HCl(g) was passed through the solution for 5 minutes and the mixture was stirred as it was allowed to warm to room temperature. The resulting wine red solution was filtered through Celite and filtrate was concentrated under reduced pressure to a red oil. This oil was passed through a short column of alumina with  $\text{CH}_2\text{Cl}_2$  and the red colour remained on the column. The eluent was concentrated and dried under vacuum yielding 0.10g (0.51 mmol, 60%) of a light yellow liquid.

**Reaction of  $[(\text{Bz-1,4-C}_6\text{H}_4\text{Me}_2)_2\text{Fe}]$  with DDQ** - 1.36g (3.02 mmol) of  $[(\text{Bz-1,4-C}_6\text{H}_4\text{Me}_2)_2\text{Fe}]$  was partially dissolved in 25 ml of acetonitrile followed by addition of 1.37g (6.05 mmol) of 2,3-dichloro-5,6-dicyanoquinone (DDQ). The resulting black solution was stirred for 30 minutes, filtered through Celite, and the filtrate was concentrated under reduced pressure to yield an oily purple solid which was chromatographed (with the purple colour remaining on the

column) and dried as above to yield 0.51g (2.6 mmol, 43%) of a light yellow liquid.

**Pyrolysis of [(Bz-1,4-C<sub>6</sub>H<sub>4</sub>Me<sub>2</sub>)<sub>2</sub>Fe]** - 1.02g (2.26 mmol) of [(Bz-1,4-C<sub>6</sub>H<sub>4</sub>Me<sub>2</sub>)<sub>2</sub>Fe] was heated to 140°C in a sealed tube for 24 hours. After cooling to room temperature the contents of the reaction flask were extracted with 40 ml of diethyl ether, filtered through Celite, and concentrated to a brown oil under reduced pressure. Chromatography of the oil as above (with the brown colour remaining on the column) and drying under vacuum yielded 0.41g (2.1 mmol, 46%) of a light yellow liquid.

<sup>1</sup>H NMR (CDCl<sub>3</sub>): δ 7.2(m,8H), 3.93(s,2H), 2.27(s,3H), 2.18(s,3H).

**8.2h Synthesis of (η<sup>4</sup>-5-Methylene-exo-6-ethyl-1,2,3,4,6-pentamethyl-1,3-cyclohexadiene) (η<sup>6</sup>-hexamethylbenzene) iron(0)**

**(14e) (η<sup>4</sup>-5-Methylene-exo-6-ethyl-1,2,3,4,6-pentamethyl-1,3-cyclohexadiene) (η<sup>6</sup>-hexamethylbenzene) iron(0)** - 1.00g (1.80 mmol) of [(Et-C<sub>6</sub>Me<sub>6</sub>)(C<sub>6</sub>Me<sub>6</sub>)Fe]PF<sub>6</sub> was partially dissolved in 30 ml of THF. The reaction flask was then cooled to 0°C and, under a stream of N<sub>2</sub>, 5.15 ml (7.21 mmol) of a 1.4 M MeLi solution in diethyl ether was added. A dark

red solution formed immediately and was stirred for 30 minutes while the solution warmed to room temperature. At this point the solvent was removed under vacuum and the residue extracted with hexanes and filtered under  $N_2$ . The hexanes solution was then concentrated under vacuum to yield a red solid in 89% yield (1.61 mmol, 0.66g) which was subsequently crystallized from hexanes at  $-60^\circ C$  yielding dark red crystals.  $^1H$  NMR ( $C_6D_6$ ):  $\delta$  4.51(s,1H), 4.33(s,1H), 2.34(s,2H), 2.08(s,3H), 1.87(s,18H), 1.72(3H), 1.58(s,3H), 1.30(s,3H), 0.99(s,3H), 0.79(s,3H);  $^{13}C$  NMR ( $C_6D_6$ ):  $\delta$  159.4s, 92.0t, 91.2s, 83.1s, 81.9s, 56.8s, 55.7s, 45.5s, 34.0t, 27.9q, 19.4q, 17.4q, 16.0q, 14.7q, 14.4q, 10.9q. IR ( $cm^{-1}$ ): 3091w, 2968m, 2903m, 1567m, 1453m, 1382m, 1328w, 1090w, 1062m, 1016m, 840m, 804m. Decomposes above  $150^\circ C$ .

### 8.2i Synthesis of [(arene)(arene')Fe] $^{2+}$ Dications

(15) ( $\eta^6$ -meta-xylene)( $\eta^6$ -hexamethylbenzene)iron(II) hexafluorophosphate - 2.00g (12.3 mmol) of  $FeCl_3$ , 2.00g (12.3 mmol) of  $C_6Me_6$ , and 4.93g (37.0 mmol) of  $AlCl_3$  was stirred in 50 ml of m-xylene for 24 hours, under  $N_2$ . The mixture was then cooled to  $0^\circ C$  and hydrolysed with 50 ml of  $H_2O$ . The aqueous phase was separated, washed with hexanes, and precipitated with  $NH_4PF_6(aq)$ . The resulting orange solid, consisting of a mixture of [(1,3- $C_6H_4Me_2$ )( $C_6Me_6$ )Fe]( $PF_6$ ) $_2$  and [(1,3- $C_6H_4Me_2$ ) $_2$ Fe]( $PF_6$ ) $_2$ , was

filtered off and fractionally recrystallized from acetone/water yielding 4.39g (7.15 mmol, 58%) of orange crystalline **15** as the first fraction.  $^1\text{H}$  NMR ( $(\text{CD}_3)_2\text{CO}$ ):  $\delta$  7.10(t,1H), 6.89(d,2H), 6.79(s,1H), 2.79(s,18H), 2.65(s,6H);  $^{13}\text{C}$  NMR ( $(\text{CD}_3)_2\text{CO}$ ):  $\delta$  112.7s, 107.2s, 96.2d, 92.4d, 92.1d, 18.3q, 17.4q. Anal. Calcd for  $\text{C}_{20}\text{H}_{28}\text{F}_2\text{FeP}_{12}$ : C, 39.11%; H, 4.59%. Found: C, 39.18%; H, 4.33%. IR ( $\text{cm}^{-1}$ ): 3095m, 2929m, 1458m, 1389m, 1035m, 841s.

(16)  $(\eta^6\text{-para-xylene})(\eta^6\text{-hexamethylbenzene})\text{iron(II)}$  hexafluorophosphate - 2.08g (12.8 mmol) of  $\text{FeCl}_3$ , 2.08g (12.8 mmol) of  $\text{C}_6\text{Me}_6$ , and 5.13g (38.4 mmol) of  $\text{AlCl}_3$  was stirred in 50 ml of p-xylene for 24 hours, under  $\text{N}_2$ . The reaction was worked up as in **15** yielding 4.01g (6.53 mmol, 51%) of **16**.  $^1\text{H}$  NMR ( $(\text{CD}_3)_2\text{CO}$ ):  $\delta$  6.89(s,4H), 2.75(s,18H), 2.60(s,6H);  $^{13}\text{C}$  NMR ( $(\text{CD}_3)_2\text{CO}$ ):  $\delta$  111.2s, 107.1s, 93.6d, 17.8q, 17.2q. Anal. Calcd for  $\text{C}_{20}\text{H}_{28}\text{F}_{12}\text{FeP}_2$ : C, 39.10; H, 4.59%. Found: C, 38.90; H, 4.67%. IR ( $\text{cm}^{-1}$ ): 3094m, 2938w, 1493m, 1450m, 1392m, 1074m, 1028m, 842s.

(17)  $(\eta^6\text{-para-xylene})(\eta^6\text{-hexaethylbenzene})\text{iron(II)}$  hexafluorophosphate - 3.02g (12.3 mmol) of  $\text{C}_6\text{Et}_6$ , 1.00g (6.2 mmol) of  $\text{FeCl}_3$ , and 2.47g (18.5 mmol) of  $\text{AlCl}_3$  was stirred in 20 ml of p-xylene under  $\text{N}_2$  for 24 hours. Product isolation as for **15** yielded 1.11g (1.59 mmol, 26%) of orange crystalline **17**.  $^1\text{H}$  NMR ( $(\text{CD}_3)_2\text{CO}$ ):  $\delta$  6.83(s,4H),

3.46(q,12H), 2.60(s,6H), 1.43(t,18H);  $^{13}\text{C}$  NMR ( $(\text{CD}_3)_2\text{CO}$ ):  $\delta$  112.5s, 111.7s, 93.4d, 23.9t, 18.2q, 15.0q. Anal. Calcd for  $\text{C}_{26}\text{H}_{40}\text{F}_{12}\text{FeP}_2$ : C, 44.72; H, 5.77%. Found C, 44.52; H, 5.89%. IR ( $\text{cm}^{-1}$ ): 3086m, 2991m, 2947m, 1497m, 1453m, 1386m, 1050m, 841s.

### 8.2j Synthesis of Products Derived from Single Carbanion Addition to [(arene)(arene')Fe] $^{2+}$ Dications

Single net addition of  $\text{H}^-$ ,  $\text{Me}^-$  and  $^t\text{Bu}^-$ , and  $\text{Et}^-$  to  $[(1,4\text{-C}_6\text{H}_4\text{Me}_2)(\text{C}_6\text{Me}_6)\text{Fe}](\text{PF}_6)_2$  and  $[(1,4\text{-C}_6\text{H}_4\text{Me}_2)(\text{C}_6\text{Et}_6)\text{Fe}](\text{PF}_6)_2$  were conducted according to the procedures in sections 8.2d, 8.2f, and 8.2b, respectively.  $\text{Me}^-$ ,  $\text{Ph}^-$ , and  $^t\text{Bu}^-$ ; and  $\text{Et}^-$  additions to  $[(1,3\text{-C}_6\text{H}_4\text{Me}_2)(\text{C}_6\text{Me}_6)\text{Fe}](\text{PF}_6)_2$  were done according the procedures described in sections 8.2f and 8.2b, respectively.

(18A)  $(\eta^5\text{-exo-5-Hydrido-1,4-dimethylcyclohexadienyl})(\eta^6\text{-hexamethylbenzene})\text{iron(II)hexafluorophosphate}$  - 0.58g (1.23 mmol, 76%) of product was obtained that contained 8% of the isomer derived from net  $\text{H}^-$  addition to the hexamethylbenzene ring.  $[(\text{H-1,4-}\text{C}_6\text{H}_4\text{Me}_2)(\text{C}_6\text{Me}_6)\text{Fe}]\text{PF}_6$  -  $^1\text{H}$  NMR ( $(\text{CD}_3)_2\text{CO}$ ):  $\delta$  6.59(d,1H), 4.30(d,1H), 2.64(m,1H), 2.42(s,18H), 1.81(s,3H), 1.50(d,1H), 1.35(d,1H), 1.26(s,3H);  $^{13}\text{C}$  NMR ( $(\text{CD}_3)_2\text{CO}$ ):  $\delta$  101.4s, 101.2s, 85.5d, 81.2d, 60.2s, 40.7d, 32.5t, 21.8q, 18.3q, 16.5q.

Anal. Calcd for  $C_{20}H_{29}FFeP_6$ : C, 51.08%; H, 6.22%. Found: C, 51.09%; H, 6.57% IR ( $cm^{-1}$ ): 2918w, 2358w, 2787m, 1445m, 1389m, 1070m, 1021m, 841s.

(18B)  $(\eta^5\text{-exo-5-Methyl-1,4-dimethylcyclohexadienyl})(\eta^6\text{-hexamethylbenzene})\text{iron(II) hexafluorophosphate}$  - 0.93g (1.92 mmol, 59%) of product was obtained which contained 13% of the isomer derived from net  $Me^-$  addition to the hexamethylbenzene ligand.  $[(Me\text{-}1,4\text{-}C_6H_4Me_2)(C_6Me_6)Fe]PF_6$  -  $^1H$  NMR ( $(CD_3)_2CO$ ):  $\delta$  6.46(dd, 1H), 4.26(d, 1H), 2.82(d, 1H), 2.43(s, 18H), 1.81(s, 3H), 1.38(s, 3H), 0.06(d, 3H), (the *endo*-H could not be located due to overlapping resonances);  $^{13}C$  NMR ( $(CD_3)_2CO$ ):  $\delta$  101.7s, 101.0s, 83.7d, 81.0d, 67.6s, 47.3d, 37.7d, 23.5q, 20.6q, 19.8q, 16.7q. Anal. Calcd for  $C_{27}H_{43}F_6FeP$ : C, 57.05; H, 7.62%. Found: C, 56.73; H, 7.65%. IR ( $cm^{-1}$ ): 2964m, 2919m, 1448m, 1389m, 1068w, 1021m, 840s.

(18C)  $(\eta^5\text{-exo-5-Ethyl-1,4-dimethylcyclohexadienyl})(\eta^6\text{-hexamethylbenzene})\text{iron(II) hexafluorophosphate}$  - 0.73g (1.46 mmol, 45%) of product was isolated that contained 17% of the isomer derived from net  $Et^-$  addition to the hexamethylbenzene ring.  $[(Et\text{-}1,4\text{-}C_6H_4Me_2)(C_6Me_6)Fe]PF_6$  -  $^1H$  NMR ( $(CD_3)_2CO$ ):  $\delta$  6.41(dd, 1H), 4.28(d, 1H), 2.84(dm, 1H), 0.42(s, 18H), 1.82(s, 3H), 1.39(s, 3H), 0.75(m, 2H), 0.40(t, 3H), (the *endo*-H could not be located due to overlapping resonances);  $^{13}C$  NMR ( $(CD_3)_2CO$ ):  $\delta$  101.3s, 101.0s, 84.1d,

81.1d, 68.9s, 45.3d, 44.1d, 31.3t, 20.5q, 18.5q, 16.4q,  
9.0q. IR( $\text{cm}^{-1}$ ): 2952m, 2923m, 1453m, 1392m, 1068m, 1012m,  
841s.

(18D)  $(\eta^5\text{-exo-5-tert-Butyl-1,4-}$   
 $\text{dimethylcyclohexadienyl})(\eta^6\text{-hexamethylbenzene})\text{iron(II)}$   
hexafluorophosphate - 1.56g (2.96 mmol, 91%) of product was  
obtained containing 7% of the isomer derived from net  ${}^t\text{Bu}^-$   
addition to the hexamethylbenzene ring. [ $({}^t\text{Bu-1,4-}$   
 $\text{C}_6\text{H}_4\text{Me}_2)(\text{C}_6\text{Me}_6)\text{Fe}] \text{PF}_6$  -  ${}^1\text{H}$  NMR ( $(\text{CD}_3)_2\text{CO}$ ):  $\delta$  6.29(d,1H),  
4.40(d,1H), 2.81(d,1H), 2.53(d,1H), 2.42(s,18H), 1.85(s,3H),  
1.47(s,3H), 0.40(s,9H);  ${}^{13}\text{C}$  NMR ( $(\text{CD}_3)_2\text{CO}$ ):  $\delta$  101.3s, 99.3s,  
85.4d, 80.7d, 68.2s, 52.9s, 44.5d, 38.8s, 27.1q, 24.1q,  
18.1q, 16.4q. Anal. Calcd for  $\text{C}_{30}\text{H}_{49}\text{F}_6\text{FeP}$ : C, 59.02; H,  
8.09%. Found: C, 58.97; H, 7.92%. IR ( $\text{cm}^{-1}$ ): 2955m, 1469m,  
1388m, 1221m, 1070w, 1019m, 840s.

(19A)  $(\eta^5\text{-exo-5-Hydrido-1,4-}$   
 $\text{dimethylcyclohexadienyl})(\eta^6\text{-hexaethylbenzene})\text{iron(II)}$   
hexafluorophosphate - 0.31g (0.56 mmol, 39%) of product was  
isolated that contained 1% of the isomer derived from net  $\text{H}^-$   
addition to the hexaethylbenzene ring. [ $(\text{H-1,4-}$   
 $\text{C}_6\text{H}_4\text{Me}_2)(\text{C}_6\text{Me}_6)\text{Fe}] \text{PF}_6$  -  ${}^1\text{H}$  NMR ( $(\text{CD}_3)_2\text{CO}$ ):  $\delta$  6.63(d,1H),  
4.28(d,1H), 2.99(q,12H), 2.70(d,1H), 2.55(dd,1H),  
1.82(s,3H), 1.39(t,18H), 1.34(d,1H), 1.26(s,3H);  ${}^{13}\text{C}$  NMR  
( $(\text{CD}_3)_2\text{CO}$ ):  $\delta$  106.7s, 101.6s, 85.3d, 80.5d, 62.9s, 41.2d,

32.9t, 23.4t, 22.6q, 18.9q, 16.2q. IR (cm<sup>-1</sup>): 2978m, 2945m, 2884m, 2782m, 1490m, 1455m, 1383m, 1051m, 124m, 838s.

(19B) ( $\eta^5$ -exo-5-Methyl-1,4-dimethylcyclohexadienyl)( $\eta^6$ -hexaethylbenzene)iron(II) hexafluorophosphate - Yield: 0.93g (1.64 mmol, 57%). <sup>1</sup>H NMR ((CD<sub>3</sub>)<sub>2</sub>CO):  $\delta$  6.33(d,1H), 4.40(d,1H), 3.01(q,12H), 2.65(q,1H), 2.53(m,1H), 2.06(s,3H), 1.81(s,3H), 1.39(t,18H), 0.07(d,3H); <sup>13</sup>C NMR ((CD<sub>3</sub>)<sub>2</sub>CO):  $\delta$  106.5s, 99.0s, 83.5d, 80.4d, 70.3s, 47.7d, 38.0d, 23.7q, 23.4t, 20.6q, 19.4q, 16.2q. Anal. Calcd for C<sub>27</sub>H<sub>43</sub>FFeP<sub>6</sub>: C, 57.05%; H, 7.67%. Found: C, 56.65%; H, 7.42%. IR(cm<sup>-1</sup>): 2979m, 2883m, 1494m, 1449m, 1385m, 1054m, 1022m, 838s.

(19C) ( $\eta^5$ -exo-5-Ethyl-1,4-dimethylcyclohexadienyl)( $\eta^6$ -hexaethylbenzene)iron(II) hexafluorophosphate - Yield: 0.33g (0.57 mmol, 20%). <sup>1</sup>H NMR ((CD<sub>3</sub>)<sub>2</sub>CO):  $\delta$  6.45(d,1H), 4.27(d,1H), 3.01(q,12H), 2.94(d,1H), 2.40(m,1H), 1.83(s,3H), 1.40(s,3H), 1.38(t,18H), 0.39(t,3H), 0.39(dm,2H); <sup>13</sup>C NMR ((CD<sub>3</sub>)<sub>2</sub>CO):  $\delta$  106.6s, 99.4s, 83.9d, 80.4d, 69.9s, 45.8d, 44.5d, 31.4t, 23.4t, 21.2q, 19.2q, 16.2q, 9.0q. IR (cm<sup>-1</sup>): 2938m, 2879m, 1500m, 1452m, 1391m, 1052m, 1025m, 840s.

(19D) ( $\eta^5$ -exo-5-tert-Butyl-1,4-dimethylcyclohexadienyl)( $\eta^6$ -hexaethylbenzene)iron(II) hexafluorophosphate - Yield: 1.68g (2.75 mmol, 96%). <sup>1</sup>H NMR ((CD<sub>3</sub>)<sub>2</sub>CO):  $\delta$  6.33(dd,1H), 4.39(dd,1H), 3.01(q,12H),

2.85(d,1H), 2.52(d,1H), 1.85(s,3H), 1.48(s,3H), 1.38(t,18H), 0.39(s,9H);  $^{13}\text{C}$  NMR ( $(\text{CD}_3)_2\text{CO}$ ):  $\delta$  106.7s, 99.6s, 85.0d, 79.9d, 71.3s, 53.0d, 45.1d, 38.9s, 27.2q, 24.8q, 23.3t, 18.7q, 16.2q. IR ( $\text{cm}^{-1}$ ): 2966m, 2881m, 1491m, 1380m, 1298m, 1052m, 1024m, 840s.

(20A - 20C) Net  $\text{Me}^-$ ,  $\text{Et}^-$ , and  $\text{Ph}^-$  addition to  $[(1,3\text{-C}_6\text{H}_4\text{Me}_2)(\text{C}_6\text{Me}_6)\text{Fe}](\text{PF}_6)_2$  resulted in mixtures of at least three products that could not be separated, nor could their NMR spectra be assigned.

(20D)  $(\eta^5\text{-exo-4-Tert-butyl-1,3-dimethylcyclohexadienyl})(\eta^6\text{-hexamethylbenzene})\text{iron(II)}$  hexafluorophosphate - 1.26g (2.39 mmol, 74%) of product was obtained that contained a minor impurity (<5%) of the isomer derived from net  $\text{tBu}^-$  addition to the hexamethylbenzene ring. [ $(\text{tBu-1,3-C}_6\text{H}_4\text{Me}_2)(\text{C}_6\text{Me}_6)\text{Fe}]\text{PF}_6$  -  $^1\text{H}$  NMR ( $(\text{CD}_3)_2\text{CO}$ ):  $\delta$  4.32(s,1H), 4.18(d,1H), 2.88(d,1H), 2.50(t,1H), 2.42(s,3H), 2.37(s,18H), 1.47(s,3H), 0.40(s,9H);  $^{13}\text{C}$  NMR ( $(\text{CD}_3)_2\text{CO}$ ):  $\delta$  101.4s, 97.9s, 85.1d, 83.8d, 66.1s, 52.2d, 47.2d, 37.8s, 27.0q, 23.9q, 18.0q, 16.1q. Anal. Calcd for  $\text{C}_{24}\text{H}_{37}\text{FFeP}_6$ : C, 54.76%; H, 7.08% Found: C, 54.58%; H, 6.79%. IR ( $\text{cm}^{-1}$ ): 2960m, 2893m, 1460m, 1387m, 1223w, 1069w, 1021m, 840s.

8.2k Synthesis of [(Ph-1,3,5-C<sub>6</sub>H<sub>3</sub>Me<sub>3</sub>)(C<sub>5</sub>H<sub>5</sub>)Fe]

(21c) ( $\eta^5$ -1,3,5-trimethyl-6-exo-phenylcyclohexadienyl)( $\eta^5$ -cyclopentadienyl)iron(II) - 1.00g (2.59 mmol) of [(1,3,5-C<sub>6</sub>H<sub>3</sub>Me<sub>3</sub>)(C<sub>5</sub>H<sub>5</sub>)Fe]PF<sub>6</sub> was partially dissolved in 30 ml of THF and degassed with N<sub>2</sub>. The reaction vessel was then cooled to 0°C and, under a stream of N<sub>2</sub>, 5.18 ml (10.4 mmol) of 2 M phenyllithium solution was added. The mixture was then allowed to warm to room temperature with stirring at which point the solvent was removed under vacuum and the residue extracted with hexanes. The orange hexanes solution was stirred with 2 ml of H<sub>2</sub>O, dried over MgSO<sub>4</sub>, and filtered. The filtrate was then concentrated under reduced pressure yielding 0.76g (2.4 mmol, 93%) of a red oil which crystallized upon cooling. Cooling of a hexanes solution of 21c to -15°C afforded moderately air- and solution-sensitive crystals suitable for X-ray crystallography. <sup>1</sup>H NMR (C<sub>6</sub>D<sub>6</sub>):  $\delta$  7.08(m,2H), 6.98(m,1H), 6.83(m,2H), 3.87(s,5H), 3.78(s,2H), 2.25(s,3H), 2.02(s,1H), 1.42(s,6H); <sup>13</sup>C NMR (C<sub>6</sub>D<sub>6</sub>):  $\delta$  143.7s, 129.6d, 126.3d, 126.1d, 89.0s, 79.0d, 75.1d, 54.8d, 42.2s, 24.5q, 21.0q. m.p. 99-100°C.

8.21 Synthesis of  $[(C_6(CH_2CH_2Ph)_6)(C_5H_5)Fe]PF_6$  and  
Decomplexation of  $C_6(CH_2CH_2Ph)_6$

(22)  $(\eta^5\text{-Cyclopentadienyl})(\eta^6\text{-hexa(phenylethyl)benzene})\text{iron(II) hexafluorophosphate}$  - 22 was prepared by a method based upon that described earlier by Astruc<sup>80</sup>. 0.70g (1.63 mmol) of  $[(C_6Me_6)(C_5H_5)Fe]PF_6$ , 3.63g (32.3 mmol) of freshly prepared  $K^+ tBuO^-$ , and 2.00 ml (16.8 mmol) of benzyl bromide were stirred in 50 ml of THF for 4 hours, under an atmosphere of dinitrogen. The solvent was then removed *in vacuo* and the residue washed thoroughly with  $H_2O$ , filtered, and washed with ether. The resulting tan solid was subsequently recrystallized from acetone/ $H_2O$  yielding 1.02g (1.05 mmol, 65%) of yellow air-stable crystals of 22.  $^1H$  NMR ( $(CD_3)_2CO$ ):  $\delta$  7.39(s, 30H), 5.28(s, 5H), 3.48(dm, 24H);  $^{13}C$  NMR ( $(CD_3)_2CO$ ):  $\delta$  141.6s, 129.6d, 129.1d, 127.5d, 104.2s, 79.5d, 38.1t, 33.7t.

(23) Hexa(phenylethyl)benzene - An acetonitrile solution (0.40g, 0.41 mmol in 100ml) of 22 afforded colourless crystals of hexa(phenylethyl)benzene after standing for five days. The crystals were collected by filtration and dried under vacuum. Yield: 0.21g (0.30 mmol, 72%).  $^1H$  NMR ( $(CD_3)_2CO$ ):  $\delta$  7.31(m, 5H), 2.97(dm, 4H);  $^{13}C$  NMR ( $(CD_3)_2CO$ ):  $\delta$  143.1s, 137.3s, 129.3d, 129.0d, 126.8d, 38.5t, 33.2t.

Chapter 9

Appendix. X-ray Crystallography

The X-ray crystal structures of [(1,3,5-C<sub>6</sub>H<sub>3</sub>Me<sub>3</sub>)<sub>2</sub>Fe](PF<sub>6</sub>)<sub>2</sub>, **1c**; [(Et-1,3,5-C<sub>6</sub>H<sub>3</sub>Me<sub>3</sub>)(1,3,5-C<sub>6</sub>H<sub>3</sub>Me<sub>3</sub>)Fe]PF<sub>6</sub>, **2c**; [(Et-C<sub>6</sub>Me<sub>6</sub>)(C<sub>6</sub>Me<sub>6</sub>)Fe]PF<sub>6</sub>, **2e**; and [(CH<sub>2</sub>Cl-1,3,5-C<sub>6</sub>H<sub>3</sub>Me<sub>3</sub>)(1,3,5-C<sub>6</sub>H<sub>3</sub>Me<sub>3</sub>)Fe]PF<sub>6</sub>, **3c**; were solved by Drs. Stanley Cameron and Anthony Linden at Dalhousie University. The X-ray structures of [(CH<sub>2</sub>Cl-C<sub>6</sub>Me<sub>6</sub>)(C<sub>6</sub>Me<sub>6</sub>)Fe]PF<sub>6</sub>, **3e**; and [(Ph-1,3,5-C<sub>6</sub>H<sub>3</sub>Me<sub>3</sub>)(C<sub>5</sub>H<sub>5</sub>)Fe], **21c**; were solved by Dr. Peter White at the University of New Brunswick. Dr. Robin Rogers solved the crystal structures of [(1,4-C<sub>6</sub>H<sub>4</sub>Me<sub>2</sub>)(C<sub>6</sub>Me<sub>6</sub>)Fe](PF<sub>6</sub>)<sub>2</sub>, **16**; [(C<sub>6</sub>(CH<sub>2</sub>CH<sub>2</sub>C<sub>6</sub>H<sub>5</sub>)<sub>6</sub>)(C<sub>5</sub>H<sub>5</sub>)Fe]PF<sub>6</sub>, **22**; and C<sub>6</sub>(CH<sub>2</sub>CH<sub>2</sub>C<sub>6</sub>H<sub>5</sub>)<sub>6</sub>, **23**; at Northern Illinois University, and Dr. Michael Zaworotko solved the crystal structures of [(<sup>t</sup>Bu-C<sub>6</sub>H<sub>6</sub>)<sub>2</sub>Fe], **8a**; and [(1,3-C<sub>6</sub>H<sub>4</sub>Me<sub>2</sub>)(C<sub>6</sub>Me<sub>6</sub>)Fe](PF<sub>6</sub>)<sub>2</sub>, **15**; from data collected at the University of Victoria by Ms. Kathy Beveridge.

## (1c) Bis(mesitylene)iron(II) hexafluorophosphate.

Table A1 Crystal Data and Refinement Parameters for  
 $[(1,3,5\text{-C}_6\text{H}_3\text{Me}_3)_2\text{Fe}](\text{PF}_6)_2$ .

---

Formula	$\text{C}_{18}\text{F}_{12}\text{FeH}_{24}\text{P}_2$
Colour	orange
Formula Wt.	586.16
Space Group	$\text{Fm}\bar{3}\text{m}$
Temp, °C	22
a, Å	13.433(4)
b, Å	13.433(4)
c, Å	13.433(4)
$\alpha$ , °	90
$\beta$ , °	90
$\gamma$ , °	90
Cell Volume, Å <sup>3</sup>	2424(2)
Z	4
$D_{\text{calc}}$ , g cm <sup>-3</sup>	1.61
Reflections Observed <sup>a</sup>	142
R	0.024
$R_w$	0.022

---

<sup>a</sup> Corrections: Lorentz-polarization, absorption.  $F_o \geq 3\sigma(F_o)$

Table A2 Final Fractional Coordinates for  
[(1,3,5-C<sub>6</sub>H<sub>3</sub>Me<sub>3</sub>)<sub>2</sub>Fe](PF<sub>6</sub>)<sub>2</sub>.

ATOM	x/a	y/b	z/c	U <sub>eq</sub> <sup>b</sup>
Fe1	0.00000(0)	0.00000	0.00000	0.0580
P1	0.25000(0)	0.25000(0)	0.25000(0)	0.0876
F1	0.2596(7)	0.2596(7)	0.1332(1)	0.1243
C1	-0.0255(2)	-0.0255(2)	-0.1547(3)	0.0739
C2	0.0199(4)	0.0199(4)	-0.2468(3)	0.0873
C3	0.0157(5)	-0.1103(2)	-0.1103(2)	0.0852

<sup>b</sup> U<sub>eq</sub> is one third of the trace of the orthogonalized U<sub>ij</sub> tensors.

Table A3 Bond Distances (Å) and Angles (°) for  
 $[(1,3,5\text{-C}_6\text{H}_3\text{Me}_3)_2\text{Fe}](\text{PF}_6)_2$ .

ATOMS	DISTANCE	ATOMS	DISTANCE
Fe - C1	2.134(1)	Fe - C3	2.109(1)
C1 - C2	1.508(1)	C1 - C3	1.400(1)
Fe - Cent	1.594(1)		

ATOMS	ANGLE	ATOMS	ANGLE
C3 - C1 - C3a	117.5(2)	C1 - C3 - C1b	122.5(2)
C2 - C1 - C3	121.3(1)	C2 - C1 - C3a	121.3(1)

a = symmetry equivalent z, x, y

b = symmetry equivalent y, z, x

(2c) [ $(\eta^5\text{-exo-Ethyl-2,4,6-trimethylcyclohexadienyl})(\eta^6\text{-mesitylene})\text{iron(II) hexafluorophosphate.}$

Table A4 Crystal Data and Refinement Parameters for  
 $[(\text{Et-1,3,5-C}_6\text{H}_3\text{Me}_3)(1,3,5\text{-C}_6\text{H}_3\text{Me}_3)\text{Fe}]\text{PF}_6$ .

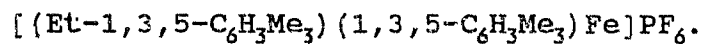
---

Formula	$\text{C}_{20}\text{F}_6\text{FeH}_{29}\text{P}$
Colour	red
Molecular Wt.	470.26
Space Group	$\text{P}2_12_12_1$
Temp., °C	22
a, Å	8.880(2)
b, Å	15.243(3)
c, Å	15.457(3)
$\alpha$ , °	90
$\beta$ , °	90
$\gamma$ , °	90
Cell Volume, Å <sup>3</sup>	2092.2
Z	4
$D_{\text{calc}}$ , g cm <sup>-3</sup>	1.455
Reflections Observed	1476
R	0.039
$R_w$	0.040

---

<sup>a</sup> Corrections: Lorentz-polarization.  $F_o \geq 2\sigma(F_o)$

Table A5 Final Fractional Coordinates for



ATOM	x/a	y/b	z/c	U <sub>eq</sub> <sup>b</sup>
Fe1	0.7670(1)	0.1175(1)	0.2143(1)	0.0319
P1	0.7652(3)	0.4714(1)	0.0432(1)	0.0457
F1	0.7551(6)	0.4160(3)	-0.0438(3)	0.0698
F2	0.8906(6)	0.4055(4)	-0.9233(4)	0.0898
F3	0.8918(5)	0.5317(4)	0.0023(4)	0.0713
F4	0.6382(6)	0.4103(4)	0.0834(4)	0.0830
F5	0.7771(7)	0.5259(4)	0.1293(3)	0.0841
F6	0.6378(6)	0.5349(5)	0.0083(4)	0.0814
C1	0.668(1)	0.2226(7)	0.5243(5)	0.0914
C2	0.666(1)	0.2538(5)	0.4318(5)	0.0655
C3	0.6430(8)	0.1841(5)	0.3611(5)	0.0504
C4	0.6406(7)	0.2221(4)	0.2711(5)	0.0378
C5	0.7734(7)	0.2511(4)	0.2347(4)	0.0397
C6	0.9130(7)	0.2110(5)	0.2607(5)	0.0393
C7	0.9032(7)	0.1408(5)	0.3194(4)	0.0403
C8	0.7641(8)	0.1156(4)	0.3541(4)	0.0403
C9	0.4891(7)	0.2547(5)	0.2370(6)	0.0556
C10	1.0610(7)	0.2370(5)	0.2217(6)	0.0580
C11	0.749(1)	0.0328(4)	0.4055(4)	0.0609
C12	0.8800(8)	0.0049(4)	0.1648(5)	0.0381
C13	0.8850(8)	0.0750(5)	0.1039(5)	0.0425

---

ATOM	x/a	y/b	z/c	$U_{eq}^b$
C14	0.7520(8)	0.1184(4)	0.0769(4)	0.0444
C15	0.6150(7)	0.0927(5)	0.1128(5)	0.0462
C16	0.6055(7)	0.0250(5)	0.1740(5)	0.0396
C17	0.7388(7)	-0.0172(4)	0.1994(4)	0.0409
C18	1.0231(8)	-0.0386(5)	0.1932(6)	0.0564
C19	0.761(1)	0.1910(5)	0.0113(4)	0.0583
C20	0.4559(7)	-0.0015(5)	0.2106(7)	0.0562

---

<sup>b</sup>  $U_{eq}$  is one third of the trace of the orthogonalized  $U_{ij}$  tensors.

**Table A6** Bond Distances (Å) and Angles (°) for  
 [(Et-1,3,5-C<sub>6</sub>H<sub>3</sub>Me<sub>3</sub>)<sub>2</sub>(1,3,5-C<sub>6</sub>H<sub>3</sub>Me<sub>3</sub>)Fe]PF<sub>6</sub>.

ATOMS	DISTANCE	ATOMS	DISTANCE
Fe1 - C4	2.139(7)	Fe1 - C5	2.061(6)
Fe1 - C6	2.056(7)	Fe1 - C7	2.056(7)
Fe1 - C8	2.161(7)	Fe1 - C12	2.130(7)
Fe1 - C13	2.104(8)	Fe1 - C14	2.127(6)
Fe1 - C15	2.103(8)	Fe1 - C16	2.106(7)
Fe1 - C17	2.081(6)	P1 - F1	1.591(5)
P1 - F2	1.587(6)	P1 - F3	1.582(6)
P1 - F4	1.590(6)	P1 - F5	1.572(5)
P1 - F6	1.583(7)	C1 - C2	1.51(1)
C2 - C3	1.54(1)	C4 - C3	1.51(1)
C3 - C8	1.50(1)	C4 - C5	1.379(9)
C4 - C9	1.527(9)	C5 - C6	1.439(9)
C6 - C7	1.41(1)	C6 - C10	1.50(1)
C7 - C8	1.400(9)	C8 - C11	1.498(9)
C12 - C13	1.43(1)	C12 - C17	1.404(9)
C12 - C18	1.50(1)	C13 - C14	1.42(1)
C14 - C15	1.39(1)	C14 - C19	1.504(9)
C15 - C16	1.40(1)	C16 - C17	1.403(9)
C16 - C20	1.50(1)		

---

ATOMS	ANGLE	ATOMS	ANGLE
F1 - P1 - F3	90.7(3)	F1 - P1 - F4	88.8(3)
F1 - P1 - F5	179.4(3)	F1 - P1 - F6	89.8(3)
F3 - P1 - F4	179.4(4)	F3 - P1 - F5	89.1(3)
F3 - P1 - F6	91.0(3)	F4 - P1 - F5	91.5(3)
F4 - P1 - F6	89.1(3)	F5 - P1 - F6	90.8(3)
C3 - C2 - C1	117.3(7)	C3 - C4 - C5	119.2(6)
C3 - C4 - C9	117.1(6)	C3 - C8 - C7	118.0(6)
C3 - C8 - C11	118.9(6)	C4 - C3 - C2	113.1(6)
C4 - C3 - C8	102.1(6)	C4 - C5 - C6	119.1(6)
C5 - C4 - C9	120.6(6)	C5 - C6 - C7	116.7(6)
C5 - C6 - C10	122.1(6)	C6 - C7 - C8	120.7(6)
C7 - C6 - C10	121.0(6)	C7 - C8 - C11	120.8(6)
C8 - C3 - C2	115.8(6)	C12 - C13 - C14	121.3(6)
C12 - C17 - C16	122.5(6)	C13 - C12 - C17	117.3(6)
C13 - C12 - C18	119.9(6)	C13 - C14 - C15	118.7(6)
C13 - C14 - C19	119.8(6)	C14 - C15 - C16	121.9(6)
C15 - C14 - C19	121.6(7)	C15 - C16 - C17	118.4(6)
C15 - C16 - C20	120.4(6)	C17 - C12 - C18	122.7(6)
C17 - C16 - C20	121.2(6)		

---

**Table A7** Least Squares Best Planes Calculations for [(Et-  
1,3,5-C<sub>6</sub>H<sub>3</sub>Me<sub>3</sub>)(1,3,5-C<sub>6</sub>H<sub>3</sub>Me<sub>3</sub>)Fe]PF<sub>6</sub>.

---

**Plane 1**

Equation of the plane:  $0.91(4)X + 9.99(4)Y + 11.56(4)Z$   
 $= 5.94(3)$

Distances (Å) to the plane from the atoms in the plane.

C11	0.001(11)	C12	-0.009(10)
C13	0.017(10)	C14	-0.015(9)
C15	0.008(10)		

$\chi^2$  for this plane is 7.575

Distances (Å) to the plane from the atoms out of the plane.

Fe1	-1.586(4)	C10	0.664(12)
-----	-----------	-----	-----------

**Plane 2**

Equation of the plane:  $1.07(3)X + 10.14(4)Y + 11.39(3)Z$   
 $= 2.89(2)$

Distances (Å) to the plane from the atoms in the plane.

C1	-0.014(13)	C2	0.008(11)
C3	-0.002(10)	C4	-0.001(9)
C5	-0.000(8)	C6	0.004(10)

$\chi^2$  for this plane is 2.111

Distances ( $\text{\AA}$ ) to the plane from the atoms out of the plane.

Fe1	1.570(4)
-----	----------

Dihedral angle between planes A and B.

A	B	Angle( $^{\circ}$ )
1	2	1.4(3)

(2e) [ $(\eta^5$ -exo-eth. 1,2,3,4,5,6-hexamethylcyclohexadienyl) ( $\eta^6$ -hexamethylbenzene) - iron(II) hexafluorophosphate

Table A8 Crystal Data and Refinement Parameters for  
[(Et-C<sub>6</sub>Me<sub>6</sub>) (C<sub>6</sub>Me<sub>6</sub>) Fe]PF<sub>6</sub>.

Formula	C <sub>26</sub> F <sub>6</sub> FeH <sub>41</sub> P
Colour	red
Molecular Wt.	554.4
Space Group	C2/c
Temp., °C	22
a, Å	34.295(5)
b, Å	10.332(2)
c, Å	16.262(3)
$\alpha$ , °	90
$\beta$ , °	115.604(13)
$\gamma$ , °	90
Cell Volume, Å <sup>3</sup>	5196.4
Z	8
D <sub>calc</sub> , g cm <sup>-3</sup>	1.417
Reflections Observed <sup>a</sup>	2038
R	0.056
R <sub>w</sub>	0.058

<sup>a</sup> Corrections: Lorentz-polarization.  $F_o \geq 2\sigma(F_o)$

Table A9 Final Fractional Coordinates for  
 $[(\text{Et}-\text{C}_6\text{Me}_6)(\text{C}_6\text{Me}_6)\text{Fe}]\text{PF}_6$ .

ATOM	x/a	y/b	z/c	$U_{\text{eq}}^b$
Fe1	-0.13587(3)	-0.76362(8)	-0.02717(6)	0.0313
P1	0.25000	0.25000	0.0000	0.0537
F1	0.2805(1)	0.3568(5)	0.0666(4)	0.1007
F2	0.2142(2)	0.2927(6)	0.0299(5)	0.1276
F3	0.2660(3)	0.1452(6)	0.0758(4)	0.1282
P2	0.50000	0.2911(3)	0.25000	0.0631
F4	0.4687(3)	0.1909(9)	0.2544(7)	0.2045
F5	0.4699(2)	0.4042(7)	0.2558(5)	0.1358
F6	0.4768(2)	0.2994(8)	0.1428(4)	0.1296
C1	-0.0515(2)	-0.378(1)	-0.1028(7)	0.0829
C2	-0.0553(3)	-0.4866(9)	-0.0296(7)	0.0830
C3	-0.0980(2)	-0.5353(7)	-0.0196(5)	0.0601
C4	-0.1261(2)	-0.6032(8)	-0.1033(5)	0.0627
C5	-0.1132(2)	-0.7199(7)	-0.1259(4)	0.0587
C6	-0.0825(2)	-0.7963(6)	-0.0554(5)	0.0519
C7	-0.0686(2)	-0.7549(7)	0.0366(4)	0.0484
C8	-0.0836(2)	-0.6368(6)	0.0543(4)	0.0468
C9	-0.1184(3)	-0.4197(8)	0.0038(7)	0.0902
C10	-0.1626(3)	-0.525(1)	-0.1752(6)	0.0857
C11	-0.1300(3)	-0.765(1)	-0.2234(5)	0.0824
C12	-0.0653(3)	-0.9204(9)	-0.0775(8)	0.0984

ATOM	x/a	y/b	z/c	$U_{eq}^b$
C13	-0.0363 (2)	-0.8386 (9)	0.1129 (6)	0.0725
C14	-0.0699 (3)	-0.5970 (9)	0.1515 (5)	0.0792
C15	-0.2011 (2)	-0.8251 (6)	-0.1139 (4)	0.0467
C16	-0.1746 (2)	-0.9360 (5)	-0.0784 (5)	0.0477
C17	-0.1500 (2)	-0.9502 (5)	0.0163 (4)	0.0420
C18	-0.1504 (2)	-0.8543 (6)	0.0758 (4)	0.0497
C19	-0.1766 (2)	-0.7411 (6)	0.0409 (4)	0.0536
C20	-0.2020 (2)	-0.7270 (6)	-0.0531 (5)	0.0478
C21	-0.2306 (2)	-0.816 (1)	-0.2156 (5)	0.0634
C22	-0.1758 (3)	-1.0438 (8)	-0.1429 (6)	0.0742
C23	-0.1243 (2)	-1.0728 (7)	0.0518 (7)	0.0664
C24	-0.1258 (3)	-0.8738 (9)	0.1774 (5)	0.0767
C25	-0.1800 (3)	-0.6413 (9)	0.1056 (6)	0.0912
C26	-0.2326 (2)	-0.6136 (7)	-0.0884 (7)	0.0703

<sup>b</sup>  $U_{eq}$  is one third of the trace of the orthogonalized  $U_{ij}$  tensors.

Table A10 Bond Distances (Å) and Angles (°) for  
 [(Et-C<sub>6</sub>Me<sub>6</sub>)(C<sub>6</sub>Me<sub>6</sub>)Fe]PF<sub>6</sub>.

ATOMS	DISTANCE	ATOMS	DISTANCE
Fe1 - C4	2.18(1)	Fe1 - C5	2.111(9)
Fe1 - C6	2.097(9)	Fe1 - C7	2.082(7)
Fe1 - C8	2.152(7)	Fe1 - C15	2.161(6)
Fe1 - C16	2.162(6)	Fe1 - C17	2.179(7)
Fe1 - C18	2.157(9)	Fe1 - C19	2.138(9)
Fe1 - C20	2.153(8)	P1 - F1	1.582(6)
P1 - F2	1.567(9)	P1 - F3	1.552(7)
P2 - F4	1.51(1)	P2 - F5	1.590(9)
P2 - F6	1.574(7)	C1 - C2	1.58(2)
C2 - C3	1.62(2)	C3 - C4	1.46(1)
C3 - C8	1.51(1)	C3 - C9	1.51(2)
C4 - C5	1.39(1)	C4 - C10	1.53(1)
C5 - C6	1.415(9)	C5 - C11	1.51(1)
C6 - C7	1.43(1)	C6 - C12	1.52(1)
C7 - C8	1.40(1)	C7 - C13	1.53(1)
C8 - C14	1.50(1)	C15 - C16	1.42(9)
C15 - C20	1.43(1)	C15 - C21	1.52(1)
C16 - C17	1.41(1)	C16 - C22	1.52(1)
C17 - C18	1.39(1)	C17 - C23	1.51(1)
C18 - C19	1.43(1)	C18 - C24	1.51(1)
C19 - C20	1.402(9)	C19 - C25	1.51(1)

---

ATOMS	DISTANCE	ATOMS	DISTANCE
C20 - C26	1.51(1)		

---

---

ATOMS	ANGLE	ATOMS	ANGLE
F1 - P1 - F2	88.1(4)	F1 - P1 - F3	92.3(4)
F2 - P1 - F3	90.3(5)	F4 - P2 - F5	90.4(6)
F4 - P2 - F6	93.4(5)	F5 - P2 - F6	89.7(4)
C1 - C2 - C3	117.4(7)	C2 - C3 - C4	108.4(9)
C2 - C3 - C8	107.2(7)	C2 - C3 - C9	108.4(8)
C4 - C3 - C8	105.3(6)	C4 - C3 - C9	115.0(7)
C8 - C3 - C9	112.1(9)	C3 - C4 - C5	120.4(7)
C3 - C4 - C10	116.7(8)	C5 - C4 - C10	120.6(7)
C4 - C5 - C6	118.7(7)	C4 - C5 - C11	121.7(7)
C6 - C5 - C11	119.6(8)	C5 - C6 - C7	118.5(7)
C5 - C6 - C12	120.6(8)	C7 - C6 - C12	121.0(7)
C6 - C7 - C8	119.4(6)	C6 - C7 - C13	118.6(7)
C8 - C7 - C13	121.9(7)	C3 - C8 - C7	117.8(7)
C3 - C8 - C14	119.6(7)	C7 - C8 - C14	118.7(6)
C16 - C15 - C20	119.6(6)	C16 - C15 - C21	119.9(7)
C20 - C15 - C21	120.4(6)	C15 - C16 - C17	120.2(7)
C15 - C16 - C22	119.3(7)	C17 - C16 - C22	120.3(6)
C16 - C17 - C18	120.4(6)	C16 - C17 - C23	118.7(7)

---

---

ATOMS	ANGLE	ATOMS	ANGLE
C18 - C17 - C23	120.8(7)	C17 - C18 - C19	119.9(6)
C17 - C18 - C24	119.9(7)	C19 - C18 - C24	120.0(7)
C18 - C19 - C20	120.2(7)	C18 - C19 - C25	120.3(6)
C20 - C19 - C25	119.3(6)	C15 - C20 - C19	119.6(6)
C15 - C20 - C26	120.5(7)	C19 - C20 - C26	119.7(8)

---

**Table A11** Least Squares Best Planes Calculations for [(Et-C<sub>6</sub>Me<sub>6</sub>) (C<sub>6</sub>Me<sub>6</sub>) Fe]PF<sub>6</sub>.

---

**Plane 1**

Equation of the plane:  $30.04(7)X + 4.94(4)Y - 7.10(5)Z = 6.05(2)$

Distances (Å) to the plane from the atoms in the plane.

C4	0.010(11)	C5	-0.018(9)
C6	0.026(10)	C7	-0.013(9)
C8	0.003(9)		

$\chi^2$  for this plane is 14.332

Distances (Å) to the plane from the atoms out of the plane.

Fe1	-1.616(4)	C3	0.596(11)
-----	-----------	----	-----------

**Plane 2**

Equation of the plane:  $30.29(5)X + 4.78(3)Y - 7.35(4)Z = 9.20(2)$

Distances (Å) to the plane from the atoms in the plane.

C15	-0.001(9)	C16	0.011(10)
C17	-0.008(9)	C18	0.001(8)
C19	0.005(9)	C20	-0.007(10)

$\chi^2$  for this plane is 2.877

Distances (Å) to the plane from the atoms out of the plane.

Fe1	1.631(3)	C21	-0.105(14)
C22	-0.067(14)	C23	-0.076(15)
C24	-0.093(13)	C25	-0.097(14)
C26	-0.133(15)		

Dihedral angle between planes A and B.

A	B	Angle(°)
1	2	1.3(3)

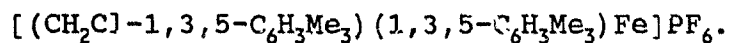
(3c) [ $(\eta^5$ -exo-chloromethyl-2,4,6-trimethylcyclohexadienyl) ( $\eta^6$ -mesitylene) iron(II) hexafluorophosphate

Table A12 Crystal Data and Refinement Parameters for  
 $[(\text{CH}_2\text{Cl-1,3,5-C}_6\text{H}_3\text{Me}_3)(1,3,5\text{-C}_6\text{H}_3\text{Me}_3)\text{Fe}]\text{PF}_6$ .

Formula	$\text{C}_{19}\text{ClF}_6\text{FeH}_{26}\text{P}$
Colour	red
Molecular Wt.	459.70
Space Group	Pbca
Temp., °C	22
a, Å	15.219(2)
b, Å	15.608(2)
c, Å	17.544(5)
$\alpha$ , °	90
$\beta$ , °	90
$\gamma$ , °	90
Cell Volume, Å <sup>3</sup>	4167.4
Z	8
$D_{\text{calc}}$ , g cm <sup>-3</sup>	1.465
Reflections Observed <sup>a</sup>	1230
R	0.052
$R_w$	0.051

<sup>a</sup> Corrections: Lorentz-polarization.  $F_o \geq \sigma(F_o)$

Table A13 Final Fractional Coordinates for



ATOM	x/a	y/b	z/c	$U_{\text{eq}}^b$
Fe1	0.37253(7)	0.25871(7)	0.11778(6)	0.0373
P1	0.6960(2)	0.4700(1)	0.1342(1)	0.0572
F1	0.6279(5)	0.5427(4)	0.1547(4)	0.1080
F2	0.6421(5)	0.4451(4)	0.0609(3)	0.1025
F3	0.7504(5)	0.4943(4)	0.2071(3)	0.0871
F4	0.7641(5)	0.3969(5)	0.1145(4)	0.1090
F5	0.6436(5)	0.3995(4)	0.1805(4)	0.1040
F6	0.7465(6)	0.5402(5)	0.0871(4)	0.1218
C1	0.5267(6)	0.0469(5)	0.1221(6)	0.0583
C2	0.4534(6)	0.1058(5)	0.1507(4)	0.0446
C3	0.4841(6)	0.1986(5)	0.1654(5)	0.0435
C4	0.5026(5)	0.2546(5)	0.1032(4)	0.0441
C5	0.4604(5)	0.2384(6)	0.0316(4)	0.0464
C6	0.3980(6)	0.1732(5)	0.0303(5)	0.0429
C7	0.3818(6)	0.1200(5)	0.0950(4)	0.0442
C8	0.5202(7)	0.2190(7)	0.2432(5)	0.0597
C9	0.4762(8)	0.2977(7)	-0.0356(5)	0.0651
C10	0.3070(7)	0.0578(6)	0.0944(6)	0.0627
C11	0.2530(7)	0.3054(5)	0.0770(5)	0.0507
C12	0.2425(5)	0.2563(6)	0.1438(5)	0.0471
C13	0.2881(7)	0.2729(6)	0.2103(5)	0.0530

---

ATOM	x/a	y/b	z/c	$U_{eq}^b$
C14	0.3471(7)	0.3419(6)	0.2106(5)	0.0562
C15	0.3593(6)	0.3944(5)	0.1457(5)	0.0506
C16	0.3131(6)	0.3744(5)	0.0785(5)	0.0463
C17	0.2034(6)	0.2857(7)	0.0048(5)	0.0563
C18	0.2741(9)	0.2185(8)	0.2815(5)	0.0816
C19	0.4222(7)	0.4688(6)	0.1467(7)	0.0724
C11	0.4947(2)	-0.0657(1)	0.1199(2)	0.0966

---

<sup>b</sup>  $U_{eq}$  is one third of the trace of the orthogonalized  $U_{ij}$  tensors.

Table A14 Bond Distances (Å) and Angles (°) for  
 $[(\text{CH}_2\text{Cl}-1,3,5-\text{C}_6\text{H}_3\text{Me}_3)(1,3,5-\text{C}_6\text{H}_3\text{Me}_3)\text{Fe}]\text{PF}_6$ .

ATOMS	DISTANCE	ATOMS	DISTANCE
Fe1 - C4	2.18(1)	Fe1 - C5	2.111(9)
Fe1 - C3	2.14(1)	Fe1 - C4	2.046(9)
Fe1 - C5	2.065(9)	Fe1 - C6	2.052(9)
Fe1 - C7	2.153(8)	Fe1 - C11	2.12(1)
Fe1 - C12	2.080(9)	Fe1 - C13	2.10(1)
Fe1 - C14	2.10(1)	Fe1 - C15	2.133(9)
Fe1 - C16	2.106(9)	P1 - F1	1.577(8)
P1 - F2	1.583(8)	P1 - F3	1.579(8)
P1 - F4	1.576(9)	P1 - F5	1.575(8)
P1 - F6	1.563(9)	C1 - C2	1.54(1)
C1 - CL1	1.785(9)	C2 - C3	1.51(1)
C2 - C7	1.50(1)	C3 - C4	1.42(1)
C3 - C8	1.51(1)	C4 - C5	1.44(1)
C5 - C6	1.39(1)	C5 - C9	1.51(1)
C6 - C7	1.42(1)	C7 - C10	1.50(2)
C11 - C12	1.40(1)	C11 - C16	1.41(1)
C11 - C17	1.514(1)	C12 - C13	1.39(1)
C13 - C14	1.40(1)	C13 - C18	1.52(1)
C14 - C15	1.40(1)	C15 - C19	1.50(1)
C15 - C16	1.42(1)		

---

ATOMS	ANGLE	ATOMS	ANGLE
F1 - P1 - F2	88.1(4)	F1 - P1 - F3	92.3(4)
F1 - P1 - F2	89.7(5)	F1 - P1 - F3	90.7(4)
F1 - P1 - F4	179.5(4)	F1 - P1 - F5	90.6(4)
F1 - P1 - F6	88.9(4)	F2 - P1 - F3	179.6(3)
F2 - P1 - F4	90.7(4)	F2 - P1 - F5	88.8(4)
F2 - P1 - F6	90.1(4)	F3 - P1 - F4	88.9(4)
F3 - P1 - F5	91.2(4)	F3 - P1 - F6	89.8(4)
F4 - P1 - F5	89.1(4)	F4 - P1 - F6	91.5(5)
F5 - P1 - F6	178.8(5)	C2 - C1 - CL1	111.0(7)
C1 - C2 - C3	111.3(8)	C1 - C2 - C7	115.3(7)
C3 - C2 - C7	102.3(7)	C2 - C3 - C4	119.7(8)
C2 - C3 - C8	117.8(8)	C4 - C3 - C8	119.8(8)
C3 - C4 - C5	118.5(8)	C4 - C5 - C6	117.2(8)
C4 - C5 - C9	120.4(6)	C6 - C5 - C9	122.0(8)
C5 - C6 - C7	121.3(8)	C2 - C7 - C6	118.1(9)
C2 - C7 - C10	119.6(8)	C6 - C7 - C10	119.5(9)
C12 - C11 - C16	117.3(9)	C12 - C11 - C17	122.3(9)
C16 - C11 - C17	120.3(9)	C11 - C12 - C13	123.1(9)
C12 - C13 - C14	118.5(9)	C12 - C13 - C18	121.3(9)
C14 - C13 - C18	120.2(9)	C13 - C14 - C15	120.9(9)
C14 - C15 - C16	118.9(9)	C14 - C15 - C19	120.7(9)
C16 - C15 - C19	120.3(9)	C11 - C16 - C15	121.1(9)

---

**Table A15** Least Squares Best Planes Calculations for  
 $[(\text{CH}_2\text{Cl}-1,3,5-\text{C}_6\text{H}_3\text{Me}_3)(1,3,5-\text{C}_6\text{H}_3\text{Me}_3)\text{Fe}^1\text{PF}_6$ .

---

**Plane 1**

Equation of the plane:  $-11.06(4)X + 9.81(5)Y + 5.04(8)Z = 2.56(3)$

Distances (Å) to the plane from the atoms in the plane.

C3	-0.016(12)	C4	0.024(10)
C5	-0.037(11)	C6	0.024(11)
C7	-0.004(12)		

$\chi^2$  for this plane is 22.471

Distances (Å) to the plane from the atoms out of the plane.

Fe1	1.570(4)	C2	-0.660(13)
-----	----------	----	------------

**Plane 2**

Equation of the plane:  $-11.07(4)X + 9.57(5)Y + 5.61(7)Z = 0.57(3)$

Distances (Å) to the plane from the atoms in the plane.

C11	-0.017(13)	C12	0.006(11)
C13	0.029(13)	C14	-0.062(13)
C15	0.042(12)	C16	-0.012(12)

$\chi^2$  for this plane is 42.294

Distances ( $\text{\AA}$ ) to the plane from the atoms out of the plane.

Fe1	-1.555(4)
-----	-----------

Dihedral angle between planes A and B.

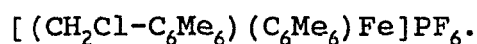
A	B	Angle( $^{\circ}$ )
1	2	2.1(4)

(3e) [ $\eta^5$ -exo-chloromethyl-1,2,3,4,5,6-hexamethylcyclohexadienyl) ( $\eta^6$ -hexamethylbenzene) iron(II) hexafluorophosphate

Table A16 Crystal Data and Refinement Parameters for  
 $[(\text{CH}_2\text{Cl}-\text{C}_6\text{Me}_6)(\text{C}_6\text{Me}_6)\text{Fe}]\text{PF}_6$ .

Formula	$\text{C}_{25}\text{ClF}_6\text{FeH}_{38}\text{P}$
Colour	red
Molecular Wt.	574.64
Space Group	$\text{C2/c}$
Temp., °C	22
a, Å	34.164(3)
b, Å	10.3435(11)
c, Å	16.219(2)
$\alpha$ , °	90
$\beta$ , °	115.680(7)
$\gamma$ , °	90
Cell Volume, Å <sup>3</sup>	5165.28
Z	8
$D_{\text{calc}}$ , g cm <sup>-3</sup>	1.478
Reflections Observed <sup>a</sup>	2286
R	0.058
$R_w$	0.066

<sup>a</sup> Corrections: Lorentz-polarization.  $F_o \geq 2.5\sigma(F_o)$

Table A17 Final Fractional Coordinates for

ATOM	x/a	y/b	z/c	B <sub>iso</sub> <sup>b</sup>
Fe1	0.13517(3)	0.23777(9)	0.02681(6)	2.34(4)
CL1	0.0614(1)	0.6362(3)	0.1053(2)	9.2(2)
C11	0.1738(2)	0.0660(7)	0.0796(5)	3.4(4)
C12	0.2006(2)	0.1774(7)	0.1141(5)	3.5(4)
C13	0.2016(2)	0.2738(7)	0.0525(5)	3.6(4)
C14	0.1759(2)	0.2579(7)	-0.0420(5)	3.5(4)
C15	0.1501(2)	0.1461(7)	-0.0755(5)	3.5(4)
C16	0.1488(2)	0.0511(7)	-0.0156(5)	3.3(4)
C111	0.1750(3)	-0.0431(9)	0.1433(7)	6.0(6)
C121	0.2305(3)	0.189(1)	0.2157(6)	5.9(5)
C131	0.2319(3)	0.3867(9)	0.0868(7)	5.9(6)
C141	0.1792(4)	0.3577(9)	-0.1080(8)	7.0(7)
C151	0.1257(3)	0.125(1)	-0.1774(6)	6.6(6)
C161	0.1235(3)	-0.0717(8)	-0.0522(7)	5.5(5)
C21	0.0978(3)	0.4669(8)	0.0169(5)	4.5(4)
C22	0.0834(2)	0.3635(7)	-0.0549(5)	3.6(4)
C23	0.0673(2)	0.2457(7)	-0.0373(5)	3.8(4)
C24	0.0816(2)	0.2064(7)	0.0550(6)	3.9(4)
C25	0.1124(2)	0.2829(8)	0.1250(5)	3.9(4)
C26	0.1262(3)	0.3988(9)	0.1022(5)	4.9(5)
C211	0.1183(3)	0.5824(9)	-0.0056(7)	6.5(6)

ATOM	x/a	y/b	z/c	B <sub>iso</sub> <sup>b</sup>
C212	0.0543 (3)	0.516 (1)	0.0235 (8)	7.0 (6)
C221	0.0689 (3)	0.404 (1)	-0.1532 (6)	6.9 (6)
C231	0.0349 (3)	0.1641 (9)	-0.1126 (7)	6.5 (6)
C241	0.0639 (3)	0.085 (1)	0.0770 (8)	7.7 (8)
C251	0.1303 (3)	0.239 (1)	0.2242 (6)	7.0 (6)
C261	0.1628 (3)	0.479 (1)	0.1751 (7)	7.8 (6)
P1	0.0	0.2118 (3)	0.25	4.9 (2)
F11	0.0302 (2)	0.0997 (7)	0.2453 (5)	10.8 (5)
F12	0.0309 (3)	0.3100 (9)	0.2462 (8)	18. (1)
F13	-0.0226 (2)	0.2034 (8)	0.1433 (4)	11.6 (5)
P2	0.75	0.25	0.0	4.3 (2)
F21	0.7189 (2)	0.3561 (6)	-0.0666 (4)	8.4 (4)
F22	0.7848 (2)	0.2909 (6)	-0.0325 (6)	10.8 (6)
F23	0.7669 (3)	0.3550 (6)	0.0760 (5)	11.3 (6)
H111A	0.151	-0.100	0.112	10. (3)
H111B	0.172	-0.008	0.196	8.0 (2)
H111C	0.202	-0.091	0.163	8.0 (2)
H121A	0.227	0.116	0.248	11.6 (3)
H121B	0.223	0.265	0.241	8. (2)
H121C	0.260	0.194	0.225	9. (3)
H131A	0.252	0.372	0.149	8. (2)
H131B	0.216	0.465	0.084	9. (2)

ATOM	x/a	y/b	z/c	B <sub>iso</sub> <sup>b</sup>
H131C	0.249	0.401	0.054	7.(2)
H141A	0.190	0.327	-0.150	16.(4)
H141B	0.197	0.431	-0.077	11.(3)
H141C	0.149	0.379	-0.136	15.(4)
H151A	0.139	0.062	-0.201	8.(2)
H151B	0.123	0.203	-0.211	13.(3)
H151C	0.097	0.097	-0.189	10.(3)
H161A	0.098	-0.052	-0.106	8.(2)
H161B	0.115	-0.104	-0.007	7.(2)
H161C	0.137	-0.145	-0.067	5.(2)
H211A	0.133	0.636	0.047	9.(3)
H211B	0.097	0.634	-0.052	8.(2)
H211C	0.139	0.559	-0.030	6.(2)
H212A	0.034	0.543	-0.036	14.(4)
H212B	0.042	0.442	0.039	8.(2)
H221A	0.064	0.328	-0.191	8.(2)
H221B	0.092	0.451	-0.158	6.(2)
H221C	0.044	0.457	-0.185	4.(2)
H231A	0.039	0.177	-0.167	8.(2)
H231B	0.006	0.193	-0.124	11.(3)
H231C	0.035	0.072	-0.105	7.(2)
H241A	0.085	0.041	0.130	11.(3)
H241B	0.054	0.023	0.028	10.(3)

---

ATOM	x/a	y/b	z/c	B <sub>iso</sub> <sup>b</sup>
H241C	0.040	0.109	0.090	9.(3)
H251A	0.159	0.271	0.259	10.(3)
H251B	0.131	0.146	0.230	9.(3)
H251C	0.111	0.274	0.248	9.(3)
H261A	0.173	0.548	0.150	13.(3)
H261B	0.187	0.428	0.215	9.(3)
H261C	0.147	0.511	0.206	8.(2)

---

<sup>b</sup> B<sub>iso</sub> is the Mean of the Principal Axes of the Thermal Ellipsoid.

Table A18 Bond Distances (Å) and Angles (°) for  
 $[(\text{CH}_2\text{Cl}-\text{C}_6\text{Me}_6)(\text{C}_6\text{Me}_6)\text{Fe}]\text{PF}_6$ .

ATOMS	DISTANCE	ATOMS	DISTANCE
Fe1 - C11	2.157(7)	Fe1 - C12	2.156(7)
Fe1 - C13	2.154(7)	Fe1 - C14	2.139(7)
Fe1 - C15	2.155(7)	Fe1 - C16	2.168(7)
Fe1 - C22	2.133(7)	Fe1 - C23	2.091(7)
Fe1 - C24	2.096(7)	Fe1 - C25	2.107(7)
Fe1 - C26	2.166(8)	P1 - F11	1.576(7)
P1 - F12	1.486(7)	P1 - F13	1.563(6)
P2 - F21	1.583(5)	P2 - F22	1.552(6)
P2 - F23	1.554(6)	C11 - C12	1.75(1)
C11 - C12	1.43(1)	C11 - C16	1.41(1)
C11 - C111	1.53(1)	C12 - C13	1.42(1)
C12 - C121	1.52(1)	C13 - C14	1.41(1)
C13 - C131	1.50(1)	C14 - C15	1.41(1)
C14 - C141	1.53(1)	C15 - C16	1.40(1)
C15 - C151	1.51(1)	C16 - C161	1.51(1)
C21 - C22	1.50(1)	C21 - C26	1.48(1)
C21 - C211	1.51(1)	C21 - C212	1.62(1)
C22 - C23	1.42(1)	C22 - C221	1.51(1)
C23 - C24	1.42(1)	C23 - C231	1.50(1)
C24 - C25	1.41(1)	C24 - C241	1.51(1)
C25 - C26	1.40(1)	C25 - C251	1.52(1)

---

ATOMS	DISTANCE	ATOMS	DISTANCE
C26 - C261	1.54(1)		

---

---

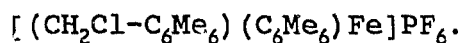
ATOMS	ANGLE	ATOMS	ANGLE
F11 - P1 - F12	90.5(5)	F11 - P1 - F13	85.7(4)
F12 - P1 - F13	90.6(5)	F21 - P2 - F22	87.9(3)
F21 - P2 - F23	88.0(4)	F22 - P2 - F23	90.2(4)
CL1 - C212 - C21	116.3(7)	C12 - C11 - C16	119.9(6)
C12 - C11 - C111	120.7(7)	C16 - C11 - C111	119.2(7)
C11 - C12 - C13	119.8(7)	C11 - C12 - C121	120.3(7)
C13 - C12 - C121	119.7(7)	C12 - C13 - C14	119.4(6)
C12 - C13 - C131	120.5(7)	C14 - C13 - C131	120.0(7)
C13 - C14 - C15	120.3(6)	C13 - C14 - C141	118.9(7)
C15 - C14 - C141	120.5(7)	C14 - C15 - C16	120.8(6)
C14 - C15 - C151	119.7(7)	C16 - C15 - C151	119.4(7)
C11 - C16 - C15	119.9(6)	C11 - C16 - C161	119.6(7)
C15 - C16 - C161	120.4(7)	C22 - C21 - C26	104.4(7)
C22 - C21 - C211	114.1(7)	C22 - C21 - C212	106.0(7)
C26 - C21 - C211	114.7(7)	C26 - C21 - C212	109.7(7)
C211 - C21 - C212	107.7(8)	C21 - C22 - C23	118.9(6)
C21 - C22 - C221	118.2(7)	C23 - C22 - C221	118.1(7)
C22 - C23 - C24	118.3(6)	C22 - C23 - C231	122.1(7)

---

---

ATOMS	ANGLE	ATOMS	ANGLE
C24 - C23 - C231	119.5(8)	C23 - C24 - C25	119.0(7)
C23 - C24 - C241	120.0(8)	C25 - C24 - C241	121.0(8)
C24 - C25 - C26	119.2(7)	C24 - C25 - C251	120.2(8)
C26 - C25 - C251	120.6(8)	C21 - C26 - C25	119.8(7)
C21 - C26 - C261	116.7(8)	C25 - C26 - C261	120.9(8)

---

Table A19 Least Squares Best Planes Calculations for**Plane 1**

Equation of the plane:  $30.00(6)X - 4.89(3)Y - 7.20(5)Z$   
 $= 4.33(2)$

Distances ( $\text{\AA}$ ) to the plane from the atoms in the plane.

C11	-0.007(10)	C12	0.003(10)
C13	0.004(11)	C14	-0.007(10)
C15	0.005(10)	C16	0.002(10)

$\chi^2$  for this plane is 1.544

Distances ( $\text{\AA}$ ) to the plane from the atoms out of the plane.

Fe1	-1.627(4)	C111	0.103(15)
C121	0.112(15)	C131	0.116(16)
C141	0.080(2)	C151	0.112(15)
C161	0.107(15)		

**Plane 2**

Equation of the plane:  $29.62(8)X - 5.12(4)Y - 6.99(5)Z$   
 $= 0.99(2)$

Distances (Å) to the plane from the atoms in the plane.

C22	0.001(11)	C23	0.005(10)
C24	-0.016(11)	C25	0.015(10)
C26	-0.010(12)		

$\chi^2$  for this plane is 5.197

Distances (Å) to the plane from the atoms out of the plane.

Fe1	1.608(4)
-----	----------

Dihedral angle between planes A and B.

A	B	Angle(°)
1	2	1.5(3)

(8a) Bis( $\eta^5$ -tert-butylcyclohexadienyl)iron(II)

Table A20 Crystal Data and Refinement Parameters for  
 [ (<sup>t</sup>Bu-C<sub>6</sub>H<sub>6</sub>)<sub>2</sub>Fe ].

Formula	C <sub>20</sub> FeH <sub>30</sub>
Colour	orange
Formula Wt.	326.30
Space Group	P $\bar{1}$
Temp, °C	20
a, Å	6.421(1)
b, Å	14.916(2)
c, Å	19.282(3)
$\alpha$ , °	99.36(1)
$\beta$ , °	91.92(1)
$\gamma$ , °	92.40(1)
Cell Volume, Å <sup>3</sup>	1819.04
Z	4
D <sub>calc</sub> , g cm <sup>-3</sup>	1.191
Reflections Observed <sup>a</sup>	3257
R	0.041
R <sub>w</sub>	0.046

<sup>a</sup> Corrections: Lorentz-polarization, absorption.  $F_o \geq 2.5\sigma(F_o)$ .

Table A21 Final Fractional Coordinates for [<sup>t</sup>Bu-C<sub>6</sub>H<sub>6</sub>)<sub>2</sub>Fe]<sup>\*</sup>.

Atom	x/a	y/b	z/c	Biso <sup>b</sup>
Fe1	0.3067(1)	0.48981(5)	0.17707(4)	3.01(4)
Fe2	0.6530(1)	0.00669(5)	0.31987(4)	3.40(4)
C1	0.3043(9)	0.6319(4)	0.1933(3)	3.5(3)
C2	0.5012(9)	0.6031(4)	0.1779(3)	3.8(3)
C3	0.5281(9)	0.5387(4)	0.1172(4)	4.2(3)
C4	0.3506(9)	0.5066(4)	0.0756(3)	3.9(3)
C5	0.1579(8)	0.5396(4)	0.0931(3)	3.2(3)
C6	0.1399(8)	0.6328(4)	0.1360(3)	3.1(3)
C7	0.1436(8)	0.7164(4)	0.0961(3)	3.8(3)
C8	0.3495(9)	0.7315(4)	0.0633(4)	6.0(4)
C9	0.1048(1)	0.8009(4)	0.1496(4)	6.3(4)
C10	-0.0334(0)	0.7023(4)	0.0398(3)	5.9(3)
C11	0.4139(9)	0.4590(4)	0.2731(3)	3.7(3)
C12	0.4479(9)	0.3892(4)	0.2187(4)	4.2(3)
C13	0.2788(9)	0.3520(4)	0.1736(3)	4.0(3)
C14	0.0833(9)	0.3898(4)	0.1849(3)	3.6(3)
C15	0.0626(8)	0.4603(4)	0.2415(3)	3.2(3)
C16	0.2058(8)	0.4694(4)	0.3057(3)	3.4(3)
C17	0.1529(8)	0.4114(4)	0.3640(3)	3.7(3)
C18	0.1644(0)	0.1009(4)	0.3375(3)	5.9(4)
C19	0.3004(0)	0.4453(6)	0.4283(4)	7.6(5)
C20	-0.0657(0)	0.4304(5)	0.3882(4)	6.4(4)

---

Atom	x/a	y/b	z/c	Biso <sup>b</sup>
C21	0.8711(8)	-0.0895(4)	0.3377(3)	3.6(3)
C22	0.8913(0)	-0.0104(5)	0.3873(4)	4.7(3)
C23	0.7213(2)	0.0219(5)	0.4260(4)	5.2(4)
C24	0.5283(1)	-0.0260(5)	0.4093(4)	5.0(4)
C25	0.5190(9)	-0.1043(4)	0.3598(3)	3.9(3)
C26	0.7068(8)	-0.1613(4)	0.3445(3)	3.6(3)
C27	0.7559(9)	-0.2306(4)	0.3946(3)	4.4(3)
C28	0.8107(1)	-0.1845(5)	0.4691(4)	7.2(4)
C29	0.9404(1)	-0.2832(5)	0.3663(4)	7.3(4)
C30	0.5715(0)	-0.2962(4)	0.3924(4)	6.4(4)
C31	0.8174(0)	0.0929(4)	0.2636(4)	4.2(3)
C32	0.6536(1)	0.1364(4)	0.2982(4)	4.8(4)
C33	0.4517(0)	0.0959(5)	0.2864(4)	4.7(3)
C34	0.4274(9)	0.0118(4)	0.2426(3)	4.2(3)
C35	0.6005(8)	-0.0279(4)	0.2104(3)	3.5(3)
C36	0.7836(8)	0.0304(4)	0.1947(3)	3.7(3)
C37	0.7767(9)	0.0731(4)	0.1263(4)	4.7(3)
C38	0.9860(1)	0.1201(5)	0.1193(4)	7.8(4)
C39	0.7398(1)	-0.0050(5)	0.0644(4)	7.1(4)
C40	0.6037(2)	0.1387(5)	0.1258(4)	8.0(5)
HC1	0.291(7)	0.664(3)	0.231(3)	3.(1)
HC2	0.612(7)	0.613(3)	0.209(3)	4.(1)

---

---

Atom	x/a	y/b	z/c	Biso <sup>b</sup>
HC3	0.656 (7)	0.513 (3)	0.107 (2)	3. (1)
HC4	0.361 (6)	0.457 (3)	0.041 (3)	3. (1)
HC5	0.033 (6)	0.509 (3)	0.069 (2)	3. (1)
HC6	0.007 (6)	0.633 (3)	0.1534 (2)	2. (1)
H1C8	0.480	0.720	0.087	4.7
H2C8	0.359	0.668	0.019	4.7
H3C8	0.346	0.780	0.030	4.7
H1C9	0.214	0.810	0.185	4.7
H2C9	0.104	0.853	0.126	4.7
H3C9	-0.038	0.788	0.165	4.7
H1C10	-0.016	0.643	0.007	4.7
H2C10	-0.187	0.679	0.060	4.7
H3C10	-0.048	0.758	0.017	4.7
HC11	0.519 (6)	0.485 (3)	0.294 (2)	2. (1)
HC12	0.591 (8)	0.370 (3)	0.203 (3)	5. (1)
HC13	0.297 (7)	0.313 (3)	0.133 (3)	4. (1)
HC14	-0.024 (7)	0.376 (3)	0.151 (3)	4. (1)
HC15	-0.061 (6)	0.491 (3)	0.243 (2)	2. (9)
HC16	0.203 (6)	0.527 (3)	0.327 (2)	3. (1)
H1C18	0.100	0.278	0.375	4.7
H2C18	0.040	0.294	0.295	4.7
H3C18	0.324	0.299	0.316	4.7
H1C19	0.446	0.442	0.423	4.7

---

Atom	x/a	y/b	z/c	Biso <sup>b</sup>
H2C19	0.396	0.403	0.394	4.7
H3C19	0.282	0.402	0.463	4.7
H1C20	-0.063	0.494	0.404	4.7
H2C20	-0.090	0.394	0.425	4.7
H3C20	-0.183	0.405	0.344	4.7
HC21	0.984(7)	0.894(3)	0.302(3)	4.(1)
HC22	1.005(7)	1.021(3)	0.390(3)	4.(1)
HC23	0.729(6)	1.075(3)	0.455(3)	3.(1)
HC24	0.419(9)	1.000(4)	0.427(3)	6.(2)
HC25	0.377(8)	0.871(3)	0.343(3)	6.(2)
HC26	0.678(8)	0.799(4)	0.297(3)	6.(2)
H1C28	0.835	0.766	0.494	4.7
H2C28	0.662	0.836	0.479	4.7
H3C28	0.914	0.870	0.481	4.7
H1C29	0.966	0.689	0.317	4.7
H2C29	0.980	0.666	0.391	4.7
H3C29	1.083	0.763	0.370	4.7
H1C30	0.461	0.736	0.423	4.7
H2C30	0.616	0.654	0.425	4.7
H3C30	0.503	0.661	0.350	4.7
HC31	0.935(7)	1.113(3)	0.273(3)	3.(1)
HC32	0.683(6)	1.190(3)	0.334(3)	3.(1)
HC33	0.345(7)	1.119(3)	0.311(3)	4.(1)

---

Atom	x/a	y/b	z/c	Biso <sup>b</sup>
HC34	0.290(7)	0.979(3)	0.240(3)	5.(1)
HC35	0.578(6)	0.911(3)	0.187(2)	3.(1)
HC36	0.905(7)	0.998(3)	0.193(2)	3.(1)
H1C38	0.994	1.161	0.084	4.7
H2C38	1.050	1.160	0.169	4.7
H3C38	1.104	1.061	0.131	4.7
H1C39	0.773	1.019	0.019	4.7
H2C39	0.896	0.951	0.072	4.7
H3C39	0.571	0.964	0.060	4.7
H1C40	0.625	1.177	0.094	4.7
H2C40	0.641	1.194	0.177	4.7
H3C40	0.467	1.103	0.126	4.7

---

<sup>b</sup> Biso is the Mean of the Principal Axes of the Thermal Ellipsoid.

\* Hydrogen atoms were located from a difference Fourier; those with e.s.d.'s were refined, those without were fixed to the appropriate carbon atom and given fixed isotropic temperature factors.

Table A22 Bond Distances (Å) and Angles (°) for [(<sup>t</sup>Bu-C<sub>6</sub>H<sub>6</sub>)<sub>2</sub>Fe].

ATOMS	DISTANCE	ATOMS	DISTANCE
Fe1 - C1	2.092 (6)	Fe1 - C2	2.056 (5)
Fe1 - C3	2.046 (6)	Fe1 - C4	2.040 (6)
Fe1 - C5	2.105 (5)	Fe1 - C11	2.081 (6)
Fe1 - C12	2.044 (6)	Fe1 - C13	2.046 (6)
Fe1 - C14	2.053 (5)	Fe1 - C15	2.108 (5)
Fe2 - C21	2.105 (6)	Fe2 - C22	2.026 (6)
Fe2 - C23	2.053 (7)	Fe2 - C24	2.045 (7)
Fe2 - C25	2.101 (6)	Fe2 - C31	2.088 (6)
Fe2 - C32	2.044 (6)	Fe2 - C33	2.056 (6)
Fe2 - C34	2.055 (6)	Fe2 - C35	2.102 (6)
C1 - C2	1.378 (8)	C1 - C6	1.504 (8)
C2 - C3	1.41 (1)	C3 - C4	1.393 (9)
C4 - C5	1.383 (8)	C5 - C6	1.509 (8)
C6 - C7	1.567 (8)	C7 - C8	1.509 (8)
C7 - C9	1.528 (9)	C7 - C10	1.529 (8)
C11 - C12	1.382 (9)	C11 - C16	1.499 (8)
C12 - C13	1.405 (9)	C13 - C14	1.407 (8)
C14 - C15	1.401 (8)	C15 - C16	1.502 (8)
C16 - C17	1.562 (8)	C17 - C18	1.508 (8)
C17 - C19	1.539 (9)	C17 - C20	1.518 (8)
C21 - C22	1.391 (9)	C21 - C26	1.496 (8)

ATOMS	DISTANCE	ATOMS	DISTANCE
C22 - C23	1.40(1)	C23 - C24	1.40(1)
C24 - C25	1.38(1)	C25 - C26	1.513(8)
C26 - C27	1.560(8)	C27 - C28	1.513(9)
C27 - C29	1.516(9)	C27 - C30	1.500(8)
C31 - C32	1.391(9)	C31 - C36	1.498(9)
C32 - C33	1.403(9)	C33 - C34	1.39(1)
C34 - C35	1.397(8)	C35 - C36	1.501(8)
C36 - C37	1.555(9)	C37 - C38	1.510(9)
C37 - C39	1.53(1)	C37 - C40	1.512(9)

ATOMS	ANGLE	ATOMS	ANGLE
C1 - C2 - C3	119.4(6)	C1 - C6 - C7	117.7(4)
C1 - C6 - C5	101.1(4)	C2 - C1 - C6	121.2(6)
C2 - C3 - C4	117.5(6)	C3 - C4 - C5	120.3(6)
C4 - C5 - C6	121.0(5)	C5 - C6 - C7	117.8(5)
C6 - C7 - C8	112.9(4)	C6 - C7 - C9	107.6(5)
C6 - C7 - C10	108.8(4)	C8 - C7 - C9	108.3(5)
C8 - C7 - C10	110.3(5)	C9 - C7 - C10	108.8(5)
C11 - C12 - C13	118.9(5)	C11 - C16 - C15	101.1(5)
C11 - C16 - C17	118.0(5)	C12 - C11 - C16	121.8(5)
C12 - C13 - C14	118.0(6)	C13 - C14 - C15	119.4(5)

---

ATOMS	ANGLE	ATOMS	ANGLE
C14 - C15 - C16	120.5(5)	C15 - C16 - C17	118.6(4)
C16 - C17 - C18	111.7(5)	C16 - C17 - C19	107.8(5)
C16 - C17 - C20	109.3(4)	C18 - C17 - C19	113.0(5)
C18 - C17 - C20	109.0(5)	C19 - C17 - C20	105.9(5)
C21 - C22 - C23	121.0(6)	C21 - C26 - C25	101.0(5)
C21 - C26 - C27	117.9(5)	C22 - C21 - C26	120.1(6)
C22 - C23 - C24	116.9(6)	C23 - C24 - C25	119.0(6)
C24 - C25 - C26	122.0(5)	C25 - C26 - C27	117.4(5)
C26 - C27 - C28	112.4(5)	C26 - C27 - C29	107.7(5)
C26 - C27 - C30	108.6(5)	C28 - C27 - C29	108.7(5)
C28 - C27 - C30	110.9(5)	C29 - C27 - C30	108.3(5)
C31 - C32 - C33	118.8(6)	C31 - C36 - C35	100.7(5)
C31 - C36 - C37	118.2(5)	C32 - C31 - C36	121.8(6)
C32 - C33 - C34	117.8(6)	C33 - C34 - C35	119.8(5)
C34 - C35 - C36	120.4(5)	C35 - C36 - C37	119.3(5)
C36 - C37 - C38	108.7(5)	C36 - C37 - C39	107.3(5)
C36 - C37 - C40	112.0(5)	C38 - C37 - C39	108.6(6)
C38 - C37 - C40	110.8(6)	C39 - C37 - C40	109.3(6)

---

Table A23 Least Squares Best Planes Calculations for [(<sup>t</sup>Bu-  
C<sub>6</sub>H<sub>6</sub>)<sub>2</sub>Fe].

---

**Plane 1**

Equation of the plane:  $0.86(2)X + 12.40(3)Y - 12.81(4)Z = 5.63(2)$

Distances ( $\text{\AA}$ ) to the plane from the atoms in the plane.

C1	-0.006(9)	C2	0.003(8)
C3	0.007(8)	C4	-0.012(8)
C5	0.007(7)		

$\chi^2$  for this plane is 4.493

Distances ( $\text{\AA}$ ) to the plane from the atoms out of the plane.

Fe1	-1.558(3)	C6	0.598(8)
-----	-----------	----	----------

**Plane 2**

Equation of the plane:  $1.31(2)X + 11.42(3)Y - 13.96(4)Z = 1.97(2)$

Distances ( $\text{\AA}$ ) to the plane from the atoms in the plane.

C11	0.000(8)	C12	0.005(8)
C13	-0.010(8)	C14	0.008(8)
C15	-0.004(8)		

$\chi^2$  for this plane is 3.301

Distances (Å) to the plane from the atoms out of the plane.

Fe1	1.552(3)	C16	-0.609(9)
-----	----------	-----	-----------

### Plane 3

Equation of the plane:  $1.39(2)X - 10.20(4)Y + 15.40(4)Z = 7.32(2)$

Distances (Å) to the plane from the atoms in the plane.

C21	0.002(8)	C22	-0.011(8)
C23	0.020(9)	C24	-0.018(9)
C25	0.005(9)		

$\chi^2$  for this plane is 10.398

Distances (Å) to the plane from the atoms out of the plane.

Fe1	-1.556(3)	C26	0.611(9)
-----	-----------	-----	----------

### Plane 4

Equation of the plane:  $0.98(2)X - 9.14(4)Y + 16.65(3)Z = 4.35(1)$

Distances (Å) to the plane from the atoms in the plane.

C31	-0.006(9)	C32	0.012(9)
C33	-0.012(9)	C34	0.004(8)
C35	0.000(9)		

$\chi^2$  for this plane is 4.192

Distances ( $\text{\AA}$ ) to the plane from the atoms out of the plane.

Fe1	1.558(3)	C26	-0.616(9)
-----	----------	-----	-----------

Dihedral angle between planes A and B.

A	B	Angle( $^{\circ}$ )
1	2	6.6(3)
3	4	6.9(3)

(15) ( $\eta^6$ -hexamethylbenzene) ( $\eta^6$ -meta-xylene) iron(II)  
hexafluorophosphate

Table A24 Crystal Data and Refinement Parameters for  
[(1,3-C<sub>6</sub>H<sub>4</sub>Me<sub>2</sub>) (C<sub>6</sub>Me<sub>6</sub>) Fe] (PF<sub>6</sub>)<sub>2</sub>.

Formula	C <sub>20</sub> F <sub>12</sub> FeH <sub>28</sub> P <sub>2</sub>
Colour	orange
Formula Wt.	614.21
Space Group	Pbc2 <sub>1</sub>
Temp, °C	22
a, Å	8.980
b, Å	16.898
c, Å	15.981
$\alpha$ , °	90
$\beta$ , °	90
$\gamma$ , °	90
Cell Volume, Å <sup>3</sup>	2425.0
Z	4
D <sub>calc</sub> , g cm <sup>-3</sup>	1.682
Reflections Observed <sup>a</sup>	1064
R	0.048
R <sub>w</sub>	0.051

<sup>a</sup> Corrections: Lorentz-polarization, absorption I<sub>0</sub> ≥  
2.5σ(I<sub>0</sub>).

Table A25 Final Fractional Coordinates for [(1,3-  
 $C_6H_4Me_2$ ) ( $C_6Me_6$ ) Fe] ( $PF_6$ )<sub>2</sub>.

Atom	x/a	y/b	z/c	B <sub>iso</sub> <sup>b</sup>
Fe	0.2630 (1)	0.40168 (6)	0.25000	2.48 (4)
P1	0.3372 (3)	0.7624 (2)	0.5187 (2)	4.0 (1)
F1	0.3038 (1)	0.7426 (7)	0.4277 (6)	13.2 (7)
F2	0.5075 (7)	0.7587 (7)	0.4971 (6)	10.2 (5)
F3	0.3314 (1)	0.8512 (5)	0.4926 (6)	12.2 (7)
F4	0.3920 (1)	0.7881 (7)	0.6080 (6)	12.7 (6)
F5	0.3484 (1)	0.6742 (4)	0.5493 (7)	11.0 (6)
F6	0.1749 (8)	0.7746 (5)	0.5466 (8)	11.8 (7)
P2	0.2109 (3)	0.0740 (1)	0.3767 (2)	3.6 (1)
F11	0.0749 (8)	0.0453 (5)	0.4308 (5)	8.7 (4)
F12	0.0974 (8)	0.1122 (4)	0.3138 (5)	8.3 (4)
F13	0.2015 (7)	-0.0061 (4)	0.3261 (5)	7.7 (4)
F14	0.3464 (7)	0.1006 (4)	0.3201 (6)	8.2 (4)
F15	0.3270 (9)	0.0349 (5)	0.4371 (6)	9.9 (5)
F16	0.2193 (8)	0.1563 (4)	0.4239 (6)	9.3 (5)
C1	0.2006 (9)	0.5194 (5)	0.2833 (6)	3.4 (4)
C2	0.203 (1)	0.4718 (6)	0.3548 (6)	3.8 (4)
C3	0.118 (1)	0.3983 (6)	0.3552 (6)	3.8 (4)
C4	0.038 (1)	0.3775 (6)	0.2838 (6)	3.4 (4)
C5	0.040 (1)	0.4231 (5)	0.2109 (6)	3.2 (4)
C6	0.1215 (9)	0.4973 (5)	0.2121 (6)	3.0 (4)

---

Atom	x/a	y/b	z/c	B <sub>iso</sub> <sup>b</sup>
C7	0.280(1)	0.5976(5)	0.2854(7)	5.2(5)
C8	0.291(1)	0.4962(8)	0.4296(7)	6.4(6)
C9	0.116(1)	0.3467(7)	0.4327(7)	6.3(6)
C10	-0.053(1)	0.3014(6)	0.2864(8)	6.3(6)
C11	-0.050(1)	0.4031(7)	0.1352(7)	6.1(6)
C12	0.116(1)	0.5486(6)	0.1364(7)	5.4(5)
C21	0.317(1)	0.2976(6)	0.1783(7)	4.5(4)
C22	0.361(1)	0.2896(6)	0.2640(7)	4.7(5)
C23	0.450(1)	0.3453(7)	0.3021(7)	5.0(5)
C24	0.4960(8)	0.4121(6)	0.2564(9)	4.1(5)
C25	0.4557(9)	0.4230(5)	0.1738(7)	3.5(4)
C26	0.3614(9)	0.3676(5)	0.1369(6)	3.2(4)
C27	0.225(1)	0.2377(7)	0.1369(9)	7.0(6)
C28	0.508(1)	0.4949(7)	0.1258(8)	5.6(5)

---

<sup>b</sup> B<sub>iso</sub> is the Mean of the Principle Axes of the Thermal Ellipsoid.

Table A26 Bond Distances (Å) and Angles (°) for  
 [(1,3-C<sub>6</sub>H<sub>4</sub>Me<sub>2</sub>)(C<sub>6</sub>Me<sub>6</sub>)Fe](PF<sub>6</sub>)<sub>2</sub>.

ATOMS	DISTANCE	ATOMS	DISTANCE
Fe - C1	2.134(8)	P2 - F16	1.583(7)
Fe - C2	2.121(9)	F11 - F12	2.20(1)
Fe - C3	2.125(8)	F14 - F15	2.18(1)
Fe - C4	2.129(9)	C1 - C2	1.40(1)
Fe - C5	2.133(9)	C1 - C6	1.39(1)
Fe - C6	2.143(8)	C1 - C7	1.50(1)
Fe - C21	2.154(9)	C2 - C3	1.46(1)
Fe - C22	2.102(9)	C2 - C8	1.49(1)
Fe - C23	2.105(9)	C3 - C4	1.39(1)
Fe - C24	2.102(8)	C3 - C	1.52(1)
Fe - C25	2.146(8)	C4 - C5	1.40(1)
Fe - C26	2.093(8)	C4 - C10	1.52(1)
P1 - F1	1.522(9)	C5 - C6	1.45(1)
P1 - F2	1.569(7)	C5 - C11	1.49(1)
P1 - F3	1.558(8)	C6 - C12	1.49(1)
P1 - F4	1.570(9)	C21 - C22	1.43(2)
P1 - F5	1.572(7)	C21 - C26	1.41(1)
P1 - F6	1.537(8)	C21 - C27	1.47(2)
P2 - F11	1.573(7)	C22 - C23	1.38(2)
P2 - F12	1.571(7)	C23 - C24	1.41(2)
P2 - F13	1.580(7)	C24 - C25	1.38(2)

ATOMS	DISTANCE	ATOMS	DISTANCE
P2 - F14	1.582(7)	C25 - C26	1.39(1)
P2 - F15	1.567(7)	C25 - C28	1.51(1)
Fe - Cent1	1.594(4)	Fe - Cent2	1.587(5)

ATOM	ANGLE	ATOMS	ANGLE
C1 - C2 - C3	119.2(8)	C1 - C2 - C8	120.3(9)
C1 - C6 - C5	120.1(8)	C1 - C6 - C12	121.6(8)
C2 - C1 - C6	121.3(8)	C2 - C1 - C7	118.8(8)
C2 - C3 - C4	118.8(8)	C2 - C3 - C9	120.1(9)
C3 - C2 - C8	120.6(9)	C3 - C4 - C5	122.6(9)
C3 - C4 - C10	117.9(9)	C4 - C3 - C9	121.1(9)
C4 - C5 - C6	118.0(8)	C4 - C5 - C11	123.1(9)
C5 - C4 - C10	119.5(9)	C5 - C6 - C12	118.3(8)
C6 - C1 - C7	119.8(8)	C6 - C5 - C11	118.7(9)
C21 - C22 - C23	121.4(9)	C21 - C26 - C25	122.4(9)
C22 - C21 - C26	116.5(9)	C22 - C21 - C27	122.(1)
C22 - C23 - C24	119.2(10)	C23 - C24 - C25	121.8(9)
C24 - C25 - C28	120.7(9)	C24 - C25 - C26	118.4(8)
C26 - C21 - C27	122.(1)	C26 - C25 - C28	121.(1)
F1 - P1 - F2	88.4(6)	F1 - P1 - F3	87.1(6)
F1 - P1 - F4	172.1(7)	F1 - P1 - F5	95.8(6)

---

ATOMS	ANGLE	ATOMS	ANGLE
F1 - P1 - F6	96.9(6)	F2 - P1 - F3	90.7(6)
F2 - P1 - F4	84.6(5)	F2 - P1 - F5	88.2(5)
F2 - P1 - F6	173.2(6)	F3 - P1 - F4	89.3(6)
F3 - P1 - F5	176.9(6)	F3 - P1 - F6	85.3(5)
F4 - P1 - F5	87.7(6)	F4 - P1 - F6	89.9(6)
F5 - P1 - F6	95.6(5)	F11 - P2 - F12	88.6(5)
F11 - P2 - F13	88.5(4)	F11 - P2 - F14	178.0(5)
F11 - P2 - F15	92.8(5)	F11 - P2 - F16	92.7(5)
F12 - P2 - F13	89.4(4)	F12 - P2 - F14	90.9(5)
F12 - P2 - F15	178.2(5)	F12 - P2 - F16	88.6(4)
F13 - P2 - F14	89.5(4)	F13 - P2 - F15	89.4(4)
F13 - P2 - F16	177.6(5)	F14 - P2 - F15	87.7(5)
F14 - P2 - F16	89.3(5)	F15 - P2 - F16	92.6(5)

---

Table A27 Least Squares Best Planes Calculations for [(1,3-  
C<sub>6</sub>H<sub>4</sub>Me<sub>2</sub>) (C<sub>6</sub>Me<sub>6</sub>)Fe] (PF<sub>6</sub>)<sub>2</sub>.

---

**Plane 1**

Equation of the plane:  $-7.22(2)X + 8.21(6)Y + 5.47(6)Z$   
 $= 4.36(3)$

Distances (Å) to the plane from the atoms in the plane.

C1	0.006(11)	C2	-0.010(12)
C3	-0.001(12)	C4	0.016(12)
C5	-0.018(12)	C6	0.006(11)

$\chi^2$  for this plane is 5.126

Distances (Å) to the plane from the atoms out of the plane.

Fe1	-1.594(4)	C7	0.090(16)
C8	-0.034(18)	C9	0.015(17)
C10	0.063(18)	C11	0.048(17)
C12	0.055(16)		

**Plane 2**

Equation of the plane:  $-7.30(3)X - 8.31(7)Y + 4.96(7)Z$   
 $= 1.07(4)$

Distances (Å) to the plane from the atoms in the plane.

C21	-0.027(14)	C22	0.006(14)
C23	0.008(15)	C24	0.004(17)
C25	-0.022(13)	C26	0.024(11)

$\chi^2$  for this plane is 11.708

Distances (Å) to the plane from the atoms out of the plane.

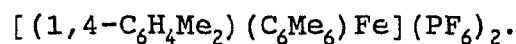
Fe1	1.587(5)	C27	-0.058(20)
C28	-0.041(19)		

Dihedral angle between planes A and B.

A	B	Angle(°)
1	2	1.9(3)

(16) ( $\eta^6$ -hexamethylbenzene) ( $\eta^6$ -para-xylene) iron(II)  
hexafluorophosphate

Table A28 Crystal Data and Refinement Parameters for



Formula	$C_{20}F_{12}FeH_{28}P_2$
Colour	orange
Formula Wt.	514.21
Space Group	Pnma
Temp, °C	20
a, Å	18.406(2)
b, Å	9.285(1)
c, Å	14.703(2)
$\alpha$ , °	90
$\beta$ , °	90
$\gamma$ , °	90
Cell Volume, Å <sup>3</sup>	2513
Z	4
$D_{calc}$ , g cm <sup>-3</sup>	1.62
Reflections Observed <sup>a</sup>	1313
R	0.056
$R_w$	0.070

<sup>a</sup> Corrections: Lorentz-polarization.  $F_o \geq 5\sigma(F_o)$ .

**Table A29** Final Fractional Coordinates for [(1,4-  
 $C_6H_4Me_2)(C_6Me_6)Fe](PF_6)_2$ .

Atom	x/a	y/b	z/c	B(eqv) <sup>b</sup>
Fe	0.87287(7)	0.7500	0.29297(9)	2.40
P1	0.6452(1)	0.7500	0.0378(2)	3.39
P2	0.5593(2)	1.2500	0.3164(2)	4.21
F1	0.6495(4)	0.7500	0.1445(4)	6.06
F2	0.6411(4)	0.7500	-0.0686(4)	6.98
F3	0.5839(2)	0.6310(6)	0.0424(4)	5.81
F4	0.7058(3)	0.6301(7)	0.0345(4)	7.18
F5	0.4841(5)	1.2500	0.2675(8)	10.05
F6	0.6326(4)	1.2500	0.3684(6)	6.70
F7	0.5876(4)	1.3684(6)	0.2497(5)	8.46
F8	0.5326(4)	1.3705(8)	0.3797(5)	10.37
C1	0.7635(3)	0.8257(7)	0.3032(4)	2.94
C2	0.8014(4)	0.9001(7)	0.2331(5)	3.08
C3	0.8367(3)	0.8244(7)	0.1636(4)	3.27
C4	0.7252(4)	0.9113(9)	0.3760(6)	4.58
C5	0.8002(5)	1.0645(8)	0.2333(7)	5.50
C6	0.8743(5)	0.906(1)	0.0888(5)	5.77
C7	0.9046(5)	0.7500	0.4337(7)	3.39
C8	0.9244(3)	0.6202(8)	0.3905(5)	3.38
C9	0.9654(3)	0.6201(8)	0.3104(5)	3.64
C10	0.9895(5)	0.7500	0.2697(7)	3.79

---

Atom	x/a	y/b	z/c	B(eqv) <sup>b</sup>
C11	0.8681(7)	0.7500	0.5224(7)	5.07
C12	1.0345(7)	0.7500	0.1883(8)	5.06

---

<sup>b</sup>  $B(\text{eqv}) = 4/3[a^2\beta_{11} + b^2\beta_{22} + c^2\beta_{33} + ab(\cos \gamma)\beta_{12} + ac(\cos \beta)\beta_{13} + bc(\cos \alpha)\beta_{23}]$ .

Table A30 Bond Distances (Å) and Angles (°) for  
 $[(1,4\text{-C}_6\text{H}_4\text{Me}_2)(\text{C}_6\text{Me}_6)\text{Fe}](\text{PF}_6)_2$ .

ATOMS	DISTANCE	ATOMS	DISTANCE
Fe - C1	2.138(6)	Fe - C2	2.109(6)
Fe - C3	2.130(6)	Fe - C7	2.15(1)
Fe - C8	2.100(6)	Fe - C9	2.102(6)
Fe - C10	2.173(9)	C1 - C2	1.423(8)
C1 - C4	1.508(9)	C1 - C1a	1.41(1)
C3 - C6	1.50(1)	C3 - C3a	1.38(1)
C7 - C8	1.410(9)	C7 - C11	1.47(1)
C8 - C9	1.399(9)	C9 - C10	1.417(9)
C10 - C12	1.46(1)	P1 - F1	1.571(7)
P1 - F2	1.565(7)	P1 - F3	1.581(5)
P1 - F4	1.576(5)	P2 - F5	1.560(8)
P2 - F6	1.551(7)	P2 - F7	1.563(6)
P2 - F8	1.535(6)	Fe - Cent1	1.60
Fe - Cent2	1.59		

ATOMS	ANGLE	ATOMS	ANGLE
C1 - C2 - C3	120.8(6)	C1 - C2 - C5	118.5(7)
C2 - C1 - C4	119.1(6)	C2 - C3 - C6	119.7(7)
C3 - C2 - C5	120.6(7)	C7 - C8 - C9	121.3(7)

---

ATOMS	ANGLE	ATOMS	ANGLE
C8 - C7 - C11	121.2(5)	C8 - C7 - C8a	117(1)
C8 - C9 - C10	121.5(8)	C9 - C10 - C9a	117(1)
C9 - C10 - C12	121.7(5)	F1 - P1 - F2	179.9(1)
F1 - P1 - F3	89.6(3)	F1 - P1 - F4	89.7(3)
F2 - P1 - F3	90.5(3)	F2 - P1 - F4	90.2(3)
F3 - P1 - F4	90.8(3)	F3 - P1 - F3a	88.6(4)
F4 - P1 - F4a	89.9(5)	F5 - P2 - F6	178.0(6)
F5 - P2 - F7	90.4(4)	F5 - P2 - F8	89.8(5)
F6 - P2 - F7	91.1(4)	F6 - P2 - F8	88.8(4)
F7 - P2 - F8	88.5(4)	F7 - P2 - F7b	89.4(6)
F8 - P2 - F8b	93.5(7)	Cent1 - Fe - Cent2	179.1

---

a = symmetry equivalent x, 1.5-y, z

b = symmetry equivalent x, 2.5-y, z

Table A31 Least Squares Best Planes Calculations for [(1,4-  
C<sub>6</sub>H<sub>4</sub>Me<sub>2</sub>) (C<sub>6</sub>Me<sub>6</sub>) Fe] (PF<sub>6</sub>)<sub>2</sub>.

---

**Plane 1**

Equation of the plane:  $15.39X + 0Y + 8.07Z = 14.20$

Distances (Å) to the plane from the atoms in the plane.

C1	-0.006	C2	0.012
C3	-0.006	C1'	-0.006
C2'	0.012	C3'	-0.006

Distances (Å) to the plane from the atoms out of the plane.

Fe1	1.595	C4	-0.008
C5	-0.005	C6	-0.031
C4'	-0.008	C5'	-0.005
C6'	-0.031		

**Plane 2**

Equation of the plane:  $15.46X + 0Y + 7.98Z = 17.42$

Distances (Å) to the plane from the atoms in the plane.

C7	0.027	C8	-0.012
C9	-0.017	C10	0.031
C8'	-0.012	C9'	-0.017

Distances ( $\text{\AA}$ ) to the plane from the atoms out of the plane.

Fe1	-1.587	C11	0.170
C12	0.078		

Dihedral angle between planes A and B.

A	B	Angle( $^{\circ}$ )
1	2	0.4

(21c) ( $\eta^5$ -Cyclopentadienyl)( $\eta^5$ -exo-6-phenyl-1,3,5-trimethylcyclohexadienyl)iron(II)

Table A32 Crystal Data and Refinement Parameters for  
 $[(C_5H_5)(C_6H_5-1,3,5-C_6H_3Me_3)Fe]$ .

Formula	$C_{20}FeH_{22}$
Colour	orange
Molecular Wt.	318.24
Space Group	$P2_1/n$
Temp., °C	22
a, Å	8.5703(5)
b, Å	8.5283(9)
c, Å	21.844(2)
$\alpha$ , °	90
$\beta$ , °	93.868(6)
$\gamma$ , °	90
Cell Volume, Å <sup>3</sup>	1592.91
Z	4
$D_{calc}$ , g cm <sup>-3</sup>	1.327
Reflections observed <sup>a</sup>	2046
R	0.035
$R_w$	0.049

<sup>a</sup> Corrections: Lorentz-polarization.  $I_o \geq 2.5\sigma(I_o)$ .

**Table A33** Final Fractional Coordinates for [(C<sub>5</sub>H<sub>5</sub>)(C<sub>6</sub>H<sub>5</sub>-  
1,3,5-C<sub>6</sub>H<sub>3</sub>Me<sub>3</sub>)Fe].

Atom	x/a	y/b	z/c	B <sub>iso</sub> <sup>b</sup>
Fe1	0.8173(4)	0.75388(5)	0.11358(2)	3.30(2)
C11	1.0341(4)	0.6508(5)	0.1243(2)	5.9(2)
C12	0.9236(5)	0.5414(4)	0.0998(2)	6.9(2)
C13	0.8600(4)	0.6016(5)	0.0434(2)	6.4(2)
C14	0.9307(4)	0.7459(4)	0.0333(2)	5.5(2)
C15	1.0391(3)	0.7767(4)	0.0837(2)	5.1(2)
C21	0.5483(3)	0.9104(3)	0.0961(1)	3.1(1)
C22	0.7131(3)	0.9752(3)	0.1078(1)	3.2(1)
C23	0.7935(3)	0.9484(3)	0.1655(1)	3.2(1)
C24	0.7602(3)	0.8127(4)	0.2003(1)	3.5(1)
C25	0.6498(3)	0.7061(3)	0.1721(1)	3.7(1)
C26	0.5738(3)	0.7407(3)	0.1143(1)	3.5(1)
C27	0.7631(4)	1.1080(4)	0.06801(1)	4.5(1)
C28	0.8497(4)	0.7759(4)	0.2607(2)	4.9(2)
C29	0.4718(4)	0.6185(4)	0.0816(2)	5.0(2)
C31	0.4213(3)	1.0025(3)	0.1266(1)	3.1(1)
C32	0.3621(3)	0.9553(4)	0.1813(1)	3.9(1)
C33	0.2488(4)	1.0426(4)	0.2083(1)	4.5(1)
C34	0.1936(3)	1.1806(4)	0.1808(2)	4.7(1)
C35	0.2496(4)	1.2281(4)	0.1269(2)	4.8(2)

---

Atom	x/a	y/b	z/c	$B_{iso}^b$
C36	0.3624(4)	1.1397(3)	0.0996(1)	4.0(1)

---

<sup>b</sup>  $B_{iso}$  is the Mean of the Principal Axes of the Thermal Ellipsoid.

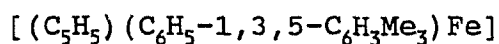
**Table A34** Bond Distances (Å) and Angles (°) for  
 $[(C_5H_5)(C_6H_5-1,3,5-C_6H_3Me_3)Fe]$ .

ATOMS	DISTANCE	ATOMS	DISTANCE
Fe1 - C11	2.055(3)	Fe1 - C12	2.059(3)
Fe1 - C13	2.060(3)	Fe1 - C14	2.063(3)
Fe1 - C15	2.060(3)	Fe1 - C22	2.088(3)
Fe1 - C23	2.027(3)	Fe1 - C24	2.050(3)
Fe1 - C25	2.028(3)	Fe1 - C26	2.091(3)
C11 - C12	1.409(6)	C11 - C15	1.395(6)
C12 - C13	1.409(6)	C13 - C14	1.397(5)
C14 - C15	1.417(5)	C21 - C22	1.522(4)
C21 - C26	1.512(4)	C21 - C31	1.531(4)
C22 - C23	1.412(4)	C22 - C27	1.507(4)
C23 - C24	1.425(4)	C24 - C25	1.422(4)
C24 - C28	1.514(4)	C25 - C26	1.413(4)
C26 - C29	1.509(4)	C31 - C32	1.398(4)
C31 - C36	1.391(4)	C32 - C33	1.387(4)
C33 - C34	1.390(5)	C34 - C35	1.363(5)
C35 - C36	1.391(4)	Fe - Cent1	1.677(2)
Fe - Cent2	1.526(1)		

---

ATOMS	ANGLE	ATOMS	ANGLE
C11 - C12 - C13	107.6(3)	C11 - C15 - C14	107.8(3)
C12 - C11 - C15	108.4(3)	C21 - C22 - C23	118.8(2)
C21 - C22 - C27	118.2(2)	C21 - C26 - C25	119.0(2)
C21 - C26 - C29	117.9(3)	C21 - C31 - C32	122.5(3)
C21 - C31 - C36	119.7(2)	C22 - C21 - C26	100.8(2)
C22 - C21 - C31	114.8(2)	C22 - C23 - C24	120.3(2)
C23 - C22 - C27	119.7(2)	C23 - C24 - C25	116.1(2)
C23 - C24 - C28	121.7(3)	C24 - C25 - C26	120.4(3)
C25 - C24 - C28	121.8(3)	C25 - C26 - C29	119.7(3)
C26 - C21 - C31	118.1(2)	C31 - C32 - C33	121.2(3)
C31 - C36 - C35	121.1(3)	C32 - C31 - C36	117.8(3)
C32 - C33 - C34	119.8(3)	C33 - C34 - C35	119.7(3)
C34 - C35 - C36	120.3(3)		

---

Table A35 Least Squares Best Planes Calculations for**Plane 1**

Equation of the plane:  $-6.425(12)X + 3.94(2)Y + 11.43(4)Z = 2.66(2)$

Distances (Å) to the plane from the atoms in the plane.

C11	0.000(5)	C12	-0.001(6)
C13	0.001(5)	C14	-0.001(5)
C15	0.000(5)		

$\chi^2$  for this plane is 0.134

Distances (Å) to the plane from the atoms out of the plane.

Fe1	1.677(2)
-----	----------

**Plane 2**

Equation of the plane:  $-6.471(7)X + 4.144(9)Y + 10.71(3)Z = 0.576(12)$

Distances (Å) to the plane from the atoms in the plane.

C22	0.004(3)	C23	-0.010(3)
C24	0.016(4)	C25	-0.013(4)
C26	0.004(6)		

$\chi^2$  for this plane is 40.24

Distances (Å) to the plane from the atoms out of the plane.

Fe1	-1.526(1)	C21	0.677(4)
C27	-0.195(5)	C28	-0.069(6)
C29	-0.193(6)		

**Plane 3**

Equation of the plane:  $5.870(8)X + 4.441(10)Y + 10.10(3)Z = 8.200(8)$

Distances (Å) to the plane from the atoms in the plane.

C31	0.005(4)	C32	-0.001(4)
C33	-0.005(4)	C34	0.006(4)
C35	0.001(4)	C36	-0.005(4)

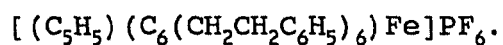
$\chi^2$  for this plane is 6.919

Dihedral angle between planes A and B.

A	B	Angle(°)
1	2	2.4(2)
2	3	92.3(1)

(22) ( $\eta^6$ -Hexa(phenylethyl)benzene) ( $\eta^5$ -  
cyclopentadienyl)iron(II) hexafluorophosphate

Table A36 Crystal Data and Refinement Parameters for




---

Formula	$C_{59}F_6FeH_{59}P$
Colour	yellow
Formula Wt.	968.93
Space Group	$Pn2_1a$
Temp, °C	20
a, Å	26.192(9)
b, Å	18.447(6)
c, Å	10.066(7)
$\alpha$ , °	90
$\beta$ , °	90
$\gamma$ , °	90
Cell Volume, Å <sup>3</sup>	4863.5
Z	4
$D_{calc}$ , g cm <sup>-3</sup>	1.32
Reflections Observed <sup>a</sup>	1807
R	0.074
$R_w$	0.079

---

<sup>a</sup> Corrections: Lorentz-polarization.  $F_o \geq 5\sigma(F_o)$

**Table A37** Final Fractional Coordinates for  
 $[(C_5H_5)(C_6(CH_2CH_2C_6H_5)_6)Fe]PF_6$ .

ATOM	x/a	y/b	z/c	B(eqv) <sup>b</sup>
Fe	-0.97838(7)	-0.25000	-0.25000	3.15
C1	-0.9581(6)	-0.1971(8)	-0.323(1)	3.15
C2	-0.9374(6)	-0.1604(8)	-0.211(2)	3.38
C3	-0.9714(6)	-0.1381(7)	-0.098(1)	2.79
C4	-1.0224(6)	-0.1542(8)	-0.103(1)	3.15
C5	-1.0443(5)	-0.1958(6)	-0.216(1)	2.10
C6	-1.0111(5)	-0.2139(7)	-0.324(1)	2.44
C7	-0.8816(5)	-0.1420(9)	-0.198(2)	4.02
C8	-0.8628(7)	-0.080(1)	-0.288(2)	5.27
C9	-0.8125(6)	-0.0465(9)	-0.236(2)	3.74
C10	-0.7787(6)	-0.077(1)	-0.157(2)	4.73
C11	-0.7326(7)	-0.040(1)	-0.114(2)	5.16
C12	-0.7269(9)	0.024(1)	-0.159(2)	6.94
C13	-0.761(1)	0.060(1)	-0.229(3)	7.96
C14	-0.8051(7)	0.025(1)	-0.281(2)	5.90
C15	-0.8051(7)	-0.2202(8)	-0.430(1)	3.73
C16	-0.9208(6)	-0.1756(9)	-0.554(2)	4.00
C17	-0.8786(7)	-0.195(1)	-0.649(2)	4.01
C18	-0.8424(9)	-0.141(1)	-0.696(2)	5.83
C19	-0.8045(8)	-0.156(1)	-0.782(3)	6.86
C20	-0.7999(9)	-0.229(2)	-0.826(3)	7.95

---

ATOM	x/a	y/b	z/c	B (eqv) <sup>b</sup>
C21	-0.8318(8)	-0.280(1)	-0.781(2)	6.25
C22	-0.8722(6)	-0.261(1)	-0.695(1)	4.42
C23	-1.0322(4)	-0.2523(9)	-0.442(1)	3.37
C24	-1.0603(7)	-0.2026(9)	-0.541(2)	4.85
C25	-1.0911(5)	-0.2358(9)	-0.643(1)	3.10
C26	-1.0793(7)	-0.302(1)	-0.702(2)	4.73
C27	-1.1060(7)	-0.334(1)	-0.803(2)	5.23
C28	-1.150(1)	-0.295(1)	-0.845(2)	7.27
C29	-1.1652(7)	-0.235(1)	-0.786(2)	6.15
C30	-1.1339(8)	-0.201(1)	-0.692(2)	5.24
C31	-1.0992(5)	-0.2259(8)	-0.213(2)	3.56
C32	-1.1410(5)	-0.1791(8)	-0.254(2)	4.18
C33	-1.1912(6)	-0.2157(9)	-0.245(2)	3.97
C34	-1.2177(8)	-0.211(1)	-0.127(2)	6.08
C35	-1.2630(8)	-0.252(1)	-0.110(2)	6.00
C36	-1.2830(6)	-0.291(1)	-0.206(3)	5.52
C37	-1.2555(9)	-0.295(1)	-0.324(3)	7.28
C38	-1.2104(6)	-0.2608(9)	-0.347(2)	3.66
C39	-1.0584(6)	-0.1314(8)	0.005(1)	3.59
C40	-1.0762(7)	-0.0541(8)	-0.017(2)	4.04
C41	-1.1196(9)	-0.030(1)	0.073(2)	5.03
C42	-1.1170(8)	-0.019(1)	0.199(3)	5.45
C43	-1.155(1)	-0.002(1)	0.286(2)	5.80

---

---

ATOM	x/a	y/b	z/c	B(eqv) <sup>b</sup>
C44	-1.202(1)	0.002(1)	0.217(3)	8.30
C45	-1.207(1)	-0.006(1)	0.092(4)	9.40
C46	-1.169(1)	-0.025(1)	0.018(2)	7.25
C47	-0.9477(7)	-0.1027(8)	0.026(2)	4.65
C48	-0.9344(7)	-0.0273(8)	0.001(2)	4.77
C49	-0.9088(7)	0.0083(9)	0.121(2)	3.70
C50	-0.9331(7)	0.0082(8)	0.249(2)	4.87
C51	-0.9090(9)	0.041(1)	0.353(2)	6.30
C52	-0.8619(9)	0.0778(9)	0.335(2)	5.68
C53	-0.8397(8)	0.071(1)	0.219(2)	5.47
C54	-0.8624(7)	0.0408(9)	0.110(2)	4.34
C55	-1.0070(7)	-0.341(1)	-0.078(3)	5.97
C56	-0.979(1)	-0.310(1)	0.022(2)	6.86
C57	-0.932(1)	-0.304(1)	-0.025(3)	8.13
C58	-0.930(1)	-0.331(2)	-0.146(3)	7.91
C59	-0.977(1)	-0.3567(9)	-0.172(2)	4.20
P1	-1.0421(3)	0.0331(4)	0.5987(7)	8.5(2)c
F1	-1.0315(6)	-0.0126(8)	0.462(2)	13.7(5)c
F2	-1.0589(8)	0.074(1)	0.721(2)	21.0(8)c
F3	-1.0100(9)	0.091(1)	0.542(3)	20.6(8)c
F4	-1.0924(8)	0.069(1)	0.527(2)	18.2(7)c
F5	-1.0023(9)	-0.005(1)	0.669(2)	20.0(8)c

---

---

ATOM	x/a	y/b	z/c	B(eqv) <sup>b</sup>
F6	-1.0851(7)	-0.025(1)	0.623(2)	18.3(7) <sup>c</sup>

---

<sup>b</sup>  $B(\text{eqv}) = 4/3[a^2\beta_{11} + b^2\beta_{22} + c^2\beta_{33} + ab(\cos \gamma)\beta_{12} + ac(\cos \beta)\beta_{13} + bc(\cos \alpha)\beta_{23}]$ .

<sup>c</sup> Isotropic refinement.

Table A38 Bond Distances (Å) and Angles (°) for  
 $[(C_5H_5)(C_6(CH_2CH_2C_6H_5)_6)Fe]PF_6$ .

ATOMS	DISTANCE	ATOMS	DISTANCE
Fe - C1	2.09(2)	Fe - C2	2.07(1)
Fe - C3	2.13(1)	Fe - C4	2.16(1)
Fe - C5	2.11(1)	Fe - C6	2.09(1)
Fe - C55	1.97(2)	Fe - C56	2.03(2)
Fe - C57	2.00(3)	Fe - C58	1.97(3)
Fe - C59	1.99(2)	P1 - F1	1.64(2)
P1 - F2	1.51(3)	P1 - F3	1.48(2)
P1 - F4	1.64(2)	P1 - F5	1.45(2)
P1 - F6	1.57(2)	C1 - C2	1.42(2)
C1 - C6	1.42(2)	C1 - C15	1.50(2)
C2 - C3	1.50(2)	C2 - C7	1.51(2)
C3 - C4	1.37(2)	C3 - C47	1.54(2)
C4 - C5	1.49(2)	C4 - C39	1.50(2)
C5 - C6	1.43(2)	C5 - C31	1.54(2)
C6 - C23	1.49(2)	C7 - C8	1.54(2)
C8 - C9	1.55(3)	C9 - C10	1.32(3)
C9 - C14	1.41(3)	C10 - C11	1.45(3)
C11 - C12	1.28(3)	C12 - C13	1.32(3)
C13 - C14	1.43(3)	C15 - C16	1.50(2)
C16 - C17	1.50(2)	C17 - C18	1.45(3)
C17 - C22	1.31(3)	C18 - C19	1.35(3)

---

ATOMS	DISTANCE	ATOMS	DISTANCE
C19 - C20	1.41(4)	C20 - C21	1.34(4)
C21 - C22	1.41(2)	C23 - C24	1.54(2)
C24 - C25	1.44(2)	C25 - C26	1.40(2)
C25 - C30	1.38(3)	C26 - C27	1.36(3)
C27 - C28	1.45(3)	C28 - C29	1.29(3)
C29 - C30	1.40(3)	C31 - C32	1.45(2)
C32 - C33	1.49(2)	C33 - C34	1.38(3)
C33 - C38	1.41(3)	C34 - C35	1.41(3)
C35 - C36	1.31(3)	C36 - C37	1.39(4)
C37 - C38	1.36(3)	C39 - C40	1.51(2)
C40 - C41	1.52(3)	C41 - C42	1.28(4)
C41 - C46	1.44(4)	C42 - C43	1.37(4)
C43 - C44	1.41(4)	C44 - C45	1.27(5)
C45 - C46	1.26(4)	C47 - C48	1.46(2)
C48 - C49	1.53(2)	C49 - C50	1.44(2)
C49 - C54	1.36(2)	C50 - C51	1.36(3)
C51 - C52	1.42(3)	C52 - C53	1.31(3)
C53 - C54	1.37(3)	C55 - C56	1.37(4)
C55 - C59	1.26(4)	C56 - C57	1.33(5)
C57 - C58	1.32(5)	C58 - C59	1.36(4)
Fe - Cent1	1.54	Fe - Cent2	1.64

ATOMS	ANGLE	ATOMS	ANGLE
F1 - P1 - F2	173(1)	F1 - P1 - F3	87(1)
F2 - P1 - F3	96(1)	F1 - P1 - F4	89(1)
F2 - P1 - F4	86(1)	F3 - P1 - F4	89(1)
F1 - P1 - F5	92(1)	F2 - P1 - F5	93(1)
F3 - P1 - F5	97(1)	F4 - P1 - F5	173(1)
F1 - P1 - F6	85(1)	F2 - P1 - F6	90(1)
F3 - P1 - F6	164(1)	F4 - P1 - F6	77(1)
F5 - P1 - F6	96(1)	C2 - C1 - C6	119(1)
C2 - C1 - C15	118(1)	C6 - C1 - C15	123(1)
C1 - C2 - C3	120(1)	C1 - C2 - C7	123(1)
C3 - C2 - C7	117(1)	C2 - C3 - C4	119(1)
C2 - C3 - C47	120(1)	C4 - C3 - C47	121(1)
C3 - C4 - C5	121(1)	C3 - C4 - C39	122(1)
C5 - C4 - C39	117(1)	C4 - C5 - C6	118(1)
C4 - C5 - C31	122(1)	C6 - C5 - C31	120(1)
C1 - C6 - C5	122(1)	C1 - C6 - C23	118(1)
C5 - C6 - C23	119(1)	C2 - C7 - C8	115(1)
C7 - C8 - C9	112(1)	C8 - C9 - C10	127(2)
C8 - C9 - C14	113(2)	C10 - C9 - C14	120(2)
C9 - C10 - C11	123(2)	C10 - C11 - C12	115(2)
C11 - C12 - C13	125(2)	C12 - C13 - C14	121(2)
C9 - C14 - C13	115(2)	C1 - C15 - C16	117(1)
C15 - C16 - C17	114(1)	C16 - C17 - C18	122(2)

---

ATOMS	ANGLE	ATOMS	ANGLE
C16 - C17 - C22	123(2)	C18 - C17 - C22	116(2)
C17 - C18 - C19	123(2)	C18 - C19 - C20	117(2)
C19 - C20 - C21	121(2)	C20 - C21 - C22	120(2)
C17 - C22 - C21	123(2)	C6 - C23 - C24	114(1)
C23 - C24 - C25	118(1)	C24 - C25 - C26	124(1)
C24 - C25 - C30	121(2)	C26 - C25 - C30	115(1)
C25 - C26 - C27	125(2)	C26 - C27 - C28	115(2)
C27 - C28 - C29	121(2)	C28 - C29 - C30	121(2)
C25 - C30 - C29	121(2)	C5 - C31 - C32	119(1)
C31 - C32 - C33	112(1)	C32 - C33 - C34	118(2)
C32 - C33 - C38	122(2)	C34 - C33 - C38	119(2)
C33 - C34 - C35	119(2)	C34 - C35 - C36	123(2)
C35 - C36 - C37	117(2)	C36 - C37 - C38	125(2)
C33 - C38 - C37	117(2)	C4 - C39 - C40	111(1)
C39 - C40 - C41	114(1)	C40 - C41 - C42	126(2)
C40 - C41 - C46	119(2)	C42 - C41 - C46	115(2)
C41 - C42 - C43	129(2)	C42 - C43 - C44	110(2)
C43 - C44 - C45	124(3)	C44 - C45 - C46	123(3)
C41 - C46 - C45	119(3)	C3 - C47 - C48	111(1)
C47 - C48 - C49	112(1)	C48 - C49 - C50	121(2)
C48 - C49 - C54	121(2)	C50 - C49 - C54	118(2)
C49 - C50 - C51	119(2)	C50 - C51 - C52	121(2)
C51 - C52 - C53	117(2)	C52 - C53 - C54	124(2)

---

ATOMS	ANGLE	ATOMS	ANGLE
C49 - C54 - C53	120(2)	C56 - C55 - C59	109(2)
C55 - C56 - C57	106(2)	C56 - C57 - C58	109(3)
C57 - C58 - C59	106(3)	C55 - C59 - C58	110(2)
Cent1 - Fe - Cent2	179.1		

---

Table A39 Least Squares Best Planes Calculations for**Plane 1**

Equation of the plane:  $-0.218X + 0.894Y - 0.392Z =$   
0.411

Distances (Å) to the plane from the atoms in the plane.

C55	0.026	C58	0.015
C56	-0.015	C59	-0.027
C57	0.000		

Distances (Å) to the plane from the atoms out of the plane.

Fe	1.640
----	-------

**Plane 2**

Equation of the plane:  $-0.191X + 0.871Y - 0.453Z =$   
3.088

Distances (Å) to the plane from the atoms in the plane.

C1	0.009	C4	0.020
C2	-0.014	C5	-0.025
C3	-0.001	C6	0.011

Distances (Å) to the plane from the atoms out of the plane.

Fe            -1.540

**Plane 3**

Equation of the plane:  $0.537X + 0.488Y - 0.689Z = -12.990$

Distances (Å) to the plane from the atoms in the plane.

C25	-0.006	C28	0.020
C26	-0.025	C29	-0.051
C27	0.019	C30	0.043

Distances (Å) to the plane from the atoms out of the plane.

C24            0.019

**Plane 4**

Equation of the plane:  $-0.513X + 0.783Y - 0.353Z = 13.745$

Distances (Å) to the plane from the atoms in the plane.

C33	0.010	C36	0.015
C34	0.013	C37	0.009
C35	-0.027	C38	-0.021

Distances (Å) to the plane from the atoms out of the plane.

C32            -0.104

**Plane 5**

Equation of the plane:  $0.163X + 0.971Y - 0.174Z = -$   
5.457

Distances ( $\text{\AA}$ ) to the plane from the atoms in the plane.

C41	0.004	C44	-0.019
C42	0.010	C45	0.035
C43	-0.003	C46	-0.027

Distances ( $\text{\AA}$ ) to the plane from the atoms out of the plane.

C40	-0.077
-----	--------

**Plane 6**

Equation of the plane:  $-0.453X + 0.859Y - 0.239Z =$   
10.597

Distances ( $\text{\AA}$ ) to the plane from the atoms in the plane.

C49	0.016	C52	0.047
C50	-0.006	C53	-0.039
C51	-0.024	C54	0.006

Distances ( $\text{\AA}$ ) to the plane from the atoms out of the plane.

C48	0.043
-----	-------

**Plane 7**

Equation of the plane:  $0.489X - 0.333Y - 0.806Z = -$   
8.208

Distances (Å) to the plane from the atoms in the plane.

C9	0.007	C12	0.037
C10	-0.021	C13	-0.049
C11	-0.001	C14	0.026

Distances (Å) to the plane from the atoms out of the plane.

C8	-0.007
----	--------

**Plane 8**

Equation of the plane:  $-0.604X + 0.199Y - 0.772Z =$   
18.219

Distances (Å) to the plane from the atoms in the plane.

C17	-0.003	C20	0.009
C18	-0.011	C21	-0.022
C19	0.008	C22	0.020

Distances (Å) to the plane from the atoms out of the plane.

C16	0.002
-----	-------

## Dihedral angle between planes A and B.

A	B	Angle(°)
1	2	4.0
1	3	54.0
1	4	18.3
1	5	25.8
1	6	16.2
1	7	95.0
1	8	52.3
2	3	50.7
2	4	20.1
2	5	26.7
2	6	19.5
2	7	91.1
2	8	50.4
3	4	69.5
3	5	47.1
3	6	70.1
3	7	49.0
3	8	72.3
4	5	42.5
4	6	8.6
4	7	103.1
4	8	42.5
5	6	36.7
5	7	96.0

Dihedral angle between planes A and B.

A	B	Angle(°)
5	8	76.8
6	7	108.3
6	8	51.1
7	8	74.9

## (23) Hexa(phenylethyl)benzene

Table A40 Crystal Data and Refinement Parameters for  
 $C_6(CH_2CH_2C_6H_5)_6$ .

---

Formula	$C_{54}H_{54}$
Colour	colourless
Formula Wt.	703.02
Space Group	$P\bar{1}$
Temp, °C	20
a, Å	11.567(5)
b, Å	12.115(6)
c, Å	15.887(8)
$\alpha$ , °	86.96(5)
$\beta$ , °	77.30(5)
$\gamma$ , °	76.01(5)
Cell Volume, Å <sup>3</sup>	2107.4
Z	2
$D_{calc}$ , g cm <sup>-3</sup>	1.11
Reflections Observed <sup>a</sup>	1854
R	0.070
$R_w$	0.088

---

<sup>a</sup> Corrections: Lorentz-polarization.  $F_o \geq 5\sigma(F_o)$

Table A41 Final Fractional Coordinates for  $C_6(CH_2CH_2C_6H_5)_6$ .

ATOM	x/a	y/b	z/c	B (eqv) <sup>b</sup>
C1	0.9779 (8)	1.1172 (7)	0.5066 (5)	2.93
C2	0.9020 (7)	1.0716 (7)	0.4686 (5)	2.47
C3	0.9258 (7)	0.9523 (7)	0.4614 (5)	2.75
C4	0.9523 (8)	1.2465 (6)	0.5205 (5)	3.19
C5	0.8748 (8)	1.2818 (7)	0.6103 (6)	3.57
C6	0.8650 (9)	1.4023 (8)	0.6358 (5)	3.24
C7	0.7591 (9)	1.4844 (8)	0.6477 (6)	4.48
C8	0.751 (1)	1.5933 (9)	0.6744 (7)	5.45
C9	0.855 (1)	1.6241 (9)	0.6834 (6)	4.82
C10	0.963 (1)	1.540 (1)	0.6720 (6)	5.44
C11	0.9667 (9)	1.4330 (8)	0.6474 (7)	4.63
C12	0.8028 (7)	1.1472 (7)	0.4306 (5)	3.14
C13	0.8497 (7)	1.1738 (7)	0.3364 (5)	3.47
C14	0.7555 (9)	1.2434 (8)	0.2908 (6)	3.58
C15	0.7166 (9)	1.1974 (9)	0.2279 (7)	5.36
C16	0.632 (1)	1.261 (1)	0.1834 (7)	6.15
C17	0.587 (1)	1.374 (1)	0.2023 (8)	5.81
C18	0.619 (1)	1.417 (1)	0.2644 (9)	7.22
C19	0.707 (1)	1.356 (1)	0.3088 (7)	5.85
C20	0.8389 (7)	0.9003 (7)	0.4257 (5)	2.91
C21	0.7374 (8)	0.8736 (8)	0.4966 (6)	3.64
C22	0.6548 (9)	0.8094 (8)	0.4682 (6)	3.20

---

ATOM	x/a	y/b	z/c	B (eqv) <sup>b</sup>
C23	0.679 (1)	0.694 (1)	0.4746 (7)	5.80
C24	0.605 (1)	0.634 (1)	0.4492 (9)	7.23
C25	0.512 (1)	0.693 (1)	0.4147 (9)	6.93
C26	0.486 (1)	0.806 (1)	0.4063 (7)	5.73
C27	0.5617 (9)	0.8652 (9)	0.4312 (6)	4.19
C28	0.4572 (8)	0.6073 (7)	0.0384 (5)	2.62
C29	0.3780 (7)	0.5332 (7)	0.0447 (5)	2.53
C30	0.4203 (8)	0.4274 (7)	0.0046 (5)	2.52
C31	0.4107 (7)	0.7251 (6)	0.0807 (5)	3.12
C32	0.4264 (8)	0.7283 (7)	0.1727 (6)	3.79
C33	0.4036 (9)	0.8488 (8)	0.2048 (5)	3.22
C34	0.285 (1)	0.9076 (9)	0.2426 (6)	4.52
C35	0.266 (1)	1.018 (1)	0.2742 (7)	5.51
C36	0.362 (2)	1.066 (1)	0.2620 (8)	6.17
C37	0.477 (1)	1.011 (1)	0.2225 (8)	6.53
C38	0.495 (1)	0.9025 (9)	0.1927 (6)	4.55
C39	0.2493 (7)	0.5707 (7)	0.0955 (5)	3.08
C40	0.1548 (7)	0.6347 (7)	0.0427 (5)	3.45
C41	0.0299 (9)	0.668 (1)	0.0988 (6)	3.90
C42	-0.047 (1)	0.595 (1)	0.1154 (7)	6.05
C43	-0.154 (2)	0.615 (2)	0.172 (1)	10.86
C44	-0.188 (3)	0.717 (2)	0.211 (2)	11.32
C45	-0.127 (2)	0.794 (2)	0.196 (2)	10.89

---

---

ATOM	x/a	y/b	z/c	B(eq $v$ ) <sup>b</sup>
C46	-0.015(1)	0.768(1)	0.1394(8)	6.83
C47	0.3320(7)	0.3512(7)	0.0067(5)	3.27
C48	0.3289(8)	0.2683(7)	0.0829(5)	3.74
C49	0.2423(9)	0.1961(9)	0.0802(6)	3.59
C50	0.276(1)	0.091(1)	0.0408(7)	6.06
C51	0.189(2)	0.028(1)	0.039(1)	9.63
C52	0.072(2)	0.077(2)	0.070(1)	11.37
C53	0.031(2)	0.181(2)	0.109(1)	8.49
C54	0.118(1)	0.237(1)	0.1113(7)	5.51

---

<sup>b</sup>  $B(\text{eqv}) = 4/3[a^2\beta_{11} + b^2\beta_{22} + c^2\beta_{33} + ab(\cos \gamma)\beta_{12} + ac(\cos \beta)\beta_{13} + bc(\cos \alpha)\beta_{23}]$ .

Table A42 Bond Distances (Å) and Angles (°) for  
 $C_6(CH_2CH_2C_6H_5)_6$ .

ATOMS	DISTANCE	ATOMS	DISTANCE
C1 - C2	1.39(1)	C1 - C4	1.54(1)
C1 - C3a	1.40(1)	C2 - C3	1.41(1)
C2 - C12	1.50(1)	C3 - C20	1.52(1)
C4 - C5	1.53(1)	C5 - C6	1.50(1)
C6 - C7	1.36(1)	C6 - C11	1.37(2)
C7 - C8	1.38(2)	C8 - C9	1.37(2)
C9 - C10	1.39(2)	C10 - C11	1.37(2)
C12 - C13	1.52(1)	C13 - C14	1.50(1)
C14 - C15	1.38(2)	C14 - C19	1.37(1)
C15 - C16	1.39(2)	C16 - C17	1.36(2)
C17 - C18	1.30(2)	C18 - C19	1.41(2)
C20 - C21	1.52(1)	C21 - C22	1.52(2)
C22 - C23	1.36(2)	C22 - C27	1.36(1)
C23 - C24	1.38(2)	C24 - C25	1.35(2)
C25 - C26	1.33(2)	C26 - C27	1.39(2)
C28 - C29	1.41(1)	C28 - C31	1.53(1)
C28 - C30b	1.40(1)	C29 - C30	1.39(1)
C29 - C39	1.50(1)	C30 - C47	1.53(1)
C31 - C32	1.52(1)	C32 - C33	1.52(1)
C33 - C34	1.40(1)	C33 - C38	1.35(2)
C34 - C35	1.40(2)	C35 - C36	1.36(2)

---

ATOMS	DISTANCE	ATOMS	DISTANCE
C36 - C37	1.37(2)	C37 - C38	1.38(2)
C39 - C40	1.56(1)	C40 - C41	1.49(1)
C41 - C42	1.38(2)	C41 - C46	1.34(2)
C42 - C43	1.34(2)	C43 - C44	1.34(4)
C44 - C45	1.28(4)	C45 - C46	1.38(3)
C47 - C48	1.53(1)	C48 - C49	1.49(2)
C49 - C50	1.38(2)	C49 - C54	1.38(2)
C50 - C51	1.41(3)	C51 - C52	1.33(3)
C52 - C53	1.37(3)	C53 - C54	1.35(3)

---

---

ATOMS	ANGLE	ATOMS	ANGLE
C2 - C1 - C4	120.6(8)	C2 - C1 - C3a	121.7(8)
C4 - C1 - C3a	117.6(9)	C1 - C2 - C3	118.3(7)
C1 - C2 - C12	121.1(7)	C3 - C2 - C12	120.5(8)
C2 - C3 - C20	119.2(7)	C2 - C3 - C1a	120.0(9)
C20 - C3 - C1a	120.6(8)	C1 - C4 - C5	111.6(7)
C4 - C5 - C6	115.2(7)	C5 - C6 - C7	123(1)
C5 - C6 - C11	119.5(8)	C7 - C6 - C11	117.1(9)
C6 - C7 - C8	122(1)	C7 - C8 - C9	120(1)
C8 - C9 - C10	118(1)	C9 - C10 - C11	120(1)
C6 - C11 - C10	122.1(9)	C2 - C12 - C13	111.3(6)

---

---

ATOMS	ANGLE	ATOMS	ANGLE
C12 - C13 - C14	115.4(7)	C13 - C14 - C15	121.7(9)
C13 - C14 - C19	121(1)	C15 - C14 - C19	117(1)
C14 - C15 - C16	122(1)	C15 - C16 - C17	119(1)
C16 - C17 - C18	120(1)	C17 - C18 - C19	123(1)
C14 - C19 - C18	119(1)	C3 - C20 - C21	112.1(7)
C20 - C21 - C22	115.7(7)	C21 - C22 - C23	119.7(9)
C21 - C22 - C27	120.6(9)	C23 - C22 - C27	120(1)
C22 - C23 - C24	121(1)	C23 - C24 - C25	118(1)
C24 - C25 - C26	124(2)	C25 - C26 - C27	118(1)
C22 - C27 - C26	120(1)	C29 - C28 - C31	120.2(7)
C29 - C28 - C30b	120.5(7)	C31 - C28 - C30b	119.3(8)
C28 - C29 - C30	119.8(7)	C28 - C29 - C39	119.0(7)
C30 - C29 - C39	121.3(8)	C29 - C30 - C47	119.4(7)
C29 - C30 - C28b	119.7(9)	C47 - C30 - C28b	120.9(7)
C28 - C31 - C32	114.5(6)	C31 - C32 - C33	112.1(7)
C32 - C33 - C34	120(1)	C32 - C33 - C38	120.5(8)
C34 - C33 - C38	120(1)	C33 - C34 - C35	119(1)
C34 - C35 - C36	119(1)	C35 - C36 - C37	122(1)
C36 - C37 - C38	119(1)	C33 - C38 - C37	122(1)
C29 - C39 - C40	115.2(7)	C39 - C40 - C41	111.0(7)
C40 - C41 - C42	122(1)	C40 - C41 - C46	123(1)
C42 - C41 - C46	115(1)	C41 - C42 - C43	125(2)
C42 - C43 - C44	115(2)	C43 - C44 - C45	125(2)

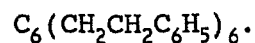
---

ATOMS	ANGLE	ATOMS	ANGLE
C44 - C45 - C46	118(2)	C41 - C46 - C45	122(2)
C30 - C47 - C48	113.4(8)	C47 - C48 - C49	110.4(8)
C48 - C49 - C50	123.8(9)	C48 - C49 - C54	120.5(9)
C50 - C49 - C54	115(1)	C49 - C50 - C51	121(1)
C50 - C51 - C52	118(2)	C51 - C52 - C53	124(2)
C52 - C53 - C54	115(2)	C49 - C54 - C53	126(1)

---

a = symmetry equivalent 2-x, 2-y, 1-z

b = symmetry equivalent 1-x, 1-y, -z

Table A43 Least Squares Best Planes Calculations for**Plane 1**

$$\text{Equation of the plane: } 0.451X + 0.334Y - 0.892Z = 0.806$$

Distances ( $\text{\AA}$ ) to the plane from the atoms in the plane.

C1	0.004	C1a	-0.004
C2	-0.004	C2a	0.004
C3	0.004	C3a	-0.004

Distances ( $\text{\AA}$ ) to the plane from the atoms out of the plane.

C4	-0.077	C20	-0.101
C12	0.074		

**Plane 2**

$$\text{Equation of the plane: } 0.062X + 0.265Y - 0.962Z = -4.102$$

Distances ( $\text{\AA}$ ) to the plane from the atoms in the plane.

C6	-0.004	C9	0.020
C7	0.016	C10	-0.008
C8	-0.024	C11	-0.000

Distances (Å) to the plane from the atoms out of the plane.

C5            -0.018

**Plane 3**

Equation of the plane:  $0.688X + 0.238Y - 0.685Z = 9.608$

Distances (Å) to the plane from the atoms in the plane.

C14	0.005	C17	0.021
C15	-0.009	C18	-0.026
C16	-0.003	C19	0.012

Distances (Å) to the plane from the atoms out of the plane.

C13            0.044

**Plane 4**

Equation of the plane:  $0.399X - 0.101Y - 0.912Z = -2.933$

Distances (Å) to the plane from the atoms in the plane.

C22	-0.021	C25	0.004
C23	0.012	C26	-0.012
C24	-0.003	C27	0.021

Distances (Å) to the plane from the atoms out of the plane.

C21            -0.001

**Plane 5**

Equation of the plane:  $-0.364X + 0.393Y - 0.845Z = -0.323$

Distances ( $\text{\AA}$ ) to the plane from the atoms in the plane.

C28	0.011	C28a	-0.011
C29	-0.011	C29a	0.011
C30	0.011	C30a	-0.011

Distances ( $\text{\AA}$ ) to the plane from the atoms out of the plane.

C31	0.019	C47	0.081
C39	-0.065		

**Plane 6**

Equation of the plane:  $-0.300X + 0.357Y - 0.885Z = -1.578$

Distances ( $\text{\AA}$ ) to the plane from the atoms in the plane.

C33	-0.025	C36	0.001
C34	0.023	C37	-0.002
C35	-0.012	C38	0.014

Distances ( $\text{\AA}$ ) to the plane from the atoms out of the plane.

C32	-0.030		
-----	--------	--	--

**Plane 7**

Equation of the plane:  $-0.543X + 0.381Y - 0.748Z = 0.427$

Distances (Å) to the plane from the atoms in the plane.

C41	-0.023	C44	-0.025
C42	0.023	C45	0.023
C43	0.000	C46	0.001

Distances (Å) to the plane from the atoms out of the plane.

C40	-0.146
-----	--------

**Plane 8**

Equation of the plane:  $-0.202X + 0.420Y - 0.885Z = -0.856$

Distances (Å) to the plane from the atoms in the plane.

C49	-0.013	C52	0.011
C50	0.022	C53	-0.003
C51	-0.021	C54	0.004

Distances (Å) to the plane from the atoms out of the plane.

C48	0.059
-----	-------

## Dihedral angle between planes A and B.

A	B	Angle(°)
1	2	26.5
1	3	21.6
1	4	8.3
1	5	53.0
1	6	48.2
1	7	64.2
1	8	44.6
2	3	40.1
2	4	28.9
2	5	26.6
2	6	22.0
2	7	38.1
2	8	18.2
3	4	28.9
3	5	65.0
3	6	61.0
3	7	76.7
3	8	55.4
4	5	54.2
4	6	49.4
4	7	64.7
4	8	46.8
5	6	4.8
5	7	11.7

Dihedral angle between planes A and B.

A	B	Angle (°)
5	8	9.7
6	7	16.1
6	8	6.7
7	8	21.3

**Chapter 10**

**References**

1. Hein, F. *Chem. Ber.* **1919**, 52, 195.
2. Fischer, E.O.; Hafner, W. *Z. Naturforsch* **1955**, B10, 655.
3. Silverthorn, W.E. *Adv. Organomet. Chem.* **1975**, 13, 47.
4. Davies, S.G.; Green, M.L.H.; Mingos, D.M.P. *Tetrahedron* **1978**, 34, 3047.
5. Semmelhack, M.F.; Clark, G.R.; Garcia, J.L.; Harrison, J.J.; Thebtaranonth, Y.; Wulff, W.; Yamashita, A. *Tetrahedron* **1981**, 37, 3957.
6. Muetterties, E.L.; Bleeke, J.R.; Wucherer, E.J. *Chem. Rev.* **1982**, 82, 499.
7. Astruc, D. *Tetrahedron* **1983**, 39, 4027.
8. Kane-Maguire, L.A.P.; Honig, E.D.; Sweigart, D.A. *Chem. Rev.* **1984**, 84, 525.
9. Sutherland, R.G.; Iqbal, M.; Piorko, A. *J. Organomet. Chem.* **1986**, 302, 307.
10. Watts, W.E. in Comprehensive Organometallic Chemistry, ed. G. Wilkinson, Pergamon Press, **1982**, 8, 1013.
11. Dines, M.B.; Bird, P.H. *J. Chem. Soc., Chem. Commun.* **1973**, 12.
12. Turner, R.W.; Amma, E.L. *J. Inorg. Nucl. Chem.* **1966**, 28, 2411.
13. Brennan, J.G.; Cloke, F.G.N.; Sameh, A.A.; Zalkin, A. *J. Chem. Soc., Chem. Commun.* **1987**, 1668.
14. Cotton, F.A.; Schwotzer, W. *J. Am. Chem. Soc.* **1986**, 108, 4657.

15. Campbell, G.C.; Cotton, F.A.; Haw, J.F.; Schwotzer, W. *Organometallics* **1986**, *5*, 274.
16. Cesari, M.; Pedretti, U.; Zazzetta, A.; Lugli, G.; Ma , W. *Inorg. Chim. Acta* **1971**, *5*, 439.
17. Cotl , F.A.; Schwotzer, W. *Organometallics* **1985**, *4*, 942.
18. Cotton, F.A.; Schwotzer, W.; Simpson, C.Q.,II. *Angew. Chem. Int. Ed. Engl.* **1986**, *25*, 637.
19. Weininger, M.S.; Rodesilar, P.F.; Amma, E.. *Inorg. Chem.* **1979**, *18*, 751.
20. Gash, A.G.; Rodesilar, P.F.; Amma, E.L. *Inorg. Chem.* **1974**, *13*, 2429.
21. Rodesilar, P.F.; Auel, Th.; Amma, E.L. *J. Am. Chem. Soc.* **1975**, *97*, 7405.
22. Auel, Th.; Amma, E.L. *J. Am. Chem. Soc.* **1968**, *90*, 5941.
23. Weininger, M.S.; Rodesilar, P.F.; Gash, A.G.; Amma, E.L. *J. Am. Chem. Soc.* **1972**, *94*, 2135.
24. Luth, H.; Amma, E.L. *J. Am. Chem. Soc.* **1969**, *91*, 7515.
25. Fischer, E.O.; Rohrscheid, F. *J. Organomet. Chem.* **1966**, *6*, 53.
26. Allegra, G.; Casagrande, G.T.; Immirzi, A.; Porri, L.; Vitulli, G. *J. Am. Chem. Soc.* **1970**, *92*, 289.
27. Coffield, T.H.; Sandel, V.; Closson, R.D. *J. Am. Chem. Soc.* **1957**, *79*, 5826.
28. Winkhaus, G.; Pratt, L.; Wilkinson, G. *J. Chem. Soc.* **1961**, 3807.

29. Pauson, P.L.; Segal, J.A. *J. Chem. Soc., Dalton Trans.* **1975**, 1677.
30. Nicholls, B.; Whiting, M.C.; *Proc. Chem. Soc. (London)* **1958**, 152.
31. Fischer, E.O.; Ofele, K. *Z. Naturforsch; Teil B* **1958**, 13, 458.
32. Natta, G.; Ercoli, R.; Calderazzo, F. *Chim. Ind. (Milan)* **1958**, 40, 287.
33. Natta, G.; Ercoli, R.; Calderazzo, F.; Santambrogio, E. *Chim. Ind. (Milan)* **1958**, 40, 1003.
34. Fischer, E.O.; Ofele, K.; Essler, H.; Frohlich, W.; Mortensen, J.P.; Semmlinger, W. *Chem. Ber.* **1958**, 91, 2763.
35. Fischer, E.O.; Ofele, K.; Essler, H.; Frohlich, W.; Mortensen, J.P.; Semmelinger, W. *Z. Naturforsch, Teil B* **1958**, 13, 458.
36. Benfield, F.W.S.; Green, M.L.H.; Ogden, J.S.; Young, D. *J. Chem. Soc., Chem. Commun.* **1973**, 866.
37. Middleton, R.; Hull, J.R.; Simpson, S.R.; Tomlinson, C.H.; Timms, P.L. *J. Chem. Soc., Dalton Trans.* **1973**, 120.
38. Skell, P.S.; Williams-Smith, D.L.; McGlinchey, M.J. *J. Am. Chem. Soc.* **1973**, 95, 3337.
39. Tsutsui, M.; Zeiss, H. *J. Am. Chem. Soc.* **1961**, 83, 825.
40. Fischer, E.O.; Schmidt, M.W. *Chem. Ber.* **1967**, 100, 3782.

41. Kang, J.W.; Childs, R.F.; Maitlis, P.M. *J. Am. Chem. Soc.* **1970**, *92*, 720.
42. Browning, J.; Green, M.; Penfold, B.R.; Spencer, J.L.; Stone, F.G.A. *J. Chem. Soc., Chem. Commun.* **1973**, 31.
43. Wang, C.; Lang, M.G.; Sheridan, J.B. *J. Am. Chem. Soc.* **1990**, *112*, 3236.
44. Oishi, S. *J. Organomet. Chem.* **1987**, *335*, 207.
45. Brauer, D.J.; Kruger, C. *Inorg. Chem.* **1977**, *16*, 884.
46. Sweet, J.R.; Graham, W.A.G. *J. Organomet. Chem.* **1983**, *241*, 45.
47. Huttner, G.; Lange, S. *Acta. Cryst.* **1972**, *B28*, 2049.
48. Fischer, E.O.; Elschenbroich, C. *Chem. Ber.* **1970**, *103*, 162.
49. Burt, R.; Cooke, M.; Green, M. *J. Chem. Soc. (A)* **1970**, 2981.
50. Dickson, R.S.; Kirsch, H.P. *Aust. J. Chem.* **1974**, *27*, 61.
51. Dickson, R.S.; Wilkinson, G. *J. Chem. Soc.* **1964**, 2699.
52. Harman, W.D.; Taube, H. *J. Am. Chem. Soc.* **1987**, *109*, 1383.
53. Omori, H.; Suzuki, H.; Take, Y.; Moro-oka, Y. *Organometallics* **1989**, *8*, 2270.
54. Neithamer, D.R.; Parkanyi, L.; Mitchell, J.F.; Wolczanski, P.T. *J. Am. Chem. Soc.* **1985**, *110*, 4421.
55. Gallop, M.A.; Johnson, B.F.G.; Lewis, J.; Raithby, P.R. *J. Chem. Soc., Chem. Commun.* **1987**, 1809.

56. Lamanna, W.M.; Gleason, W.B. *Organometallics* **1987**, *6*, 1583.
57. Duff, A.W.; Jones, K.; Goddard, R.; Kraus, H.J.; Kruger, C. *J. Am. Chem. Soc.* **1983**, *105*, 5479.
58. Lamanna, W.M. *J. Am. Chem. Soc.* **1986**, *108*, 2096.
59. Kealy, T.J.; Pauson, P.L. *Nature* **1951**, *168*, 1039.
60. Ernst, R.D. *Chem. Rev.* **1988**, *88*, 1255.
61. Powell, P. *Adv. Organomet. Chem.* **1986**, *26*, 125.
62. Ernst, R.D. *Struct. Bonding* **1984**, *57*, 1.
63. Ernst, R.D. *Acc. Chem. Res.* **1985**, *18*, 56.
64. Yasuda, H.; Nakamura, A. *J. Organomet. Chem.* **1985**, *285*, 15.
65. Helling, J.F.; Braitsch, D.M. *J. Am. Chem. Soc.* **1970**, *92*, 7207.
66. Helling, J.F.; Braitsch, D.M. *J. Am. Chem. Soc.* **1970**, *92*, 7209.
67. Clerk, M.D.; Zaworotko, M.J.; Borecka, B.; Cameron, T.S.; Hooper, D.L.; Linden, A. *Can. J. Chem.* **1990**, *68*, 1923.
68. Sturge, K.C.; Zaworotko, M.J. *J. Chem. Soc., Chem. Commun.* **1990**, 1244.
69. Astruc, D. *Chem. Rev.* **1988**, *88*, 1189.
70. Astruc, D. *Acc. Chem. Res.* **1986**, *19*, 377.
71. Michaud, P.; Mariot, J.P.; Varret, F.; Astruc, D. *J. Chem. Soc., Chem. Commun.* **1982**, 1383.

72. Abd-El-Aziz, A.S.; Baranski, A.S.; Piorko, A.; Sutherland, R.G. *Inorg. Chim. Acta.* **1988**, 147, 77.
73. Helling, J.F.; Hendrickson, W.A. *J. Organomet. Chem.* **1979**, 168, 87.
74. Sutherland, R.G.; Steele, B.R.; Demchuk, K.J.; Lee, C.C. *J. Organomet. Chem.* **1979**, 181, 411.
75. Lee, C.C.; Gill, U.S.; Sutherland, R.G. *J. Organomet. Chem.* **1981**, 206, 89.
76. Lee, C.C.; Abd-El-Aziz, A.S.; Chowdhury, R.L.; Gill, U.S.; Piorko, A.; Sutherland, R.G. *J. Organomet. Chem.* **1986**, 315, 79.
77. Abd-El-Aziz, A.S.; Lee, C.C.; Piorko, A.; Sutherland, R.G. *J. Organomet. Chem.* **1988**, 348, 95.
78. Sutherland, R.G.; Abd-El-Aziz, A.S.; Piorko, A.; Gill, U.S.; Lee, C.C. *J. Heterocyclic Chem.* **1988**, 25, 1107.
79. Piorko, A.; Abd-El-Aziz, A.S.; Lee, C.C.; Sutherland, R.G. *J. Chem. Soc., Perkin Trans.* **1989**, 469.
80. Hamon, J.R.; Saillard, J.Y.; LeBeuze, A.; McGlinchey, M.J.; Astruc, D. *J. Am. Chem. Soc.* **1982**, 104, 7549.
81. Moulines, F.; Astruc, D. *J. Chem. Soc., Chem. Commun.* **1989**, 614.
82. Iverson, D.J.; Hunter, G.; Blount, J.F.; Damewood, Jr. J.R.; Mislow, K. *J. Am. Chem. Soc.* **1981**, 103, 6073.
83. Hunter, G.; Blount, J.F.; Damewood, Jr. J.R.; Iverson, D.J.; Mislow, K. *Organometallics* **1982**, 1, 448.

84. Hunter, G.; Weakley, T.J.R.; Mislow, K.; Wong, M.G. *J. Chem. Soc., Dalton Trans.* **1986**, 577.
85. McGlinchey, M.J.; Fletcher, J.L.; Sayer, B.G.; Bougeard, P.; Faggiani, R.; Lock, C.J.L.; Bain, A.D.; Rodger, C.; Kundig, E.P.; Astruc, D.; Hamon, J.R.; Le Maux, P.; Top, S; Jaouen, G. *J. Chem. Soc., Chem. Commun.* **1983**, 634.
86. McGlinchey, M.J.; Bougeard, P.; Sayer, B.G.; Hofer, R.; Lock, C.J.L. *J. Chem. Soc., Chem. Commun.* **1984**, 789.
87. Blount, J.F.; Hunter, G.; Mislow, K. *J. Chem. Soc., Chem. Commun.* **1984**, 170.
88. Hunter, G.; Mislow, K. *J. Chem. Soc., Chem. Commun.* **1984**, 172.
89. Pomeroy, R.K.; Harrison, D.J. *J. Chem. Soc., Chem. Commun.* **1980**, 661.
90. Zennek, U.; Elschenbroich, C.; Mockel, R. *J. Organomet. Chem.* **1981**, 219, 177.
91. Hu, X.; Duchowski, J.; Pomeroy, R.K. *J. Chem. Soc., Chem. Commun.* **1988**, 362.
92. Nambu, M.; Siegel, J.S. *J. Am. Chem. Soc.* **1988**, 110, 3675.
93. Chudek, J.A.; Hunter, G.; MacKay, R.L.; Farber, G.; Weissensteiner, W. *J. Organomet. Chem.* **1989**, 377, C69.
94. Downton, P.A.; Mailvaganam, B.; Frampton, C.S.; Sayer, B.G.; McGlinchey, M.J. *J. Am. Chem. Soc.* **1990**, 112, 28.

95. Dubois, R.H.; Zaworotko, M.J.; White, P.S. *J. Organomet. Chem.* **1989**, 362, 155.
96. Zaworotko, M.J.; Sturge, K.C.; Nunez, L.; Rogers, R.D. *Organometallics*, **1990**, in press.
97. Sweigart, D.A.; Neto, C.C. *J. Chem. Soc., Chem. Commun.* **1990**, 1703.
98. Cameron, T.S.; Clerk, M.D.; Linden, A.; Sturge, K.C.; Zaworotko, M.J. *Organometallics* **1988**, 7, 2571.
99. Gaudet, M.V.; Hanson, A.W.; White, P.S.; Zaworotko, M.J. *Organometallics* **1989**, 8, 286.
100. Sutherland, R.G.; Chowdhury, R.L.; Piorko, A.; Lee, C.C. *Can. J. Chem.* **1986**, 64, 2031.
101. Wilmoth, M.A.; Bernhardt, R.J.; Eyman, D.P.; Huffman, J.C. *Organometallics* **1986**, 5, 2559.
102. Bae, H.K.; Jung, I.N.; Chung, Y.K. *J. Organomet. Chem.* **1986**, 317, C1.
103. Fish, R.H.; Kim, H.S.; Fong, R.H. *Organometallics* **1990**, 9, 1327.
104. Mandon, D.; Astruc, D. *J. Organomet. Chem.* **1989**, 369, 383.
105. Pike, R.D.; Ryan, W.J.; Carpenter, G.B.; Sweigart, D.A. *J. Am. Chem. Soc.* **1989**, 111, 8535.
106. Mandon, D.; Toupet, L.; Astruc, D. *J. Am. Chem. Soc.* **1986**, 108, 1320.
107. Mandon, D.; Astruc, D. *J. Organomet. Chem.* **1986**, 307, C27.

108. Astruc, D.; Michaud, P.; Madonik, A.M.; Saillard, J.Y.; Hoffman, R. *Nouv. J. Chim.* **1985**, *9*, 41.
109. Zaworotko, M.J.; Sturge, K.C.; White, P.S. *J. Organomet. Chem.* **1990**, *389*, 333.
110. Michaud, P.; Astruc, D.; Ammeter, J.H. *J. Am. Chem. Soc.* **1982**, *104*, 3755.
111. Madonik, A.M.; Mandon, D.; Michaud, P.; Lapinte, C.; Astruc, D. *J. Am. Chem. Soc.* **1984**, *106*, 3381.
112. Khand, I.U.; Pauson, P.L.; Watts, W.E. *J. Chem. Soc. (C)* **1969**, 2024.
113. Green, M.L.H.; Mitchard, L.C.; Silverthorn, W.E. *J. Chem. Soc., Dalton Trans.* **1973**, 1952.
114. Walker, P.J.C.; Mawby, R.J. *J. Chem. Soc., Dalton Trans.* **1973**, 622.
115. Semmelhack, M.F.; Bisaha, J.; Czarny, M. *J. Am. Chem. Soc.* **1979**, *101*, 769.
116. Semmelhack, M.F.; Hill, H.T. *J. Am. Chem. Soc.* **1974**, *96*, 7091.
117. Semmelhack, M.F.; Hall, H.T. *J. Am. Chem. Soc.* **1974**, *96*, 7092.
118. Semmelhack, M.F.; Hall, H.T., Jr.; Farina, R.; Yoshifuji, M.; Clark, G.; Bargar, T.; Hirotsu, K.; Clardy, J. *J. Am. Chem. Soc.* **1979**, *101*, 3536.
119. Chung, Y.K.; Williard, P.G.; Sweigart, D.A. *Organometallics* **1982**, *1*, 1053.

120. Helling, J.F.; Cash, G.G. *J. Organomet. Chem.* **1974**, *73*, C10.
121. Chung, Y.K.; Choi, H.S.; Sweigart, D.A.; Connelly, N.G. *J. Am. Chem. Soc.* **1982**, *104*, 4245.
122. Lai, Y.H.; Tam, W.; Vollhardt, K.P.C. *J. Organomet. Chem.* **1981**, *216*, 97.
123. Jenker, H.; Schmidt, H.W. *Ger. Pat. Appl.* 1 048 275 (1955) (*Chem. Abstr.* **1960**, *54*, 19 486).
124. Neumann, W.P.; Niermann, H. *Liebigs Ann. Chem.* **1962**, *653*, 164.
125. Glockling, F.; Light, J.R.C. *J. Chem. Soc. (A)* **1967**, 623.
126. Blitzer, S.M.; Pearson, T.H. *US Pat.* 2 859 228 (1959) (*Chem. Abstr.* **1959**, *53*, 9150).
127. Ziegler, K. *US Pat.* 3 124 604 (1956) (*Chem. Abstr.* **1964**, *60*, 15 909).
128. Eisch, J.J. *J. Am. Chem. Soc.* **1962**, *84*, 3605.
129. Pasynkiewicz, S. *Przem. Chem.* **1960**, *39*, 225.
130. Zietz, J.R., Jr.; Robinson, G.C.; Lindsay, K.L. in Comprehensive Organometallic Chemistry, ed. G. Wilkinson, Pergamon Press, **1982**, *7*, 365.
131. Helling, J.F.; Rice, S.L.; Braitsch, D.M.; Mayer, T. *J. Chem. Soc., Chem. Commun.* **1971**, 930.
132. Gunther, H. NMR Spectroscopy, John Wiley and Sons, **1980**, 7/-86.

133. Johnson, C.K.; ORTEP; Report ORNL-3794, revised, Oak Ridge National Laboratory, Oak Ridge, Tennessee, 1965.
134. DiMauro, P.T.; Wolczanski, P.T. *Organometallics* **1987**, *6*, 1947.
135. DiMauro, P.T.; Wolczanski, P.T.; Parkanyi, L.; Petach, H.H. *Organometallics* **1990**, *9*, 1097.
136. Lee, C.C.; Zhang, C.H.; Abd-El-Aziz, A.S.; Piorko, A.; Sutherland, R.G. *J. Organomet. Chem.* **1989**, *364*, 217.
137. Zhang, C.H.; Chowdhury, R.L.; Piorko, A.; Lee, C.C.; Sutherland, R.G. *J. Organomet. Chem.* **1988**, *346*, 67.
138. Sutherland, R.G.; Zhang, C.H.; Piorko, A.; Lee, C.C. *Can. J. Chem.* **1989**, *67*, 137.
139. Coates, G.E.; Green, M.L.H.; Powell, P.; Wade, K. Principles of Organometallic Chemistry, Methuen and Co. Ltd. **1968**, 198.
140. Braitsch, D.M.; Kumarappan, R. *J. Organomet. Chem.* **1975**, *84*, C37.
141. Darchen, A. *J. Organomet. Chem.* **1986**, *302*, 389.
142. Ashby, E.C.; Goel, A.B. *J. Organomet. Chem.* **1981**, *221*, C15.
143. Goldman, A.S.; Tyler, D.R. *Inorg. Chem.* **1987**, *26*, 253.
144. Nesmeyanov, A.N.; Vol'kenau, N.A.; Petrakova, V.A. *J. Organomet. Chem.* **1977**, *136*, 363.
145. Nesmeyanov, A.N.; Vol'kenau, N.A.; Bolesova, I.N. *Tetrahedron Lett.* **1963**, 1725.

146. Atwood, J.L. in Inclusion Compounds ed. J.L. Atwood; J.E.D. Davies; D.D. MacNicol, Academic Press, 1984, 1, 375.
147. Atwood, J.L. in Recent Developments in Separation Science, ed. N.N. Li, CRC Press 1977, 3, 195.
148. Atwood, J.L.; Atwood, J D. in Inorganic Compounds with Unusual Properties, ed. R.B. King, American Chemical Society, 1976, 112.
149. Atwood, J.L.; Milton, P.A.; Seale, S.K. *J. Organomet. Chem.* 1971, 28, C29.
150. Weller, F.; Wilson, I.L.; Dehnicke, K. *J. Organomet. Chem.* 1971, 30, C4.
151. Atwood, J.L.; Newberry, W.R.,III *J. Organomet. Chem.* 1974, 66, 15.
152. Atwood, J.L.; Newberry, W.R.,III *J. Organomet. Chem.* 1974, 65, 145.
153. Shakir, R.; Zaworotko, M.J.; Atwood, J.L. *J. Organomet. Chem.* 1979, 171, 9.
154. Zaworotko, M.J.; Rogers, R.D.; Atwood, J.L. *Organometallics* 1982, 1, 1179.
155. Atwood, J.L.; Crissinger, K.D.; Rogers, R.D. *J. Organomet. Chem.* 1978, 155, 1.
156. Atwood, J.L.; Seale, S.K. *J. Organomet. Chem.* 1976, 114, 107.
157. Hines, M.R. B.Sc. Honours Thesis April 1990, Saint Mary's University, Halifax, Nova Scotia.

158. Bohm, M.C.; Eckert-Maksic, M.; Ernst, R.D.; Wilson, D.R.; Gleiter, R. *J. Am. Chem. Soc.* **1982**, 104, 2699.
159. Mathew, M.; Palenik, G.J. *Inorg. Chem.* **1972**, 11, 2809.
160. Astruc, D.; Hamon, J.R.; Roman, E.; Michaud, P. *J. Am. Chem. Soc.* **1981**, 103, 7502.
161. Rybinskaya, M.I.; Kudinov, A.R.; Kaganovich, V.S. *J. Organomet. Chem.* **1983**, 246, 279.
162. Kaganovich, V.S.; Kudinov, A.R.; Rybinskaya, M.I. *J. Organomet. Chem.* **1987**, 323, 111.
163. Bennett, M.A.; Matheson, T.W. *J. Organomet. Chem.* **1979**, 175, 87.
164. Winkhaus, G.; Singer, H. *J. Organomet. Chem.* **1967**, 7, 487.
165. Bennett, M.A.; Smith, A.K. *J. Chem. Soc., Dalton Trans.* **1974**, 233.
166. Dr. Don Arnold (Dalhousie University), private communication.
167. Bottrill, M.; Green, M.; O'Brien, E.; Smart, L.E.; Woodward, P. *J. Chem. Soc., Dalton, Trans.* **1980**, 292.
168. Chinn, Jr. J.W.; Hall, M.B. *J. Am. Chem. Chem.* **1983**, 105, 4930.
169. Wilkinson, G. *J. Organomet. Chem.* **1975**, 100, 273.
170. Fischer, E.O.; Bottcher, R. *Chem. Ber.* **1956**, 89, 2397.
171. Clerk, M.D.; Sturge, K.C.; White, P.S.; Zaworotko, M.J. *J. Organomet. Chem.* **1989**, 368, C33.

172. Dunitz, J.D.; Orgel, L.E.; Rich, A. *Acta. Cryst.* **1956**,  
9, 373.
173. Cameron, T.S.; Linden, A.; Sturge, K.C.; Zaworotko,  
M.J. *Acta Cryst.*, submitted for publication.
174. Han, J.C.; Hutchinson, J.P.; Ernst, R.D. *J. Organomet.*  
*Chem.* **1987**, 321, 389.
- 175 Wilson, D.R.; Ernst, R.D.; Cymbaluk, T.H.  
*Organometallics* **1983**, 2, 1220.
176. Astruc, D.; Hamon, J.R.; Althoff, G.; Roman, E. *J. Am.*  
*Chem. Soc.* **1979**, 101, 5445.
177. Ernst, R.D. (University of Utah), private  
communication.